Functional characterization of the African horse sickness virus VP5 protein, and studies regarding virus-induced apoptosis in cultured mammalian cells

by

Liesel Stassen

Submitted in partial fulfilment of the requirements for the degree
Philosophiae Doctor
in the Faculty of Natural and Agricultural Sciences
University of Pretoria
Pretoria

May 2011

DECLARATION

I declare that the thesis, which I hereby submit for the degree, Philosophiae Doctor (Microbiology) at the University of Pretoria, is my own work and has not previously been submitted by me for a degree at another University.

Signed: …….. Date: ……..

ACKNOWLEDGEMENTS

I would like to express by sincere appreciation to the following people for their contribution towards the completion of this thesis:

Prof. J. Theron for granting me the opportunity to commence my PhD under his supervision.

Alan Hall for his assistance in the microscopy analysis.

Flip Wege for cell culture maintenance and titration of the AHSV strains.

Wayne Barnes for technical assistance with the flow cytometry.

My family and friends, especially Johann, for their continued support and encouragement.

The National Research Foundation for financial assistance towards this research.

Dedicated to Karli

SUMMARY

Functional characterization of the African horse sickness virus VP5 protein, and studies regarding virus-induced apoptosis in cultured mammalian cells

by

LIESEL STASSEN

Supervisor: Prof. J. Theron
Department of Microbiology and Plant Pathology
University of Pretoria

Co-supervisor: Prof. H. Huismans
Department of Genetics
University of Pretoria

for the degree PhD

African horse sickness virus (AHSV) is a member of the genus *Orbivirus* in the family *Reoviridae* and is the causative agent of African horse sickness (AHS), an acute disease in horses with a high mortality rate. AHSV consists of two concentric capsids that enclose the viral double-stranded RNA genome. The outer capsid is composed of two major structural proteins of the virion, VP2 and VP5. A focus of this investigation was on the functional characterization of the VP5 protein, which is known only to play a supportive role to VP2 in enhancing the protective immune response in horses and is cytotoxic when expressed in *Spodoptera frugiperda* insect cells. Silencing of VP5 gene expression in AHSV-infected mammalian cells by short hairpin RNA (shRNA) and small interfering RNA (siRNA) proved inefficient as means to determine the *in vivo* functional role of the VP5 protein. Subsequently, characterization of a series of baculovirus-expressed N- and C-terminal truncated VP5 proteins in *S. frugiperda* cells, as well as relevant peptides based on the predicted structural features of the VP5 protein,

indicated that the N-terminal 43 amino acids of the VP5 protein correlated with increased membrane permeabilization. These results suggest that this property of VP5 may be of importance during the initial stages of virus entry into susceptible host cells by facilitating the release of core particles from early endosomes.

Infection of mammalian cell cultures with AHSV is known to result in dramatic cytopathic effects (CPE), but no CPE is observed in infected insect cell cultures despite productive virus replication. The basis for this phenomenon has not yet been investigated, but is suggestive of apoptosis being induced following virus infection of the mammalian cells. A second focus of this investigation was therefore to determine whether AHSV can induce apoptosis in infected mammalian cells and by which mechanism. To investigate, *Culicoides sonorensis* (KC) insect cells and BHK-21 mammalian cells were infected with AHSV-9 and analyzed for morphological and biochemical hallmarks of apoptosis. In contrast to KC cells, infection of BHK-21 cells with AHSV-9 resulted in ultrastructural changes and nuclear DNA fragmentation, both of which are associated with the induction of apoptosis. Results also indicated that AHSV-9 infection of BHK-21 cells resulted in activation of caspase-3, a key agent in apoptosis, and in mitochondrial membrane depolarization. Cumulatively, the data indicate that the intrinsic pathway is activated in AHSV-induced apoptosis.

CONTENTS

LIST OF ABBREVIATIONS

Å	angstrom
aa	amino acid
ABTS	2,2-azino-bis(3-ethylbenzthiazoline-6-sulphonic acid)
AcNPV	*Autographa californica* nuclear polyhedrosis virus
Ago	Argonaute
AHS	African horse sickness
AHSV	African horse sickness virus
AIS	average internal stability
Apaf-1	apoptotic protease activating factor-1
ATP	adenosine-5'-triphosphate
ATPase	adenosine triphosphatase
BHK	Baby hamster kidney
BIR	baculoviral IAP repeat
BLAST	Basic Local Alignment Search Tool
bp	base pair
BSA	bovine serum albumin
BTV	bluetongue virus
˚C	degrees Celsius
ca.	approximately
CARD	caspase-recruitement domain
cDNA	complementary DNA
CER	chicken embryo-related
CLP	core-like particle
cm^2	cubic centimeter
CMV	cytomegalovirus
CO_2	carbon dioxide
CP	crossing point
CPE	cytopathic effect
DD	death domain
DED	death effector domain
DEVD	Asp-Glu-Val-Asp
DISC	death-inducing signaling complex

DMSO	dimethyl sulfoxide
DNA	deoxyribonucleic acid
DNase	deoxyribonuclease
dNTP	deoxyribonucleoside-5'-triphosphate
DR	death receptor
ds	double-stranded
DSSE	differential stability of siRNA duplex ends
E	PCR efficiency
e.g.	*exempli gratia* (for example)
EDTA	ethylenediaminetetra-acetic acid
EHDV	epizootic haemorrhagic disease virus
eGFP	enhanced green fluorescent protein
et al.	*et alia* (and others)
FADD	Fas-Associated protein with Death Domain
FasL	Fas ligand
FBS	foetal bovine serum
FCCP	carbonyl cyanide *p*-(trifluoro-methoxy) phenylhydrazone
Fig.	figure
FLICE	FADD-like interleukin-1 beta-converting enzyme
FLIP	FLICE-like inhibitory protein
GST	glutathione *S*-transferase
GTase	guanylyltransferase
h	hour
i.e.	that is
IAP	inhibitor of apoptosis protein
IFN	interferon
IPTG	isopropyl-β-D-thiogalactopyranoside
JNK	c-Jun N-terminal kinases
kb	kilobase pairs
KC	*Culicoides sonorensis*
kcal	kilocalorie
kDa	kilodalton
LB	Luria-Bertani
LDH	lactate dehydrogenase

M	molar
mA	milliampere
MAPK	mitogen-activated protein kinase
MCS	multiple cloning site
MEM	minimum essential medium
mg	milligram
min	minute
ml	millilitre
mm	millimetre
mM	millimolar
MOI	multiplicity of infection
M_r	molecular weight
mRNA	messenger ribonucleic acid
N	normal
NF-κβ	nuclear factor-kappaβ
ng	nanogram
nm	nanometer
nM	nanomolar
nt	nucleotides
NTPase	nucleoside triphosphate phosphohydrolase
OAS	2'-5'-oligoadenylate synthetase
OD	optical density at 405 nm
OIE	Office International des Epizootics
ORF	open reading frame
p	probability
PI3K	phosphatidylinositol 3-kinase
PAGE	polyacrylamide gel electrophoresis
PBS	phosphate-buffered saline
PCD	programmed cell death
PCR	polymerase chain reaction
PFU	plaque forming units
PKR	dsRNA-activated protein kinase R
pmol	picomole
*p*NA	*p*-nitroanilide

Pol	polymerase
PSB	protein solvent buffer
REST	Relative Expression Software Tool
RGD	arginine-glycine-aspartate
RISC	RNA-induced silencing complex
RNA	ribonucleic acid
RNAi	RNA interference
RNase	ribonuclease
rpm	revolutions per minute
RT-PCR	reverse transcription-PCR
s	second
SD	standard deviation
SDS	sodium dodecyl sulphate
Sf-9	*Spodoptera frugiperda* clone 9 cells
shRNA	short hairpin RNA
shUNeg	control non-silencing shRNA
shVP5-1311	VP5-directed shRNA targeting nucleotides 1311-1331
shVP5-148	VP5-directed shRNA targeting nucleotides 148-168
shVP5-651	VP5-directed shRNA targeting nucleotides 651-671
shVP5-826	VP5-directed shRNA targeting nucleotides 826-846
siRNA	small interfering RNA
siUNeg	control non-silencing siRNA
siVP5-138	VP5-directed siRNA targeting nucleotides 138-156
siVP5-528	VP5-directed siRNA targeting nucleotides 528-546
siVP5-984	VP5-directed siRNA targeting nucleotides 984-1002
Smac	second mitochondria-derived activator of caspase
ss	single-stranded
TEMED	N',N',N',N'-tetramethylethylenediamine
TLR	Toll-like receptor
TNF	tumor necrosis factor
TNFR	tumor necrosis factor receptor
TRAIL	TNF-related apoptosis inducing ligand
U	units
U937	Human leukemic monocyte lymphoma cells

UHQ	ultra-high quality
UTR	untranslated regions
UV	ultraviolet
V	volts
v.	version
v/v	volume per volume
VIB	viral inclusion body
w/v	weight per volume
X-Gal	5-bromo-4-chloro-3-indolyl β-D-galactopyranoside
β2-MG	β2-microglobulin
µg	microgram
µl	microlitre
µm	micrometre
µM	micromolar

LIST OF FIGURES

FIGURE

LIST OF TABLES

CHAPTER ONE

LITERATURE REVIEW

1.1 GENERAL INTRODUCTION

Just under a 120 years ago, in 1892, Dimitry Ivanovsky demonstrated that the sap of leaves infected with tobacco mosaic disease remained infectious, even after filtration through a Chamberland filter capable of retaining bacteria. In 1898, Beijerinck showed that the tobacco mosaic agent could pass through the fine filter of an agar plug, that it required growing cells (unlike most bacteria) and that it survived drying but not boiling. In the same year, Loeffler and Frosch showed that the agent causing foot-and-mouth disease of cattle could not be removed by filtration. Not only did these reports point to the existence of disease agents smaller than any known before, but they are considered to be the first reports to establish the existence of viruses. Indeed, the term filterable agent was the name first used to describe these organisms well before the term viruses were specifically applied to them (Levy *et al.*, 1994). Today, hundreds of viruses are known and many of them are of agricultural and medical importance. Amongst these is African horse sickness virus (AHSV), the causative agent of African horse sickness (AHS). This disease is one of the most lethal diseases of equids and is characterized by clinical signs that develop as a consequence of damage to the circulatory and respiratory systems, thus giving rise to serious effusion and haemorrhage in various organs and tissues (Mellor and Hamblin, 2004). Since the first demonstration by Clem *et al*. (1991) that apoptotic cell death plays a major role in viral disease mechanisms, it is now recognized that many animal viruses are capable of inducing apoptosis in infected cells (Clarke and Tyler, 2009) and that apoptosis contributes significantly to their pathogenesis (O'Donnell *et al.*, 2005; Umeshappa *et al.*, 2010).

Much of the pioneering research on AHS was performed by Sir Arnold Theiler during the early 20th century. In 1900, he demonstrated the filterability of the pathogen through Berkefield and Chamberland filters, thereby indicating that the pathogen was indeed a virus. Theiler's research also indicated that there existed immunologically distinct strains of the AHS agent, since immunity acquired against one strain did not always protect the horse when challenged by a heterologous strain. In 1903, Theiler and Pitchford-Watkins established that AHSV may be transmitted by biting insects and, in 1921, Theiler reported the first detailed descriptions of the clinical signs and lesions produced by infections with AHSV (reviewed in Coetzer and Erasmus, 1994). During the late 1960s and 1970s, several studies were undertaken aimed at characterizing the structure and morphology of AHSV (Verwoerd and Huismans, 1969; Oellerman *et al.*, 1970;

Bremer, 1976). With the advent of gene cloning, genetic engineering and protein expression technologies, much progress has been made regarding structure-function relationships of different AHSV genes and encoded gene products (Uitenweerde *et al.*, 1995; Maree and Huismans, 1997; van Niekerk *et al.*, 2001; de Waal and Huismans, 2005). Despite this progress, much still remains to be learned, amongst other, regarding the role of individual AHSV proteins within the context of infected host cells, the interaction of individual viral proteins with host cellular proteins, as well as viral proteins and cellular mechanisms that contribute to the molecular basis of AHS disease and pathogenesis. During the last decade, the phenomenon of RNA interference (RNAi), a post-transcriptional gene silencing process in which double-stranded RNA (dsRNA) initiates specific cleavage of cytoplasmic mRNA (Fire *et al.*, 1998), has emerged as a powerful genetic tool whereby some of these types of questions may be addressed.

The review will summarize the current information concerning AHSV and will highlight the role of individual viral proteins in the infectious cycle of the virus. This will be followed by discussions of RNAi and its development as a tool for heterologous gene silencing in mammalian cells, as well as signalling pathways involved in virus-induced apoptosis in mammalian cells.

1.2 AFRICAN HORSE SICKNESS (AHS)

African horse sickness (AHS) is caused by African horse sickness virus (AHSV), a member of the *Orbivirus* genus in the family *Reoviridae*. It is a highly infectious disease of equines with high mortality rates in horses (Coetzer and Erasmus, 1994; Guthrie, 2007). Although zebras have long been considered the natural vertebrate host and reservoir of AHSV (Erasmus *et al*., 1978; Lord *et al*., 1997; Barnard, 1998), antibodies to AHSV have been identified in camels, dogs, cattle, sheep, buffalo, donkeys and mules (Van Rensburg *et al*., 1981; Coetzer and Erasmus, 1994; Fassi-Fihri *et al*., 1998; el Hasnaoui *et al*., 1998). A single incident of AHSV infection in humans by neurotropic strains of the virus (serotypes 1 and 6) has also been reported (Swanepoel *et al*., 1992).

African horse sickness is endemic in sub-Saharan Africa, however, outbreaks have occurred in North Africa, the Middle East and in southern European countries (Mellor and Hamblin, 2004).

Multiannual disease incidences have been reported between 1996 and 2008 within South Africa and neighboring countries, notably Zimbabwe, Lesotho, Swaziland, Namibia and Botswana, as well as other African countries such as Ethiopia, Nigeria and Senegal (OIE World Animal Health Information Database). Although all 9 serotypes of AHSV occur in eastern and southern Africa, the increase in the number of serotypes present within the northern limits of the virus' range in sub-Saharan Africa is disconcerting and of substantial concern due to potential spread of AHS from Africa into adjacent regions (Dufour *et al*., 2008; Gale *et al*., 2009; MacLachlan and Guthrie, 2010).

AHSV is transmitted between susceptible equid hosts by biting midges of the genus *Culicoides* (Wetzel *et al*., 1970; Mellor *et al*., 1975; Mellor, 1993). In Africa, the major vector of AHSV is *C. imicola* (Mellor, 1994; Mellor and Hamblin, 2004) and, recently, a second African species, *C. bolitinos*, has been identified as a potential field vector of AHSV (Venter *et al*., 2000). After transfer of the virus by the bite of infective midges, AHSV is transported to the regional lymph nodes of the animal where initial virus multiplication takes place. This is followed by virus dissemination throughout the body via the blood (primary viraemia) and virus replication in target organs and endothelial cells gives rise to secondary viraemia (Coetzer and Erasmus, 1994). According to the extent and severity of clinical symptoms caused by the infection, the disease can be classified into four distinct forms, *i.e.* the pulmonary (acute), cardiac (subacute), mixed pulmonary and cardiac (cardio-pulmonary), and fever forms (Erasmus, 1973; Brown and Dardiri, 1990).

Based on its potential economic and international importance, AHS has been listed as a notifiable disease by the Office International des Epizootics (OIE). Such diseases are defined as transmissible diseases that have the potential for very serious and rapid spread, with particularly serious socio-economic or public health consequences, and are of major importance in the international trade of animals and animal products (www.oie.int/animal-health-in-the-world/oie-listed-diseases-2011/). In southern Africa, AHS is controlled by vaccination using polyvalent, live attenuated vaccines that are administered twice in the first and second year of life of susceptible animals, and annually thereafter (Erasmus, 1976; Taylor *et al*., 1992; MacLachlan *et al*., 2007). These vaccines are, however, not without their risks and drawbacks. These include

incomplete protection (Coetzer and Erasmus, 1994), weak immunogenicity of some vaccine strains (Laegreid, 1996) and possible reversion to virulence (Mellor and Hamblin, 2004). In addition, even limited replication of AHSV attenuated strains *in vivo* could complicate the distinction between vaccinated and infected animals for import/export purposes (Laviada *et al*., 1995).

1.3 AFRICAN HORSE SICKNESS VIRUS (AHSV)

1.3.1 Taxonomic classification

AHSV is a member of the genus *Orbivirus* in the family *Reoviridae* (Calisher and Mertens, 1998). The family encompasses viruses with segmented dsRNA genomes (10-12 segments) encapsidated within single non-enveloped virus particles with a diameter of 55-80 nm, which exhibit icosahedral symmetry. According to the International Committee on Taxonomy of viruses (2009), fifteen genera of *Reoviridae* exist and are divided into two subfamilies. The subfamily *Sedoreovirinae* contains the six genera *Orbivirus*, *Cardoreovirus*, *Mimoreovirus*, *Phytoreovirus*, *Rotavirus* and *Seadornavirus*. The subfamily *Spinareovirinae* contains the nine genera *Aquareovirus*, *Coltivirus*, *Cypovirus*, *Dinovernavirus*, *Fijivirus*, *Idnoreovirus, Orthoreovirus*, *Mycoreovirus* and *Oryzavirus*. These viruses have broad host ranges and have been isolated from a wide variety of terrestrial and non-terrestrial vertebrates and invertebrates, as well as plants (Francki *et al*., 1991; Gorman, 1992). The orbiviruses can be distinguished from other members of the *Reoviridae* in that they replicate in both insects and vertebrates (Calisher and Mertens, 1998), show greater sensitivity to lipid solvents and detergents, and virus infectivity is lost in mildly acidic conditions (Gorman and Taylor, 1985). Within the genus, viruses are divided into 21 distinct serogroups based on cross-reactivities in complement fixation tests, and serotypes within a serogroup are recognized by specific serum-neutralization tests (Gorman, 1979; 1985; Knudson and Monath, 1990; Brown *et al*., 1991). Nine different AHSV serotypes have been distinguished serologically (McIntosh, 1958; Howell, 1962).

1.3.2 Virion structure

The AHSV virion is non-enveloped with two concentric protein layers that enclose a dsRNA genome consisting of ten segments (Verwoerd *et al*., 1972; Bremer *et al.*, 1990). The outer capsid is composed of the two major structural proteins VP2 and VP5, while the inner capsid is comprised mainly of the two major proteins VP3 and VP7 that enclose the three minor proteins VP1, VP4 and VP6 (Roy *et al*., 1994b).

The structure of the AHSV particle is comparable to that of bluetongue virus (BTV), of which the structure of single- and double-shelled virus particles has been determined by cryoelectron microscopy and by X-ray crystallography (Hewat *et al.*, 1992; Prasad *et al.*, 1992; Grimes *et al.*, 1998; Stuart and Grimes, 2006). Based on these analyses, it is possible to segregate the core into two distinct layers. A thin inner layer is formed from 120 molecules of VP3, arranged as 60 dimers, to form a smooth-surfaced shell. The VP3 shell is stabilized by the outer layer of the core that comprises 260 VP7 trimers, organized into pentametric and hexameric rings that protrude 5 nm from the surface with channels between them (Prasad *et al.*, 1992; Stuart *et al.*, 1998). The core contains the dsRNA genome and the three minor proteins VP1 (10 or 12 copies), VP4 (20 or 24 copies that form dimers) and VP6 (60 or 72 copies that may form hexamers), each of which plays a significant role in genome RNA replication (Stuart and Grimes, 2006). The icosahedral and fibrillar outer capsid consists of 360 globular-shaped VP5 molecules, which are arranged in 120 trimers that are located in the channels formed by the six-membered rings of the VP7 trimers. The 180 copies of VP2 form 60 triskelion-type motifs that cover all of the VP7 trimers and protrude 4 nm above the globular VP5 proteins (Hewat *et al.*, 1992; Stuart *et al.*, 1998; Roy and Noad, 2006). A schematic diagram at the BTV particle is presented in Fig. 1.1.

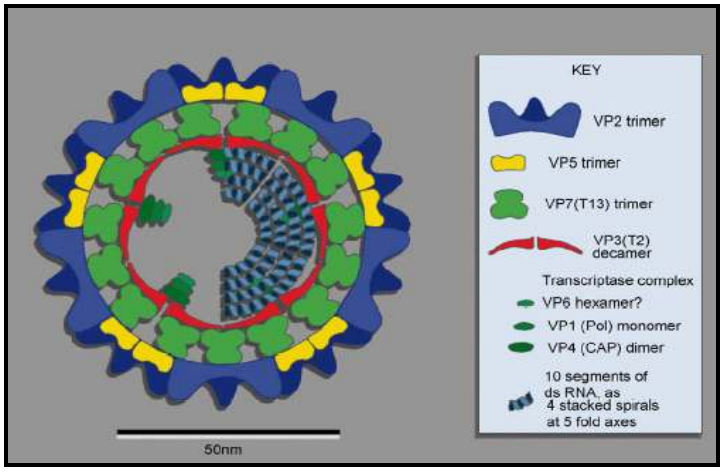

Fig. 1.1 **Schematic representation of the BTV particle (Mertens, 2004).** The core particle, which comprises VP3 and VP7, encloses the three minor core proteins, namely VP1, VP4 and VP6, and the ten dsRNA viral genome segments. The core is surrounded by the outer capsid composed of VP2 and VP5.

1.3.3 Viral genome

The AHSV genome consists of ten dsRNA segments, which are grouped according to size into large (L1-L3), medium (M4-M6) and small (S7-S10) genome segments (Bremer *et al.*, 1990). Each genome segment is monocistronic, except for S10, which encodes the two related nonstructural proteins NS3 and NS3A (van Staden and Huismans, 1991; Grubman and Lewis, 1992). The total viral genome is *ca.* 19.2 kilobase pairs (kb) in length. The 5' non-coding region of the genome segments ranges in size between 12 and 35 base pairs (bp), while the 3' non-coding regions are 29 to 100 bp in length (Roy *et al*., 1994b). In contrast to BTV, the terminal hexanucleotide sequences of AHSV are not conserved through all the segments (Rao *et al*., 1983; Roy *et al.*, 1994b). Nevertheless, the 5'- and 3'-terminal sequences of each genome segment display partial inverted complementarity. This feature is thought to play a role in determining the secondary structure of the viral mRNA, which may be of importance for initiation of transcription and/or in the sorting and assembly of genome segments during virus replication (Cowley *et al*., 1992; Mizukoshi *et al.*, 1993).

1.3.4 AHSV proteins

In addition to seven structural proteins (VP1-VP7), four non-structural proteins (NS1, NS2, NS3 and NS3A) are also encoded by the viral genome. The ten orbivirus dsRNA genome segments, together with their encoded proteins and likely functions, are summarized in Table 1.1.

1.3.4.1 Nonstructural proteins

The nonstructural viral proteins, NS1, NS2, NS3 and NS3A, are considered to play important roles in the replication and morphogenesis of orbiviruses (Roy, 2008). In AHSV-infected cells, NS1 and NS2 are synthesized abundantly, and their synthesis coincides with the appearance of two virus-specific structures, namely tubules and granular viral inclusion bodies (VIBs), respectively (Lecatsas, 1968). Tubules are composed entirely of the NS1 protein (Huismans and Els, 1979; Maree and Huismans, 1997). Although the function of the NS1 tubules in virus replication is still unclear, it has been proposed that the NS1 protein may be a major determinant of BTV pathogenesis in the vertebrate host since it augments virus-cell association that ultimately leads to lysis of the infected cell (Owens *et al*., 2004).

The NS2 protein is a major component of the VIBs observed in orbivirus-infected cells (Thomas *et al*., 1990; Brookes *et al*., 1993), and is solely responsible for their formation (Thomas *et al*., 1990; Uitenweerde *et al*., 1995). The VIBs are the sites of virus replication and of early viral assembly, and contain ssRNA, dsRNA, NS1, as well as incomplete virus particles (Eaton *et al*., 1988; Eaton *et al*., 1990; Brookes *et al*., 1993). The NS2 protein has a strong affinity for single-stranded RNA (ssRNA) (Huismans *et al.*, 1987b; Theron and Nel, 1997; Lymperopoulos *et al*., 2003), suggesting that NS2 may play a role in the recruitment of viral mRNA for replication, and in the selection and condensation of the ten viral ssRNA species into precursor subviral particles. NS2 is the only virus-specific phosphoprotein and it has been suggested that the phosphorylation of NS2 might down-regulate its ssRNA-binding ability (Huismans *et al*., 1987b; Theron *et al*., 1994). In BTV, phosphorylation of NS2 is required for VIB formation and dephosphorylation of the NS2 protein is proposed to allow disassembly of the VIBs with the subsequent release of assembled cores for attachment of the outer capsid proteins prior to virus release (Modrof *et al.*, 2005; Kar *et al.*, 2007).

Table 1.1 BTV genome segments and their encoded proteins (adapted from Stuart *et al.*, 1998 and Mertens, 2004)

Segment	No. of bp	Encoded protein	No. of amino acids	Size (M_r)	Copy number / particle	Location	Function
L1	3965	VP1	1305	150292	10 / 12	Within the subcore at the five-fold axis	RNA-dependent RNA polymerase
L2	3203	VP2	1051	122043	180	Outer capsid	Serotype-specific antigen, adsorption, neutralization, structural protein involved in determination of virulence, possible role in cell exit via vimentin association
L3	2792	VP3	905	103269	120	Inner capsid	Structural protein, forms scaffold for VP7 trimers, controls overall size and organization of capsid structure, interacts with internal minor proteins
M4	1978	VP4	642	75826	20 / 24	Within the subcore at the five-fold axis	Capping enzyme, guanylyltransferase, methyltransferase
M5	1748	NS1	548	63377	0	Nonstructural protein, forms tubules	Forms tubules in the cell cytoplasm, characteristic of orbivirus replication, unknown function
M6	1566	VP5	504	56900	360	Outer capsid	Structural protein, helps control virus serotype, fusion protein involved in membrane penetration during initiation of infection
S7	1167	VP7	349	37916	780	Outer layer of the core particle	Group-specific structural protein, trimer forms outer core surface, T=13 symmetry, possibly involved in cell entry in vector
S8	1166	NS2	365	41193	0	Cytoplasm, forms viral inclusion bodies	Important viral inclusion body matrix protein, binds ssRNA
S9	1169	VP6	369	38464	60 / 72	Within the subcore at the five-fold axis	Binds ssRNA and dsRNA, helicase, NTPase
S10	756	NS3 NS3A	217 206	23659 22481	0 0	Cell membrane	Membrane glycoprotein involved in virus release, may be involved in determination of virulence

In contrast to NS1 and NS2, the two closely related nonstructural proteins NS3 and NS3A are synthesized in low abundance in orbivirus-infected cells (Huismans, 1979; French *et al*., 1989; van Staden *et al*., 1995). The segment 10 gene, encoding NS3, contains two in-phase translation initiation codons that initiate the synthesis of NS3 and NS3A, respectively (van Staden and Huismans, 1991). The NS3/NS3A proteins are the only virus-encoded membrane-associated proteins (Wu *et al*., 1992; van Niekerk *et al*., 2001) and are localized to sites of virus release (Hyatt *et al*., 1993; Stoltz *et al*., 1996). NS3 proteins are therefore thought to be involved in the final stages of viral morphogenesis by facilitating the release of progeny virions from infected cells (Han and Harty, 2004; Celma and Roy, 2009; Meiring *et al.*, 2009).

1.3.4.2 Core proteins

The major core proteins VP3 and VP7 form the outer layer of the viral core particle, and assemble spontaneously into core-like particles (CLPs) when co-expressed by recombinant baculoviruses (Maree *et al*., 1998). Of the two proteins, VP7 is the most abundant protein in the core particle and self-assembles into trimers (Basak *et al.*, 1992), which form the outermost shell of the core. In both BTV and AHSV, VP7 has been demonstrated to be a serogroup-specific antigen (Huismans and Erasmus, 1981; Chuma *et al*., 1992). The crystal structure of BTV and AHSV VP7 (Basak *et al*., 1992; Basak *et al.*, 1996) revealed that the proteins are structurally similar, and can be divided into two domains: a bottom domain (residues 1 to 120 and 250 to 349) that interacts with VP3, and a top domain (residues 121 to 249) that contains a surface-exposed Arg-Gly-Asp (RGD) tripeptide motif, which, in the case of BTV, has been shown to be responsible for attachment of cores to *Culicoides* cells (Tan *et al*., 2001). Notably, in contrast to BTV, AHSV VP7 forms flat hexagonal crystals in the cytoplasm of virus-infected cells (Burroughs *et al*., 1994) and when expressed by a recombinant baculovirus (Chuma *et al.*, 1992). The functional significance of the AHSV VP7 crystals remains to be determined. The VP3 protein plays a major role in the structural integrity of the virus core and forms the protein scaffold on which the VP7 capsomers are assembled (Stuart *et al.*, 1998; Kar *et al.*, 2004). The BTV VP3 protein contains group-specific antigenic determinants (Inumaru *et al*., 1987) and is capable of interacting with ssRNA (Loudon and Roy, 1992).

The three minor core proteins VP1, VP4 and VP6 form part of the transcriptase complex, and are solely responsible for the synthesis of capped and methylated transcripts of each dsRNA segment during the infectious cycle (Mertens and Diprose, 2004). The VP1 protein is a RNA-dependent RNA polymerase and exhibits detectable RNA-elongation activity (Roy *et al*., 1988; Urakawa *et al*., 1989; Boyce *et al*., 2004). The VP4 protein possesses nucleoside triphosphate phosphohydrolase (NTPase), guanylyltransferase (GTase) and both methyltransferse type 1 and 2 activities (Le Blois *et al*., 1992; Ramadevi *et al*., 1998; Ramadevi and Roy, 1998). The role of VP6 as an RNA-dependent ATPase with helicase activity has been confirmed (Stauber *et al*., 1997; Kar and Roy, 2003). It has been proposed that BTV VP6 is involved in unwinding of the dsRNA genome prior to the initiation of transcription, or to separate the parental and newly synthesized RNAs following transcription. Based on its ss- and dsRNA-binding ability, VP6 may also be involved in the encapsidation of the RNA (Roy *et al*., 1990; Hayama and Li, 1994; de Waal and Huismans, 2005).

1.3.4.3 Outer capsid proteins

The VP2 protein, one of the two outer capsid proteins, is the most variable of the viral proteins (Oldfield *et al*., 1991; Williams *et al*., 1998; Potgieter *et al*., 2003), and is the major serotype-specific antigen (Huismans and Erasmus, 1981; Kahlon *et al*., 1983) and viral heamagglutinin (Cowley and Gorman, 1987; Eaton and Crameri, 1989). BTV and AHSV VP2 elicit neutralizing antibodies (DeMaula *et al*., 2000; Martinez-Torrecuadrada *et al*., 2001) that confer protection against subsequent challenge with the homologous virus serotype (Huismans *et al*., 1987a; Martinez-Torrecuadrada *et al*., 1994). Moreover, VP2 is involved in attachment of the virus to cells and has been reported to bind to sialic acid moieties of cellular receptors prior to internalization of the virus particle (Hassan and Roy, 1999; Zhang *et al*., 2010). In addition to its role in attachment, VP2 is also emerging as a key player in the control of BTV assembly and egress from infected cells. The N-terminal of the protein interacts with vimentin and this interaction contributes to virus egress (Bhattacharya *et al*., 2007; Celma and Roy, 2009).

Compared to VP2, the second outer capsid protein VP5 is more highly conserved (Gould and Pritchard, 1988; Wade-Evans *et al*., 1988; Oldfield *et al*., 1991). In contrast to BTV VP5, which may play a supportive role to VP2 in enhancing the immune response (Marshall and Roy, 1990;

Roy *et al*., 1992; Roy *et al*., 1994a), the AHSV VP5 protein is able to induce neutralizing antibodies, albeit at lower titres than those induced by VP2 (Martinez-Torrecuadrada *et al.*, 1999). The biological function of AHSV VP5 remains unknown, but it may be analogous to that of its BTV counterpart. Recent studies on BTV VP5 showed that the protein permeabilizes host cell membranes (Hassan *et al.*, 2001) and has the ability to induce cell-cell fusion when expressed on the cell surface (Forzan *et al*., 2004). Both these activities are mediated by two N-terminal amphipathic helices and are believed to play a major role in destabilizing the membrane of the endocytosized vesicle, thus allowing release of the viral core into the cytoplasm (Forzan *et al*., 2007; Zhang *et al*., 2010). BTV VP5 also interacts with membrane lipid rafts via a WHAL motif, and is likely to play an important part in docking VP5 with plasma membranes for assembly and/or egress via membrane fusion (Bhattacharya and Roy, 2008).

1.4 ORBIVIRUS REPLICATION AND MORPHOGENESIS

Unlike other vertebrate-infecting members of the family *Reoviridae*, unraveling of the orbivirus replication cycle at the molecular level is compounded by their ability to replicate in both vertebrate hosts and arthropod vectors. Moreover, the effect of orbivirus replication in these distinct host types is markedly different. For BTV and AHSV, replication of the virus in insect cells results in persistent infection with little or no cytopathic effect (Mirchamsy *et al.*, 1970; Mertens *et al.*, 1996). However, infection of mammalian cells results in cell death (Osawa and Hazrati, 1965; Mortola *et al.*, 2004). Although it is likely that the basic replication strategies may be similar in the different host types, orbiviruses must have evolved specific replication mechanisms to enable the survival of its arthropod vector to ensure infection of a new vertebrate host. Using BTV as a model for orbivirus replication and morphogenesis (Fig. 1.2), four major events in the replication cycle of orbiviruses have been identified and are discussed below in greater detail. These events are adsorption and penetration, uncoating and formation of replicative complexes, formation of virus tubules and virus inclusion bodies, and movement of virus to and release from the cell surface (Mertens, 2004; Roy, 2008).

In mammalian cells, binding of BTV to a receptor(s) is mediated by VP2 (Hassan and Roy, 1999; Zhang *et al*., 2010). The virus enters the cell through AP2-dependent clathrin-mediated

endocytosis and is incorporated into early endosomes (Forzan *et al*., 2007). The low pH environment within the endosome causes removal of VP2 and triggers conformational changes in VP5 that allows the protein to permeabilize the endosomal membrane (Hassan *et al*., 2001). Subsequently, the transcriptionally active core is released into the cytoplasm (Forzan *et al*., 2007). The replication of BTV is initiated by the synthesis and extrusion of capped and methylated mRNA from transcriptionally active cores within the cytoplasm. The mRNA transcripts function to encode proteins, and are also used as templates for production of minus-strands to form the dsRNA genome segments encapsidated in the progeny virions (Mertens and Diprose, 2004). However, the mechanism by which viral mRNAs are selected and encapsidated prior to replication is not yet known.

Soon after the initiation of transcription of BTV mRNAs, granular matrix structures accumulate near the core particles (Hyatt *et al.*, 1987). These VIBs increase both in size and number as the viral infection progresses (Eaton *et al.*, 1990). Newly synthesized viral transcripts, the four subcore viral proteins (VP1, VP3, VP4 and VP6), as well as assembled cores and subcores have been identified in the VIBs, implicating VIBs as the sites of orbivirus replication and early viral assembly (Hyatt and Eaton, 1988). More recently, co-expression of the BTV structural proteins with NS2 have indicated that VP7 requires co-expression of VP3 to be recruited to the VIBs and that neither of the outer capsid proteins VP5 and VP2 have an affinity for the VIBs (Modrof *et al.*, 2005; Kar *et al.*, 2007). Therefore, it would appear that progeny core particles are first produced in the VIBs, then moved to periphery of the VIBs where they are coated by the outer capsid proteins VP5 and VP2 (Kar *et al.*, 2007). The nascent virions are subsequently released from the VIBs, possibly through dephosphorylation of NS2 (Modrof *et al.*, 2005). In an alternative model, it was recently reported that VP5 of BTV associates with lipid rafts in the plasma membrane and that the core particles are transported to these sites for the final assembly of the outer capsid proteins (Bhattacharya and Roy, 2008). In addition to VIBs, NS1-rich tubules form part of the 'insoluble' phase of the cell and become a characteristic structure of the cell from an early stage of infection (Huismans and Els, 1979; Eaton *et al.*, 1988).

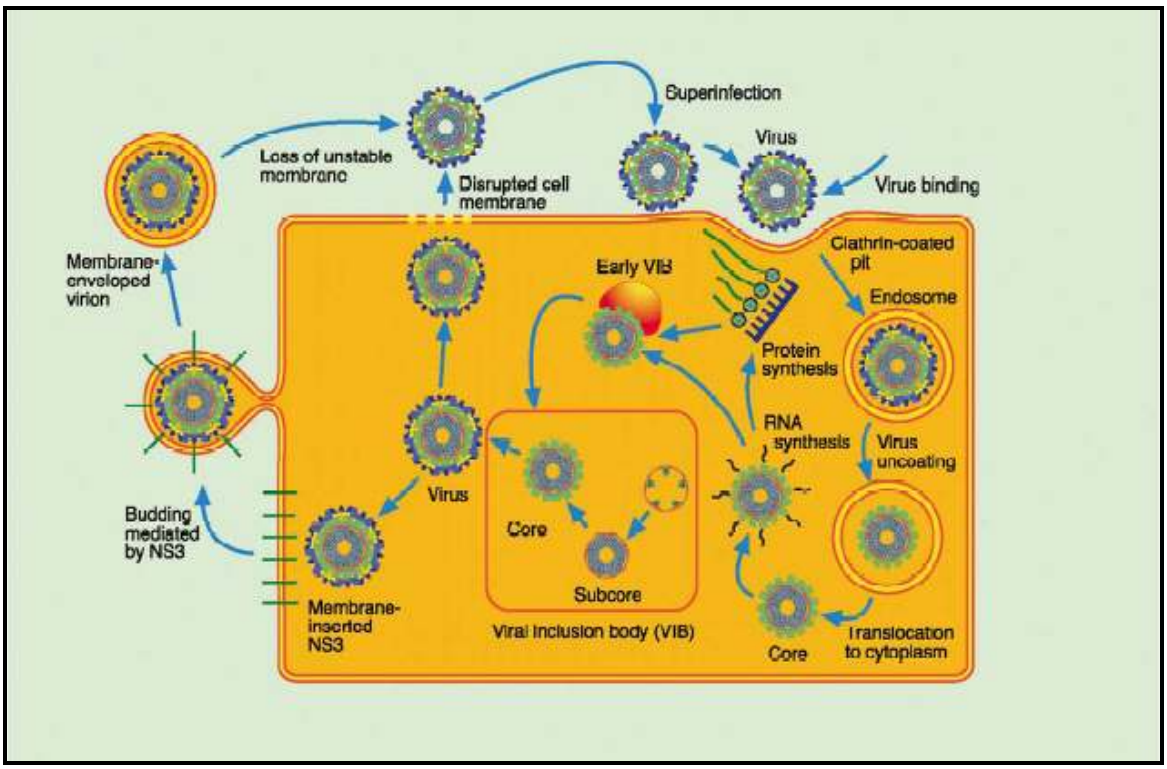

Fig. 1.2 **Schematic diagram of the replication cycle of BTV (Mertens, 2004).** The adsorption of the virus involves a receptor of unknown nature in the cell membrane of susceptible host cells. The viruses enter the cell via endocytosis, after which clathrin-coated vesicles, containing the virions, form and are drawn to the cell nucleus. The outer capsid proteins are removed to yield core particles in the cell cytoplasm. Transcription of the virion RNA occurs and the proteins generated by translation of the viral mRNA condense with the viral ssRNA around the parental cores to form VIBs. Structural proteins are translated and condense at the VIB periphery to form cores and subcores. The outer capsid proteins are added, after which the virions are released from the cells via lysis, budding or extrusion from the cells.

Investigations regarding virus release from mammalian cells have demonstrated a strong correlation between the presence of NS3 and NS3A, and virus release (Hyatt *et al.*, 1991; Stoltz *et al.*, 1996). The virions may leave infected cells by budding through the plasma membrane (Gould and Hyatt, 1994) or virions are extruded through a locally disrupted plasma membrane surface (Hyatt *et al.*, 1989; Han and Harty, 2004). More recently, the NS3 protein of BTV has also been shown to interact with the cellular proteins p11 and Tsg101, and these interactions were furthermore shown to assist in the egress of virus particles from infected cells in a non-lytic manner (Beaton *et al.*, 2002; Wirblich *et al.*, 2006; Celma and Roy, 2009).

1.5 RNA INTERFERENCE (RNAi)

RNA interference (RNAi) is an evolutionary conserved gene silencing mechanism in which the expression of a gene is specifically inhibited by its cognate dsRNA (Fire *et al.*, 1998). The natural function of RNAi is thought to be the protection of the host against transposons (Blumenstiel and Hartl, 2005; van Rij and Berezikov, 2009), and to maintain normal growth and development (Grishok *et al.*, 2001). Also, RNAi has been shown to be an innate antiviral defense mechanism in plants, insects, nematodes and, recently, higher vertebrates (Lecellier *et al.*, 2005; Nayak *et al.*, 2010; Sidahmed and Wilkie, 2010). Due to its apparent universal applicability, high specificity and simplicity, RNAi has progressed to become an important experimental tool both *in vitro* and *in vivo* for the analysis of gene function (Shrey *et al.*, 2009; Hirsch, 2010; Mohr *et al.*, 2010). Consequently, in this part of the literature review, aspects relating to the molecular mechanism underlying RNAi and the development of RNAi tools for use in mammalian cells will be addressed.

1.5.1 The mechanism of RNAi

Biochemical and genetic analyses have provided a mechanistic understanding of RNAi-mediated gene silencing (Meister and Tuschl, 2004; Hutvagner and Simard, 2008; Ohrt *et al.*, 2008; Carthew and Sontheimer, 2009). In the first step, referred to as the RNAi initiating step, long dsRNA is typically cleaved into discrete 21-nucleotide (nt) RNA fragments, termed small interfering RNA (siRNA), by the RNase III-like enzyme Dicer (Bernstein *et al.*, 2001; Provost *et al.*, 2002). Dicers are *ca.* 200-kDa multidomain proteins, which include a DEAH RNA

helicase/ATPase domain, dual RNase III domains (RIIIa and RIIIb), a dsRNA-binding domain (dsRBD) and a PAZ domain (Cerutti and Casas-Mollano, 2006). One end of the dsRNA engages the Dicer PAZ domain, and each of the two RNAse III active sites cleaves two nearby phosphodiester bonds on opposite RNA strands (Sun *et al*., 2005; Gan *et al*., 2006; Macrae *et al*., 2006). Cleavage of the dsRNA results in siRNA duplexes that are typically 21-nt in length, have 5' phosphate and 3' hydroxyl groups and 2-nt overhangs at the 3'-termini (Zhang *et al.*, 2004; Vermeulen *et al*., 2005).

In the second step, referred to as the effector step of RNAi, the siRNAs are assembled into a RNA-induced silencing complex (RISC) (Hammond *et al.*, 2000), which subsequently guides the sequence-specific recognition of the target mRNA (Zamore *et al*., 2000; Martinez *et al.*, 2002; Martinez and Tuschl, 2004). Every RISC contains a member of the Argonaute (Ago) protein family, which is characterized by the presence of a PAZ domain and a PIWI domain (Carmell *et al.*, 2002). These domains specifically recognize the 2-nt 3' overhang (Lingel *et al.*, 2004; Ma *et al*., 2004) and 5'-end of a siRNA duplex (Parker *et al.*, 2005), respectively, thereby allowing for transfer of the siRNA into RISC. The formation of RISC on siRNA duplexes requires ATP, but once formed, RISC can mediate robust sequence-specific cleavage of its target in the absence of ATP (Nykänen *et al.*, 2001; Bernstein *et al.*, 2001). The ATP is most likely required for energy-driven unwinding of the siRNA duplex (Tomari *et al.*, 2004; Pham *et al.*, 2004). Unwinding of the siRNA duplex is accompanied by Ago cleavage and removal of the siRNA passenger strand to form holo-RISC (Matranga *et al*., 2005; Kim *et al*., 2007). It has also been reported that thermodynamic differences in the base-pairing of the two siRNA strands determine which siRNA strand is assembled into RISC (Khvorova *et al.*, 2003; Schwarz *et al.*, 2003). This strand bias is presumably caused by a rate-limiting unwinding step that occurs during transition from the siRNA duplex-containing ribonucleoprotein particle to the RISC complex, which allows the 5'-end of the strand positioned at the weakly paired end of the siRNA to enter RISC first (Khvorova *et al.*, 2003).

To guide sequence-specific degradation of complementary mRNA, the holo-RISC transiently contacts single-stranded mRNA non-specifically and promotes siRNA-target mRNA annealing. Efficient target recognition and cleavage requires the annealing of nt 2-15 at the 5'-end of the

siRNA (Ameres *et al*., 2007). Thermodynamically unfavorable association, as caused by 5'-end mismatches, leads to immediate dissociation of RISC, whereas stable association results in the 3'-end of the siRNA annealing (Haley and Zamore, 2004; Ameres *et al*., 2007). The current model of Argonaute Slicer activity indicates that the siRNA guide strand interacts with the PAZ domain of the Argonaute protein, while the mRNA substrate enters a binding groove formed by the N-terminal, middle and PIWI domains. The 5'-end of the mRNA is predicted to lie between the PAZ domain and N-terminus of Argonaute, with the latter functioning as an mRNA grip. The mRNA is positioned so that the active site, located in the PIWI domain, is 10 nt from the 5'-end of the siRNA/mRNA double-stranded region, thus allowing for cleavage of the mRNA target between 11 and 12 nt from the 3'-end of the siRNA guide (Tomari and Zamore, 2005). The 5' mRNA fragments generated by RISC cleavage are rapidly degraded from their 3'-ends by the exosome ERI-1, a multimeric assembly of 3'-to-5' exonucleases, while the 3' mRNA fragments are degraded from their 5'-ends by XRN1, a major cytoplasmic 5'-to-3' exonuclease (Parker and Song, 2004). A two-step mechanistic model for RNAi-mediated gene silencing is presented in Fig. 1.3.

1.5.2 Developing RNAi for use in mammalian cells

The introduction of long dsRNA (>30 bp) into the cytoplasm of mammalian cells has been reported to induce the interferon (IFN) pathway by activating the IFN-inducible dsRNA-activated protein kinase R (PKR), 2',5'-oligoadenylate synthetase (OAS) and RNA-responsive Toll-like receptor 3 (TLR3) (Stark *et al.*, 1998; Alexopoulou *et al*., 2001; Olejniczak *et al.*, 2009). Predominant amongst these responses triggered is activation of PKR and OAS, the product of which is an essential co-factor for the non-specific RNase L (Olejniczak *et al*., 2009). Their activation result in a systemic, non-specific inhibition of protein synthesis (Manche *et al*., 1992; Stark *et al.*, 1998; Olejniczak *et al*., 2009). In order to apply RNAi technology to studies using mammalian systems, without inducing the dsRNA-activated IFN response, the gene-silencing pathway has to be induced without the use of long dsRNA. This problem was overcome when Elbashir *et al.* (2001a) and Caplen *et al.* (2001) reported that the introduction of synthetic siRNAs of 21 to 22 nt in length, directly into the cytoplasm of mammalian cells, efficiently and specifically silenced expression of the homologous genes. This discovery opened the door to RNAi approaches in mammalian cells, albeit that the gene silencing is transient.

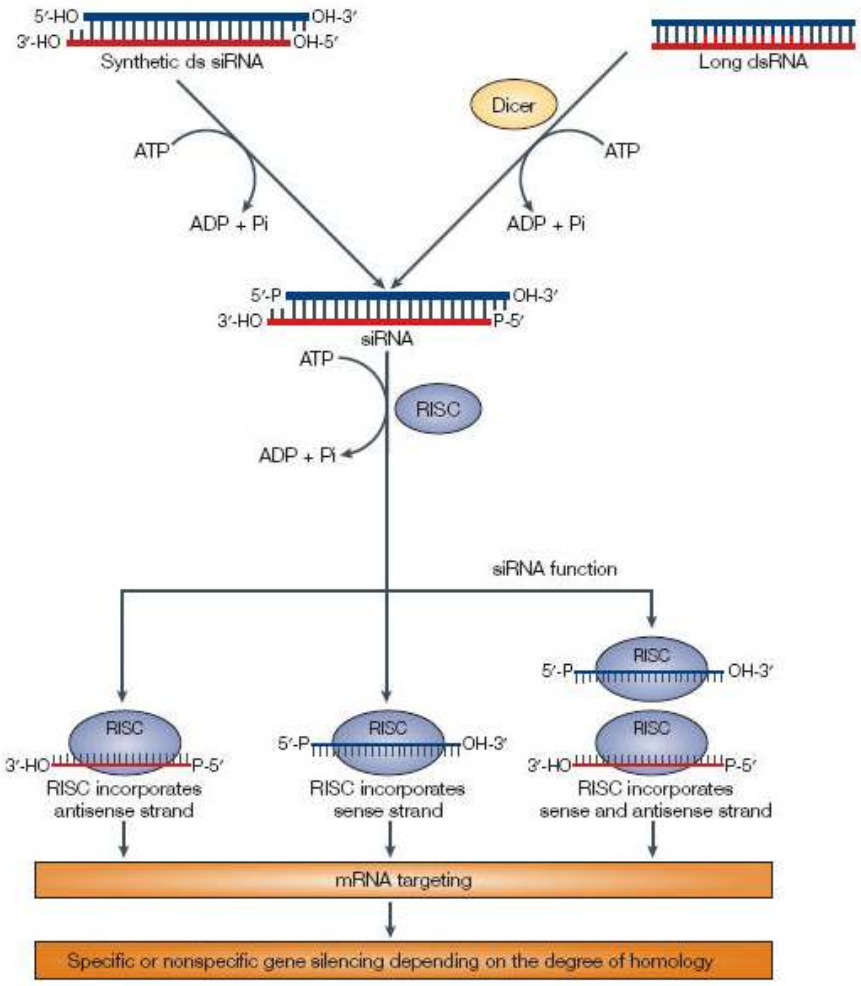

Fig. 1.3 **RNAi-mediated gene silencing (Mittal, 2004).** The processing of long dsRNA by Dicer leads to the formation of siRNAs, which consists of 21-nt RNA duplexes with symmetric 2-nt 3' overhangs and 5' phosphate groups. Exogenously provided synthetic siRNAs are converted into active functional siRNAs by an endogenous kinase that provides 5' phosphate groups in the presence of ATP. siRNAs associate with cellular proteins to form an RNA-induced silencing complex (RISC), which contains a helicase that unwinds the duplex siRNA in an ATP-dependant reaction. In an ideal situation, the antisense strand guides the RISC to the target mRNA for endonucleolytic cleavage. In theory, each of the siRNA strands can be incorporated into RISC and direct RNAi. The antisense strand of a siRNA can direct the cleavage of a corresponding sense RNA target, whereas the sense strand of a siRNA can direct the cleavage of an antisense target.

1.5.2.1 siRNA design, synthesis and delivery

At present, it is not possible to predict with complete certainty the degree of gene silencing a particular siRNA will produce and the design of an effective siRNA is still an empirical process. In addition to a number of general guidelines and recommendations (Elbashir *et al.*, 2001a-c; Caplen *et al.*, 2001; Mittal, 2004; Peek and Behlke, 2007), several siRNA design algorithms (Reynolds *et al.*, 2004; Ui-Tei *et al.*, 2004; Shah *et al.*, 2007; Naito *et al.*, 2009) have also been developed that may increase the probability of producing an effective siRNA. These guidelines and algorithms are, however, only predictive and do not guarantee a gene silencing effect. Nevertheless, the two most important factors influencing siRNA efficiency appears to be the structural characteristics of the siRNA (Mittal, 2004; Reynolds *et al.*, 2004) and the target site within the gene (Ameres *et al.*, 2007; Westerhout and Berkhout, 2007).

Chemical synthesis of synthetic siRNAs represents the gold standard in RNAi assays, and allows for the synthesis of higher concentrations of siRNAs with uniform composition and a wide range of chemical modifications (Braasch *et al.*, 2003; Subramanya *et al*., 2010). Synthetic siRNA can also be obtained through phage T7 RNA polymerase-mediated *in vitro* transcription from short double-stranded DNA oligonucleotide cassettes, which contain the promoter sequence immediately upstream of the siRNA strand template sequence to be transcribed (Donze and Picard, 2002; Sohail *et al.*, 2003). Alternatively, a pool of enzymatically-generated siRNAs can be obtained by digesting long dsRNA, prepared by *in vitro* transcription, with *E. coli* RNase III or recombinant human Dicer (Yang *et al.*, 2002; Kawasaki *et al.*, 2003; Myers *et al.*, 2003). Although effective gene silencing is achieved without the need to identify an individual effective siRNA, unprocessed or partially processed long dsRNA can activate PKR, resulting in non-specific translational inhibition.

For siRNAs to initiate gene-silencing effects they must be introduced into the cytoplasm of mammalian cells and chemical transfection or electroporation have been used for this purpose (Elbashir *et al.*, 2002; Weil *et al.*, 2002). Whereas electroporation has been reported to be well suited for cells in suspension (Weil *et al*., 2002; Randall *et al*., 2003), chemical transfection is widely used for introducing siRNAs into adherent cells and the transfectant reagents are typically cationic lipids (Elbashir *et al.*, 2002). An inherent problem associated with siRNA-mediated

gene silencing is the variability in transfection efficiency, particularly in difficult-to-transfect cell lines. In addition, the siRNAs induce a transient response and are therefore not suitable for long-term studies. To overcome these problems, plasmids and viral vectors, which stably express short hairpin RNA (shRNA), have been developed.

1.4.2.2 Plasmid- and viral vector-expressed shRNAs

The most commonly used approach for the synthesis of shRNAs involves RNA polymerase (Pol) III-mediated transcription of shRNA with a perfectly double-stranded stem of 19 to 29 bp, identical in sequence to the target mRNA, and a short loop of 6 to 9 bases, which is removed *in vivo* by Dicer activity (Brummelkamp *et al.*, 2002a; Paddison *et al.*, 2002a; 2002b). Although RNA Pol II promoters have been used to express shRNAs in mammalian cells (Xia *et al.*, 2002; Giering *et al.*, 2008), RNA polymerase III promoters, such as mammalian U6 or H1 promoters, are more commonly used (Miyagishi and Taira, 2002; Paddison *et al.*, 2002a; Paul *et al.*, 2002; Sui *et al.*, 2002; Yu *et al.*, 2003). RNA Pol III promoters are active in all cell types and normally transcribe large amounts of small, non-coding transcripts that bear well defined ends (Paule and White 2000; Rossi, 2008). For the expression of a shRNA, an expression cassette encoding, in the following order, the sense strand of the hairpin, the hairpin loop, the antisense strand of the hairpin, and the terminator, is inserted immediately downstream of the promoter. Less commonly, the two strands of a shRNA can be transcribed from separate U6 promoters on either the same (Lee *et al.*, 2002) or two separate plasmids (Yu *et al.*, 2002). Several strategies have been used to express multiple shRNAs. In one such strategy, expression of multiple shRNAs, driven by different Pol III promoters were found to have a synergistic effect in repressing the target gene without additional cell toxicity (Henry *et al.*, 2006; ter Brake *et al.*, 2006; Gou *et al.*, 2007).

An alternative to the construction of plasmid vectors expressing shRNAs is to generate shRNA expression cassettes (SECs), which contain a U6 promoter, followed by the sense strand, a loop, the antisense strand and a terminator sequence. The shRNAs generated by this method are highly specific and efficient, and the suppression of gene expression is comparable to chemically synthesized 21-nt siRNA duplexes or an expression plasmid containing the same shRNA (Castanotto *et al.*, 2002; Gou *et al.*, 2003; Scherer *et al.*, 2004). SECs are, however, difficult to

transfect into cells. In addition to vector-expressed shRNA, effective RNAi-mediated gene silencing can also be obtained by transfecting cells with *in vitro*-transcribed shRNA (Wang *et al*., 2005; Vlassov *et al*., 2007) or synthetic shRNA (Kim *et al*., 2005; Siolas *et al*., 2005).

The use of viral vectors, such as retroviruses, lentiviruses and adenoviruses, has reportedly allowed shRNA delivery of hard-to-transfect cells. Adenoviruses and adeno-associated viruses (AAV) efficiently transduce many different cell types, including terminally differentiated cells, but they do not integrate into the host genome (Shen *et al.*, 2003; Zhao *et al.*, 2003). In contrast, stable integration of shRNA expression cassettes into the genome of host cells has been achieved by delivery via retroviruses (Brummelkamp *et al.*, 2002b; Liu *et al.*, 2004; Schuck *et al.*, 2004) or lentiviruses (Qin *et al.*, 2003; Rubinson *et al.*, 2003; Zinke *et al*., 2009). Lentivirus-mediated delivery has the added advantages of integration into the genome of non-dividing cells, it can accommodate relatively large sequences of transgenes and is less toxic than adenoviral-mediated transduction (Manjunath *et al*., 2009; Moore *et al*., 2010). Disadvantages associated with retroviral systems include the potential for insertional mutagenesis of chromosomal genes and the possibility of mutations in the shRNA expression cassette due to error-prone viral reverse transcriptase (Hacein-Bey-Abina *et al.*, 2003). Furthermore, both lentivirus and retrovirus delivery systems have been reported to induce the interferon response, resulting in non-specific gene silencing (Bridge *et al*., 2003; Fish and Kruithof, 2004).

Although plasmid- and viral vector-based constitutive expression of shRNAs frequently results in stable and efficient suppression of target genes, the inability to adjust levels of suppression has imposed limitations in the analysis of essential genes. To overcome this obstacle, regulated or inducible vector-based shRNA expression systems have been developed (Wadhwa *et al.*, 2004; Wiznerowicz *et al*., 2006). To date, several Pol III-inducible systems have been reported (van de Wetering *et al.*, 2003; Czauderna *et al.*, 2003b; Gupta *et al*., 2004; Heinonen *et al*., 2005), and inducible Pol II systems also exist (Unwalla *et al*., 2004; Chen *et al*., 2007). A disadvantage of inducible promoters is that the inducer/repressor must be co-expressed in the cells targeted by the shRNA. However, vectors that harbor both the inducible promoter and repressor genes have been developed (Aagaard *et al*., 2007; Gray *et al*., 2007).

1.5.2.3 Specificity of siRNA

A critical assumption in RNAi-based approaches to study gene function is that RNAi is sequence-specific and that the siRNA will selectively inhibit the homologous gene only. The siRNAs are designed to be perfectly complementary to their targets, and it has been reported that mismatches of more than 1 to 2 nt between the antisense strand of the siRNA and the target mRNA could abolish siRNA activity (Tuschl *et al*., 1999; Elbashir *et al*., 2001b; 2001c; Chiu and Rana, 2002). It has also been reported that, depending on the position of the mismatch, siRNA activity is affected to different extents (Jackson *et al*., 2003; Du *et al*., 2005; Ge *et al*., 2010). Single mutations within the centre of a siRNA duplex appears to be more discriminating than mutations located at the 5'- and 3'-ends (Amarzguioui *et al*., 2003; Czauderna *et al*., 2003a), and in some cases there is enough activity left to mediate significant gene silencing (Holen *et al*., 2002; Miller *et al*., 2003).

Several reports have indicated that siRNAs and shRNAs can silence expression of genes other than the intended target gene. The sequence-specific silencing of non-target genes, *e.g.* those involved in diverse cellular functions, has been observed and attributed to the cross-hybridization of transcripts containing regions of partial homology with the siRNA sequence (Jackson *et al*., 2003). Off-target silencing effects have been demonstrated in transcripts with complementarity as low as 7 nt with the siRNA guide strand (Lin *et al*., 2005). Base-pairing between the hexamer seed region of a siRNA guide strand (nt 2-7) and complementary sequences in the 3' UTR of mature transcripts has been implicated as an important element in off-target gene silencing and false positive phenotypes (Doench *et al*., 2003; Jackson *et al*., 2006; Anderson *et al*., 2008). In addition, some studies have reported that siRNAs, as well as shRNAs produced from plasmid and lentiviral vectors, may induce the interferon pathway (Bridge *et al*., 2003; Sledz *et al*., 2003; Kariko *et al*., 2004a; 2004b). However, these effects were shown to be concentration dependent and could be overcome by using the lowest effective dose of siRNAs or shRNA-encoding vectors. Notably, more recently, it was reported that siRNAs of 19-bp in length, even when used at a high concentration, do not up-regulate PKR, while longer siRNAs (23-27 nt) are capable of inducing the PKR-dependent type I IFN response and upregulating OAS2 in a concentration-dependent manner (Reynolds *et al*., 2006).

1.5.3 Application of RNAi to viruses with a segmented dsRNA genome

Since the initial report by Elbashir *et al.* (2001a), whom identified RNAi activity in mammalian cells, numerous publications have subsequently described the use of RNAi to inhibit viruses from diverse virus families (Ketzinel-Gilad *et al.*, 2006; Stram and Kuzntzova, 2006; Kanzaki *et al.*, 2008; Csorba *et al.*, 2009). However, despite its impact in probing gene function, there have been only a few studies exploring the potential for RNAi approaches to members of the *Reoviridae* family and these have focused mostly on rotaviruses. RNAi has been used to study *in vivo* the role of both structural proteins (Déctor *et al.*, 2002; López *et al.*, 2005a; Ayala-Breton *et al.*, 2009) and non-structural proteins (Campagna *et al.*, 2005; López *et al.*, 2005b; Cuadras *et al.*, 2006; Montero *et al.*, 2006), and more recently to study the importance of different heat shock proteins (Broquet *et al.*, 2007; Dutta *et al.*, 2009) and endosomal chaperones (Maruri-Avidal *et al.*, 2008) on the morphogenesis of rotavirus infectious particles. Although RNAi has also been applied to reoviruses with the aim of understanding the function of reovirus proteins associated with the formation of viral inclusions (Kobayashi *et al.*, 2006; Carvalho *et al.*, 2007; Kobayashi *et al.*, 2009), there is a paucity of RNAi-based studies undertaken on orbiviruses.

With the exception of studies performed by Wirblich *et al.* (2006), illustrating the importance of the cellular Tsg101 protein in BTV release, and Forzan *et al.* (2007), illustrating that the clathrin-AP2 adaptor complex is required for host cell internalization of BTV, only one other study has reported the use of RNAi to silence orbivirus gene expression. Specifically, siRNAs were used to silence expression of the VP7 gene of AHSV, which encodes for a structural protein required for stable capsid assembly (Stassen *et al.*, 2007). These studies nevertheless indicate that RNAi can be an important genetic tool for the study of orbiviruses and for the analysis of specific viral genes important for orbivirus biology.

1.6 APOPTOSIS

Apoptosis is a physiological process of controlled cell suicide in response to a variety of stimuli (Kerr *et al*., 1972) and is important for maintaining homeostasis (Elmore, 2007), organ and tissue remodeling (Penaloza *et al*., 2006), cellular proliferation and differentiation (Lamkanfi *et al*., 2007), and cell fate determination (Kumar, 2007; Chowdhury *et al.*, 2008). The induction of apoptosis by viruses is thought to contribute to the tissue injury associated with their

pathogenesis (Callus and Vaux, 2007; Galluzzi *et al*., 2008; Clarke and Tyler, 2009). Knowledge regarding the viral processes and/or proteins that underlie apoptosis induction in infected cells may therefore not only provide a window on critical molecular events in the cell, but also enable the development of new antiviral agents. Since induction of apotosis following infection of susceptible host cells with AHSV is a focus of this investigation, the molecular mechanisms of apoptosis, a form of cell death that is mediated by caspases, will be discussed in the following sections.

1.6.1 Caspases

A caspase-cascade system plays a central role in the induction, transduction and amplification of intracellular apoptotic signals (Jin and El-Deiry, 2005; Duprez *et al*. 2009). Caspases belong to a family of highly conserved aspartate-specific cysteine proteases and are members of the interleukin-1β-converting enzyme family (Alnemri *et al*., 1996). They exist as inactive precursors, called procaspases, consisting of a large internal domain (p20; 17-21 kDa) that contains the catalytic subunit, a small C-terminal domain (p10; 10-13 kDa) and a death domain (DD; 3-24 kDa) (Chowdhury *et al*., 2008). An aspartate cleavage site seperates the DD from the internal domain, and an interdomain linker, containing one or two aspartate cleavage sites, separates the internal and C-terminal domains (Li and Yuan, 2008). The DD is involved in the transduction of apoptotic signals (Martinon *et al*., 2001; Weber and Vincenz, 2001) and has two subdomains, the death effector domain (DED) and the caspase-recruitment domain (CARD) (Fesik, 2000). Upon receiving an apoptotic signal, the inactive procaspases undergo two proteolytic processing events at specific aspartic acid residues to generate two subunits that comprise the active enzyme (Fuentes-Prior and Salvesen, 2004). Active caspases are thus present in a tetramer, comprising two large and two small subunits as heterodimers ($p20_2$-$p10_2$) (Sattar *et al*., 2003; Schweizer *et al*., 2003; Bao and Shi, 2007).

Apoptotic caspases (initiator and executioner caspases) play key roles in the execution of apoptosis (Yuan *et al*., 1993; Duprez *et al*., 2009). The initiator caspases contain a long DD (>90 amino acids) with either DED (caspase-8 and -10) or CARD (caspase-2 and -9) domains, which mediate recruitment of the procaspase to specific death signaling complexes. Initiator caspases are subsequently autocatalytically activated by a mechanism termed ‘proximity-induced’

activation (Degterev *et al*., 2003). Effector or executioner caspases (caspase-3, -6 and -7) contain short DD (20-30 amino acids) and their activation requires cleavage by activated initiator caspases (Degterev *et al*., 2003; Fuentes-Prior and Salvesen, 2004; Bao and Shi, 2007). Executioner caspase targets include cellular and nuclear structural proteins, DNA metabolism and repair proteins (PARP, DNA-PKcs, Rad51, DNA-replication protein, DNA topoisomerases, RNA polymerase), cell-cycle related proteins and endonuclease inhibitors (Jin and El-Deiry, 2005; Timmer and Salvesen, 2007; Li and Yuan, 2008). The cleavage of several of these substrates by executioner caspases contributes to some of the morphological and biochemical changes associated with apoptosis (Kerr *et al*., 1972; Wyllie *et al*., 1981; Earnshaw, 1995; Martelli *et al*., 2001).

1.6.2 Caspase signaling pathways

The two major pathways to caspase activation are indicated in Fig. 1.4, and are referred to as the mitochondria-mediated pathway (intrinsic pathway) and the death receptor-mediated pathway (extrinsic pathway) (Jin and El-Deiry, 2005; Xu and Shi, 2007; Duprez *et al*., 2009).

1.6.2.1 The intrinsic pathway

In the intrinsic pathway, apoptotic stimuli (cytotoxic stress, oxidative stress, heat shock and DNA damage) trigger internal sensors, such as the tumor suppressor protein p53, which induces BH3-only domain proteins (such as Bid) to translocate from the cytosol to the mitochondria (Wang *et al*., 1996). Bid binds to the proapoptotic protein Bax and facilitates its assembly into the pores of the outer mitochondrial membrane, resulting in permeabilization of the mitochondrial outer membrane (Wang *et al*., 1996; Desagher *et al*., 1999; Korsmeyer *et al*., 2000). Intermembrane space proteins, such as cytochrome c and the second mitochondria-derived activator of caspase (Smac), also known as DIABLO, are released from the mitochondrial intermembrane space to the cytosol (Finkel, 2001; Chowdhury *et al*., 2006; Chipuk and Green, 2008). Cytochrome c binds to the WD40 domains of cytosolic, monomeric apoptotic protease activating factor-1 (Apaf-1), resulting in oligomerization of Apaf-1 and formation of the apoptosome complex (Acehan *et al*., 2002; Riedl and Salvesen, 2007). Thereafter, the apoptosome binds to procaspase-9, via the caspase recruitment domains in Apaf-1, and activates caspase-9 by dimerization and

autocleavage (Hu *et al*., 1998; Acehan *et al*., 2002). Caspase-9 subsequently cleaves and activates the effector caspases (caspase-3 and -7), which are also recruited by the apoptosome (Boatright *et al*., 2003). While cytochrome c activates Apaf-1, Smac/DIABLO relieves the inhibition on caspases by binding to and neutralizing the inhibitory activity of inhibitor of apoptosis proteins (IAPs) (Du *et al*., 2000; Verhagen *et al*., 2000; Ekert *et al*., 2001). Phosphatidylserine, on the inside of the plasma membrane, is peroxidized by cytosolic cytochrome c and exported to the outer leaflet of the plasma membrane where it provides a signal to phagocytes (Jiang *et al*., 2003; Brown and Borutaite, 2008). The cells are subsequently cleared by phagocytosis and degraded by lysosomal enzymes (Wu *et al*., 2006).

1.6.2.2 The extrinsic pathway

The extrinsic cell death pathways are initiated by death receptors of the tumor necrosis factor (TNF) family. The TNF-receptor (TNFR) superfamily has three main members, namely (i) Fas and Fas ligand (FasL) (Itoh *et al*., 1991; Suda *et al*., 1993), (ii) "death receptors" (DR4 and DR5) and TNF-related apoptosis inducing ligand (TRAIL) (Wiley *et al*., 1995; Pitti *et al*., 1996), and (iii) TNFa and the TNF receptor (TNF-R1) (Tartaglia *et al*., 1993; Krammer, 1998). Ligation of the death receptor results in the formation of the death-inducing signaling complex (DISC) that activates caspase-8 (Boatright *et al*., 2003). The processing of procaspase-8 includes two cleavage events, firstly between the protease domains, and thereafter between the DD and the large protease subunit (Scaffidi *et al*., 1997; Chang *et al*., 2003). Both cleavage products remain bound to the DISC, where an active caspase-8 heterotetramer is formed. The active caspase-8 heterotetramer is then released to the cytosol and triggers apoptosis. Although procaspase-10 is also activated at the DISC, to form an active heterotetramer, its function remains unclear (Kischkel *et al*., 2001; Sprick *et al*., 2002; Takahashi *et al*., 2006). Although the activation of caspase-8 by the DISC may be sufficient to induce the activation of downstream effector caspases, in cells with an insufficient amount of activated caspase-8, however, death receptor and mitochondrial apoptosis may cross-interact by a mitochondrial amplification step. This step involves caspase-8 cleavage of the Bid protein to generate tBid (Li *et al*., 1998; Luo *et al*., 1998), and tBid-mediated release of cytochrome c from the mitochondria to the cytosol (Korsmeyer *et al*., 2000). Subsequent activation of caspase-9 and caspase-3 amplifies the original signal (Luo *et al*., 1998; Li *et al*., 2002).

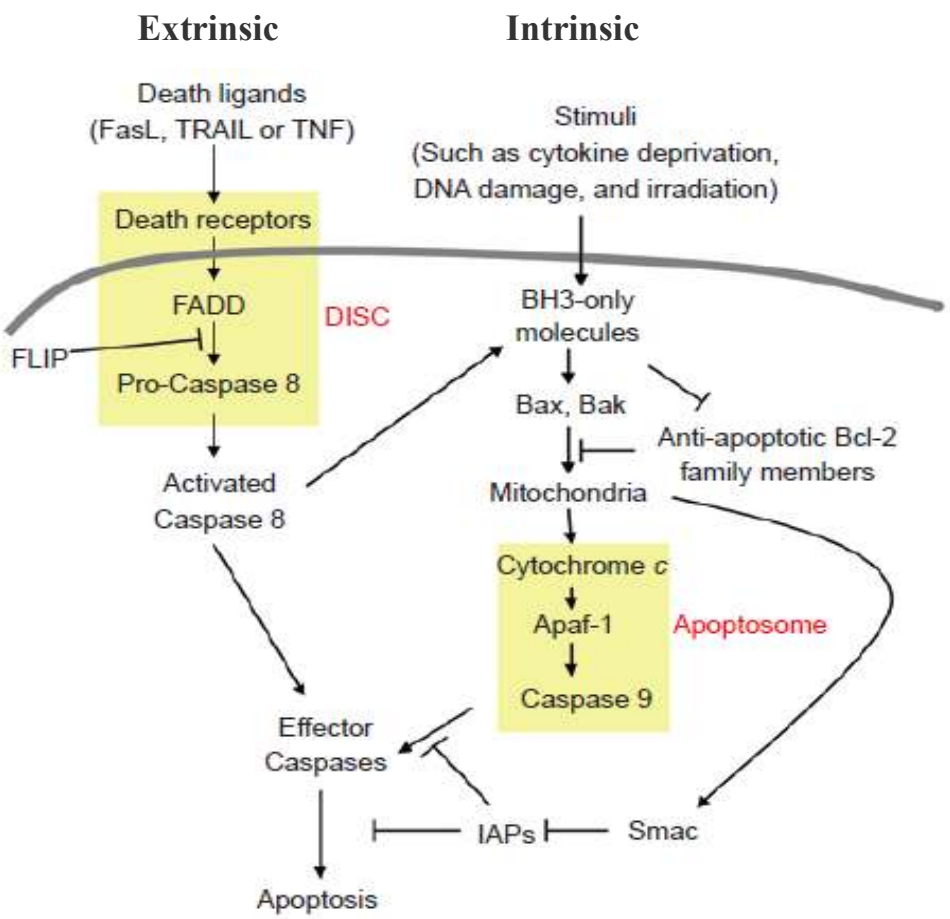

Fig. 1.4 **Schematic diagram of the extrinsic and intrinsic apoptotic signaling pathways (Xu and Shi, 2007).** The extrinsic pathway is triggered by the binding of death ligands to their death receptors, resulting in the formation of the death-inducing signaling complex (DISC), which allows the activation of caspase-8 and/or caspase-10. In the intrinsic pathway, the loss of mitochondrial transmembrane potential results in the release of cytochrome c and DIABLO from the mitochondrial intermembrane space to the cytosol. Cytochrome c forms an apoptosome complex with Apaf-1 and procaspase-9, thereby activating the latter. The initiator caspases in both pathways are responsible for activating the executioner caspases (caspase-3, -6 and -7), which execute the apoptosis process.

1.6.3 Regulation of apoptosis and caspase activation

In the death receptor-mediated apoptosis pathway, the expression of ligands for death receptors, as well as the expression of death receptors, is regulated (Chen and Wang, 2002). In addition, FLICE-like inhibitory proteins (FLIPs) are well-known inhibitors of death receptor-induced apoptosis (Yeh *et al*., 2000; Golks *et al*., 2005). Moreover, Fas-mediated apoptosis is controlled by a host of regulators of the mitochondrial cell death pathway, as described below.

The mitochondrial apoptosis pathway is regulated by Bcl-2 family members and inhibitor of apoptosis proteins (IAPs). The Bcl-2 family is divided into one anti-apoptotic group and two proapoptotic groups. Anti-apoptotic members of the Bcl-2 family of proteins, such as Bcl-2 (Vaux *et al*., 1988), Bcl-xL (Boise *et al*., 1993), Bcl-w (Gibson *et al*., 1996), Bcl-B (Ke *et al*., 2001), and Mcl-1 (Kozopas *et al*., 1993), predominantly prevent mitochondrial changes, and share three or four Bcl-2 homology (BH) domains. One group of the proapoptotic Bcl-2 family members, such as Bax (Oltvai *et al*., 1993) and Bak (Kiefer *et al*., 1995), contain two or three BH domains. The second group of proapoptotic Bcl-2 family members shares only the BH3 domain and includes, amongst other, Bad (Yang *et al*., 1995) and Bid (Wang *et al*., 1996). Bax and Bak activation is triggered by BH3-only proteins, and permeabilize the outer membrane of mitochondria by forming size-indeterminate openings in the outer mitochondrial membrane, resulting in release of proapoptotic factors such as cytochrome c (Wolter *et al*., 1997; Murphy *et al*., 2000). This activation of Bax and Bak is inhibited by the anti-apoptotic Bcl-2 family proteins. The anti-apoptotic protein Bcl-2 converges on mitochondria and competes with proapoptotic Bax to regulate the release of cytochrome c in response to an apoptotic signal (Gross *et al*., 1999; Danial and Korsmeyer, 2004). However, activated BH3-only proteins, such as Bid, can suppress the capacity of Bcl-2 to inhibit apoptosis by interacting with it to displace and subsequently activate Bax (Letai *et al*., 2002; Kuwana *et al*., 2005).

Apoptosis is also regulated at the level of the apoptosome, and at each of the subsequent activated caspases. Caspase activity can be modulated by caspase-binding proteins of the inhibitor of apoptosis protein (IAP) family (Duckett *et al*., 1996; Uren *et al*., 1996; Clarke and Clem, 2003). The overexpression of IAP family proteins inhibits apoptosis induced by Bax and other pro-apoptotic Bcl-2 family proteins (Deveraux and Reed, 1999). The IAPs are characterized by a

novel domain of 70-80 amino acids, termed the baculoviral IAP repeat (BIR) (Birnbaum *et al*., 1994; Rothe *et al*., 1995; Uren *et al*., 1998; Shi, 2002). All members of the family contain one to three N-terminal BIR domains, which bind to the surface of caspases and block the catalyzing grooves of caspases. Whereas BIR3 interacts with and inhibits the activity of caspase-9 (Johnson and Jarvis, 2004), the linker region between BIR1 and BIR2 targets and inhibits both caspase-3 and caspase-7 (Deveraux *et al*., 1997; Roy *et al*., 1997; Deveraux and Reed, 1999). In the mitochondrial pathway, XIAP, c-IAP1 and c-IAP2 bind directly to procaspase-9 and prevent its activation (Deveraux *et al*., 1998). IAPs also inhibit the extrinsic apoptotic pathway by modulating caspase activity (Deveraux *et al*., 1997; Roy *et al*., 1997; Deveraux *et al*., 1998). Although most IAPs bind and directly suppress caspase catalytic activity, some of them function to downregulate caspase expression by acting as E3 ligases for their ubiquitination and degradation (Suzuki *et al*., 2001). IAPs themselves are negatively regulated by IAP antagonists, which share a highly conserved IAP binding motif and function as proapoptotic proteins (Pronk *et al*., 1996; Zhou *et al*., 2005). Caspase activity can also be regulated by post-translational modification, such as nitrosylation, oxidation, ubiquitination and phosphorylation (Jin and El-Deiry, 2005). In addition, many signaling pathways, such as nuclear factor-kappaβ (NF-κβ) (Wertz and Dixit, 2010), p53 (Chowdhury *et al*., 2006), mitogen-activated protein kinases (MAPKs)/c-Jun N-terminal kinases (JNKs) (Papadakis *et al*., 2006), as well as phosphatidylinositol 3-kinase (PI3K) and its downstream kinase effector Akt (Osaki *et al*., 2004), are all able to regulate caspase activation and apoptosis.

1.6.4 Viruses and apoptosis

In virus-infected cells, the induction of apoptosis may represent an antiviral mechanism used to limit viral replication and reduce the viral population (Benedict *et al*., 2002). Therefore, in order to maximize virus progeny, viruses have evolved mechanisms to inhibit apoptosis of the host cell. Many viruses encode proteins that have been shown to suppress apoptosis (Lagunoff and Caroll, 2003; Fischer *et al*., 2007; Howie *et al*., 2009). Viral proteins can disrupt apoptosis by degrading p53 (Wang *et al*., 1995), activating the cell-survival pathways (Bagchi *et al*., 2010), controlling the release of cytochrome c by Bcl-2 family members (Sundararajan and White, 2001), or encoding orthologs of the anti-apoptotic regulator Bcl-2 (White, 1998). In addition, some viruses regulate death receptor signaling by producing neutralizing soluble TNF decoy receptors

(Reading *et al*., 2002), TRAILR2 orthologs (Brojatsch *et al*., 1996), viral FLICE (Bertin *et al*., 1997) or by modulating cell surface amounts of Fas (Shisler *et al*., 1997) and TRAIL (Benedict *et al*., 2001). Caspase inhibitors, such as the cowpox and vaccinia virus CrmA protein (Renatus *et al*., 2000; Stennicke *et al*., 2002), and the baculovirus p35 and p49 proteins (Xu *et al*., 2001; Clem, 2007) bind to the caspase active sites, forming an irreversible stable complex.

Viruses can also induce apoptosis to facilitate the spread of viral progeny to neighboring cells, while evading host inflammatory responses (O'Brien, 1998; Roulston *et al*., 1999). In this regard, virions have been shown to be associated with the apoptosome, which aids in their dissemination and protect progeny virions from the host immune response (Barton *et al*., 2001; Mi *et al*., 2001; Hay and Kannourakis, 2002; Courageot *et al*., 2003). Apoptosis induction can often be ascribed to specific viral proteins. A virus protein, such as the influenza virus NS1 protein, may often exhibit both anti- and proapoptotic activities. In these instances, cells are initially protected from apoptosis to permit viral replication, and during later stages of infection, the spread of virus progeny to neighboring cells is facilitated by apoptosis induction (Lowy, 2003). In a further example, the adenovirus E1B 19K, E1B 55K, E3 14.7K and E3 10.4/14.5K proteins inhibit apoptosis, however, during late stages of infection, the protective effects of these proteins are overcome by the expression of the adenovirus death protein (ADP), that is required for efficient release of virus from infected cells (Schaack, 2005). Members of the *Reoviridae* family, including avian and mammalian reoviruses, BTV and rotaviruses, are known to induce apoptosis in infected cells and the induction of apoptosis is thought to contribute to the tissue injury associated with their pathogenesis (O'Donnell *et al*., 2005; Sato *et al*., 2006; Umeshappa *et al*., 2010).

1.7 AIMS OF THIS INVESTIGATION

From the review of the literature, it is evident that many aspects regarding AHSV replication, morphogenesis and release, as well as the role of individual viral proteins in these processes still need to be elucidated. This is especially true for the VP5 protein of AHSV. Apart from reports indicating that expression of VP5 in heterologous hosts is cytotoxic (du Plessis and Nel, 1997; Martinez-Torrecuadrada *et al*., 1999) and studies related to its immunogenicity (Martinez-

Torrecuadrada *et al*., 1996; 1999), no functional studies have been undertaken on the AHSV VP5 protein. Mapping the role of the VP5 protein in the virus replication cycle may benefit significantly through the use of RNAi technology, as it represents a potentially powerful tool to generate loss-of-function phenotypes that can facilitate investigations regarding virus gene function in the context of virus-infected cells (Wirblich *et al.*, 2006; Ayala-Breton *et al.*, 2009).

In contrast to other vertebrate-infecting members of the *Reoviridae* family, unraveling of the orbivirus replication cycle is complicated by their ability to replicate in both the vertebrate host and vector insect. Moreover, the effect of orbivirus replication in these distinct host types is markedly different. For AHSV and BTV, replication of the virus in insect cells results in persistent infection with no CPE, whilst infection of mammalian cells results in cell death (Osawa and Hazrati, 1965; Mirchamsy *et al*., 1970; Mortola *et al.*, 2004). For BTV, the data indicate that the virus induces apoptosis in mammalian cells by inducing caspase-dependent apoptotic pathways (Mortola *et al*., 2004; Nagaleekar *et al*., 2007). Whether the same holds true for AHSV has yet to be determined.

Therefore, based on the above, the aims of this investigation were the following:

1. To develop an RNAi assay whereby the *in vivo* functional role of the VP5 protein of AHSV can be investigated.

2. To determine which regions within the VP5 protein of AHSV is responsible for its membrane permeabilizing and cytotoxic effects.

3. To determine whether AHSV induces apoptosis and by which mechanism, following infection of mammalian and insect vector cells.

CHAPTER TWO

SILENCING OF AFRICAN HORSE SICKNESS VIRUS VP5 GENE EXPRESSION BY SHORT HAIRPIN RNA AND SMALL INTERFERING RNA IN MAMMALIAN CELLS

2.1 INTRODUCTION

African horse sickness virus (AHSV), a member of the *Orbivirus* genus in the family *Reoviridae*, is an arthropod-borne virus that causes disease in equids, and especially high mortality in horses (Coetzer and Erasmus, 1994; Guthrie, 2007). Like bluetongue virus (BTV), the prototype orbivirus, AHSV consists of two concentric protein layers that encapsidate the genome of ten double-stranded RNA (dsRNA) segments (Verwoerd *et al.*, 1972; Bremer *et al.*, 1990). The core particle is composed of two major (VP3 and VP7) and three minor (VP1, VP4 and VP6) structural proteins, and is surrounded by the outer capsid, composed of the two major structural proteins, VP2 and VP5 (Roy *et al.*, 1994b; Roy, 2008).

In the case of BTV, it has been reported that each of the two outer capsid proteins plays a role in virus entry. The outermost capsid protein VP2 is associated with cell binding and entry of virions (Hassan and Roy, 1999; Zhang *et al.*, 2010), whereas the less exposed VP5 protein is involved in cell permeabilization and translocation of the transcriptionally active core particles into the cytoplasm of infected cells (Hassan *et al.*, 2001; Forzan *et al.*, 2007) to initiate the transcription and, subsequently, the synthesis of viral proteins. In addition to their roles during the initial stages of infection, the VP2 protein has more recently been implicated in virus release from infected cells via its interaction with vimentin (Bhattacharya *et al.*, 2007), while VP5, through its interaction with membrane lipid rafts, is proposed to participate in docking of virus particles with the plasma membrane for assembly and/or egress (Bhattacharya and Roy, 2008). Moreover, it has been reported that extracellular treatment of mammalian cells with a combination of both VP2 and VP5 is sufficient to trigger apoptosis (Mortolla *et al.*, 2004). In contrast to BTV, the biological importance of the AHSV outer capsid proteins has not yet been investigated. The current investigation is therefore aimed at redressing this imbalance by focusing on the role of VP5 in the replication cycle of AHSV. It can be envisaged that a clearer understanding of the *in vivo* biological role of the VP5 protein may be obtained by observing phenotypic consequences resulting from its inactivation. In this regard, RNA interference (RNAi) can provide an investigative tool that may greatly facilitate studies aimed at generating such loss-of-function phenotypes. Indeed, this approach has been used successfully to investigate the role of different structural proteins in the rotavirus infectious cycle (Déctor *et al.*, 2002; López *et al*., 2005a; Ayala-Breton *et al.*, 2009).

RNA interference (RNAi) is a conserved gene silencing mechanism that recognizes dsRNA as a signal to trigger the sequence-specific degradation of homologous mRNA (Fire *et al*., 1998; Montgomery *et al.*, 1998). Biochemical and genetic studies in several experimental systems have indicated that dsRNA-induced gene silencing proceeds via a two-step mechanism. Initially, long dsRNA molecules are recognized and cleaved into 21-nt small interfering RNA duplexes (siRNAs) by the action of an endogenous dsRNA-specific endonuclease, Dicer, a member of the RNAse III family. Subsequently, the siRNAs are incorporated into the RNA-induced silencing complex (RISC), which identifies substrates through their homology to siRNAs and target these cognate mRNA for destruction (Hutvagner and Simard, 2008; Jinek and Doudna, 2009; Wang *et al.*, 2009). RNAi is commonly achieved by introducing chemically synthesized siRNA into cells or, alternatively, by short hairpin RNA (shRNA) that is expressed intracellularly from plasmid or viral vectors (Brummelkamp *et al.*, 2002a; 2002b; Shen *et al.*, 2003; Giering *et al.*, 2008; Moore *et al.*, 2010). The expressed shRNAs, bearing a fold-back stem-loop, are converted *in vivo* by Dicer into functional siRNAs.

As indicated above, the biological role of AHSV VP5 has not yet been investigated in any great detail. The segmented nature of the AHSV genome, however, makes it amenable to analysis by RNAi. RNAi technology is therefore well suited to silence expression of individual AHSV genes without affecting the expression of others, thus allowing for characterization of the function of proteins in the context of the whole virus (Wirblich *et al.*, 2006; Stassen *et al.*, 2007). Towards the long-term goal of elucidating the functional significance of VP5 in the AHSV infectious cycle, the primary aims of this part of the investigation were to develop and evaluate RNAi assays whereby expression of the VP5 gene of AHSV-9 could be silenced in mammalian cells. For this purpose, different VP5-directed shRNAs and siRNAs were designed, and their efficacy to inhibit VP5 gene expression was examined in Vero and BHK-21 mammalian cells.

2.2 MATERIALS AND METHODS

2.2.1 Bacterial strains and plasmids

The *Escherichia coli* strains were cultured in LB broth (1% [w/v] tryptone; 1% [w/v] NaCl; 0.5% [w/v] yeast extract; pH 7.4) (Sambrook and Russell, 2001) at 37°C with shaking at 200 rpm, and maintained at -70°C as glycerol cultures. For plasmid DNA selection and maintenance in *E. coli*, the culture medium was supplemented with 50 µg/ml of kanamycin (Roche Diagnostics). One Shot® TOP10 chemically competent *E. coli* cells and the shRNA delivery vector pENTR™/H1/TO were both obtained from Invitrogen.

2.2.2 Cell culture and viruses

Baby hamster kidney-21 (BHK-21; ATCC CL-10) and Vero (ATCC CL-81) cells were propagated and maintained as monolayers in 75 cm^2 tissue culture flasks, and cultured in Minimum Essential Medium (MEM) (Sigma-Aldrich) supplemented with 2.5% or 5% (v/v) fetal bovine serum (FBS) and antibiotics (60 mg/ml penicillin; 60 mg/ml streptomycin; 150 mg/ml Fungizone) (Highveld Biological). The flasks were incubated at 37ºC with a constant supply of 5% CO_2. African horse sickness virus serotype 9 (AHSV-9), used in virus challenge assays, was provided by Mr. Flip Wege (Department of Genetics, University of Pretoria). AHSV-9 was propagated in confluent BHK-21 monolayers using a low-passage stock virus as inoculum.

2.2.3 DNA oligonucleotides for shRNA construction

Oligonucleotides used to produce shRNAs targeting four distinct regions of the AHSV-9 VP5 mRNA (GenBank Acc. No. U74489) were designed with the RNAi Designer tool of Invitrogen (available at https://rnaidesigner.invitrogen.com). The RNAi Designer tool uses a proprietary algorithm to design shRNA sequences that are compatible for cloning into the pENTR™/H1/TO vector. The forward oligonucleotide was designed to incorporate the following features in the indicated order: a 5'-CACC sequence required to facilitate directional cloning, a transcription initiation site of the shRNA sequence at an adenosine or guanosine, a sense target sequence of 21 nt with low G+C-content (30-50%), a 5'-CGAA-3' loop sequence, followed by the 21-nt antisense target sequence. The complementary reverse oligonucleotide contained a 5'-AAAA sequence to facilitate directional cloning. To ensure that the target sequences did not contain

homology to other cellular and viral genes, they were compared to the entries of the GenBank database by making use of the BLAST-N program (Altschul *et al*., 1997) available on the National Centre for Biotechnology Information web page (http://www.ncbi.nlm.nih.gov/). A control non-silencing shRNA, designated shUNeg, was designed similarly by using a sequence that reportedly lacks homology to all known viral and cellular genes (Qiagen). The DNA oligonucleotides were supplied in lyophilized, desalted form and were each suspended in 1 × TE buffer (10 mM Tris-HCl; 1 mM EDTA; pH 7.6) at a concentration of 200 µM prior to storage at -20°C. The oligonucleotides used for shRNA construction are shown in Table 2.1 and were obtained from Integrated DNA Technologies.

2.2.4 Construction of recombinant pENTR™/H1/TO vectors

All molecular cloning techniques used in the construction of recombinant pENTR™/H1/TO shRNA delivery vectors were performed according to the procedures described by the supplier (Invitrogen). The plasmid constructs were confirmed by nucleotide sequencing.

2.2.4.1 Preparation of double-stranded DNA oligonucleotides

To prepare annealed oligonucleotide inserts for cloning, 5 µl of each the complementary forward and reverse oligonucleotides were mixed with 2 µl of 10 × Oligo annealing buffer (100 mM Tris-HCl; 10 mM EDTA; 1 M NaCl; pH 8.0) and DNase/RNase-free water was added to a final volume of 20 µl. Following incubation at 95°C for 4 min, the reaction mixtures were allowed to cool to room temperature and the annealed oligonucleotides were diluted to a final concentration of 5 nM. To confirm the presence of annealed oligonucleotides, an aliquot (5 µl) of each reaction mixture was analyzed on a 20% (w/v) polyacrylamide gel with 1 × TAE buffer (40 mM Tris-HCl; 20 mM NaOAc; 1 mM EDTA; pH 8.5) as the electrophoresis buffer (Sambrook and Russell, 2001). Electrophoresis was performed in a Hoefer Mighty Small™ SE260 electrophoresis unit for 2 h at 70 V. The gels were then stained for 30 min in 1 × TAE buffer supplemented with ethidium bromide (10 µg/µl) and examined on an UV transilluminator. Annealed double-stranded DNA oligonucleotides were sized according to their migration in the polyacrylamide gel as compared to that of a low-molecular-weight DNA ladder (New England Biolabs).

.

Table 2.1 VP5 target sites and sequences of oligonucleotides cloned into the pENTR™/H1/TO vector

Oligonucleotide	VP5 coding region targeted	DNA target sequence		Oligonucleotide sequence *
shVP5-148	148-168	5' - GGAGTAATGCAAGGAACAATT - 3'	Forward	5'- CACC**GGAGTAATGCAAGGAACAATT***CGAA***AATTGTTCCTTGCATTACTCC**-3'
			Reverse	5'-AAAAGGAGTAATGCAAGGAACAATTTTCGAATTGTTCCTTGCATTACTCC-3'
shVP5-651	651-671	5' - GCAGGAAATGTTGGATTTAAG - 3'	Forward	5'-CACC**GCAGGAAATGTTGGATTTAAG***CGAA***CTTAAATCCAACATTTCCTGC**-3'
			Reverse	5'-AAAAGCAGGAAATGTTGGATTTAAGTTCGCTTAAATCCAACATTTCCTGC-3'
shVP5-826	826-846	5' - GCGGATATCCACCCTCATATA - 3'	Forward	5'-CACC**GCGGATATCCACCCTCATATA***CGAA***TATATGAGGGTGGATATCCGC**-3'
			Reverse	5'-AAAAGCGGATATCCACCCTCATATATTCGTATATGAGGGTGGATATCCGC-3'
shVP5-1311	1311-1331	5' - GCATAAGAGAAGATTGCAACG - 3'	Forward	5'-CACC**GCATAAGAGAAGATTGCAACG***CGAA***CGTTGCAATCTTCTCTTATGC**-3'
			Reverse	5'-AAAAGCATAAGAGAAGATTGCAACGTTCGCGTTGCAATCTTCTCTTATGC-3'
shUNeg	None	None	Forward	5'-CACC**GTTCTCCGAACGTGTCACGTTT***CGAA***AAACGTGACACGTTCGGAGAA**-3'
			Reverse	5'-AAAATTCTCCGAACGTGTCACGTTTTTCGAAACGTGACACGTTCGGAGAAC-3'

* The sense and antisense shRNA target sequences are indicated in bold, loop sequences in italics, and the sequences required for directional cloning are indicated in red and blue.

2.2.4.2 Cloning of double-stranded DNA oligonucleotides

The pENTR™/H1/TO vector is supplied in a linear form with 4-nt 5' overhangs on each strand to facilitate cloning, as indicated in Fig. 2.1A. The annealed double-stranded DNA oligonucleotides (5 µl) were ligated to the pENTR™/H1/TO vector (1.5 ng) at room temperature for 2 h in a reaction mixture that contained 4 µl of 5 × Ligation Buffer (250 mM Tris-HCl [pH 7.6]; 50 mM $MgCl_2$; 25 mM ATP; 5 mM DTT; 25% [w/v] PEG-8000), 1 µl of T4 DNA Ligase (1 Weiss unit/µl) and DNase/RNase-free water to a final volume of 20 µl. One Shot® TOP10 chemically competent *E. coli* cells were subsequently transformed by mixing 50 µl of the cells with 2 µl of the ligation reaction mixture and the tubes were incubated on ice for 30 min. After a heat-shock at 42ºC for 30 s, the tubes were briefly incubated on ice and then 250 µl of pre-warmed (25ºC) SOC medium (2% [w/v] tryptone; 0.5% [w/v] yeast extract; 10 mM NaCl; 2.5 mM KCl; 10 mM MgCl; 210 mM $MgSO_4$; 20 mM glucose) was added. The transformation mixtures were incubated at 37ºC for 1 h with shaking (200 rpm). Aliquots of 20-100 µl were subsequently plated onto LB agar supplemented with kanamycin, and the agar plates were incubated overnight at 37ºC.

2.2.4.3 Plasmid DNA extraction and quantification

Plasmid DNA was extracted and purified using the Qiagen Plasmid Midi Kit (Qiagen) according to the manufacturer's instructions. A single bacterial colony was inoculated into 10 ml of selective LB medium and incubated at 37°C for 8 h with vigorous shaking (200 rpm). The starter culture was diluted 1:500 in 25 ml of selective LB medium and grown at 37°C for 16 h with vigorous shaking (200 rpm). Bacterial cells were harvested by centrifugation at 15 000 rpm for 15 min, and the cell pellet was suspended in 4 ml of Resuspension Buffer P1 (50 mM Tris-Cl [pH 8.0]; 10 mM EDTA; 100 µg/ml RNase A), followed by addition of 4 ml of Lysis Buffer P2 (200 mM NaOH; 1% [w/v] SDS). Following incubation at room temperature for 5 min, 4 ml of chilled Neutralization Buffer P3 (3 M KOAc; pH 5.5) was added and the suspension was incubated on ice for 15 min. The lysate was subsequently added to a DNA-binding column, washed twice with 10 ml of Buffer QC (1 M NaCl; 50 mM MOPS [pH 7.0]; 15% [v/v] isopropanol), and the DNA was eluted in 5 ml of Buffer QF (1.25 M NaCl; 50 mM Tris-Cl [pH 8.5]; 15% [v/v] isopropanol). Plasmid DNA was precipitated by addition of 0.7 volumes of isopropanol and recovered by centrifugation at 15 000 rpm for 30 min. The DNA pellet was

washed with 70% ethanol, vacuum-dried and suspended in 100 µl of UHQ water. The plasmid DNA concentration and purity was determined with a NanoDrop® ND-1000 spectrophotometer and ND-1000 v.3.3 software (NanoDrop Technologies, Inc.).

2.2.4.4 Nucleotide sequencing

The presence and integrity of the cloned double-stranded DNA oligonucleotide inserts was determined using the ABI-PRISM® BigDye™ Terminator v.3.1 Cycle Sequencing Ready Reaction kit (Perkin-Elmer Applied Biosystems) according to the instructions of the manufacturer. Oligonucleotides H1 forward (5'-TGTTCTGGGAAATCACCATA-3') and pUC/M13 reverse (5'-CAGGAAACAGCTATGAC-3') were used in the sequencing reactions. Each sequencing reaction contained 60-100 ng of purified template DNA, 2 µl of BigDye™ Terminator Ready Reaction mix, 2 µl of 5 × BigDye™ Terminator Sequencing buffer, 10 pmol of sequencing oligonucleotide and UHQ water to a final volume of 10 µl. Cycle sequencing reactions were performed in a GeneAmp® 2400 thermal cycler (Applied Biosystems) with 25 of the following cycles: denaturation at 96ºC for 30 s, annealing at 50ºC for 15 s and extension at 60ºC for 4 min. The extension products were subsequently precipitated by addition of 34.5 µl of UHQ water, 3 µl of 3 M NaOAc (pH 4.6) and 62.5 µl of filter-sterilized absolute ethanol. The tubes were incubated at room temperature in the dark for 15 min, centrifuged at 15 000 rpm for 30 min and the supernatant carefully aspirated. The pellet was rinsed with 250 µl of 70% ethanol, vacuum-dried and stored at -20ºC until required. Prior to electrophoresis, the purified extension products were suspended in 3 µl of sequencing loading buffer, denatured at 95ºC for 2 min and loaded onto an ABI PRISM® Model 377 DNA sequencer. Nucleotide sequences were analyzed with BioEdit Sequence Alignment Editor v.5.0.6. (Hall, 1999) software.

2.2.5 Short hairpin RNA (shRNA)-mediated silencing of AHSV-9 VP5 gene expression in Vero cells

2.2.5.1 Generation of stably transfected Vero cell lines

A kill curve experiment was initially performed to determine the minimum concentration of Zeocin™ (Invitrogen) required to kill untransfected Vero cells within two weeks of incubation. For this purpose, cells were seeded in 6-well tissue culture plates (Nunc) at *ca.* 20% confluency and cultured in the presence of different concentrations of Zeocin™, ranging from 50 to 1000

µg/ml. The tissue culture plates were incubated at 37°C in a CO_2 incubator for two weeks and the selective medium was replenished every 72 h. An untreated Vero cell monolayer was included in the analysis as a positive control for cell viability. The cells were examined daily by microscopy to monitor cell viability, the results of which indicated that the minimum concentration of Zeocin™ required to kill 100% of the Vero cells within two weeks was 600 µg/ml.

To select for stable transfectants, Vero cells were seeded in 35-mm-diameter wells to reach 80% confluency within 12 h of incubation in a CO_2 incubator. The cells were transfected with purified recombinant pENTR™/H1/TO plasmid DNA using Lipofectamine™ 2000 (Invitrogen) according to the manufacturer's instructions. For each transfection, 4 µg of purified plasmid DNA and 10 µl of the Lipofectamine™ 2000 reagent were separately diluted in 250 µl of incomplete MEM medium (lacking FBS and antibiotics). Following incubation at room temperature for 5 min, the two solutions were mixed and then incubated at room temperature for 20 min to allow the formation of DNA-lipofectamine complexes. Prior to transfection the medium was aspirated and the cells were rinsed three times with 2 ml of incomplete MEM medium. The cells were overlaid with the DNA-lipofectamine complexes and following addition of 1.5 ml of MEM medium supplemented with 2.5% (v/v) FBS, the tissue culture plates were incubated at 37°C in a CO_2 incubator. At 24 h post-transfection, plasmid DNA-transfected Vero cells were trypsinized and replated into a 25 cm^2 tissue culture flask containing 5 ml of selective MEM medium (containing 5% [v/v] FBS, antibiotics and 600 µg/ml Zeocin™). Untransfected Vero cell monolayers grown in the presence of Zeocin™ were included as controls to determine the efficiency of the transfection, while monolayers grown in the absence of Zeocin™ were used to monitor cell viability. The cells were incubated at 37°C in a CO_2 incubator and the selective medium was replenished every 72 h until the untransfected control cells died completely. Zeocin™-resistance colonies were expanded into 75 cm^2 cell culture flasks containing 10 ml of selective MEM medium. Stable cell lines were maintained as monolayers in 75 cm^2 cell culture flasks and propagated in selective MEM medium for three further generations. For long-term storage in liquid nitrogen, the stable Vero cell lines were frozen in MEM containing 20% (v/v) FBS, antibiotics and 10% (v/v) DMSO.

2.2.5.2 Viral challenge assay

The stable Vero cell lines were trypsinized, diluted in selective MEM medium and seeded in 6-well tissue culture plates (Nunc) to reach 80% confluency (*ca.* 9.6×10^5 cells/well) within 12 h of incubation at 37°C in a CO_2 incubator. The cell monolayers were rinsed twice with incomplete MEM medium and then infected with AHSV-9 at a multiplicity of infection (MOI) of 2 PFU/cell, 1 PFU/cell or 0.5 PFU/cell. Following virus infection at room temperature for 2 h, the virus inoculum was removed and 2 ml of selective MEM medium was added. At 24 h post-infection, cells were processed for quantitative real-time PCR analysis as described below (Section 2.2.7).

2.2.6 Small interfering RNA (siRNA)-mediated silencing of AHSV-9 VP5 gene expression in BHK-21 cells

2.2.6.1 siRNAs

siRNAs targeting three different regions of the AHSV-9 VP5 mRNA were designed with the siRNA application module of the Sfold 2.0 application server available at the Wadsworth Center, New York State Department of Health (http://sfold.wadsworth.org). This application module is used to predict target site accessibility and to determine the RNA duplex thermodynamics for rational siRNA design. Target regions were selected that had the highest total siRNA duplex score, calculated using the sum of the target accessibility score [0; 8], duplex feature score [-2; 10] and duplex thermodynamics score [0; 2]. Selected siRNA duplexes had a target accessibility score of ≥ 4, a duplex feature score of ≥ 6, a duplex thermodynamics score of 2 and G+C-content between 30 and 50%. The asymmetry rule of Schwarz *et al*. (2003) was enforced by DSSE (differential stability of siRNA duplex ends) and was > 0 kcal/mol. The rule of relative instability at the cleavage site (nt 9-14) was enforced by AIS (average internal stability) and was > -8.6 kcal/mol (Khvorova *et al*., 2003). The siRNA sequences were subjected to a BLAST-N search against entries in the GenBank database to ensure lack of sequence homology to sequences other than the intended target gene. The siRNAs were supplied by Ambion, whereas a control non-silencing siRNA, designated siUNeg, was obtained from Qiagen. The siRNAs were supplied as lyophilized, desalted duplexes and were suspended in RNAse-free UHQ water at a concentration of 100 µM prior to storage at -20°C. The siRNAs used in this study are shown in Table 2.2.

Table 2.2 Target sites, as well as sense and antisense sequence of siRNAs directed against AHSV-9 VP5 mRNA

siRNA	Coding region	DNA target sequence	siRNA sequence *	G+C-content	AHSV-9 gene
siVP5-138 (Sense)	138-156	5' - GGCGATAGATGGAGTAATG - 3'	5' - GGCGAUAGAUGGAGUAAUGdTT - 3'	43%	VP5
siVP5-138 (Antisense)	138-156	5' - GGCGATAGATGGAGTAATG - 3'	5' - CAUUACUCCAUCUAUCGCCdTT - 3'	43%	VP5
siVP5- 528 (Sense)	528-546	5' - CCAAACGGAAGAGGATTTA - 3'	5' - CCAAACGGAAGAGGAUUUAdTT - 3'	38%	VP5
siVP5- 528 (Antisense)	528-546	5' - CCAAACGGAAGAGGATTTA - 3'	5' -UAAAUCCUCUUCCGUUUGGdTT - 3'	38%	VP5
siVP5- 984 (Sense)	984-1002	5' - GGAATACGAAAAGCATGAT - 3'	5' - GGAAUACGAAAAGCAUGAUdTT - 3'	33%	VP5
siVP5- 984 (Antisense)	984-1002	5' - GGAATACGAAAAGCATGAT - 3'	5' - AUCAUGCUUUUCGUAUUCCdTT - 3'	33%	VP5
siUNeg (Sense)	None	None	5' - UUCUCCGAACGUGUCACGUdTT - 3'	48%	None
siUNeg (Antisense)	None	None	5' - ACGUGACACGUUCGGAGAAdTT - 3'	48%	None

* The AHSV-9 VP5 open reading frame was selected as the targeted region, avoiding regions within 100 nt from the initiation and termination codons. The siRNA was 21 nt in length, with the sequence motif 5'-(N_{19})TT-3', consisting of a 19-nt duplex RNA and 2-nt deoxythymidine 3'-end overhangs. Target regions with a G+C-content between 30-50% were selected. The rule of relative instability at the cleavage site (nt 9-14) and asymmetry rule was enforced by AIS > -8.6 kcal/mol and DSSE > 0 kcal/mol, respectively.

2.2.6.2 Viral challenge assay

BHK-21 cells were transfected with the respective siRNAs, as described previously (Burger, 2006). BHK-21 cells were seeded in 35-mm-diameter wells to reach 80% confluency within 12 h of incubation at 37ºC in a CO_2 incubator. The BHK-21 cells were then transfected with the respective siRNAs using Lipofectamine™ 2000 (Invitrogen). Briefly, 10 µl of Lipofectamine™ 2000 reagent was diluted in 250 µl of incomplete MEM medium and, following incubation at room temperature for 5 min, was added to 250 µl of incomplete MEM medium containing 200 pmol of the appropriate siRNA. The mixture was then incubated at room temperature for 20 min to allow formation of RNA-lipofectamine complexes. The cell monolayers were rinsed three times with 2 ml of incomplete MEM medium and overlaid with the RNA-lipofectamine complexes. Following addition of 1.5 ml of MEM medium containing 5% (v/v) FBS, the tissue culture plates were incubated at 37ºC in a CO_2 incubator. At 8 h post-transfection, the cells were infected with AHSV-9 at a MOI of 1 PFU/cell. A second transfection was performed after 2 h of infection, as described above, and the tissue culture plates were incubated for a further 24 h. AlexaFluor488-labelled siRNA (Allstars Negative Alexafluor488-siRNA; Qiagen) was used to assay for transfection efficiency, and, under the experimental conditions used in this study, typically resulted in the transfection of 80-90% of the BHK-21 cells. Following incubation, the cells were processed for quantitative real-time analysis.

2.2.7 Quantitative real-time polymerase chain reaction (real-time PCR)

2.2.7.1 Oligonucleotides

Quantification of specific mRNA by real-time PCR was performed using oligonucleotides based on the sequence of the AHSV-9 VP5 gene (GenBank Acc. No. U74489), and the β2-microglobulin (β2-MG) gene for Vero (GenBank Acc. No. AY570381) and BHK-21 (GenBank Acc. No. X17002) cells. The amplicons were 121, 138 and 101 bp in size, respectively. The oligonucleotides were designed with Primer3 (Rozen and Skaletsky, 2000) and DNAMAN v.4.13 (Lynnon Biosoft) software programs, while optimal oligonucleotide pairs were analyzed by PerlPrimer v.1.1.6 (Marshall, 2004). The target sequence specificity of each newly designed oligonucleotide pair was verified by a BLAST-N search against entries in the GenBank database. The oligonucleotides, indicated in Table 2.3, were obtained from Integrated DNA Technologies.

Table 2.3 Oligonucleotides used in quantitative real-time PCR

Primer	Nucleotide sequence	Tm (°C)	Annealing position	Target mRNA
RT-VP5F	5' - GAAAGCGCTAAAGGGCATGCTG - 3'	67	456-477	AHSV-9 VP5
RT-VP5R	5' - CGCTGATCATCCTCGTTTCATCC - 3'	65	555-577	AHSV-9 VP5
MG-F	5' - ATCCAGCGTGCTCCAAAGATTCAG - 3'	67	61-84	Vero β2-MG
MG-R	5'- ATCAGATGGATGAAACCCAGACACATAG - 3'	66	135-162	Vero β2-MG
MG-FBHK	5' - AGTGGAGCTGTCAGATCTGTCCTTC - 3'	64	9-34	BHK β2-MG
MG-RBHK	5' - TGACCACCTTGGGCTCCTTC - 3'	64	127-147	BHK β2-MG

2.2.7.2 RNA extraction

Total RNA was extracted from Vero and BHK-21 cells with the Aurum™ Total RNA extraction kit (BioRad) according to the manufacturer's instructions. The culture medium was aspirated and the cells were rinsed once with 1 × PBS (137 mM NaCl; 2.7 mM KCl; 4.3 mM $Na_2HPO_4.2H_2O$; 1.4 mM KH_2PO_4; pH 7.4), trypsinized and then collected by centrifugation at 3 000 rpm for 10 min. The cell pellets were suspended in 350 µl of the supplied lysis solution, lysed by vigorous pipetting and then transferred to a 2-ml Eppendorf tube. Following addition of an equal volume of 70% ethanol, the cell lysate was centrifuged through a RNA-binding column at 15 000 rpm for 30 s. The column was rinsed with wash solution, treated with RNase-free DNase I to remove contaminating genomic DNA (15 min at room temperature) and the RNA was then eluted from the column using the supplied elution buffer.

2.2.7.3 cDNA synthesis

The extracted RNA was reverse transcribed with the QuantiTect® Reverse Transcription kit (Qiagen) according to the manufacturer's instructions. Prior to reverse transcription, each RNA preparation (0.5-1 µg) was incubated at 42ºC for 2 min with 1 × genomic DNA wipeout buffer (supplied in the kit) to ensure complete removal of contaminating genomic DNA. To reverse transcribe the RNA, 4 µl of 5 × Quantiscript® RT buffer, 1 µl of Quantiscript® Reverse Transcriptase and 1 µl of RT primer mix, which contains an optimized blend of oligo-dT and random primers, were added to the RNA preparation in a final volume of 20 µl. Reverse transcription was performed at 42ºC for 30 min, after which the enzyme was inactivated by heating to 95ºC for 3 min. The cDNA was stored at -20ºC until required.

2.2.7.4 Control PCR reactions

To confirm the absence of contaminating DNA in the RNA preparations and to determine the amplification specificity of the designed oligonucleotide pairs (Table 2.3), conventional PCR reactions were performed. Each of the PCR reaction mixtures (100 µl) contained 5 µl of the RNA or cDNA preparation, 10 pmol of each the gene-specific forward and reverse oligonucleotides, 1 × PCR buffer (75 mM Tris-HCl [pH 8.8]; 16 mM $(NH_4)_2SO_2$; 0.1% [v/v] Tween-20), $MgCl_2$ at 1.5 mM, each deoxynucleotide triphosphate (dNTP) at a concentration of 250 µM and 2 U of SUPERTHERM *Taq* DNA polymerase (Southern Cross Biotechnology). Reactions mixtures lacking template were also included as controls. Thermal cycling was performed in a GeneAmp® 2400 thermal cycler (Applied Biosystems) with the following cycling parameters: initial denaturation at 94°C for 3 min, followed by 30 cycles of denaturation at 94°C for 30 s, annealing at 60°C for 30 s and elongation at 72°C for 45 s. The reaction mixtures were analyzed by agarose gel electrophoresis on a 2% (w/v) agarose gel in the presence of an appropriate DNA molecular weight marker.

2.2.7.5 Quantitative real-time PCR

Quantitative real-time PCR was performed with the QuantiTect™ SYBR® Green PCR kit (Qiagen) and a LC480 LightCycler® (Roche Diagnostics). Each reaction mixture (20 µl) contained 1 µl of the reverse transcription reaction mixture, 10 pmol of the gene-specific forward and reverse oligonucleotides and 10 µl of 2 × QuantiTect™ SYBR® Green PCR master mix (consisting of HotStar*Taq*® DNA polymerase, dNTP mixture inclusive of dUTP, SYBR® Green I, ROX passive reference dye and 5 mM $MgCl_2$). For each target gene, reaction mixtures identical to those described above were prepared, except template was omitted. The reaction mixtures were incubated at 95ºC for 15 min to activate the HotStar *Taq*® DNA polymerase enzyme and then subjected to 55 cycles of denaturation at 94ºC for 15 s, oligonucleotide annealing at 60ºC for 20 s and extension at 72ºC for 10 s. Aliquots of each reaction mixture were subsequently analyzed by agarose gel electrophoresis in the presence of an appropriate DNA molecular weight marker. During each cycle, data acquisition was performed during the extension step and analyzed using LightCycler® v.3.5.3 software (Rasmussen, 2001). To compare the amplification efficiencies of different target sequences, a dilution series of each target was prepared in triplicate and each dilution series was amplified. To confirm specific amplification, melt-curve analysis of

the amplicons was performed by decreasing the temperature from 95ºC to 65ºC with a temperature transition rate of 20ºC/s and then increasing the temperature to 95ºC at a rate of 0.1ºC/s with continuous fluorescence measurement.

2.2.7.6 Data analysis

The *BestKeeper* software tool (Pfaffl *et al*., 2004) was used to determine the stability of the β2-microglobulin (β2-MG) housekeeping gene. Quantitative real-time PCR data were analyzed with the Relative Expression Software Tool (REST©) v.2.0.7 (Pfaffl *et al.*, 2002), where the relative expression of target (VP5) normalized to an endogenous reference (β2-MG) in a sample (VP5 sh/siRNA-treated, AHSV-9 infected cells) relative to an experimental control (sh/siUNeg-siRNA-treated, AHSV-9 infected cells), is given by $R = (E_{target})^{\Delta CPtarget\ (control\ -\ sample)}/(E_{ref})^{\Delta CPref\ (control\ -\ sample)}$. In this formula, R represents the expression ratio of the target gene, E is the PCR efficiency, ΔCP is the crossing point difference of an unknown sample versus a control sample, and ref represents a reference gene. For Crossing Point (CP) determination, the Second Derivate Maximum Method was used, which is included in the LightCycler® software.

2.3 RESULTS

2.3.1 Characterization of the β2-microglobulin (β2-MG) gene as an appropriate reference gene for quantitative real-time PCR

Quantitative real-time PCR has become the favored tool in mRNA expression analysis (Mackay *et al.*, 2002; Ding and Cantor, 2004). However, the most prominent problem in quantitative mRNA expression analysis is the selection of an appropriate reference gene. The use of such genes relies on the premise that they exhibit a constant basal level of expression that is consistent, non-regulated and independent of cell cycle (Thellin *et al.*, 1999; Suzuki *et al.*, 2000). One of the most widely used reference genes in RNAi assays is the β-actin gene (Weisinger *et al*., 1999). However, there is a growing body of evidence suggesting that β-actin is an unsuitable control in quantitative mRNA expression analysis due to setting-dependent variations in its expression (Chang *et al*., 1998; Foss *et al*., 1998; Schmittgen and Zakrajsek, 2000; Selvey *et al*., 2001; Radonić *et al.*, 2004). In a recent study, ten different potential reference genes were compared for their use in experiments investigating cellular mRNA expression of virus-infected human cell

lines (Radonić *et al.*, 2005). Whereas β2-microglobulin (β2-MG) showed stable expression in virus-infected cells, β-actin showed significant variations with an increasing degree of infection and the other genes showed moderate expression stability. Consequently, the β2-MG housekeeping gene was selected and its suitability as a reference gene for use in subsequent quantitative real-time PCR analyses evaluated.

To investigate, AHSV-9 infected Vero cells that had been stably transfected with recombinant pENTR™/H1/TO shRNA delivery vectors, as well as virus-infected BHK-21 cells that had been transfected with control or VP5-directed siRNAs were harvested at 24 h post-infection. Total RNA was extracted and treated extensively with RNase-free DNase prior to performing reverse transcription and quantitative real-time PCR. The data was analyzed using the *BestKeeper* software tool (Pfaffl *et al.*, 2004) in order to examine the stability of the β2-MG housekeeping gene under these experimental settings.

Using the *BestKeeper* software tool, descriptive statistics of the derived crossing points (CP), generated by the real-time PCR platform, were computed for the β2-MG housekeeping gene. All CP data were compared over the entire study, comprising of the control AHSV-9 infected sh/siUNeg-treated cells and all test groups (AHSV-9 infected, VP5-directed sh/siRNA-treated cells). Any studied housekeeping gene with a standard deviation (SD) higher than 1 can be considered inconsistent and should thus not be used as a reference gene (Pfaffl *et al.*, 2004). In this regard, β2-MG had a standard deviation below 1 for stably transfected Vero cell lines infected with AHSV-9 at a MOI of 2 PFU/cell (SD = 0.42), a MOI of 1 PFU/cell (SD = 0.59) and a MOI of 0.5 PFU/cell (SD = 0.32). For siRNA-treated BHK-21 cells infected with AHSV-9 at a MOI of 1 PFU/cell, the standard deviation was also below 1 (SD = 0.15). Consequently, the β2-MG gene was considered to be a suitable reference gene since it was stably expressed between the respective control and test samples in these experimental settings. Thus, β2-MG was subsequently used as endogenous reference gene for data normalization and for calculation of fold changes in VP5 transcripts with the REST© software program (Pfaffl *et al.*, 2002).

2.3.2 Short hairpin RNA (shRNA)-mediated silencing of AHSV-9 VP5 gene expression in stable Vero cell lines

Towards developing a plasmid DNA vector-based RNAi assay whereby AHSV-9 VP5 gene expression could be silenced in Vero cells, the pENTR™/H1/TO shRNA delivery vector was selected for use in this investigation. This vector allows for cloning of a double-stranded DNA oligonucleotide encoding a shRNA downstream of the H1/TO promoter to create an H1/TO RNAi cassette. The H1 RNA polymerase III promoter in the vector has been modified to include two prokaryotic tetracycline operator ($TetO_2$) sequences, which enables tetracycline-dependent expression of the shRNA of interest in cells that express the tetracycline repressor (TetR) protein. Alternatively, the recombinant vector can be transfeced into non-TetR expressing mammalian cells, thus allowing for constitutive expression of the shRNA of interest. An added advantage of the pENTR™/H1/TO shRNA delivery vector is that it harbors a Zeocin™ selection marker to generate a stable cell line (Invitrogen).

2.3.2.1 Construction of recombinant pENTR™/H1/TO RNAi entry vectors

To construct recombinant pENTR™/H1/TO shRNA delivery vectors (Fig. 2.1A), complementary oligonucleotides corresponding to four different VP5-specific sequences and a control non-silencing shRNA sequence (Table 2.1) were synthesized. The complementary oligonucleotides were annealed to generate double-stranded DNA oligonucleotides (Fig. 2.1B) and then cloned into the linear vector DNA. Following transformation of competent One Shot® TOP10 *E. coli* cells, plasmid DNA was extracted from randomly selected transformants and characterized by nucleotide sequencing to confirm the presence of cloned insert DNA and to verify that no mutations were introduced into oligonucleotides during their chemical synthesis. No nucleotide differences were observed between the cloned oligonucleotide insert DNA and their intended AHSV-9 VP5 target regions. The recombinant plasmids, harboring oligonucleotide inserts corresponding to AHSV-9 VP5-specific shRNA sequences, were designated pENTR-shVP5-148, pENTR-shVP5-651, pENTR-shVP5-826 and pENTR-shVP5-1311. A recombinant plasmid, designated pENTR-shUNeg, harbored an oligonucleotide insert of which the corresponding shRNA sequence does not display homology to known viral and cellular genes, and thus served as a non-silencing control in subsequent assays.

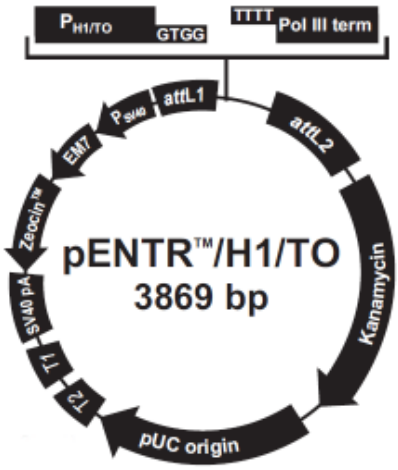

Fig. 2.1A **Plasmid map of the linear pENTR™/H1/TO vector.** The vector contains 4-nt 5' overhangs to facilitate ligation of a target-specific double-stranded DNA oligonucleotide, a Zeocin™ resistance gene to allow stable selection in transfected mammalian cells, and a hybrid promoter consisting of the human H1 promoter and two tetracycline operator (TO) sequences for RNA polymerase III-dependent regulated expression of the shRNA if desired.

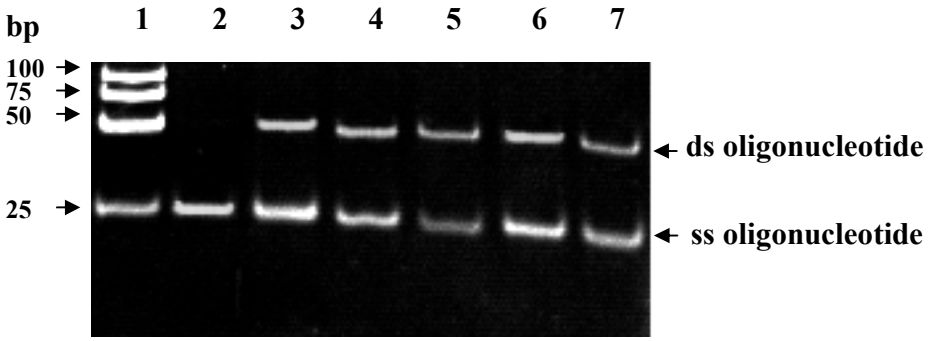

Fig. 2.1B **Polyacrylamide gel electrophoretic analysis of annealed DNA oligonucleotides.** Lane 1, DNA molecular weight marker; lane 2, single-stranded (ss) oligonucleotide; lanes 3-7, aliquots of oligonucleotide annealing reactions containing oligonucleotides corresponding in sequence to shUNeg (lane 3), shVP5-148 (lane 4), shVP5-651 (lane 5), shVP5-826 (lane 6) and shVP5-1311 (lane 7). The sizes of the DNA molecular weight marker, low-molecular-weight DNA ladder (New England Biolabs), are indicated to the left of the figure. Due to the formation of secondary structure, the ss oligonucleotides (50 nt in length) do not resolve at the expected size.

2.3.2.2 shRNA-mediated gene silencing of AHSV-9 VP5 gene expression in Vero cells

To generate stable Vero cell lines the constructed recombinant pENTR™/H1/TO shRNA delivery vectors, harboring a control non-silencing shRNA or four different VP5-directed shRNAs, were transfected into Vero cells. Transfectants were selected by supplementation of the culture medium with 600 µg/ml of Zeocin™, a concentration that produced the optimal kill curve on untransfected Vero cells (Materials and Methods, Section 2.2.5.1). Following selection, the derived cell lines, designated Vero-shUNeg, Vero-shVP5-148, Vero-shVP5-651, Vero-shVP5-826 and Vero-shVP5-1311, were seeded in tissue culture plates. Based on results indicating that different MOIs may significantly influence the silencing efficiency of a given shRNA (Chen *et al*., 2007), the respective Vero cell monolayers were therefore infected with AHSV-9 at a MOI of 2 PFU/cell, 1 PFU/cell or 0.5 PFU/cell. At 24 h post-infection, the abundance of VP5 mRNA in the virus-infected cells was examined by quantitative real-time PCR.

The results indicated that infection of Vero cells expressing the different VP5-directed shRNAs with AHSV-9 at a MOI of 2 PFU/cell did not result in a reduction in VP5 mRNA expression. Indeed, the level of VP5 mRNA expression was similar to that in cells expressing the control non-silencing shRNA (shUNeg) (Fig. 2.2A). In contrast, VP5 mRNA expression was reduced in the stably transfected Vero cells when the cells were infected with AHSV-9 at MOI of 1 PFU/cell (Fig. 2.2B) and 0.5 PFU/cell (Fig. 2.2C). Under these experimental conditions, the different VP5-directed shRNAs respectively induced, on average, a 0.25-fold and 0.65-fold reduction in VP5 mRNA transcripts as compared to Vero cells expressing the control non-silencing shRNA. Despite this reduction in VP5 mRNA expression, there was, however, no statistical significant difference ($p \geq 0.001$) between VP5 mRNA expression in Vero cells expressing the respective VP5-directed shRNAs and cells expressing the control non-silencing shRNA, irrespective of the MOI used to infect the Vero cells.

The possibility of DNA contamination in the RNA preparations used above was eliminated by performing RNase-free DNase I treatments and verified by subjecting the samples to PCR amplification, using *Taq* DNA polymerase and the gene-specific oligonucleotides (Table 2.1). No amplicons were obtained from control reaction mixtures lacking template or from the RNA preparations that were subsequently used for cDNA synthesis. In addition, the amplification specificity of the real-time PCR was verified by agarose gel electrophoresis and a single

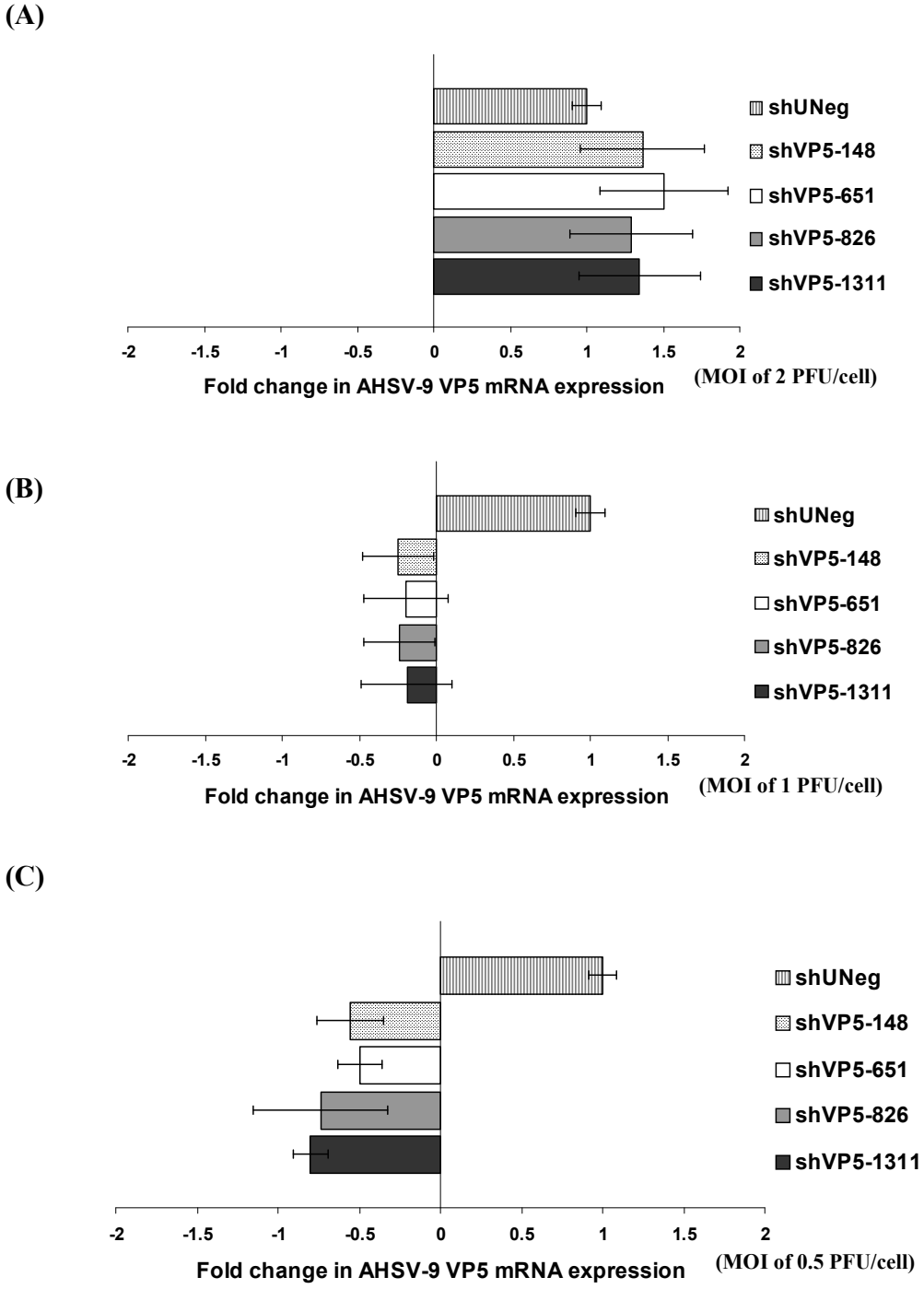

Fig. 2.2 **Quantification of VP5 mRNA expression in AHSV-9 infected Vero-shUNeg, Vero-shVP5-148, Vero-shVP5-651, Vero-shVP5-826 and Vero-shVP5-1311 cell lines.** The respective Vero cell lines were infected with AHSV-9 at MOI of 2 PFU/cell (A), 1 PFU/cell (B) and 0.5 PFU/cell (C), and fold changes in VP5 mRNA expression levels were calculated as compared with AHSV-9 infected Vero-shUNeg cells. Real-time PCR for β2-microglobulin gene transcripts was included in the assays as endogenous reference and used for data normalization of VP5 mRNA fold changes. Data are shown as the means ± S.D. of three samples.

amplicon of the expected length for each target was obtained (VP5, 121 bp; β2-MG, 138 bp). Furthermore, to confirm its reproducibility, melt curve analysis was performed and the efficiency of the real-time PCR was also calculated. Serial dilutions, in triplicate, of the cDNA prepared from Vero cells stably transfected with recombinant pENTR™/H1/TO shRNA delivery vectors and then infected with AHSV-9, were subjected to quantitative real-time PCR. Using the REST© software tool (Pfaffl *et al.*, 2002), the calculated PCR efficiencies (*E*) for both the VP5 and β2-MG targets at a MOI of 2 PFU/cell (E_{VP5} =1.829 and $E_{\beta2\text{-MG}}$ = 1.836), 1 PFU/cell (E_{VP5} =1.753 and $E_{\beta2\text{-MG}}$ = 1.800) and 0.5 PFU/cell (E_{VP5} =1.913 and $E_{\beta2\text{-MG}}$ = 1.769) were close to the theoretic maximum and optimum efficiency of *E* = 2.0, thus indicating that the quantitative real-time PCR had a high level of reproducibility and sensitivity.

Based on the above results, it was concluded that none of the VP5-directed shRNAs were capable of silencing AHSV-9 VP5 gene expression. Indeed, each of the designed shRNAs appeared to be equally inefficient in silencing VP5 mRNA expression. Although VP5 mRNA expression was reduced in stably transfected Vero cells infected with AHSV-9 at a MOI of 1 and 0.5 PFU/cell, respectively, the reduction in VP5 transcript levels was not statistically significant. Taking the above into consideration, focus was placed on developing an AHSV-9 VP5 gene silencing assay based on the use of siRNAs rather than designing and testing additional VP5-directed shRNAs.

2.3.3 siRNA-mediated silencing of AHSV-9 VP5 gene expression in BHK-21 cells

Based on the inability to silence AHSV-9 VP5 gene expression with plasmid vector-expressed shRNAs and considering that siRNAs have been used previously to successfully silence AHSV gene expression (Wirblich *et al.*, 2006; Stassen *et al.*, 2007), it was next investigated whether VP5-directed siRNAs may inhibit synthesis of AHSV-9 VP5 mRNA. To investigate, siRNAs directed to three different sites on the AHSV-9 VP5 mRNA were designed and chemically synthesized. The siRNAs were designated siVP5-138, siVP5-528 and siVP5-984, respectively. BHK-21 cell monolayers were subsequently transfected with the VP5-directed siRNAs or a control non-silencing siRNA (siUNeg), followed by infection with AHSV-9 at a MOI of 1 PFU/cell and a second round of transfection with the respective siRNAs. At 24 h post-infection, total RNA was isolated from the cells and subjected to reverse transcription followed by quantitative real-time PCR.

The data, presented in Fig. 2.3, indicated that the different VP5-directed siRNAs differed in their ability to reduce VP5 mRNA expression in the AHSV-9 infected BHK-21 cells. In BHK-21 cells transfected with either siVP5-528 or siVP5-984, the VP5 mRNA transcripts were reduced by 2.1-fold and 1.8-fold, respectively, as compared with cells transfected with the control non-silencing siRNA (siUNeg). In contrast, VP5 mRNA expression was reduced to the greatest extent in BHK-21 cells transfected with siVP5-138 (2.5-fold reduction). Analysis of the data indicated that the difference between the VP5 mRNA transcripts in cells transfected with the respective VP5-specific siRNAs and that of cells transfected with the control siRNA (siUNeg) was statistically significant ($p \leq 0.001$).

The absence of DNA contamination in the RNA preparations, as well as the specificity and reproducibility of the quantitative real-time PCR was confirmed, as described above. The results indicated the absence of amplicons from RNA preparations that were used for cDNA synthesis, whereas a single amplicon of the expected length for each target was obtained (VP5, 121 bp; β2-MG, 101 bp) following the real-time PCR. Moreover, the results also indicated that the calculated PCR efficiencies (E) for both the VP5 and β2-MG targets (E_{VP5} =1.83 and $E_{\beta2\text{-MG}}$ = 1.72) were close to the theoretic maximum and optimum efficiency of $E = 2.0$.

Based on the above, it was concluded that the respective VP5-directed siRNAs were indeed capable of reducing the accumulation of VP5 mRNA in BHK-21 cells infected with AHSV-9. Although expression of VP5 mRNA was reduced by 41-54% in the siRNA-treated cells, this is well below the level of knockdown (at least 70%) generally accepted as being meaningful in loss-of-gene function studies (Caplen *et al.*, 2001; Banan and Puri, 2004; Hsieh et *al.*, 2004). Consequently, this approach as a means to investigate AHSV-9 VP5 function was not pursued further.

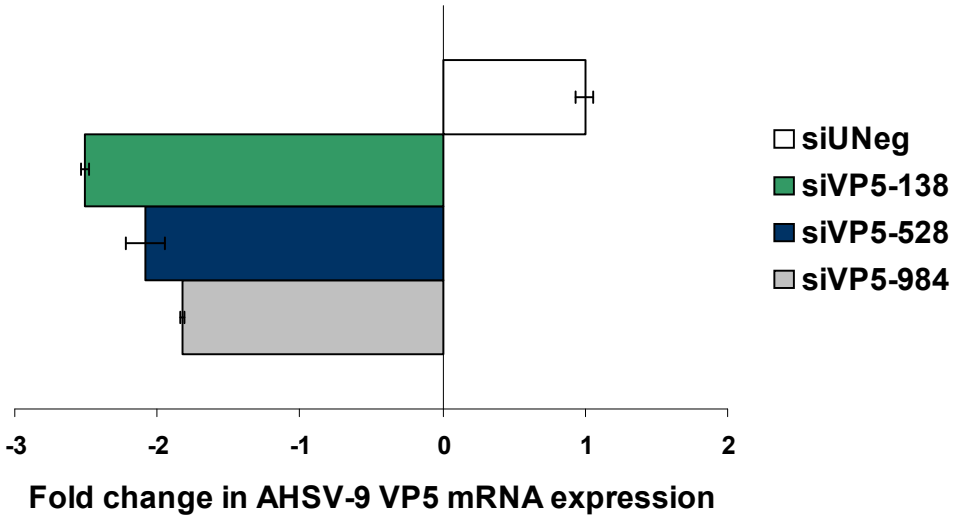

Fig. 2.3 **Real-time RT-PCR analysis for quantification of VP5 mRNA expression in AHSV-9 infected BHK-21 cells.** Fold changes in VP5 mRNA expression levels were calculated by quantification of VP5 mRNA in infected cells transfected with VP5-directed siRNAs (siVP5-138, siVP5-528 and siVP5-984) as compared to that in infected cells transfected with a control non-silencing siRNA (siUNeg). Real-time PCR for β2-microglobulin gene transcripts was included in the assays as endogenous reference and used for data normalization of VP5 mRNA fold changes. Data are shown as the means ± S.D. of three samples.

2.4 DISCUSSION

A number of recent studies on BTV have indicated that the orbivirus outer capsid proteins may have varied functions. In addition to their role in cell binding and entry (Forzan *et al.*, 2007; Zhang *et al.*, 2010), the VP2 and VP5 proteins have also been implicated in processes such as virus morphogenesis and release (Bhattacharya *et al.*, 2007; Bhattacharya and Roy, 2008), as well as the induction of apoptosis in mammalian cells (Mortola *et al.*, 2004). In contrast to BTV, much less is known regarding the role of AHSV outer capsid proteins during the virus replication cycle. A major constraint in these types of studies has been the lack of a reverse genetic system for AHSV that would allow for genetic manipulation of the viral genome in order to study protein function in greater detail. Therefore, in this investigation, RNAi-based approaches were adopted in an attempt to functionally characterize the AHSV outer capsid protein VP5.

RNAi-mediated gene silencing can be obtained in cultured mammalian cells either by endogenous expression of shRNAs (Brummelkamp *et al*., 2002a; Paddison *et al*., 2002b; Sui *et al*., 2002) or by transfection of chemically synthesized siRNAs (Elbashir *et al.*, 2001a; Caplen *et al.*, 2001). Both of these approaches are associated with their own advantages and disadvantages. Although plasmid DNA vector-based RNAi systems are economical to use and have the ability to mediate persistent gene silencing, they have often been reported to induce an interferon response (Dykxhoorn *et al.*, 2003; Bridge *et al.*, 2003; Cullen, 2006). In the case of siRNA-transfected cells, immediate and significant gene silencing can be achieved, but the silencing effect is transient and chemical synthesis of the siRNAs is a costly process (Dykxhoorn *et al.*, 2003). Moreover, the efficacy of shRNA- versus siRNA-mediated gene silencing also appears to be a matter of debate. Several reports have claimed that endogenously expressed shRNAs are as effective and even more effective than siRNAs to mediate gene silencing (Wang *et al.*, 2005; McAnuff *et al.*, 2007; Takahashi *et al.*, 2009), whereas others have claimed the opposite (Bridge *et al.*, 2003; Peng *et al.*, 2005; Lambeth *et al.*, 2007). Consequently, in this investigation, both approaches were evaluated for their ability to silence AHSV-9 VP5 gene expression in cultured mammalian cells.

Since the goal with RNAi protocols is to reduce protein levels in cells and to study the functional consequences of their removal, a key parameter for achieving effective gene silencing is therefore

the design of effective RNAi effector molecules. This is not a trivial matter, as only a limited number of RNAi effector molecules are capable of inducing highly effective gene silencing (Elbashir *et al.*, 2001a; Hsieh *et al.*, 2004; Reynolds *et al.*, 2004; Mittal, 2004). For siRNA, criteria for selecting an effective target site within a gene (Elabashir *et al.*, 2001a-c; Caplen *et al.*, 2001; Peek and Behlke, 2007) and siRNA design algorithms that have a statistically significant ability to discriminate between effective and ineffective siRNAs (Ui-Tei *et al.*, 2004; Shah *et al.*, 2007; Naito *et al.*, 2009) are well established. In contrast, much controversy surrounds the development of rules for the design of effective shRNA (Li *et al.*, 2007a; Zhou and Zheng, 2009). Since the shRNA is processed intracellularly by Dicer to a siRNA, it has been suggested that shRNA design be based on the design rules for siRNA (Amarzguioui *et al.*, 2005). However, algorithms and the design criteria for siRNAs often show little or no efficiency at predicting a functional shRNA (Root *et al.*, 2006; Taxman *et al.*, 2006). In the light of such uncertainty and considering that it is still not possible to predict with complete certainty the degree of gene silencing a particular RNAi effector molecule will produce, it is generally recommended that the silencing capability of several (at least three) candidate RNAi effector molecules be evaluated.

Initial attempts at silencing AHSV-9 VP5 gene expression relied on the use of plasmid DNA vector-expressed shRNAs. Four different VP5-directed shRNAs were designed and their ability to down-regulate VP5 transcripts were evaluated in stably transfected Vero cell lines that had been infected with AHSV-9 at different MOIs. The different VP5-directed shRNAs did induce a silencing effect in cell monolayers infected at a MOI of 1 and 0.5 PFU/cell, respectively, but not in cell monolayers infected at a MOI of 2 PFU/cell. However, in none of these assays was the reduction in VP5 mRNA expression significantly different from that in cells expressing a control non-silencing shRNA (Fig. 2.2). Moreover, the VP5-directed shRNAs appeared to be all equally inefficient at silencing VP5 mRNA expression. This result, together with the fact that not one of the four shRNAs was capable of causing a significant reduction in VP5 transcript levels, is cause for suspicion. Since each of the shRNAs were designed with the same software and considering the lack of satisfactory shRNA design tools, these results can be interpreted as simply indicating that the shRNAs were all ineffective and thus screening of a greater number of candidate shRNAs would be required in order to identify an effective shRNA. However, an alternative and more

plausible explanation for these results may be related to the induction of apoptosis in mammalian cells infected with AHSV-9.

Subsequent to performing the shRNA-mediated gene silencing assays reported in this investigation, it was shown that stable RNAi, in contrast to RISC-dependent RNAi by 21-bp siRNAs, fails soon after the induction of apoptosis. This is due to caspase-3–mediated cleavage and inactivation of Dicer, thereby resulting in a lack of processing of the vector-expressed shRNA transcripts into functional siRNA (Ghodgaonkar *et al*., 2009; Kandan-Kulangara *et al*., 2010). In this regard, it is particularly interesting to note that results obtained over the course of this study indicated that caspase-3, a key executioner molecule of the caspase cascade that leads to apoptosis (Hengartner *et al.*, 2000), is activated at 12 h post-infection in mammalian cells infected with AHSV-9 (Chapter 4). It is therefore to be expected that this early activation of caspase-3 in the AHSV infection cycle and subsequent inactivation of Dicer would yield only a small pool of processed VP5-directed shRNAs that are available for silencing of VP5 gene expression. It furthermore follows that under such conditions it may not be possible to distinguish between effective and ineffective shRNAs, as they are all likely to display similar inefficient gene silencing profiles. This explanation is also in agreement with results obtained by other members of our research group (H.J. Roos and M.A. Nieuwoudt, personal communication). Screening of plasmid DNA-expressed shRNAs for their ability to silence expression of an eGFP-tagged target gene of interest frequently results in the identification of highly effective shRNAs. However, when these apparently effective shRNAs are used in viral challenge assays, similar to that used in this study, the shRNAs are ineffective and do not result in significant levels of AHSV gene silencing.

Although outside the scope of this investigation, various strategies may be explored to maximize the yield of processed shRNAs prior to the induction of apoptosis. Several reports have demonstrated that efficient RNAi-mediated gene silencing can be obtained by *in vitro*-transcribed shRNA (Wang *et al.*, 2005; Vlassov *et al.*, 2007) or by synthetic shRNA (Kim *et al.*, 2005; Siolas *et al.*, 2005) that are transfected directly into the cells. In these studies it was also reported that 27- to 29-mer shRNAs were more potent inducers of RNAi than 21-mer shRNAs (used in this investigation). The enhanced potency of the longer duplexes was attributed to enhanced Dicer-mediated processing of the siRNA precursors (Kim *et al.*, 2005). However, if plasmid DNA

vector-expressed shRNAs are to be used consideration may be given to the choice of promoter. Similar to results reported by Chen *et al*. (2007), the silencing efficiency of the VP5-directed shRNAs was more pronounced at low MOIs (1 and 0.5 PFU/cell) as compared to a high MOI (2 PFU/cell). Since stably transfected cell lines were used in the assays, these results imply that the transcription efficiency from the H1 promoter present in the shRNA delivery vector is low. It can therefore be envisaged that an increase in transcription efficiency may be required for increased resistance. In this regard, it is important to note that several reports have suggested that the promoter choice may affect shRNA efficiency and the potency of inhibition (Boden *et al*., 2003; Wooddell *et al*., 2005; Alembekov *et al*., 2009). Indeed, Hassani *et al*. (2007) reported that silencing of a luciferase target gene by shRNA produced from a hybrid construct composed of the CMV enhancer/promoter placed immediately upstream of an H1 promoter exceeded that obtained with the H1 promoter alone (50% versus 20% silencing, respectively). Alternatively, siRNAs may be used (see below), which by virtue of their small size are incorporated directly into the RNAi pathway and therefore bypass the need for processing by the Dicer enzyme.

In contrast to the shRNA-mediated VP5 gene silencing assays, three VP5-directed siRNAs were each shown to be capable of significantly reducing VP5 mRNA expression in BHK-21 cells infected with AHSV-9 at a MOI of 1 PFU/cell. In these assays, the cell monolayers were transfected with the respective siRNAs prior to and following AHSV-9 infection, since pre-treatment of cultured mammalian cells with siRNA prior to virus infection reportedly increases the siRNA-mediated gene silencing effect (Wirblich *et al*., 2006; Zinke *et al*., 2009). The results indicated that of the three VP5-directed siRNAs used, the silencing effect of siVP5-528 and siVP5-984 were comparable (2.1- and 1.8-fold reduction in VP5 mRNA expression, respectively), whereas siVP5-138 was the most efficient (2.5-fold reduction) (Fig. 2.3).

The above results indicated that the different VP5-directed siRNAs differed in their efficacy to silence VP5 gene expression. These results are in agreement with several previous reports, indicating that siRNAs targeted to different sites on the same mRNA differ in their silencing efficiency (Holen *et al*., 2002; Harborth *et al*., 2003; Vickers *et al*., 2003; Scherer *et al*., 2004; Patel *et al*., 2009). At present, there is still a lack of clear understanding of the mechanisms that determine gene silencing efficiency of a given siRNA. Nevertheless, a number of hypotheses have been proposed in the literature, including the thermodynamic properties of the siRNA that

play a role in its stability, as well as strand bias in duplex unwinding and retention by RISC (Khvorova *et al.*, 2003; Schwartz *et al.*, 2003; Lu and Mathews, 2007), binding of viral and/or cellular proteins on the mRNA that may cause positional effects (Holen *et al.*, 2002), and the local secondary and tertiary structure of the targeted mRNA that may affect the accessibility of the siRNA (Kretschner-Kazemi Far and Sczakiel, 2003; Luo and Chang, 2004; Shao *et al.*, 2007; Gredell *et al.*, 2008). Indeed, several reports have argued that local secondary structures in the target mRNAs may restrict the accessibility of RISC and attenuate or even abolish RNAi efficiency (Brown *et al.*, 2005; Heale *et al.*, 2005; Overhoff *et al.*, 2005; Tafer *et al.*, 2008). Despite the respective VP5-directed siRNAs targeting accessible sites on VP5 mRNA, as evidenced by a predicted target accessibility score of greater than 4 with the Sfold 2.0 software, it is difficult to accurately model the complex secondary structure of mRNA (Kawasaki *et al.*, 2003). Moreover, the relevance of such predictions is also uncertain since it does not take into account either tertiary structure or RNA-protein interactions. Although these predictions should therefore be viewed as merely predictive, it is nevertheless tempting to speculate that the accessibility of the target site of the respective VP5-directed siRNAs may have differed from each other, thus resulting in binding differences with the RISC/siRNA complex and, consequently, differences in their degradation of the target mRNA.

In conclusion, the results obtained in this investigation indicated that the use of siRNAs, in contrast to plasmid DNA vector-expressed shRNAs, represents a viable means whereby AHSV-9 VP5 gene expression can be silenced in infected mammalian cells. However, further optimization and the screening of additional candidate siRNAs is required in order to obtain meaningful silencing of AHSV-9 VP5 mRNA expression. The greater efficacy of siRNAs can be attributed to the availability of appropriate siRNA design tools, its immediate availability for gene silencing once transfected into cells and the fact that siRNA-mediated gene silencing is not affected by the induction of apoptosis (Ghodgaonkar *et al.*, 2009). Despite the promise shown by this approach, the reduction in the level of VP5 mRNA transcripts in virus-infected cells is, however, not sufficient for loss-of-function studies. Consequently, an alternative approach was adopted whereby the VP5 protein could be functionally characterized. The details of these studies are provided in the following Chapter.

CHAPTER THREE

EXPRESSION AND FUNCTIONAL CHARACTERIZATION OF THE AFRICAN HORSE SICKNESS VIRUS VP5 PROTEIN

3.1 INTRODUCTION

The African horse sickness virus (AHSV) particle is considered to be structurally similar to that of bluetongue virus (BTV), the type species of the genus *Orbivirus* in the family *Reoviridae*. The virus particles are composed of seven discrete proteins, which are organized into two capsids that encapsidate the ten double-stranded RNA (dsRNA) genome segments (Roy *et al*., 1994b; Stuart *et al.*, 1998). In contrast to other members of the *Reoviridae* family, the outer capsid, which is composed of the two major structural proteins VP2 and VP5, is very fragile and virus infectivity is lost in mildly acidic conditions (Gorman and Taylor, 1985). This feature is considered to be consistent with a role for these two outer capsid proteins during the early stages of infection. Subsequent studies have shown that the VP2 protein of BTV is the receptor binding protein (Hassan and Roy, 1999; Zhang *et al.*, 2010). Some studies of the VP5 protein, focussing on its role during virus entry into the host cell, have also been undertaken. It was shown that VP5 of BTV is involved in cell permeabilization, suggesting a role for the protein in the translocation of the transcriptionally active core into the cytoplasm (Hassan *et al.*, 2001). More recently, it was demonstrated that VP5 has a pH-dependent fusogenic activity when expressed on the cell surface (Forzan *et al.*, 2004). Based on these results, a model of how the orbivirus core particles gain access to the cytoplasm of infected cells has been proposed (Forzan *et al.*, 2007; Roy, 2008). According to this model, VP2 mediates attachment of the virion to the cell surface and its subsequent internalization. After internalization, endocytic vesicles are formed within which VP5 may be unmasked following low-pH removal of VP2. The permeabilization activity associated with N-terminal amphipathic helices within VP5 may subsequently result in the formation of pores in the endosomal membrane and the transcriptionally active core particles are thus released into the cytoplasm.

In the previous Chapter, it was shown that expression of the VP5 gene of AHSV could be silenced by making use of VP5-directed small interfering RNAs (siRNAs), but not by intracellularly expressed short hairpin RNAs (shRNAs). The modest level of gene knockdown (41-54%), however, necessitated that an alternative approach be adopted in order to functionally characterize the AHSV VP5 protein. In previous studies, a combination of mutagenesis and re-expression of AHSV proteins in heterologous hosts has allowed progress to be made in relation to the structure-function relationships among some of the AHSV proteins, and has also allowed

for mapping of the function of some of the proteins. Indeed, the expression of individual AHSV proteins by appropriately constructed baculovirus recombinants in *Spodoptera frugiperda* (Sf-9) insect cell culture has made significant contributions to the structure-function relationships of nonstructural proteins such as NS1 (Maree and Huismans, 1997), NS2 (Uitenweerde *et al.*, 1995) and NS3 (van Staden *et al.*, 1995; van Niekerk *et al.*, 2001), as well as structural proteins such as VP6 (de Waal and Huismans, 2005) and VP7 (Burroughs *et al.*, 1994; Basak *et al.*, 1996).

Characterization of VP5 of AHSV has been limited to comparative sequence analyses of the VP5-encoding gene (Iwata *et al.*, 1992; du Plessis and Nel, 1997; Williams *et al.*, 1998), although expression of the VP5 protein in Sf-9 cells (du Plessis and Nel, 1997) and in *Escherichia coli* (Martinez-Torrecuadrada *et al.*, 1999) has been noted to be cytotoxic, causing rapid cell lysis and resulting in low levels of protein expression. In addition, AHSV VP5 has been reported to play a supportive role to VP2 in enhancing the protective neutralizing activity of VP2 in horses (Martinez-Torrecuadrada *et al.*, 1996; 1999). Apart from its immunogenicity, no functional studies have been undertaken on the VP5 protein of AHSV nor has the basis of its apparent cytotoxicity been investigated. To gain an understanding of the function of the AHSV VP5 protein and to determine which regions within the VP5 protein are responsible for its cytotoxic effect, a series of N- and C-terminal truncations of the full-length VP5 were generated, expressed in Sf-9 cells using the baculovirus system and the ability of each truncated VP5 protein to permeabilize Sf-9 cell membranes was determined. The data was furthermore substantiated by synthesis of relevant peptides and subsequent assessment of their effect on membrane permeabilization.

3.2 MATERIALS AND METHODS

3.2.1 Bacterial strains and plasmids

The *Escherichia coli* strains were routinely cultured in LB broth (1% [w/v] tryptone; 1% [w/v] NaCl; 0.5% [w/v] yeast extract; pH 7.4) (Sambrook and Russell, 2001) at 37ºC with shaking at 200 rpm, and maintained at 4ºC on LB agar (LB broth containing 1.2% [w/v] bacteriological agar) or at -70ºC as glycerol cultures. For plasmid DNA selection and maintenance in *E. coli*, 100 µg/ml of ampicillin was used (Roche Diagnostics). Recombinant plasmid pBSVP5,

containing a full-length cDNA copy of AHSV-9 genome segment M6, was obtained from Dr. W. Fick (Department of Genetics, University of Pretoria). The pGEM®-T Easy cloning vector and the baculovirus transfer vector, pAcGHLT-B, were obtained from Promega and BD Biosciences, respectively.

3.2.2 DNA amplification

3.2.2.1 Oligonucleotides

Oligonucleotides used to amplify the full-length AHSV-9 VP5 gene (GenBank Acc. No. U74489), as well as those used in the construction of truncated VP5 fragments, were designed based on the nucleotide sequence obtained from sequencing the VP5 gene contained in plasmid pBSVP5. To facilitate subsequent cloning procedures involving the PCR-amplified products, unique restriction endonuclease recognition sites were included at the 5'-terminus of the different oligonucleotides. To prevent incorporation of vector-derived sequences, the oligonucleotides were also designed to incorporate a stop codon (TCA) at the 3'-terminus of truncated VP5 fragments. The oligonucleotides, indicated in Table 3.1, were synthesized by EuroFins MWG.

Table 3.1 Oligonucleotides used in this part of the study

Oligonucleotides	Nucleotide sequence	Restriction enzyme site
PCR amplification*:		
VP5*Pst*I	5'- *ctgcag*ATGGGTAAGTTCACAT - 3'	*Pst*I
VP5*Bgl*505	5' - *agatct***TCA**AGCTACTTTCACACC - 3'	*Bgl*II
VP5*Kpn*280	5' - *ggtacc*CCTCATATAATTGAGAAAG - 3'	*Kpn*I
VP5*Kpn*1	5' - *ggtacc*CATGGGTAAGTTCACATC - 3'	*Kpn*I
VP5*Bgl*220	5' - *agatct***TCA**CATTTCCTGCACAG - 3'	*Bgl*II
VP5*Pst*23	5' - *ctgcag*GCAGCCAAGAGGATG - 3'	*Pst*I
VP5R*Bgl*	5' - *agatct***TCA**AGCTACTTTCACACCAAAG - 3'	*Bgl*II
VP5*Pst*44	5' - *ctgcag*GGAAGTGCGGCG - 3'	*Pst*I
VP5*Bgl*43	5' - *agatct***TCA**CACTTCACTTTCCAC - 3'	*Bgl*II
VP5*Pst*124	5' - *ctgcag*GGGGAGGATCTATTAAA - 3'	*Pst*I
Nucleotide sequencing:		
M13-F	5' - TGTAAAACGACGGCCAGT - 3'	
M13-R	5' - CAGGAAACAGCTATGAC - 3'	
VP5IF628	5 - GGCAATTGAACTTGAACAGCAGG - 3'	

* Restriction endonuclease recognition sequences are indicated in italics, and stop codons are indicated in bold.

3.2.2.2 Polymerase chain reaction (PCR)

Each of the PCR reaction mixtures (100 µl) contained 100 ng of template DNA, 100 pmol each of the forward and reverse oligonucleotides, 1 × PCR buffer (75 mM Tris-HCl [pH 8.8]; 16 mM $(NH_4)_2SO_2$; 0.1% [v/v] Tween-20), 1.5 mM $MgCl_2$, 200 µM of each dNTP and 2 U of SUPERTHERM *Taq* DNA polymerase (Southern Cross Biotechnology). The PCR was performed in a GeneAmp® 2400 thermal cycler (Applied Biosystems). The DNA was initially denatured at 94°C for 3 min, followed by 30 cycles of denaturation at 94°C for 30 s, annealing at 60°C for 30 s and elongation at 72°C for 1.5 min. The last cycle was followed by an elongation step at 72°C for 5 min to complete synthesis of all DNA strands. A negative control was also included in which the DNA template had been omitted. Aliquots of the reaction mixtures were analyzed by electrophoresis on a 0.8% (v/v) agarose gel in the presence of an appropriate DNA molecular weight marker.

3.2.3 Agarose gel electrophoresis

DNA was analyzed by agarose gel electrophoresis (Sambrook and Russell, 2001). For this purpose, horizontal 0.8% (w/v) agarose gels were cast and electrophoresed at 90 V in 1 × TAE buffer (40 mM Tris-HCl; 20 mM NaOAc; 1 mM EDTA; pH 8.5). The agarose gels were supplemented with 0.5 µg/ml ethidium bromide to allow visualization of the DNA on an UV transilluminator. Where appropriate, DNA fragments were sized according to their migration in the agarose gel as compared to that of standard DNA molecular weight markers (obtained from Fermentas).

3.2.4 Recovery of DNA fragments from agarose gels

DNA fragments were purified from agarose gels with a silica suspension, as described by Boyle and Lew (1995). For this purpose, the excised DNA fragment was mixed with 2.5 volumes of a 6 M NaI solution. The agarose was dissolved by incubating the gel slice at 55ºC for 5-10 min with occasional vortexing, after which 7 µl of a silica suspension was added to the sample. Following incubation on ice for 15 min with intermittent vortexing, the silica-bound DNA was pelleted by centrifugation at 15 000 rpm for 30 s and washed three times with ice-cold NEW wash solution (50 mM NaCl; 10 mM Tris [pH 8]; 2.5 mM EDTA; 50% ethanol). The DNA was eluted from

the silica matrix by resuspending the pellet in 7 µl of UHQ water and incubating the suspension at 55ºC for 5 min. Following centrifugation at 15 000 rpm for 1 min, the supernatant was collected. The purified DNA fragments were analyzed by electrophoresis on a 0.8% (w/v) agarose gel to assess both their purity and concentration.

3.2.5 Cloning of DNA fragments into plasmid vectors

3.2.5.1 Ligation of DNA fragments to vector DNA

PCR amplicons were ligated to pGEM®-T Easy vector DNA (Promega) according to the specifications of the manufacturer (Promega). Briefly, 300 ng of purified insert DNA was ligated to 50 ng of vector DNA at 15ºC for 16 h in a reaction mixture containing 5 µl of 2 × Rapid Ligation Buffer, 1 µl of T4 DNA ligase (3 U/µl) and UHQ water to a final volume of 10 µl. Digested DNA fragments (300 ng) and pAcGHLT-B baculovirus transfer vector DNA (100 ng) were ligated at 22ºC for 1 h in a reaction mixture consisting of 1 µl of T4 DNA ligase (5 U/µl), 4 µl of 5 × Rapid Ligation Buffer (Fermentas) and UHQ water to a final volume of 20 µl.

3.2.5.2 Preparation of competent cells

Competent *E. coli* DH5α cells were prepared and transformed according to the $CaCl_2$ method of Cohen *et al*. (1972), as described by Sambrook and Russell (2001) with slight modifications. A single colony from a freshly streaked culture of *E. coli* DH5α was inoculated into 100 ml of LB broth. The culture was incubated at 37°C with shaking (200 rpm) until an OD_{600} of 0.8 was reached, after which the cells were harvested by centrifugation at 5 000 rpm for 8 min at 4°C in a Sorvall centrifuge. The cell pellet was suspended gently in 5 ml of filter-sterilized, ice-cold transformation buffer (80 mM $CaCl_2$; 50 mM $MgCl_2$) and incubated on ice for 10 min. The cells were harvested, as above, and suspended in 10 ml of the transformation buffer. Following incubation on ice for 10 min the cells were again harvested and suspended in 5 ml of filter-sterilized, ice-cold 100 mM $CaCl_2$. Following addition of 1.5 ml of 50% (v/v) glycerol, the cells were aliquotted (200 µl) into 1.5-ml Eppendorf tubes and snap-frozen in liquid nitrogen prior to storage at -70°C.

3.2.5.3 Transformation of competent cells

Prior to transformation, the competent *E. coli* DH5α cells were allowed to thaw on ice. Each ligation reaction was mixed with 200 µl of competent cells and incubated on ice for 30 min. Following a heat-shock at 37°C for 5 min, 800 µl of pre-warmed (37°C) LB broth was added and the transformation mixtures incubated at 37°C with shaking for at least 30 min. Aliquots of 200 µl of transformed cells were plated onto LB agar supplemented with 100 µg/ml ampicillin. In instances where PCR amplicons were cloned into pGEM®-T Easy, 10 µl of 100 mM IPTG and 50 µl of 2% (w/v) X-Gal were also added. A positive control (10 ng of pUC18 plasmid DNA) and negative control (competent cells only) were also included to determine the competency of the *E. coli* DH5α cells and to test for contamination, respectively. The agar plates were incubated overnight at 37ºC.

3.2.5.4 Plasmid DNA extraction

Plasmid DNA was isolated using the alkaline lysis method (Birnboim and Doly, 1979), as described by Sambrook and Russell (2001). For small-scale plasmid extractions, a single bacterial colony was inoculated into 5 ml of LB broth, containing the appropriate antibiotic, and incubated overnight at 37ºC with active aeration (200 rpm). The cells from 3 ml of the overnight cultures were harvested by centrifugation at 15 000 rpm for 1 min and the cell pellet was suspended in 100 µl of ice-cold Solution I (50 mM glucose; 10 mM EDTA; 25 mM Tris; pH 8.0), followed by incubation at room temperature for 5 min and 1 min on ice. The cells were lysed by addition of 200 µl of freshly prepared Solution II (0.2 N NaOH; 1% [w/v] SDS) and incubated on ice for 5 min, after which 150 µl of ice-cold Solution III (3 M NaOAc; pH 4.8) wad added. After incubation on ice for 10 min and centrifugation at 15 000 rpm for 10 min, the plasmid DNA was precipitated from the recovered supernatants by addition of 2.5 volumes of 96% ethanol and incubation at -70ºC for 30 min. The plasmid DNA was pelleted by centrifugation at 15 000 rpm for 20 min, rinsed with 70% ethanol, vacuum-dried and then suspended in 30 µl of 1 × TE buffer (10 mM Tris-HCl; 1 mM EDTA; pH 8.0). Contaminating RNA was degraded by addition of 1 µl of RNase A (10 mg/ml), followed by incubation for 30 min at 37ºC.

Since *S. frugiperda* 9 (Sf-9) insect cells are sensitive to impurities in plasmid DNA preparations, which can influence transfection efficiencies, highly purified parental and recombinant

pAcGHLT-B baculovirus transfer plasmid DNA was prepared with the GeneJet™ plasmid miniprep kit (Fermentas) according to the manufacturer's instructions. Briefly, the cells from 3 ml of the overnight cultures were harvested by centrifugation at 15 000 rpm for 1 min. Following sequential addition of 200 µl each of a Resuspension solution and Lysis solution, 350 µl of neutralization solution was added to the cell pellet. The cell lysate was centrifuged at 11 000 rpm for 5 min and the cleared lysate was centrifuged through a GeneJet™ DNA-binding column at 11 000 rpm for 1 min. The column was washed twice in wash solution and the plasmid DNA was eluted in 50 µl of the supplied Elution buffer. The concentration and purity of the plasmid DNA was determined with a NanoDrop® ND-1000 spectrophotometer and ND-1000 v.3.3 software (NanoDrop Technologies, Inc.).

3.2.5.5 Restriction endonuclease digestions

Restriction endonuclease digestions were performed in Eppendorf tubes in a final volume of 15 µl and contained the appropriate concentration of salt (using the 10× buffer supplied by the manufacturer) for the specific enzyme and 1 U of enzyme per µg of plasmid DNA. The reaction mixtures were incubated for 1-2 h at 37ºC. Plasmid DNA digested with two enzymes that required different salt concentrations for optimal activity was first digested with the enzyme requiring a lower salt concentration, after which the salt concentration was adjusted and the second enzyme added. All restriction enzymes were supplied by Roche Diagnostics or Fermentas. The digestion products were analyzed on a 0.8% (w/v) agarose gel in the presence of appropriate DNA molecular weight markers.

3.2.6 Nucleotide sequencing and sequence analysis

The nucleotide sequence of cloned insert DNA was determined using the ABI-PRISM® BigDye™ Terminator v.3.1 Cycle Sequencing Ready Reaction kit (Perkin-Elmer Applied Biosystems) on a ABI PRISM® Model 377 DNA sequencer. In addition to the universal pUC/M13 forward and reverse sequencing oligonucleotides, a VP5-specific internal oligonucleotide was also used in the sequencing reactions (Table 3.1). The sequencing reactions were performed as described previously (Chapter 2, Section 2.2.4.4). Nucleotide sequences were analyzed with DNAMAN v.4.13 (Lynnon BioSoft) and BioEdit Sequence Alignment Editor v.5.0.6 (Hall, 1999) software programs. The hydrophobicity profile of the deduced AHSV-9 VP5 amino acid sequence was

predicted using the algorithm of Kyte and Doolittle (1982) with a window size of 13, while the Predict Protein server (www.predictprotein.org) was used for secondary structure analysis. Two putative α-helices, located at the N-terminus of VP5, were modeled as a helical wheel with the BioEdit software.

3.2.7 Plasmid constructs

All molecular cloning techniques employed in the construction of recombinant pAcGHLT-B baculovirus transfer vectors were performed according to the procedures described in the preceding sections. All plasmid constructs were verified by restriction endonuclease digestions and by nucleotide sequencing.

- **pAC-VP5**

Oligonucleotides VP5*PstI* and VP5*Bgl*505 were used with plasmid pBSVP5 as template DNA to amplify the full-length coding sequence of VP5. The 1.515-kb amplicon was cloned into pGEM®-T Easy to generate pGEM-VP5, and then recloned into the *Pst*I and *Bgl*II sites of pAcGHLT-B to generate pAC-VP5.

- **pAC-VP5Δ44-505**

Oligonucleotides VP5*KpnI* and VP5*Bgl*43 were used with plasmid pBSVP5 as template DNA to amplify a 129-bp amplicon, encoding the N-terminal 43 amino acids of VP5, which was cloned into pGEM®-T Easy to generate pGEM-VP5Δ44-505. The insert DNA was recovered and cloned into the *Kpn*I and *Bgl*II sites of pAcGHLT-B to generate pAC-VP5Δ44-505.

- **pAC-VP5Δ221-505**

Oligonucleotides VP5*KpnI* and VP5*Bgl*220 were used with plasmid pBSVP5 as template DNA to amplify a 660-bp amplicon, encoding the N-terminal 220 amino acids of VP5, which was cloned into pGEM®-T Easy to generate pGEM-VP5Δ221-505. The insert DNA was recovered and cloned into the *Kpn*I and *Bgl*II sites of pAcGHLT-B to generate pAC-VP5Δ221-505.

- **pAC-VP5Δ1-22**

Oligonucleotides VP5*Pst*23 and VP5R*Bgl* were used with plasmid pBSVP5 as template DNA to amplify a 1.446-kb amplicon, of which the N-terminal 22 amino acids of VP5 were deleted. The

amplicon was cloned into pGEM®-T Easy to generate pGEM-VP5Δ1-22. The insert DNA was recovered and cloned into the *Pst*I and *Bgl*II sites of pAcGHLT-B to generate pAC-VP5Δ1-22.

- **pAC-VP5Δ1-43**

Oligonucleotides VP5*Pst*44 and VP5R*Bgl* were used with plasmid pBSVP5 as template DNA to amplify a 1.386-kb amplicon, of which the N-terminal 43 amino acids of VP5 were deleted. The amplicon was cloned into pGEM®-T Easy to generate pGEM-VP5Δ1-43. The insert DNA was recovered and cloned into the *Pst*I and *Bgl*II sites of pAcGHLT-B to generate pAC-VP5Δ1-43.

- **pAC-VP5Δ1-123**

Oligonucleotides VP5*Pst*124 and VP5R*Bgl* were used with plasmid pBSVP5 as template DNA to amplify a 1.146-kb amplicon, of which the N-terminal 123 amino acids of VP5 were deleted. The amplicon was cloned into pGEM®-T Easy to generate pGEM-VP5Δ1-123. The insert DNA was recovered and cloned into the *Pst*I and *Bgl*II sites of pAcGHLT-B to generate pAC-VP5Δ1-123.

- **pAC-VP5Δ1-279**

Oligonucleotides VP5*Kpn*I and VP5*Bgl*505 were used with plasmid pBSVP5 as template DNA to amplify a 675-bp amplicon, of which the N-terminal 279 amino acids of VP5 were deleted. The amplicon was cloned into pGEM®-T Easy to generate pGEM-VP5Δ1-279. The insert DNA was recovered and cloned into the *Kpn*I and *Bgl*II sites of pAcGHLT-B to generate pAC-VP5Δ1-279.

3.2.8 Generation of recombinant baculoviruses

3.2.8.1 Cells and culture conditions

Spodoptera frugiperda clone 9 (Sf-9) cells were propagated at 27ºC, either as monolayers in 75 cm^2 tissue culture flasks or as suspension cultures in Spinner flasks, in TC-100 medium (Sigma-Aldrich) supplemented with 10% (v/v) fetal bovine serum (FBS) and the appropriate antibiotics (60 mg/ml penicillin; 60 mg/ml streptomycin; 150 mg/ml Fungizone) (Highveld Biological). For suspension cultures, the cell density was determined using a haemocytometer. Cultures were seeded at an initial density of 5×10^5 cells/ml and subcultured when they reached 2×10^6 cells/ml. Viability of the cells was determined by staining the cells with Trypan blue (0.4% [w/v] in 1 × PBS), as described by Summers and Smith (1987).

3.2.8.2 Co-transfection of Sf-9 cells

Sf-9 cells were seeded at a density of 2×10^6 cells in 60-mm tissue culture plates (Falcon®) and allowed to attach at 27ºC for 30 min. For each transfection, 0.5 µg of linearized BaculoGold™ DNA (BD Biosciences) and 2-5 µg of parental or recombinant baculovirus transfer vector were combined, mixed well by gentle vortexing and incubated at room temperature for 5 min before addition of 1 ml of Transfection Buffer B (25 mM HEPES [pH 7.1]; 125 mM $CaCl_2$; 140 mM NaCl). In the meantime, the medium was aspirated from the cell monolayers and the cells were rinsed twice with 2 ml of incomplete TC-100 medium (lacking serum and antibiotics), before being replaced with 1 ml of Transfection Buffer A (Grace's Medium supplemented with 10% [v/v] FBS). Following dropwise addition of the Transfection Buffer B-DNA solution, the cell monolayers were incubated at 27°C for 4 h. The transfection mixtures were then removed and the cell monolayers were rinsed once with 3 ml of complete TC-100 medium (containing 10% [v/v] FBS and antibiotics). The medium was aspirated and replaced with 3 ml of complete TC-100 medium, after which the plates were incubated at 27°C for 5 days. Mock-infected cells were included as a control whereby infection of the cells could be monitored.

3.2.8.3 Plaque assays

Plaque assays were performed to determine the virus titre, as described by Brown and Faulkner (1977) with slight modifications. Sf-9 cells were seeded in 35-mm-diameter wells (1×10^6 cells/well) and after adsorption at 27°C for 1 h the medium was replaced with 900 µl of the virus dilution (10^{-4} to 10^{-9} prepared in incomplete TC-100 medium). After incubation at room temperature for 1 h to allow virus particles to infect the cells, the virus dilutions were removed and the cells were overlaid gently with 2 ml of 3% (w/v) low melting temperature agarose (Sigma-Aldrich) diluted 1:1 in TC-100 medium. The tissue culture plates were incubated at 27°C for 5-7 days in a humid environment. The cells were stained with 500 µl of 0.1% (w/v) Thiazolyl Blue Tetrazolium Bromide (Sigma-Aldrich) and incubation was continued at 27°C until plaques became visible. For each recombinant virus, a plaque was plucked as an agarose plug with an Eppendorf pipette and placed in an Eppendorf tube containing 1 ml of TC-100 medium. The viruses were eluted from the agarose plugs by incubation overnight at 4°C, followed by vigorous vortexing. Each well of a 6-well tissue culture plate was seeded at 1×10^6 cells/well and 400 µl of each plaque pickup was added to separate wells in a final volume of 2 ml of complete TC-100

medium. Following incubation at 27°C for 3 days, the virus-containing supernatant of this passage one stock was collected and centrifuged at 1 000 rpm for 5 min at 4°C to remove cell debris. The supernatants were stored at 4°C, titrated as described above, and then used to prepare large-scale virus stocks.

3.2.8.4 Preparation of large-scale virus stocks

To prepare stocks of the parental and respective recombinant baculoviruses, 100 ml of Sf-9 cells, propagated as a suspension culture at 1×10^6 cells/ml in complete TC-100 medium, were infected with the recombinant baculoviruses at a multiplicity of infection (MOI) of 0.1 PFU/cell. Following incubation at 27°C for 5 days, the supernatants were collected by centrifugation at 3 000 rpm for 10 min, filter-sterilized using a 0.2-µm low protein-binding filter (Cameo 25AS) and then stored at 4°C in the dark. The titre of the respective baculovirus stocks was determined, as described above.

3.2.9 Analyses of recombinant baculovirus-expressed proteins

3.2.9.1 Expression of recombinant fusion proteins

Parental and recombinant baculoviruses were used to infect Sf-9 cell monolayers in 75 cm^2 tissue culture flasks (1×10^7 cells/flask) at a MOI of 10 PFU/cell. Following incubation at 27°C for 30-72 h, mock-infected or baculovirus-infected Sf-9 cells were harvested from the surface of tissue culture flasks with a syringe, collected by centrifugation at 3 000 rpm for 5 min and washed once with 1 × phosphate-buffered saline (PBS: 137 mM NaCl; 2.7 mM KCl; 4.3 mM $Na_2HPO_4.2H_2O$; 1.4 mM KH_2PO_4; pH 7.4). The cell pellets were each suspended in 5 ml of ice-cold Insect Cell Lysis Buffer (10 mM Tris [pH 7.5]; 130 mM NaCl; 1% Triton X-100; 10 mM NaF; 10 mM NaPi; 10 mM NaPPi), containing reconstituted Protease Inhibitor Cocktail (50 mM PMSF, 800 µg/ml benzamidine HCl, and 500 µg/ml of each phenanthroline, aprotinin, leupeptin and pepstatin A), and incubated on ice for 45 min. Prior to SDS-PAGE analysis, an equal volume of 2 × protein solvent buffer (PSB: 125 mM Tris-HCl [pH 6.8]; 4% [w/v] SDS; 20% [v/v] glycerol; 10% [v/v] 2-mercaptoethanol; 0.002% [w/v] bromophenol blue) was added to each cell lysate, and the samples were heated for 10 min in boiling water.

3.2.9.2 SDS-polyacrylamide gel electrophoresis (SDS-PAGE)

Protein samples were analyzed by SDS-PAGE, as described by Laemmli (1970). A 5% (w/v) acrylamide stacking gel and 12% (w/v) acrylamide separating gel was used, of which the acrylamide:bisacrylamide ratio was 30:0.8. The low-porosity separating gel (0.375 M Tris-HCl [pH 8.8]; 0.1% [w/v] SDS) and high-porosity stacking gel (0.125 M Tris-HCl [pH 6.8]; 0.1% [w/v] SDS) were each polymerized by addition of 0.08% (w/v) ammonium persulphate and 0.008% (v/v) TEMED. The TGS electrophoresis buffer consisted of 0.025 M Tris-HCl (pH 8.3), 0.192 M Glycine and 0.1% (w/v) SDS. Electrophoresis was performed in a Hoefer Sturdier™ SE400 electrophoresis unit for 16 h at 70 V or in a Hoefer Mighty Small™ SE260 electrophoresis unit for 2.5 h at 120 V. After electrophoresis, the gels were stained for 20 min with 0.125% (w/v) Coomassie brilliant blue (prepared in 50% methanol, 10% acetic acid) and the proteins were visualized by counterstaining the gels in a solution containing 25% methanol and 10% glacial acetic acid.

3.2.9.3 Immunoblot analysis

Immunoblot analysis of the recombinant baculovirus-expressed proteins was performed, as described by Sambrook and Russell (2001). Following SDS-PAGE, the gel, two sheets of filter paper and a Hybond™-C^+ nitrocellulose membrane (Amersham Pharmacia Biotech AB), cut to the same size as the gel, were equilibrated for 30 min in transfer buffer (25 mM Tris; 186 mM Glycine). The proteins were electroblotted onto the membrane for 1.5 h at 28 V and 120 mA, using a Mighty Small™ Transphor blotting apparatus (Hoefer). Following transfer, the gel was recovered and stained with Coomassie brilliant blue to determine the efficiency of the transfer process. The membrane was washed once in 1 × PBS for 5 min and non-specific binding sites were blocked by incubating the membrane overnight at 4ºC in blocking solution (1% [w/v] fat-free milk powder in 1 × PBS). The membrane was transferred to 1 × PBS containing the primary antibody. These comprised either a polyclonal anti-GST antibody (Calbiochem) or an AHSV-9 antiserum (Onderstepoort Veterinary Institute), which was diluted 1:200 and 1:100 in 1 × PBS, respectively. Following incubation at room temperature for 2 h with gentle agitation, the unbound primary antibodies were removed by washing the membrane three times for 5 min each in wash buffer (0.05% [v/v] Tween-20 in 1 × PBS). The secondary antibody, Protein-A conjugated to horseradish peroxidase (Sigma-Aldrich) diluted 1:1000 in 1 × PBS, was added to

the membrane and then incubated at room temperature for 1 h. The membrane was washed three times for 5 min each in wash buffer, and once for 5 min in 1 × PBS. To detect immuno-reactive proteins, the membrane was immersed in a freshly prepared enzyme substrate solution (60 mg 4-chloro-1-naphtol in 20 ml of ice-cold methanol and 60 µl of H_2O_2 in 100 ml of 1 × PBS, mixed just before use). Once the bands became visible, the membrane was rinsed with distilled water and air-dried.

3.2.10 Cytotoxicity assays

3.2.10.1 Determination of the optimal cell concentration

To determine the optimal cell concentration for use in cytotoxicity assays, Sf-9 cells (2×10^6 cells/ml) were titrated by two-fold serial dilutions across a 96-well flat-bottom microtitre plate (Greiner BioOne) by adding 100 µl of the cells to 100 µl of assay medium (TC-100 medium supplemented with 2% [v/v] FBS and antibiotics). Following cell attachment at 27°C for 30 min, the medium was aspirated and 100 µl of fresh assay medium was added to each well. For each cell concentration, three experimental controls were performed in triplicate. The background control consisted of 200 µl of assay medium per well, which provided information regarding the lactate dehydrogenase (LDH) activity contained in the assay medium. The low control consisted of 100 µl of assay medium added to 100 µl of cells, and provided information regarding spontaneous LDH release from Sf-9 cells. For the high control, 100 µl of assay medium, supplemented with Triton X-100 at a final concentration of 2% (v/v), was used to lyse the cells in order to determine the maximum LDH release from Sf-9 cells. The cells were incubated at 27°C for 24 h in a humidified incubator. Following incubation, the microtitre plates were centrifuged at 1 000 rpm for 10 min, using a Sigma-Aldrich 4K15C plate centrifuge fitted with a 09100F swing-out rotor, and the supernatant (100 µl) was transferred to corresponding wells of an optically clear microtitre plate. To determine the LDH activity in these supernatants, 100 µl of freshly prepared reaction mixture (250 µl of Catalyst [Diaphorase/NAD^+] and 11.25 ml of Dye solution [Iodotetrazolium chloride and sodium lactate] per 100 reactions) was added to each well and incubated at 25°C for 30 min in the dark. The samples were read at 492 nm against the assay medium (background control) as the blank with a Multiskan Ascent ELISA plate reader. The cell concentration in which the difference between the low and high control is at a maximum, was used in subsequent assays.

3.2.10.2 Cytotoxicity of baculovirus-expressed VP5 proteins

The cytotoxicity resulting from recombinant VP5 protein expression in Sf-9 cells was analyzed using a Cytotoxicity Detection Kit (Roche Applied Science) according to the specifications of the manufacturer. Since FBS contains various amounts of LDH, which may increase background absorbance in the assay, the assay was performed in the presence of low serum concentrations (*i.e.* 2% [v/v]). Moreover, low and high control samples, as described above, were included in each experiment to respectively correct for the spontaneous and maximum release of LDH from uninfected cells. Sf-9 cells were seeded in 96-well flat-bottom microtitre plates (Greiner BioOne) at a density of 1.5×10^4 cells/well and allowed to attach at 27ºC for 30 min. The cells were infected with recombinant baculovirus at a MOI of 10 PFU/cell in 30 µl of incomplete TC-100 medium. Following virus adsorption at room temperature for 1 h, 170 µl of TC-100 medium (supplemented with 2% [v/v] FBS and antibiotics) was added to each well, and the microtitre plates were incubated at 27°C for 30 h. Following incubation, the microtitre plates were centrifuged at 1 000 rpm for 10 min, the supernatants were transferred to corresponding wells of an optically clear microtitre plate and processed for the detection of LDH activity as described above. The percent cytotoxicity of each recombinant VP5 protein was calculated by substitution of the mean absorbance values at 492 nm in the following equation: cytotoxicity (%) = [(experimental value) – (low control) / (high control – low control)] × 100. Three independent experiments, each consisting of triplicate samples, were performed.

3.2.10.3 Cytotoxicity of synthetic VP5 peptides

Different synthetic VP5 peptides, indicated in Table 3.2 and synthesized by Genscript Corporation, were used to confirm the VP5 expression data. Stock solutions (4 mg/ml) of the peptides were prepared by suspension of the lyophilized peptides in sterile UHQ water and aliquots were stored at -20°C until required. Working solutions of each synthetic VP5 peptide were prepared by diluting the peptides to a final concentration of 50 µM in 50 µl of TC-100 medium (containing 2% [v/v] FBS and antibiotics). Sf-9 cells were seeded in 96-well flat-bottom microtitre plates at a density of 1.5×10^4 cells/well. Following cell attachment at 27°C for 30 min, the Sf-9 cell monolayers were overlaid with the VP5 peptides and incubated at room temperature for 1 h. Thereafter, 150 µl of TC-100 medium (supplemented with 2% [v/v] FBS and antibiotics) was added to each well, followed by incubation at 27ºC for 24 h. The

cytotoxicity assays, inclusive of appropriate controls, were performed in triplicate as described above.

Table 3.2 Synthetic peptides used in cytotoxicity assays

Peptide	Amino acid sequence	VP5 coding region
VP5(1-43)	MGKFTSFLKRAGSATKKALTSDAAKRMYKMAGKTLQKVVESEV	aa 1 to 43
VP5(1-22)	MGKFTSFLKRAGSATKKALTSD	aa 1 to 22
VP5(23-43)	AAKRMYKMAGKTLQKVVESEV	aa 23 to 43
VP5(280-301)	PHIIEKAMLKDKIPDNELAMAI	aa 280 to 301

3.3 RESULTS

3.3.1 Secondary structure analysis of AHSV-9 VP5

The nucleotide sequence of the full-length cDNA copy of AHSV-9 genome segment M6, contained in plasmid pBSVP5, was determined by automated sequencing procedures, and the deduced amino acid sequence was used in secondary structure analyses. The hydrophobic profile of the 505 residues of the AHSV-9 VP5 protein indicated a clear partition between two domains: an N-terminal domain (amino acids 1 to 220) and a C-terminal domain (amino acids 280 to 505), separated by a hydrophobic hinge region (amino acids 220 to 280) that is rich in alanine and glycine residues (Fig. 3.1A). Two amphipathic α-helices were also identified in the first 43 residues at the N-terminus of VP5, which were immediately followed by a stretch of hydrophobic residues (amino acids 43 to 60) (Fig 3.1A). Helical wheel representation of amino acids 1 to 22 (α-helix 1) and amino acids 23 to 43 (α-helix 2) of VP5 revealed that both helices have a net-positive charge on their hydrophilic faces as a result of the clustering of positively charged lysine residues (K) (Fig. 3.1B). The latter may allow the helices to interact with negatively charged phospholipids present in cell membranes. Indeed, cationic amphipathic α-helices are motifs common to many polypeptides with membrane-destabilizing properties and have been implicated in the membrane-binding activity of viral fusion proteins (Epand *et al*., 1995; Weissenhorn *et al*., 2007; White *et al*., 2008). The results of these analyses therefore provide support for the notion that VP5 may be a membrane-destabilizing protein.

(A)

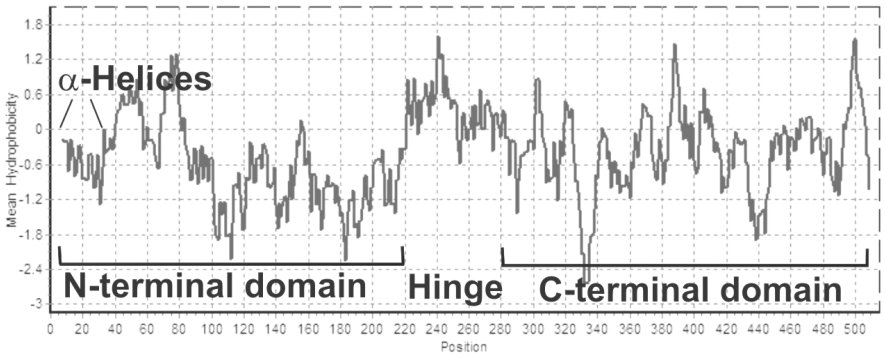

(B)

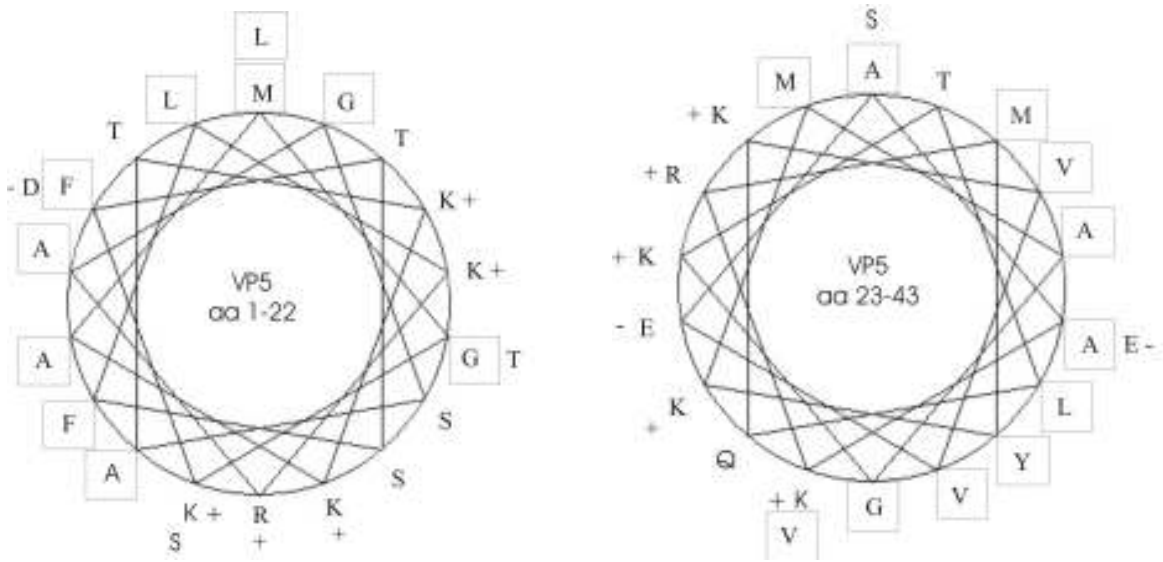

Fig. 3.1 **Structural features and domains of the AHSV-9 VP5 protein.** (A) Hydrophobicity profile of VP5, as predicted using the algorithm of Kyte and Doolittle (1982) with a window setting of 13. (B) Helical wheel diagrams showing the amphipathic nature of each predicted α-helix at the N-terminus of VP5. Each panel represents an α-helix viewed along the helix axis. Hydrophobic amino acid residues are boxed.

3.3.2 Construction of recombinant baculoviruses expressing full-length and truncated VP5 proteins

Towards determining which region(s) of the VP5 protein plays a role in its reported cytotoxicity (du Plessis and Nel, 1997; Martinez-Torrecuadrada *et al*., 1999), full-length and different truncated VP5 fragments were generated by PCR amplification using plasmid pBSVP5 as template DNA and oligonucleotides complementary to the relevant AHSV-9 VP5 coding sequence (Table 3.1). In the case of BTV VP5, it has been reported that glutathione *S*-transferase (GST) fusion proteins are expressed at higher levels than is untagged VP5 protein, suggesting that masking of the N-terminus allows higher levels of proteins to stably accumulate (Hassan *et al*., 2001). Consequently, the PCR amplicons were first ligated to pGEM®-T Easy vector DNA and then cloned into the GST baculovirus transfer vector pAcGHLT-B, as described under Materials and Methods (Section 3.2.7).

To confirm successful cloning of the respective VP5 fragments into pAcGHLT-B (Fig. 3.2A), transformants were selected randomly and the extracted plasmid DNA was characterized by agarose gel electrophoresis, following restriction enzyme digestion with enzymes of which the recognition sequences had been incorporated into the designed oligonucleotides. In all cases, insert DNAs of the expected sizes were excised by digestion with *Pst*I and either *Kpn*I or *Bgl*II (Fig. 3.2B). The integrity of the cloned insert DNA was furthermore confirmed by automated sequencing procedures, the results of which indicated the presence of an open reading frame fused in-frame with the GST tag sequence and the absence of nucleotide alterations.

The recombinant baculovirus transfer vector encoding the full-length VP5 protein was designated pAC-VP5, while those encoding the N-terminal 43 or 220 amino acids of VP5 were designated pAC-VP5Δ44-505 and pAC-VP5Δ221-505, respectively. Recombinant baculovirus transfer vectors encoding VP5 proteins of which the N-terminal 22, 43, 123 and 279 amino acids were deleted, were respectively designated pAC-VP5Δ1-22, pAC-VP5Δ1-43, pAC-VP5Δ1-123 and VP5Δ1-279.

(A)

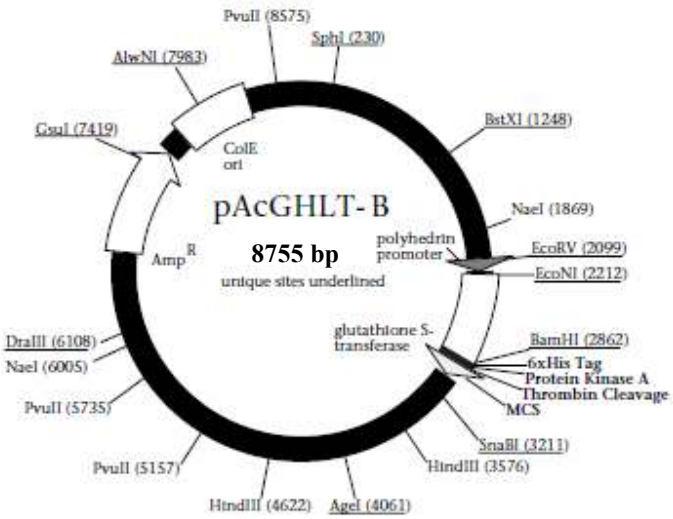

(B)

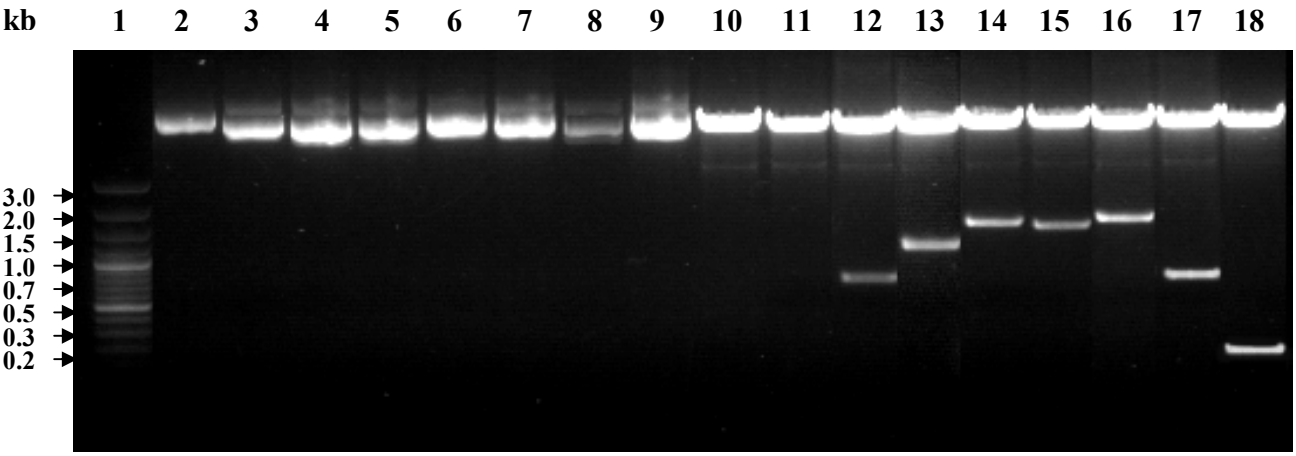

Fig. 3.2 **Construction of recombinant pAcGHLT-B vectors.** (A) Plasmid map of the pAcGHLT-B baculovirus transfer vector. (B) Agarose gel electrophoretic analysis of the recombinant pAcGHLT-B baculovirus transfer vectors. Lane 1, DNA molecular weight marker; lane 2, uncut parental pAcGHLT-B vector DNA; lane 3, uncut recombinant plasmid pAC-VP5Δ280-505; lane 4, uncut recombinant plasmid pAC-VP5Δ124-505; lane 5, uncut recombinant plasmid pAC-VP5Δ44-505; lane 6, uncut recombinant plasmid pAC-VP5Δ23-505; lane 7, uncut recombinant plasmid pAC-VP5; lane 8, uncut recombinant plasmid pAC-VP5Δ1-220; lane 9, uncut recombinant plasmid pAC-VP5Δ1-43; lane 10, parental pAcGHLT-B vector DNA digested with both *Pst*I and *Bgl*II; lane 11, parental pAcGHLT-B vector DNA digested with both *Kpn*I and *Bgl*II; lane 12, pAC-VP5Δ280-505 vector DNA digested with both *Kpn*I and *Bgl*II; lane 13, recombinant plasmid pAC-VP5Δ124-505 DNA digested with both *Pst*I and *Bgl*II; lane 14, recombinant plasmid pAC-VP5Δ44-505 DNA digested with both *Pst*I and *Bgl*II; lane 15, recombinant plasmid pAC-VP5Δ23-505 DNA digested with both *Pst*I and *Bgl*II; lane 16, recombinant pAC-VP5 vector DNA digested with both *Pst*I and *Bgl*II; lane 17, pAC-VP5Δ1-220 vector DNA digested with both *Kpn*I and *Bgl*II; lane 18, recombinant plasmid pAC-VP5Δ1-43 DNA digested with both *Kpn*I and *Bgl*II. The sizes of the DNA molecular weight marker, GeneRuler™ 100-bp DNA Ladder Plus (Fermentas), are indicated to the left of the figure.

3.3.3 Characterization of VP5 proteins synthesized in recombinant baculovirus-infected Sf-9 cells

Recombinant baculoviruses were obtained by co-transfecting Sf-9 cells with the respective recombinant baculovirus transfer vectors and linearized BaculoGold™ DNA. BaculoGold™ DNA (BD Biosciences) is a modified *Autographa californica* nuclear polyhedrosis virus (AcNPV) DNA, which contains a lethal deletion and does not code for viable virus. Co-transfection of the recombinant pAcGHLT-B transfer vector and the linearized BaculoGold™ DNA into Sf-9 cells allows recombination between homologous sites, transferring the heterologous gene from the vector to the BaculoGold™ DNA, thereby rescuing the lethally deleted virus and giving rise to recombinant baculoviruses. Virus stocks were subsequently prepared from plaque-purified viruses. A representation of the full-length and truncated VP5 fusion proteins used in this study is shown in Fig. 3.3A.

To determine whether the full-length and truncated VP5 proteins were expressed in Sf-9 cells by the respective baculovirus recombinants, cell monolayers were mock-infected or infected at a MOI of 10 PFU/cell. The recombinant proteins were expressed at maximal levels between 30 and 48 h post-infection, after which the expression levels declined significantly (results not shown). Expression of the respective VP5 fusion proteins, analyzed 48 h after infection by SDS-PAGE, is presented in Fig. 3.3B. Analysis of the Coomassie blue-stained gel indicated the presence of a unique protein in each of the cell lysates prepared from cell monolayers infected with the baculovirus recombinants. The molecular mass of these proteins was in agreement with the predicted molecular mass of the GST-tagged full-length or truncated AHSV-9 VP5 proteins (Fig. 3.3A). Subsequent immunoblot analyses indicated that the recombinant fusion proteins were recognized by both a polyclonal anti-GST antibody (Fig. 3.3C) and an anti-AHSV-9 polyvalent serum (Fig. 3.3D), thus confirming successful expression of GST-tagged full-length and truncated VP5 by means of the generated baculovirus recombinants. However, the recombinant proteins VP5Δ1-279, VP5Δ1-123 and VP5Δ44-505 reacted weakly with the AHSV-9 antiserum, possibly due to the antigenic determinants of VP5 being located at the N-terminal end of the protein (Martinez-Torrecuadrada *et al*., 1999).

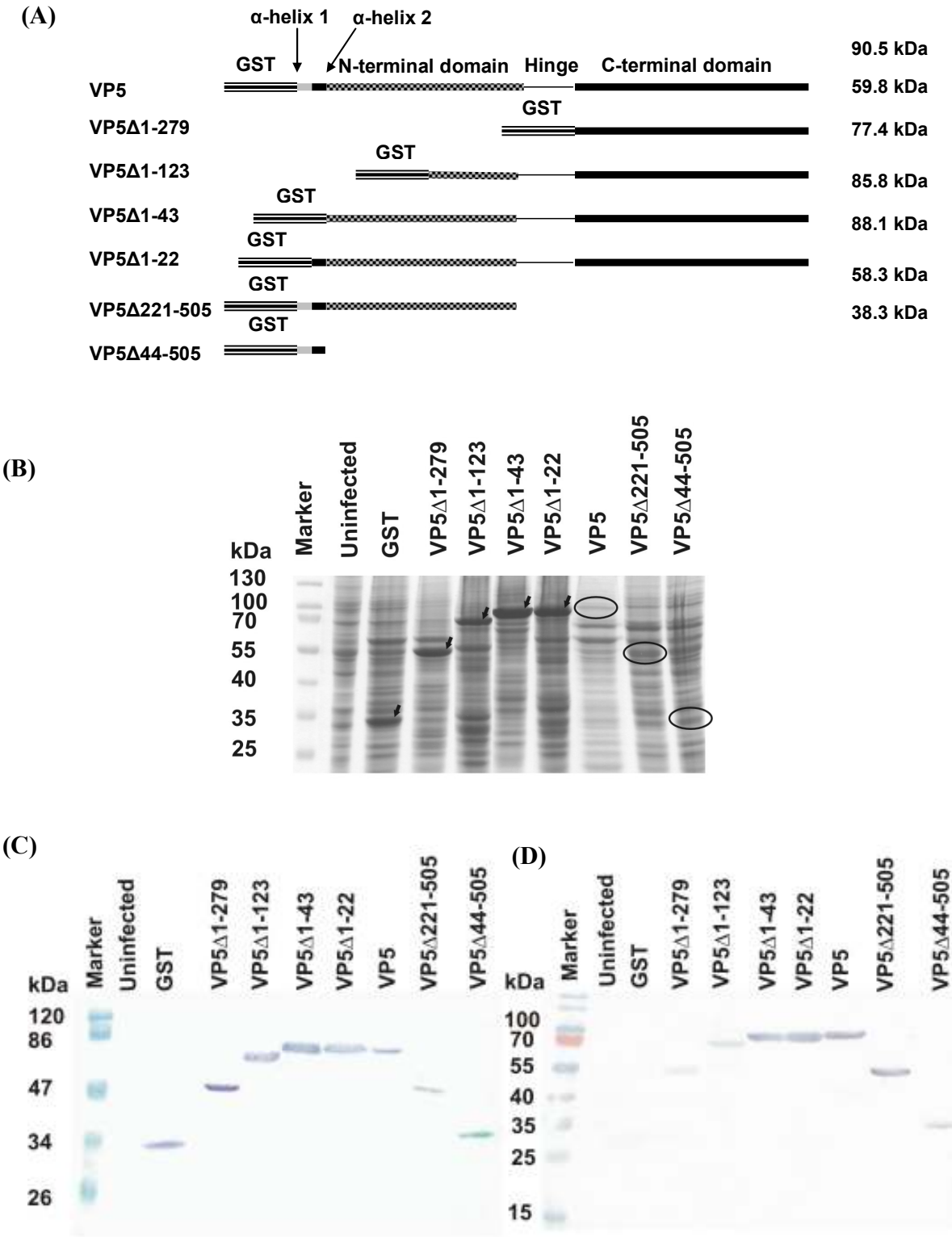

Fig. 3.3 **Baculovirus expression of full-length and truncated VP5 fusion proteins in Sf-9 cells.** (A) Schematic representation of the full-length and truncated VP5 proteins expressed as GST fusion proteins in Sf-9 cells. (B) SDS-PAGE analysis of Sf-9 lysates recovered after 48 h of infection by each of the recombinant baculoviruses. The low expression of the full-length and C-terminal truncated VP5 fusion proteins is indicated. (C) Immunoblot analyses were performed with polyclonal anti-GST or (D) anti-AHSV-9 antibodies. The sizes of molecular mass markers (kDa) are indicated to the left of the figures. Uninfected Sf-9 cells and a GST-expressing baculovirus were included as controls.

Notably, compared to the full-length VP5 fusion protein, deletions from the N-terminus resulted in an increase in the amount of VP5 fusion protein produced. Indeed, the GST-tagged truncated VP5 proteins VP5Δ1-279, VP5Δ1-123, VP5Δ1-43 and VP5Δ1-22 were each expressed at levels approximating that of the GST protein (33.6 kDa). In contrast, expression of the VP5Δ221-505 and VP5Δ44-505 recombinant proteins were barely detectable, indicating that deletions from the C-terminus resulted in a decrease in the amount of VP5 fusion protein produced (Figs 3.3B and C). This inverse correlation between the presence of the VP5 N-terminus and the level of expression observed suggested a sequence-specific effect rather than it being the result of differences in the size of the synthesized protein products.

3.3.4 Effect of baculovirus-expressed full-length and truncated VP5 proteins on plasma membrane permeability of Sf-9 cells

The cytopathic effects of several viruses may result from the altered membrane permeability of the host cell due to the expression of a single viral polypeptide (Guinea and Carrasco, 1994; Denisova *et al*., 1999; Davis *et al*., 2008). Therefore, the ability of the recombinant baculovirus-expressed full-length and truncated VP5 fusion proteins to permeabilize Sf-9 cells was evaluated, and cytotoxicity (cell leakage) was determined using a Cytotoxicity Detection Kit (Roche Applied Science). This quantitative assay measures levels of lactate dehydrogenase (LDH), a stable cytoplasmic enzyme that is released when the plasma membrane is damaged. The amount of LDH present in the supernatant is directly proportional to the number of lysed cells. This assay reveals low-level damage to cell membranes, gives values similar to those obtained using ^{51}Cr release assays (Korzeniewski and Callewaert, 1983; Decker and Lohmann-Matthes, 1988) and has been used successfully in other virus-induced cytotoxicity studies (Newton *et al*., 1997; Hassan *et al*., 2001).

Sf-9 cells were infected with the respective recombinant baculoviruses and the cytotoxicity of each of the expressed full-length and truncated GST-VP5 fusion proteins was determined at 30 h post-infection by measuring the amount of released LDH (Fig. 3.4A). Expression of the GST-tagged full-length VP5 protein, as well as expression of VP5 fusion proteins with C-terminal deletions (*i.e.* VP5Δ221-505 and VP5Δ44-505) induced substantial release of LDH, with VP5Δ44-505 exhibiting the highest activity (cytotoxicity of *ca*. 98%). In contrast, expression of

VP5 fusion proteins with deletions from the N-terminus (*i.e.* VP5Δ1-123, VP5Δ1-43 and VP5Δ1-22) resulted in comparatively low levels of LDH release (Fig. 3.4A). Based on the low cytotoxicity (*ca.* 3.3%) associated with the expression of the GST protein only, and considering that GST is unable to associate with liposomes (Davis *et al*., 2008), these results therefore indicated that the cytotoxicity observed with the VP5 fusion proteins was mediated by the VP5 component. Notably, the presence of the two amphipathic α-helices at the N-terminus of VP5 correlated strongly with increased cytotoxicity and thus membrane permeabilization.

3.3.5 Effect of synthetic VP5 peptides on plasma membrane permeability of Sf-9 cells

To ascertain whether the two predicted N-terminal amphipathic α-helices individually or in combination trigger LDH release, four synthetic VP5 peptides were generated. Two of these peptides, designated VP5(1-22) and VP5(23-43), were composed of amino acids 1 to 22 (α-helix 1) and amino acids 23 to 43 (α-helix 2), respectively, whereas the third peptide, designated VP5(1-43), encompassed both α-helices. The fourth peptide, designated VP5(280-301), was composed of residues at the VP5 C-terminal region (amino acids 280-301). This peptide was used as a control since baculovirus expression of the VP5 fusion protein VP5Δ1-279 resulted in neglible cytotoxicity (Fig. 3.4A). Uninfected Sf-9 cell monolayers were incubated with each synthetic peptide for 24 h, and the cell culture supernatants were subsequently assayed for the amount of LDH released. The results of this assay indicated that the VP5(1-43) peptide caused substantial release of LDH (cytotoxicity of *ca*. 100%), while none of the other three VP5 peptides assessed showed any such effect (Fig. 3.4B). This data therefore indicated that both N-terminal amphipathic α-helices of VP5 were required to permeabilize the plasma membrane of Sf-9 cells.

3.4 DISCUSSION

In order for a virus to infect a cell, the virus must be able to attach to the cell surface, penetrate and subsequently become sufficiently uncoated to make its genome accessible for the viral or host machinery for transcription or translation to occur. In contrast to enveloped viruses that posses virus-encoded integral membrane proteins that are responsible for membrane fusion (White *et al*., 2008), AHSV and other members of the *Reoviridae* family are non-enveloped viral particles (Calisher and Mertens, 1998). It is therefore to be expected that the proteins constituting

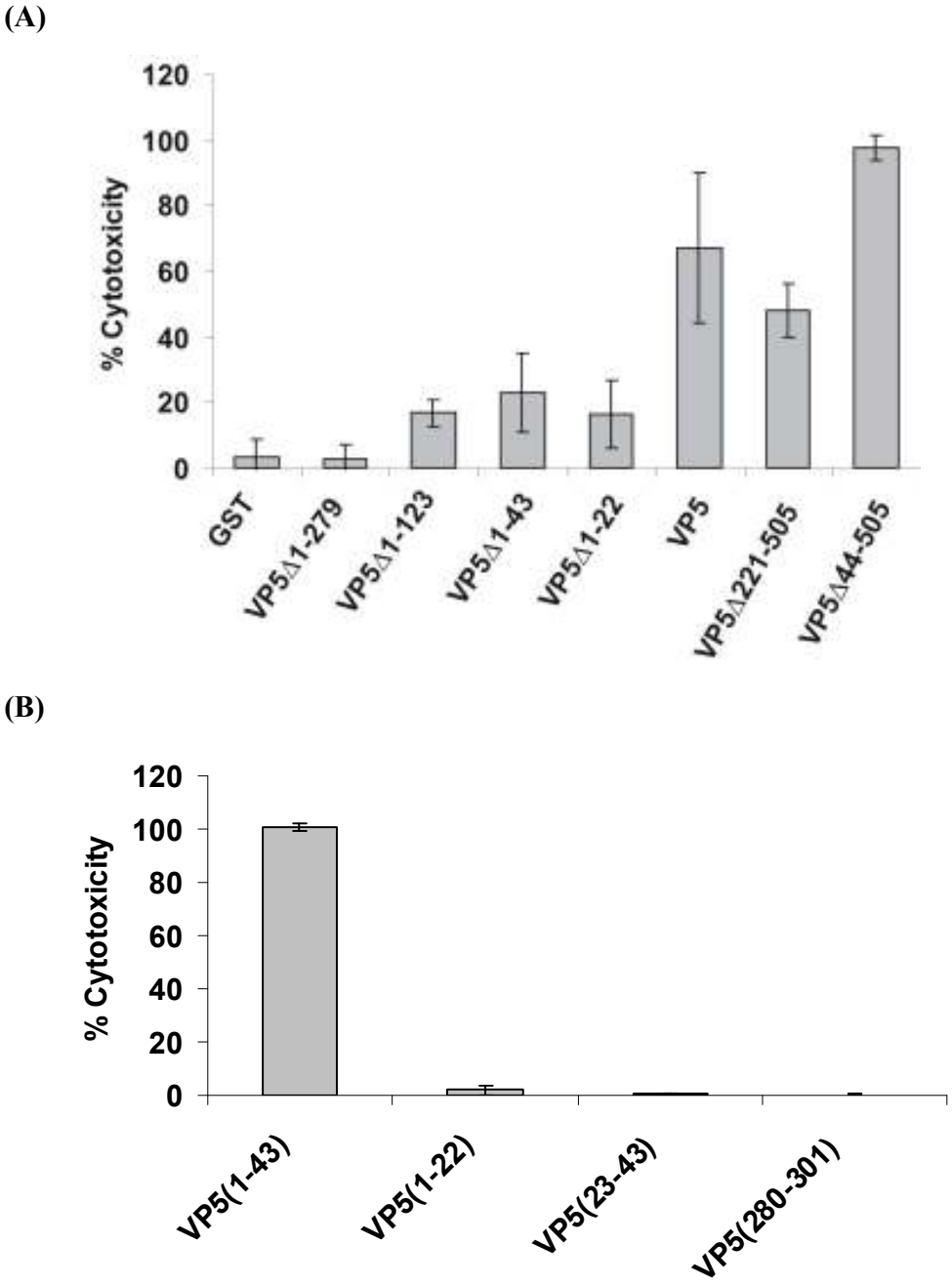

Fig. 3.4 **Membrane permeabilization of Sf-9 cells by VP5.** (A) Cell cytotoxicity of baculovirus-expressed full-length and truncated VP5 fusion proteins expressed in Sf-9 cells by recombinant baculoviruses at 30 h post-infection. Sf-9 cells infected with a baculovirus expressing GST only served as a control. (B) Cell cytotoxicity of three synthetic N-terminal peptides encompassing the amphipathic helices [VP5(1-43), VP5(1-22) and VP5(23-43)] and a control C-terminal peptide [VP5(280-301)]. Each peptide was added to Sf-9 cells, followed by LDH release assays at 24 h post-treatment. In both assays, the amount of LDH release was measured (OD_{492}) from triplicate wells and used to calculate the percent cytotoxicity, as described under Materials and Methods. Bars show mean ± SD of three independent experiments.

the outer surface of the virus must adopt a structural organization such that they can perform essentially the same function as the lipid-embedded proteins of enveloped viruses, *e.g.* the transport of virus through the lipid bilayer from the extracellular medium and delivery of the virus capsid or genomes into the host cell (Tsai, 2007; Banerjee and Johnson, 2008). For BTV, the outer capsid protein VP5, which is highly cytotoxic to cells, has been implicated in virus-cell penetration during the early stages of infection (Hassan *et al.*, 2001). Likewise, the AHSV VP5 protein is also cytotoxic when expressed in heterologous hosts (du Plessis and Nel, 1997; Martinez-Torrecuadrada *et al.*, 1999), but is biological function has not yet been investigated. Consequently, this part of the investigation was aimed at identifying the domain(s) within the AHSV-9 VP5 protein responsible for the observed cytotoxicity with a view to gain an understanding of its biological function.

Secondary structure analyses of AHSV-9 VP5 revealed that the N-terminus of the protein contains two amphipathic α-helices. Such amphipathic structures are generally found in fusion peptides and allow the peptides to bind to and alter the structure of lipid bilayers by forming pores that destabilize the membrane potential (Wiley and Skehel, 1987; White, 1990; Chan *et al*., 1997; Baker *et al*., 1999). Consequently, N-terminally GST-tagged VP5 fusion proteins were examined in the baculovirus/insect cell expression system and VP5 cytotoxicity was investigated with a LDH release assay. The results confirmed earlier observations (du Plessis and Nel, 1997; Martinez-Torrecuadrada *et al.*, 1999) that VP5 is cytotoxic to cells, and mutation analysis indicated that the presence of two amphipathic α-helices at the N-terminus correlated with cell toxicity and membrane damage. These results are in agreement with several reports indicating that the ability of viruses to modify membrane permeability and induce cell lysis is mediated by a single viral gene product and does not require the assembly of virus particles (Guinea and Carrasco, 1994; Denisova *et al*., 1999; Hassan *et al.*, 2001; Davis *et al*., 2008). By making use of *in vitro*-synthesized peptides, together with LDH release assays, it was furthermore shown that the peptide representing both α-helices of VP5 produced the highest level of LDH release, whereas no activity was shown for each of the individual α-helices. This data therefore indicated that α-helix 1 (amino acids 1-22) exerts its membrane-permeabilizing activity in concert with α-helix 2 (amino acids 23-43) and that both of these helices may be cooperatively involved in the formation of membrane integral pores. These results are in contrast to those of BTV VP5, in

which the most N-terminal α-helix (amino acids 1 to 20) exhibits a significantly higher permeabilizing activity than the adjacent α-helix (amino acids 22 to 41) (Hassan *et al*., 2001).

The data, based on the structural features and cytotoxic activity of the AHSV VP5 protein, indicate that VP5 acts as membrane-permeabilization protein. It is therefore tempting to speculate that this property of VP5 may be of importance during the early stages of virus entry into susceptible host cells. In contrast to enveloped viruses (White *et al*., 2008; Falanga *et al*., 2009; Thorley *et al*., 2010), there is a paucity of information regarding the precise mechanism by which non-enveloped viruses, including AHSV, penetrate and deliver their genome across host-cell membranes in the absence of membrane fusion. However, short membrane-altering amphipathic or hydrophobic sequences have been identified in several non-enveloped viruses, which either form a transmembrane pore or rupture intracellular endosome membranes through which the viral genome is transported to the cytoplasm (Tsai, 2007; Banerjee and Johnson, 2008). Notably, motifs similar to those described above have also been identified in polypeptides encoded by members of the *Reoviridae* family such as the VP4 protein of rotavirus (Denisova *et al.*, 1999) and the μ1 protein of reovirus (Agosto *et al.*, 2006).

In the case of rotavirus the VP4 outer capsid spike protein is proteolytically cleaved by trypsin to generate two fragments, designated VP5* and VP8* (Estes *et al.*, 1981; Denisova *et al.*, 1999), of which VP5* is required for viral entry into cells (Baker and Prasad, 2010). It has been reported that two discrete domains within VP5* is required for pore formation, namely an N-terminal basic domain that permits VP5* to peripherally associate with membranes and an internal hydrophobic domain that is required for membrane permeabilization (Dowling *et al*., 2000; Galantsova *et al*., 2004). For reovirus, it has been reported that the membrane penetration protein μ1, which contains two amphipathic helices (amino acids 534-551 and 591-604), undergoes a structural rearrangement to a protease-sensitive conformation, designated μ1*, following removal of the outer capsid protein σ3 (Chandran *et al.*, 2002). Subsequent autocatalytical cleavage of μ1* generates an N-myristoylated μ1N fragment and a μ1C fragment (Nibert *et al*., 1991; Zhang *et al*., 2006). Of these, the μ1N peptide is released from virus particles during membrane penetration and directly mediates pore formation in membranes (Odegard *et al*., 2004; Agosto *et*

al., 2006), leading to rupture of the membrane vesicle and delivery of transcriptionally active reovirus core particles into the host cell cytoplasm (Danthi *et al*., 2010).

In contrast to rotaviruses and reoviruses, each orbivirus protein is a product of a single gene and is not derived from a precursor protein (van Dijk and Huismans, 1988; Roy, 2008). Furthermore, the VP5 protein of BTV (Hassan *et al.*, 2001) and AHSV (this study) does not require a proteolytic activation step to render it functional. It therefore follows that in the case of VP5 a conformational change is most likely required to enable its interaction with and subsequent permeabilization of membranes. Recent structural studies, based on a 7-Å resolution structure of the BTV virion obtained by cryoelectron microscopy, have provided new insights as to how VP5 may accomplish membrane penetration (Zhang *et al.*, 2010). Mapping of the BTV VP5 amino acid sequence to secondary structural elements identified by cryoelectron microscopy indicated the presence of 15 amphipathic helices located on the external surface of VP5. Of these, an amphipathic helix and two hydrophobic helices located at the C-terminal of VP5 are thought to anchor VP5 to the membrane. It was suggested that the external surface of VP5 with its 12 additional amphipathic helical regions could swing up to the membrane, where the amphipathic helices could roll to make extensive hydrophobic contact with the membrane and perforate it. This unfurling of VP5 is furthermore thought to result in its detachment from the core, thus allowing release of the uncoated transcriptionally active core particle (Zhang *et al.*, 2010).

In conclusion, the results obtained in this part of the investigation indicated that AHSV VP5 has an intrinsic membrane permeabilizing activity and that this activity is mediated by two N-terminal amphipathic α-helices. These findings suggest that the VP5 protein is a membrane-destabilizing protein that could possibly be involved in the entry of AHSV into susceptible host cells, as had been proposed for VP5 of BTV.

CHAPTER FOUR

INDUCTION OF APOPTOSIS BY AFRICAN HORSE SICKNESS VIRUS IN MAMMALIAN CELLS

4.1 INTRODUCTION

Apoptosis, or programmed cell death (PCD), is a selective process of physiological cell deletion in response to numerous developmental and environmental stimuli (Kerr *et al*., 1972; Wyllie *et al*., 1981). There are two major pathways of apoptotic cell death induction: extrinsic signaling through death receptors and intrinsic signaling mainly through mitochondria (Jin and El-Deiry, 2005; Xu and Shi, 2007; Chowdhury *et al*., 2008). The extrinsic pathway is triggered by the binding of external (death) ligands to their cognate (death) receptors on cell membranes, as exemplified by members of the tumor necrosis factor (TNF) superfamily (Duprez *et al*., 2009). Receptor-ligand engagement results in formation of the death-inducing signaling complex (DISC), which allows the activation of caspase-8 (Boatright *et al.*, 2003). The intrinsic pathway is initiated in response to diverse stimuli, and leads to the loss of mitochondrial membrane potential and the release of several proapoptotic proteins, including cytochrome c and the second mitochondria-derived activator of caspase (Smac, also known as DIABLO), from the mitochondrial intermembrane space to the cytosol (Korsmeyer *et al.*, 2000; Finkel, 2001; Chowdhury *et al.*, 2006). Cytochrome c forms an apoptosome complex with Apaf-1 and procaspase-9, resulting in activation of the latter (Acehan *et al.*, 2002; Riedl and Salvesen, 2007). The initiator caspases caspase-8 in the extrinsic pathway and caspase-9 in the intrinsic pathway are responsible for activating the effector caspases (caspase-3, -6 and -7), which execute the apoptosis process through the proteolytic cleavage of a number of intracellular substrates (Martin and Green, 1995; Boatright *et al.*, 2003; Li and Yuan, 2008). Apoptotic cells exhibit characteristic morphological and biochemical features that include cell membrane blebbing, chromatin condensation, the formation of apoptotic bodies (Kerr *et al*., 1972; Wyllie *et al*., 1980; Earnshaw, 1995; Martelli *et al*., 2001), genomic DNA fragmentation (Wyllie, 1980), and phosphatidylserine externalization (Martin *et al*., 1995).

Infection by most viruses triggers apoptosis (Roulston *et al*., 1999) and in some virus-induced diseases, apoptosis is a pathogenic mechanism that contributes *in vivo* to cell death, tissue injury and disease severity (Samuel *et al*., 2007; Clarke and Tyler, 2009; Clarke *et al*., 2009). Bluetongue virus (BTV), the prototype virus of the genus *Orbivirus* in the family *Reoviridae*, is known to produce disparate cellular responses in insect and mammalian cells. In insect cells, BTV causes persistent and asymptomatic infections despite productive replication (Mertens *et*

al., 1996; Mortola *et al*., 2004; Li *et al*., 2007b). However, in mammalian cells, BTV causes severe cytopathic effects and rapid cell death (Mortola *et al*., 2004; Nagaleekar *et al*., 2007). In infected mammalian cells, BTV attachment and uncoating, but not replication, has been shown to trigger apoptosis through activation of the MAP kinase-dependent and NF-κβ pathways (Mortola *et al*., 2004; Mortola and Larsen, 2009; Stewart and Roy, 2010). Studies have also suggested that BTV induces apoptosis through both the intrinsic and extrinsic pathways (Li *et al*., 2007b; Nagaleekar *et al*., 2007; Mortola and Larsen, 2009). Moreover, it has been suggested that apoptosis may contribute to the pathogenesis of bluetongue disease in the mammalian host (DeMaula *et al*., 2001; Mortola and Larsen, 2009) and, recently, the induction of apoptosis was implicated in the pathogenesis of BTV in sheep (Umeshappa *et al*., 2010).

For other members of the *Reoviridae* family, such as rotaviruses (Sato *et al*., 2006) and reoviruses (Richardson-Burns and Tyler, 2004), induction of apoptosis in infected mammalian cells also contributes to virus pathogenesis. Rotavirus attachment, penetration and gene expression induce apoptosis in mammalian cells through activation of the mitochondrial pathway (Chaïbi *et al*., 2005; Martin-Latil *et al*., 2007). Reovirus attachment and disassembly transiently activates NF-κβ (Connolly and Dermody, 2002; Danthi *et al*., 2008), as well as genes involved in apoptotic signaling (Connolly *et al*., 2000; DeBiasi *et al*., 2003; O'Donnell *et al*., 2006). Furthermore, reovirus infection activates TNF-α-induced cell death via the release of TRAIL (TNF-related apoptosis inducing ligand) from infected cells, resulting in DISC formation, the activation of caspase-8 and, consequently, activation of the effector caspases-3 and -7 (Clarke *et al*., 2001; Kominsky *et al*., 2002b; Richardson-Burns *et al*., 2002). Moreover, activated caspase-8 cleaves the proapoptotic protein Bid, which translocates to the mitochondria and initiates activation of the mitochondrial apoptotic pathway (Kominsky *et al*., 2002a; Clarke *et al*., 2004).

African horse sickness virus (AHSV) is the causative agent of African horse sickness (AHS), a highly infectious arthropod-borne (*Culicoides* spp.) disease of equids, of which the mortality rate in horses may exceed 90% (Coetzer and Erasmus, 1994; Guthrie, 2007). A previous report regarding examination of the endothelial cells of capillaries in the myocardium, lung, spleen and liver of AHSV-infected animals noted ultrastructural alterations that included cytoplasmic projections, alteration of intercellular junctions, an electron-dense cytoplasm and condensation of

the cellular nucleus. In association with these cellular changes, oedema, haemorrhages and microthromboses were detected, particularly in the myocardium and lung (Gómez-Villamandos *et al*., 1999). These findings thus suggest that apoptosis may contribute to the pathogenesis of AHS disease in the mammalian host. Moreover, AHSV infection of mammalian cell cultures results in dramatic cytopathic effects (CPE) and is associated with irregular-shaped cells, cell rounding, shrinkage and detachment, as well as darkly Giemsa-stained nuclei within the infected cells (Osawa and Hazrati, 1965). In contrast, propagation of AHSV-9 in *Aedes albopictus* cell lines results in persistent infection and maturation of complete virus, although no CPE is observed (Mirchamsy *et al*., 1970). This difference in host cell CPE following virus infection furthermore suggests that apoptosis may be induced in mammalian cells.

In contrast to BTV and other members of the *Reoviridae* family, no investigations into the mechanism of cell death of AHSV-infected cells have been undertaken, and the pathogenic mechanisms of AHS remain poorly characterized. Whether the correlation between CPE and apoptosis holds for AHSV, as with other arboviruses (Karpf *et al*., 1997; Karpf and Brown, 1998; Mortola *et al*., 2004), also remains to be determined. Consequently, the primary aim of this part of the investigation was to determine whether AHSV induces apoptosis in infected Baby hamster kidney (BHK-21) mammalian cells and *Culicoides sonorensis* (KC) insect cells. For this purpose, infected cells were examined for morphological and biochemical alterations associated with the induction of apoptosis, and the involvement of the intrinsic pathway in AHSV-induced apoptosis was furthermore investigated.

4.2 MATERIALS AND METHODS

4.2.1 Cells and viruses

Baby hamster kidney (BHK-21; ATCC CCL-10) cells were propagated and maintained as monolayers in 75 cm^2 tissue culture flasks, and cultured in Minimum Essential Medium (MEM) (Sigma-Aldrich) supplemented with 5% (v/v) fetal bovine serum (FBS) and antibiotics (60 mg/ml penicillin; 60 mg/ml streptomycin; 150 µg/ml Fungizone) (Highveld Biological). The cells were incubated at 37°C in an incubator with a constant supply of 5% (v/v) CO_2. Embryonic *Culicoides sonorensis* (KC) cells were propagated at 27°C in modified Schneider's *Drosophila*

medium (Highveld Biological) supplemented with 10% (v/v) FBS and antibiotics (60 mg/ml penicillin; 60 mg/ml streptomycin; 150 µg/ml Fungizone).

African horse sickness virus serotype 9 (AHSV-9), supplied by Mr. Flip Wege (Department of Genetics, University of Pretoria), was used for all cell infections. For infections, BHK-21 or KC cell monolayers were rinsed with serum-free MEM medium or modified Schneider's *Drosophila* medium, and then infected with AHSV-9 at a multiplicity of infection (MOI) of 1 PFU/cell. Virus infection was performed at room temperature for 2 h, followed by incubation of the cell monolayers in MEM medium supplemented with 5% (v/v) FBS or modified Schneider's *Drosophila* medium supplemented with 10% (v/v) FBS.

4.2.2 Analyses of AHSV-infected BHK-21 and KC cells

4.2.2.1 Preparation of AHSV-infected cell lysates

BHK-21 and KC cell monolayers were propagated in 6-well tissue culture plates (Nunc) until 100% confluent, and then either mock-infected or infected with AHSV-9 at a MOI of 1 PFU/cell. The cells were harvested at different time intervals post-infection from the surface of tissue culture plates, collected by centrifugation at 3 000 rpm for 10 min and washed once in 1 × phosphate-buffered saline (PBS: 137 mM NaCl; 2.7 mM KCl; 4.3 mM $Na_2HPO_4.2H_2O$; 1.4 mM KH_2PO_4; pH 7.4). The cells were suspended in 40-100 µl of 1 × PBS and an equal volume of 2 × protein solvent buffer (PSB: 125 mM Tris-HCl [pH 6.8]; 4% [w/v] SDS; 20% [v/v] glycerol; 10% [v/v] 2-mercaptoethanol; 0.002% [w/v] bromophenol blue) was added to each sample. The samples were heated for 10 min in boiling water.

4.2.2.2 SDS-polyacrylamide gel electrophoresis (SDS-PAGE)

Protein samples were analyzed by SDS-PAGE, as described by Laemmli (1970). A 5% (w/v) acrylamide stacking gel and 12% (w/v) acrylamide separating gel was used, of which the acrylamide:bisacrylamide ratio was 30:0.8. The low-porosity separating gel (0.375 M Tris-HCl [pH 8.8]; 0.1% [w/v] SDS) and high-porosity stacking gel (0.125 M Tris-HCl [pH 6.8]; 0.1% [w/v] SDS) were each polymerized by addition of 0.08% (w/v) ammonium persulphate and 0.008% (v/v) TEMED. The TGS electrophoresis buffer consisted of 0.025 M Tris-HCl (pH 8.3),

0.192 M Glycine and 0.1% (w/v) SDS. Electrophoresis was performed in a Hoefer Mighty Small™ SE260 electrophoresis unit for 2.5 h at 120 V. After electrophoresis, the gels were stained for 20 min with 0.125% (w/v) Coomassie brilliant blue (prepared in 50% methanol, 10% acetic acid) and the proteins were visualized by counterstaining the gels in a solution containing 25% methanol and 10% glacial acetic acid.

4.2.2.3 Immunoblot analysis

Immunoblot analysis of AHSV-infected cells was performed, as described by Sambrook and Russell (2001). Following SDS-PAGE, the gel, two sheets of filter paper and a Hybond™-C^+ nitrocellulose membrane (Amersham Pharmacia Biotech AB), cut to the same size as the gel, were equilibrated for 30 min in transfer buffer (25 mM Tris; 186 mM Glycine). The proteins were electroblotted onto the membrane for 1.5 h at 28 V and 120 mA, using a Mighty Small™ Transphor blotting apparatus (Hoefer). Following transfer, the gel was recovered and stained with Coomassie brilliant blue to determine the efficiency of the transfer process. The membrane was washed once in 1 × PBS for 5 min and non-specific binding sites were blocked by incubating the membrane overnight at 4ºC in blocking solution (1% [w/v] fat-free milk powder in 1 × PBS). The membrane was transferred to 1 × PBS containing an AHSV-9 antiserum, diluted 1:100 (Onderstepoort Veterinary Institute). Following incubation at room temperature for 2 h with gentle agitation, the unbound primary antibodies were removed by washing the membrane three times for 5 min each in wash buffer (0.05% [v/v] Tween-20 in 1 × PBS). The secondary antibody, Protein-A conjugated to horseradish peroxidase (Sigma-Aldrich) and diluted 1:500 in 1 × PBS, was added to the membrane and then incubated at room temperature for 1 h. The membrane was washed three times for 5 min each in wash buffer, and once for 5 min in 1 × PBS. To detect immuno-reactive proteins, the membrane was immersed in a freshly prepared enzyme substrate solution (60 mg 4-chloro-1-naphtol in 20 ml of ice-cold methanol and 60 µl of H_2O_2 in 100 ml of 1 × PBS, mixed just before use). Once the bands became visible, the membrane was rinsed with distilled water and air-dried.

4.2.3 Microscopy

BHK-21 and KC cells were seeded onto coverslips in 6-well tissue culture plates (Nunc) and either mock-infected or infected with AHSV-9 at a MOI of 1 PFU/cell. The coverslips were removed at 24, 48 and 72 h post-infection (BHK-21 cells) or at 7 days post-infection (KC cells), placed on glass slides in the absence of fixatives and sealants, and examined for AHSV-induced cytopathic effects (CPE) with a Zeiss Axiovert 200 inverted microscope at magnifications ranging from 20-40×. The images were captured using a Nikon DXM 1200 digital camera and analyzed with Nikon ACT-1 v.2.20 software. For detection of morphological cell alterations characteristic of apoptosis, confluent BHK-21 and KC cell monolayers were infected in 75 cm^2 tissue culture flasks with AHSV-9 at a MOI of 1 PFU/cell and subsequently prepared for examination by transmission electron microscopy. Cells from virus-infected and mock-infected cell monolayers were harvested at 24, 48 and 72 h post-infection (BHK-21 cells) or at 7 days post-infection (KC cells) by centrifugation at 3 000 rpm for 10 min. The cells were fixed at room temperature for 30 min in 1 × PBS containing 2.5% (v/v) formaldehyde and 0.1% (v/v) glutaraldehyde, and post-fixed in 1% osmium tetroxide. After fixing, the cells were washed three times in 1 × PBS and dehydrated through a series of graded ethanol solutions (15 min each in 50%, 70%, 90% and 100% [v/v] ethanol). The treatment with 50-90% ethanol was performed once, while treatment with 100% ethanol was repeated three times to ensure complete dehydration of the samples. The fixed cells were embedded in Quetol. Ultrathin cell sections were obtained on an ultramicrotome, collected on copper grids, stained in a 5% solution of uranyl acetate, washed in ddH_2O and counterstained in 3% lead citrate. The preparations were examined and photographed in a Philips 301 transmission electron microscope.

4.2.4 DNA fragmentation analysis

Chromosomal DNA fragmentation was detected with an Apoptotic DNA-ladder kit (Roche Diagnostics) according to the specifications of the manufacturer. Mock-infected or AHSV-infected BHK-21 and KC cells (*ca*. 2 × 10^6 cells), in a sample volume of 200 µl of 1 × PBS, were incubated with an equal volume of Nucleic Acid Binding and Lysis buffer (6 M guanidine-HCl; 10 mM urea; 10 mM Tris-HCl; 20% [v/v] Triton X-100; pH 4.4). Following incubation at room temperature for 10 min, 100 µl of isopropanol was added to each sample, mixed thoroughly and pipetted into a DNA-binding column. Following centrifugation at 8 000 rpm for 1 min, cellular

impurities were removed from the bound DNA by washing the column twice with Wash buffer (20 mM NaCl; 2 mM Tris-HCl; pH 7.5) and the DNA was then eluted in 200 µl of prewarmed (70°C) Elution buffer (10 mM Tris; pH 8.5). As a positive control of chromosomal DNA fragmentation, lyophilized apoptotic U937 cells (supplied in the kit) were suspended in 400 µl of the Nucleic Acid Binding and Lysis buffer and treated identically. Aliquots of the extracted chromosomal DNA were analyzed by electrophoresis in a 1% (w/v) agarose gel.

4.2.5 Quantification of apoptosis

Apoptosis in AHSV-infected BHK-21 cells was quantified by making use of the Cell Death Detection ELISA^{PLUS} kit (Roche Diagnostics) according to the manufacturer's instructions. This *in vitro* enzyme immunoassay allows for the quantification of histone-associated-DNA-fragments (mono- and oligonucleosomes) that are released into the cytoplasm of cells that died from apoptosis. BHK-21 cells were seeded in the wells of a 96-well flat-bottom microtitre plate (Greiner BioOne) and incubated at 37ºC in a CO_2 incubator until they reached 100% confluence. The cells were infected with AHSV-9 at an MOI of 1 PFU/cell, while uninfected BHK-21 cells were included as a control in these assays. The cells were harvested at different times post-infection by centrifugation at 1 000 rpm for 10 min with a Sigma-Aldrich 4K15C plate centrifuge fitted with a 09100F swing-out rotor. The cell pellets were each suspended in 200 µl of the supplied Lysis Buffer and incubated at 25°C for 30 min to lyse the cells. The cell lysates were centrifuged at 1 000 rpm for 10 min and 20 µl of the supernatants was transferred into a streptavidin-coated 96-well microtitre plate. To each well, 80 µl of immunoreagent was added, which comprised 4 µl of biotinylated anti-histone antibodies, 4 µl of peroxidase-labelled anti-DNA antibodies and 72 µl of Incubation Buffer (1% [w/v] BSA; 0.5% [v/v] Tween-20; 1 mM EDTA in PBS). The microtitre plate was incubated at 25°C for 2 h on a shaker and unbound antibodies were subsequently removed by three washes each with 300 µl of Incubation buffer. The peroxidase-labelled complexes retained were incubated with 100 µl of the peroxidase substrate ABTS (2,2-azino-bis(3-ethylbenzthiazoline-6-sulphonic acid). Following color development for 20 min at 25°C, the samples were read at 405 nm against Incubation buffer (containing ABTS) as the blank with a Multiscan Ascent ELISA plate reader. To calculate the specific enrichment factor of nucleosomes released into the cytoplasm of AHSV-infected BHK-21 cells, the absorbance measurements of the samples were averaged and the background value

was subtracted from each of these averages. The enrichment factor was then calculated as follows: Enrichment factor = mU of the sample (AHSV-infected BHK-21 cells) / mU of the negative control (uninfected BHK-21 cells), where mU = absorbance (10^{-3}). Two independent photometric enzyme immunoassays were performed.

4.2.6 Caspase-3 activation assays

Caspase-3 activation assays were performed with an ApoTarget™ Caspase-3 Colorimetric Protease Assay kit (BioSource International) according to the specifications of the manufacturer. BHK-21 cells were propagated in 25 cm^2 tissue culture flasks until 100% confluent and then infected with AHSV-9 at MOI of 1 PFU/cell. At different times post-infection, *ca*. 2.5 × 10^6 cells were collected by centrifugation at 2 500 rpm for 5 min and suspended in 50 µl of chilled Cell Lysis Buffer (supplied in the kit). Following incubation on ice for 10 min, cellular debris was pelleted by centrifugation at 10 000 rpm for 1 min. The protein concentration of each cytoplasmic extract was determined with the Quick Start Bradford Protein Assay kit (BioRad) and bovine serum albumin (BSA) as the standard. Each cytoplasmic extract was then diluted in 50 µl of Cell Lysis Buffer to yield *ca.* 200 µg total cellular protein and pipetted into the wells of a 96-well flat-bottom microtitre plate (Greiner BioOne). Following addition of 50 µl of 2 × Reaction buffer (10 mM DTT; 4 mM DEVD-*p*NA), the microtitre plate was incubated at 37°C in the dark for 2 h. The samples were read at 405 nm against Reaction buffer as the blank with a Multiscan Ascent ELISA plate reader. The values of AHSV-infected samples were compared with uninfected BHK-21 controls to determine the increase in caspase-3 enzymatic activity. Three independent caspase-3 activation assays were performed.

4.2.7 Detection of mitochondrial membrane depolarization

Mitochondrial membrane depolarization was assessed using DePsipher™ (5,5,6,6-tetrachloro-1,1,3,3-tetraethylbenzimidazolylcarbocyanin iodide) (Trevigen, Inc.) according to the manufacturer's instructions. DePsipher™ is a lypophilic cation that is susceptible to changes in mitochondrial membrane potential. It has the property of aggregating upon membrane polarization forming a red fluorescent compound with absorption/emission maxima of 585/590 nm. If the potential is disrupted, the dye cannot access the mitochondrial transmembrane space and remains in its green fluorescent monomeric form with absorption/emission maxima of

510/527 nm. To investigate, BHK-21 cells were seeded in 6-well tissue culture plates (1×10^6 cells/well) with or without glass cover slips, and infected with AHSV-9 at a MOI of 1 PFU/cell. The tissue culture plates were incubated at 37°C in a CO_2 incubator and processed at different times post-infection for flow cytometry or confocal microscopy, as described below. In these assays, uninfected BHK-21 cells were included as a control for healthy cells with polarized mitochondrial membranes, whereas BHK-21 cells incubated for 24 h with 20 µM FCCP (carbonyl cyanide *p*-[trifluoro-methoxy] phenylhydrazone) served as a positive control for cells with depolarized mitochondrial membranes (Dispersyn *et al*., 1999).

4.2.7.1 Flow cytometry

At 6-h intervals post-infection, control and AHSV-infected BHK-21 cells were harvested by centrifugation at 1 000 rpm for 5 min and suspended in 1 ml of DePsipher™ solution, which had been diluted in the supplied 1 × Reaction buffer to a final concentration of 5 µg/ml. Following incubation of the samples at 37°C in the dark for 20 min in a CO_2 incubator, the cells were rinsed twice with 1 × PBS and suspended in 1 ml of the same buffer. Cell fluorescence was recorded using a BD FACSAria™ flow cytometer (BD Biosciences) equipped with a 488-nm argon laser and using neutral density filter 2. A minimum of 10 000 events were analyzed for each sample with FACSDiva™ v.6.1.1 software (BD Biosciences). Data collection was gated, utilizing forward light scatter and side light scatter, to exclude cell debris and cell aggregates. The green Desipher™ monomer was detected using the fluorescein channel (FITC-A; FL1) and the red Desipher™ aggregates were detected using the propidium iodide channel (PE-A; FL2). The results are presented as a green/red fluorescence ratio (geomean FL1/FL2), the increase of which indicates mitochondrial membrane depolarization (Markovic *et al*., 2007; Isakovic *et al*., 2008).

4.2.7.2 Confocal laser scanning microscopy of AHSV-infected BHK-21 cells

At 24 h post-infection, the cell culture medium of control and AHSV-infected BHK-21 cells was aspirated and replaced with 1 ml of DePsipher™ solution (5 µg/ml). The tissue culture plates were incubated at 37°C in the dark for 30 min in a CO_2 incubator, after which the DePsipher™ solution was aspirated and the cells rinsed once with 1 ml of 1 × Reaction buffer. The glass cover slips were removed from the tissue culture plates and the cells were examined with a Zeiss LSM S10 META confocal laser scanning microscope at 40× magnification, using bypass filters

for fluorescein (505-550 nm) and rhodamine (560-615 nm). Fluorescent images were captured with a Zeiss Axiocam Series 5 digital camera and analyzed with Zeiss v.3.2SP2 software.

4.3 RESULTS

4.3.1 Microscopic examination of AHSV-infected BHK-21 and KC cells

It has been reported previously that replication of AHSV in insect (*Aedes albopictus*) cells results in persistent infection with no CPE, while virus infection of mammalian cells shows dramatic CPE (Osawa and Hazrati, 1965; Mirchamsy *et al*., 1970). To determine whether this difference in host cell CPE following AHSV infection is linked to the induction of apoptosis, BHK-21 mammalian cell and KC insect cell monolayers were infected with AHSV-9 and analyzed for morphological hallmarks of apoptosis. The KC cells used in this study are derived from *Culicoides sonorensis*, which has been reported to experimentally transmit AHSV (Wetzel *et al*., 1970; Mellor *et al*., 1975; Mellor, 1993).

To characterize the induction of apoptosis by AHSV-9 in BHK-21 cells, the virus-infected cells were analyzed over a time course of 72 h. Immunoblot analysis of the infected cells, using an anti-AHSV-9 polyvalent serum, confirmed expression of viral proteins (Fig. 4.1A). Light microscopy of the AHSV-infected cells at 72 h post-infection indicated that the virus-infected cells showed signs of severe CPE. In contrast to mock-infected BHK-21 cells, virus infection resulted in cell rounding, shrinkage and surface detachment (Fig. 4.1B). To detect ultrastructural alterations associated with apoptosis, the AHSV-infected cells were examined by transmission electron microscopy. The virus-infected BHK-21 cells showed a continuum of nuclear chromatin alterations, including margination of the nuclear chromatin against the nuclear periphery, although the nuclear envelope remained morphologically intact (Fig. 4.1C; III), progressive condensation of chromatin (Fig. 4.1C; IV and VIII) and, ultimately, nuclear fragmentation into apoptotic bodies (Fig. 4.1C; V and IX). In addition, nucleolar segregation (Fig. 4.1C; VII and VIII), cytoplasm compactness (Fig 4.1C; VI) and plasma membrane blebbing (Fig. 4.1C; VII, VIII and IX) was also observed in the AHSV-infected BHK-21 cells. None of these morphological alterations were noted in mock-infected BHK-21 cells (Fig. 4.1C; I and II).

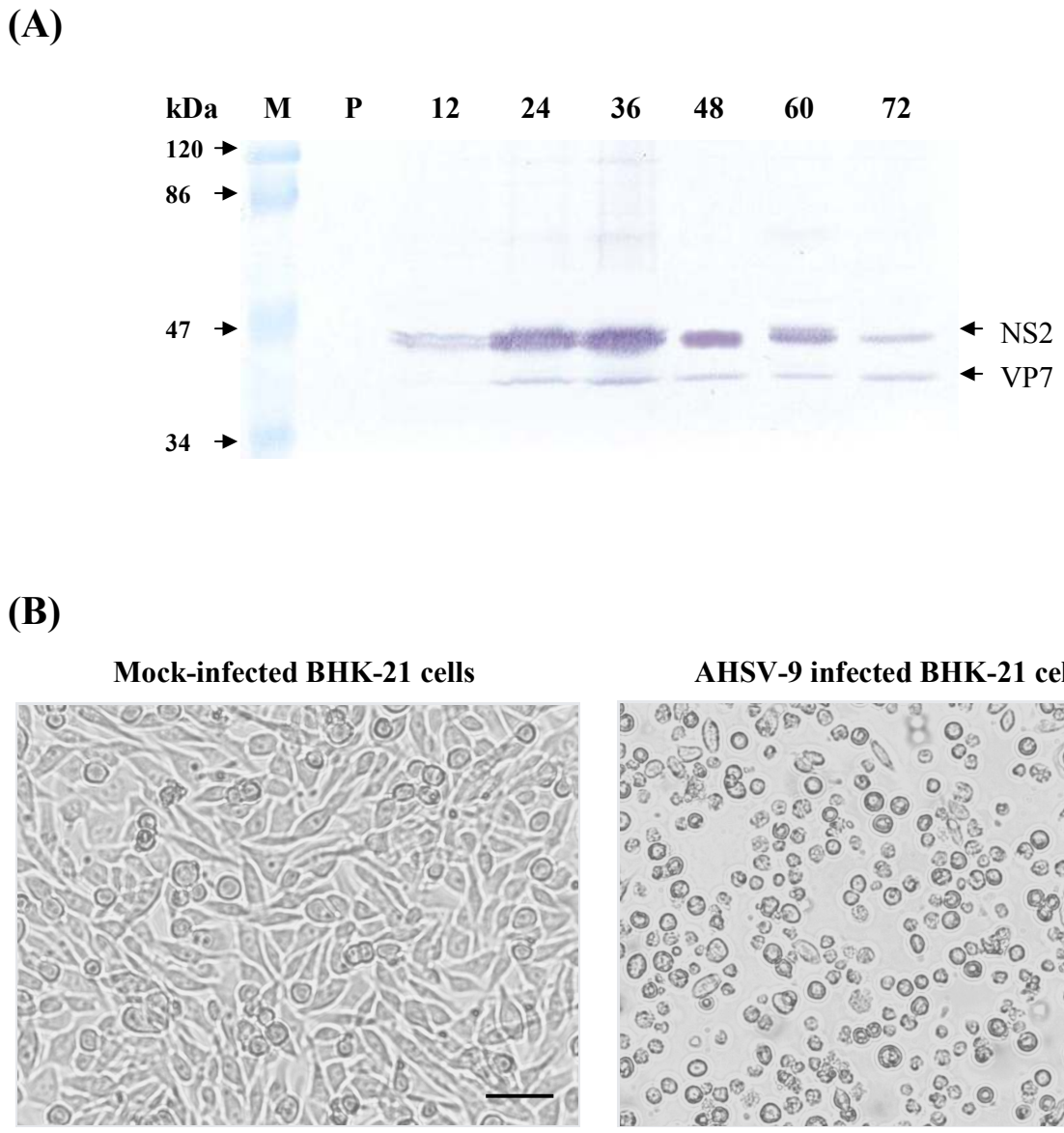

Fig. 4.1 **AHSV-9 induces apoptosis in mammalian cells.** (A) Immunoblot analysis of cell lysates from mock-infected (P) and AHSV-infected BHK-21 cells over a time course of 72 h using an AHSV-9 antiserum. The sizes of the molecular weight marker (M; Fermentas) are indicated to the left of the figure. (B) Micrographs of mock-infected and AHSV-infected BHK-21 cells. The AHSV-infected cells show clear signs of shrinkage, rounding and detachment. Bar = 50 µm.

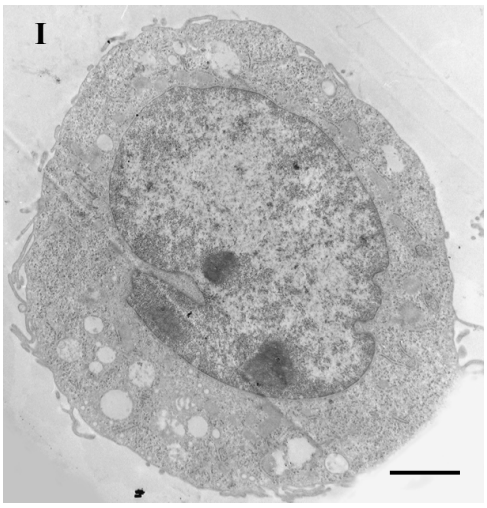

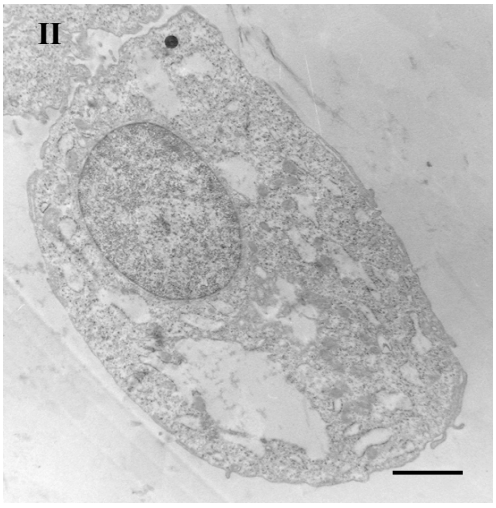

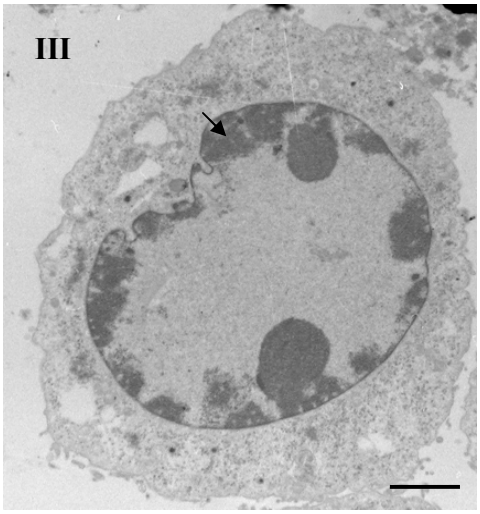

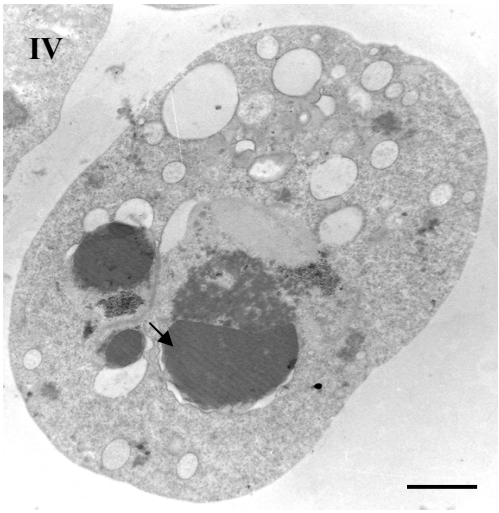

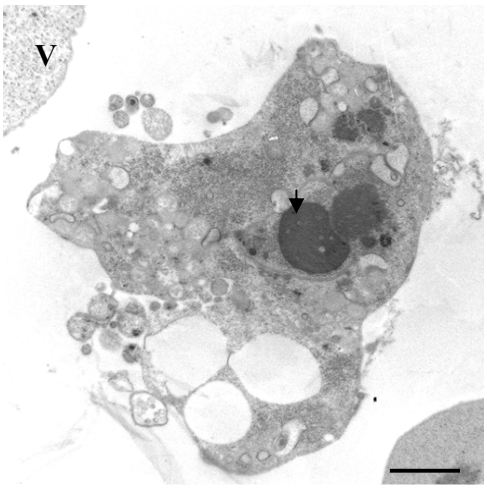

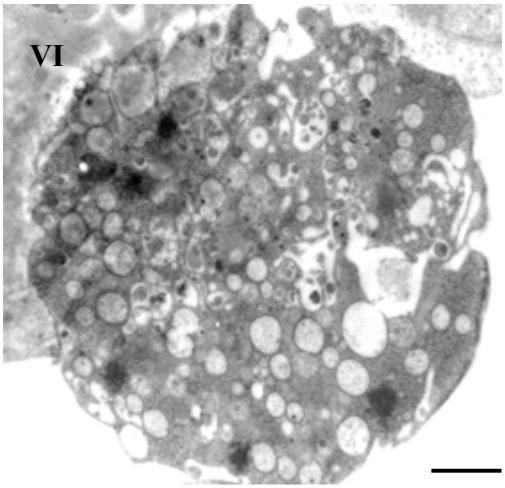

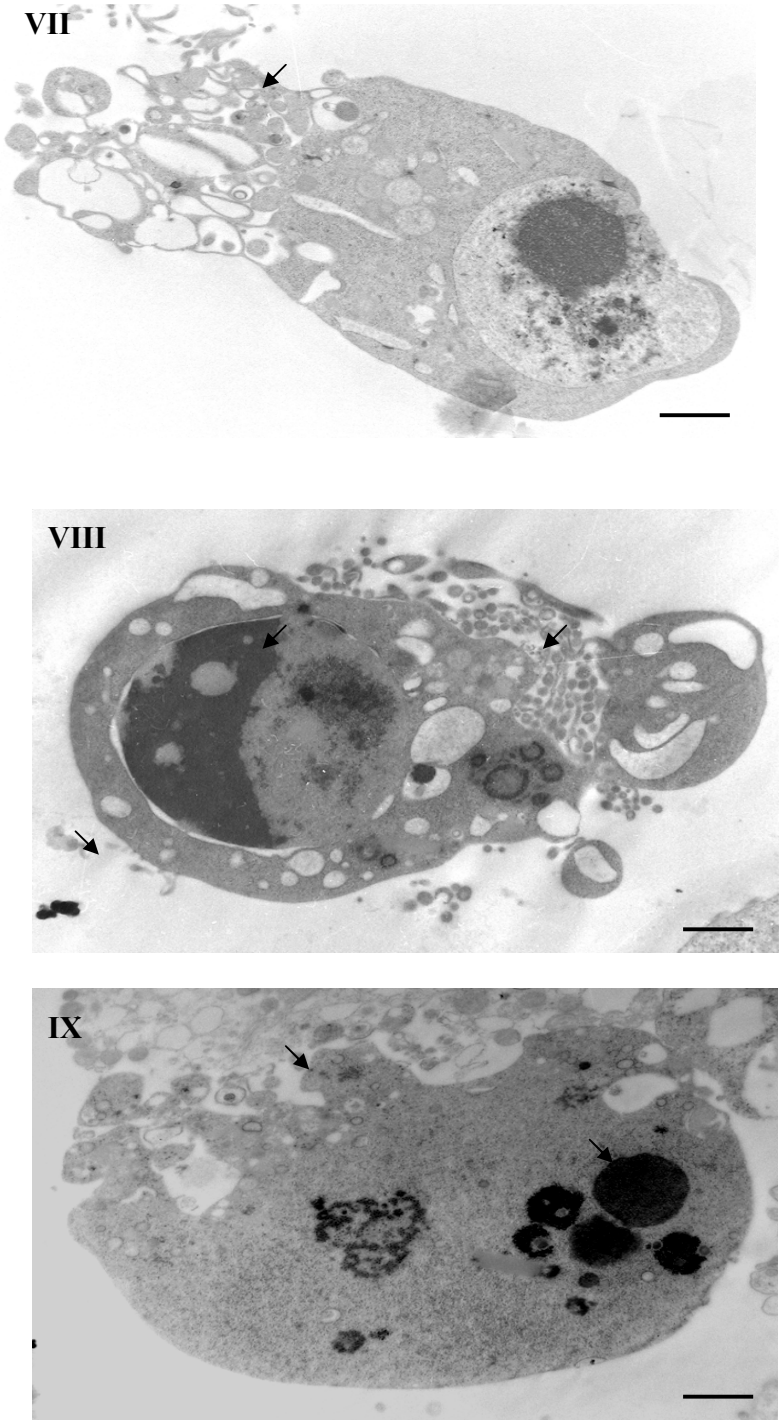

Fig. 4.1C **Transmission electron micrographs of BHK-21 cells infected with AHSV-9.** In contrast to mock-infected BHK-21 cells (I and II), AHSV-infected cells show morphological hallmarks of apoptosis, as indicated by the arrows. These included progressive condensation of chromatin (III, IV and VIII), the formation of apoptotic bodies (V and IX), cytoplasm compactness (VI) and plasma membrane blebbing (VII, VIII and IX). Bar = 1 µm.

To determine whether AHSV-9 infection induces morphological changes in *Culicoides sonorensis* cells similar to those observed in BHK-21 cells, the KC cells were infected with AHSV-9 and examined daily over the course of 7 days for induction of apoptosis. Despite production of viral proteins (Fig. 4.2A), the virus-infected KC cells did not display any morphological features that could be associated with apoptotic events. Indeed, microscopic examination (Fig. 4.2B) and transmission electron micrographs (Fig. 4.2C) of the AHSV-infected KC cells at 7 days post-infection indicated that they were indistinguishable from the mock-infected KC cells. These results therefore suggested that, in contrast to AHSV-infected BHK-21 mammalian cells, apoptosis is not induced in virus-infected KC insect cells.

4.3.2 DNA fragmentation analysis in AHSV-infected BHK-21 and KC cells

In cells undergoing apoptosis morphological changes, such as chromatin condensation and cytoplasmic blebbing, are associated with the incidence of nucleosome excisions from chromatin through the activation of an intracellular endonuclease (Wyllie, 1980). Since the 180-200 base pairs of DNA wrapped around a histone core are conformationally protected from digestion, the endonuclease-mediated nucleosome excision results in the appearance of a ladder of nucleosomal DNA fragments in agarose gels that has become the biochemical hallmark of apoptosis (Hewish and Burgoyne, 1973; Kornberg, 1974; Wyllie *et al*., 1980). Thus, to confirm that the morphological alterations observed in AHSV-infected BHK-21 cells were due to apoptosis, the infected cells were analyzed by a DNA fragmentation assay. AHSV-infected KC cells, which did not display any morphological changes despite productive virus replication, were included in the analysis to verify the absence of apoptosis. To investigate, nuclear DNA was extracted from virus-infected BHK-21 cells over a time course of 72 h, as well as from virus-infected KC cells over a time course of 7 days, and analyzed by agarose gel electrophoresis.

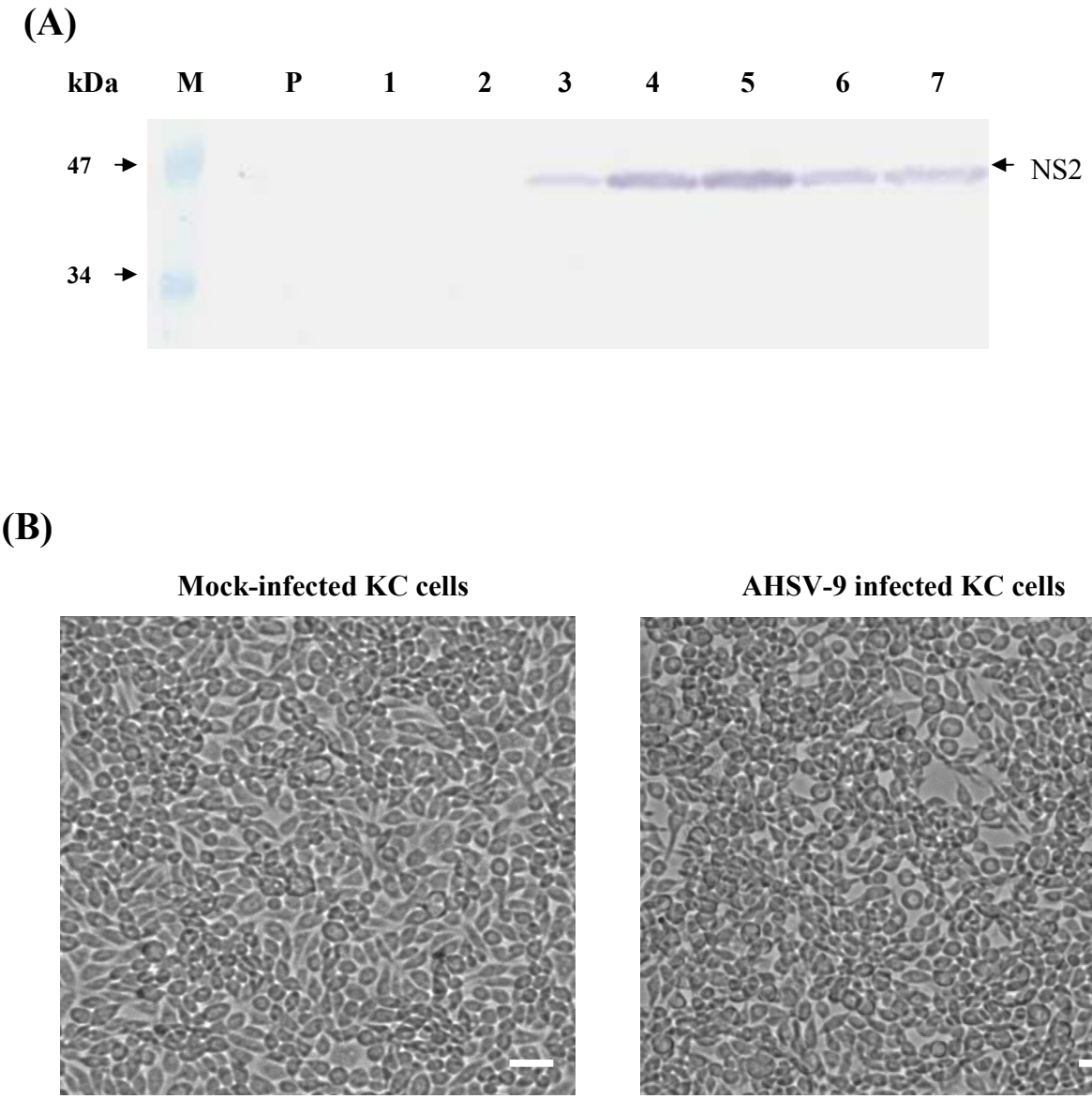

Fig. 4.2 **AHSV-9 does not induce apoptosis in insect cells.** (A) Immunoblot analysis of cell lysates from mock-infected (P) and AHSV-infected KC cells over a time course of 7 days using an AHSV-9 antiserum. The sizes of the molecular weight marker (M; Fermentas) are indicated to the left of the figure. (B) Micrographs of mock-infected and AHSV-infected KC cells at 7 days post-infection, indicating a lack of CPE. Bar = 20 µm.

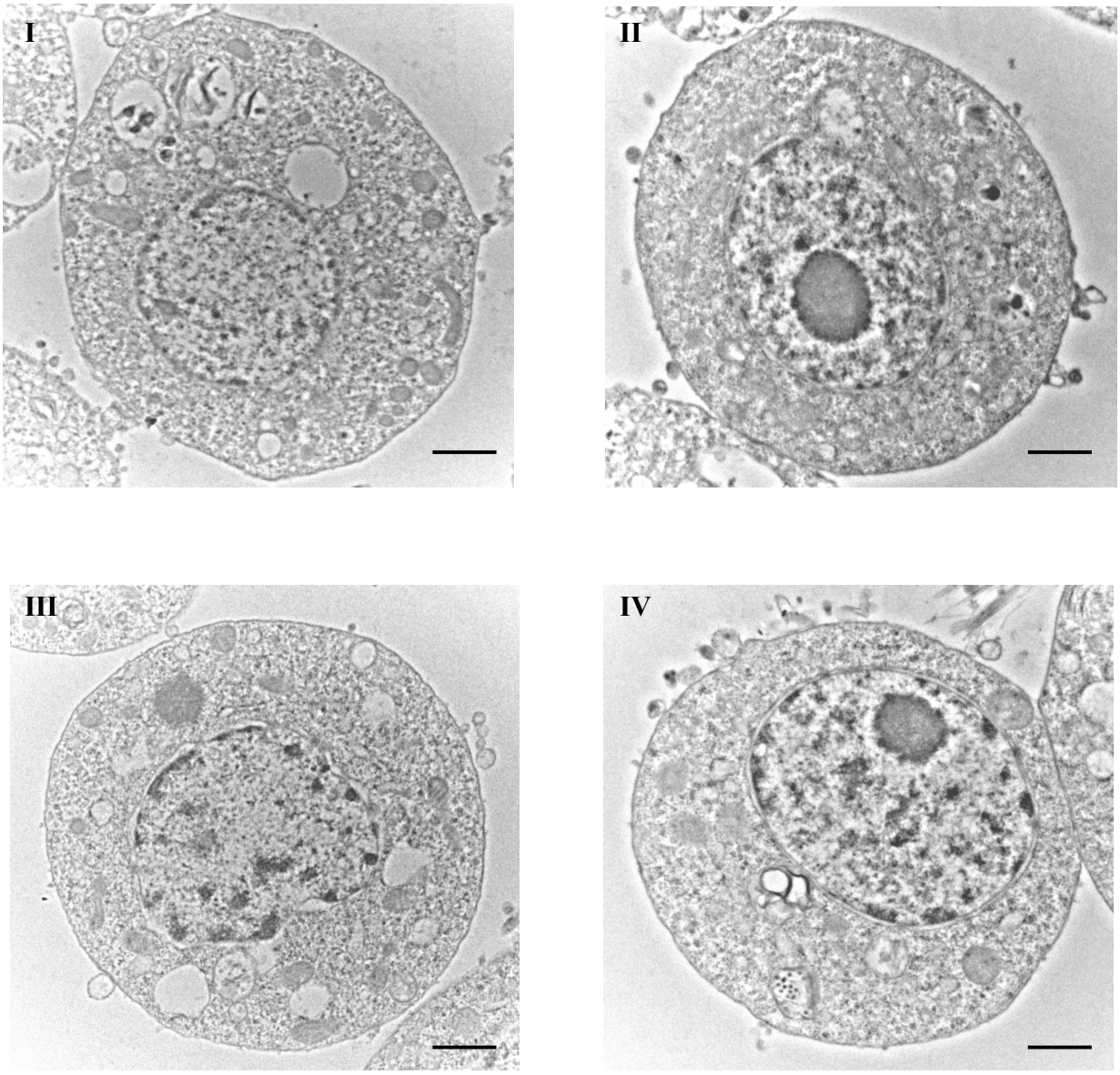

Fig. 4.2C **Transmission electron micrographs of KC cells infected with AHSV-9.** The AHSV-infected KC cells (III and IV) showed no detectable morphological hallmarks of apoptosis and were similar in appearance to mock-infected KC cells (I and II). The electron micrographs were taken at 7 days post-infection. Bar = 1 µm.

In contrast to mock-infected BHK-21 cells, which showed no evidence of DNA fragmentation, an oligonucleosomal DNA ladder was detected in AHSV-infected cells from 12 to 72 h post-infection. The fragmented chromosomal DNA ladder resembled that observed in apoptotic U937 cells, which served as a positive control in this assay (Fig. 4.3A). Furthermore, fragmentation of the chromosomal DNA in AHSV-infected BHK 21 cells at 72 h post-infection appears to be precise and non-random, as evidenced in a second independent sample that displayed an identical DNA-laddering pattern. In contrast to these results, there was no detectable chromosomal DNA fragmentation in the AHSV-infected KC cells over a time course of 7 days (Fig. 4.3B). These results therefore provided supporting biochemical evidence that the gross morphological changes observed in AHSV-infected BHK-21 cells was due to the induction of apoptosis in the mammalian cells.

To determine more accurately when apoptosis is induced in the AHSV-infected BHK-21 cells, the nucleosomes present in the cytoplasm of virus-infected cells was quantified over a time course of 72 h with a photometric enzyme immunoassay. This assay is based on a sandwich-enzyme immunoassay principle using monoclonal antibodies directed against histones and DNA, respectively, and allows for specific detection and quantification of mono- and oligonucleosomes that are released into the cytoplasm of cells that died from apoptosis.

The results, presented in Fig. 4.4, indicated that there was limited release of nucleosomes into the cytosol of AHSV-infected BHK-21 cells during the first 6 h of infection. This is reflected by a 0.6-fold increase in the nucleosome enrichment factor from 0 to 6 h post-infection. However, there was a significant increase in the release of nucleosomes between 6 and 12 h post-infection, as evidenced by a 12-fold increase in the nucleosome enrichment factor over this time period. Between 12 and 24 h post-infection, there was a slight increase (1.4-fold) in the release of nucleosomes. No further increases in the nucleosome enrichment factor were observed between 24 and 72 h post-infection, possibly as a consequence of the chromosomal DNA having been fragmented in most infected cells (Fig. 4.3A). These results therefore indicate that apoptosis is induced at 12 h post-infection and maximal apoptosis is reached at 24 h post-infection. Cumulatively, the above data provide evidence that infection of BHK-21 cells with AHSV results in apoptosis at 12 h post-infection.

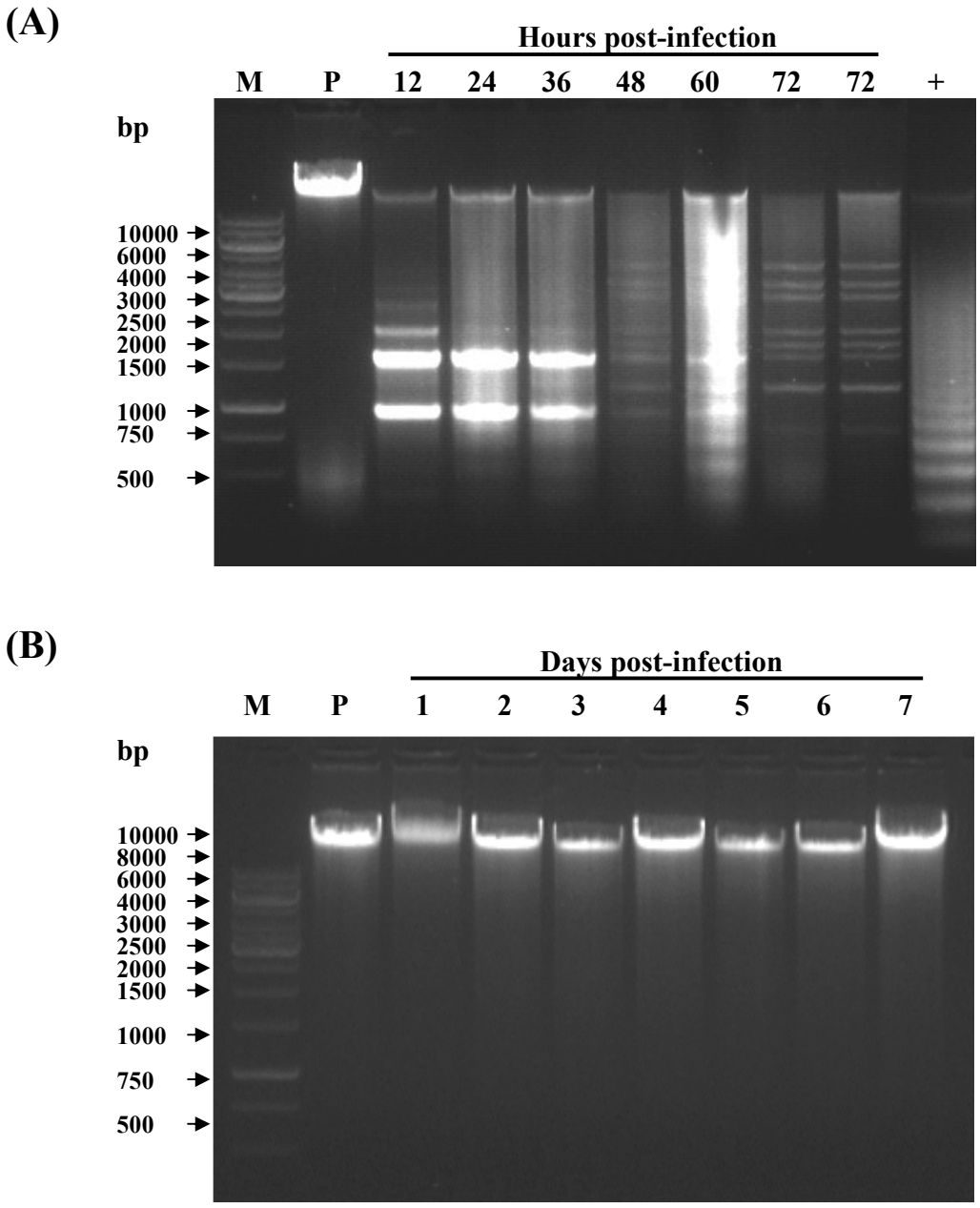

Fig 4.3 **DNA fragmentation analysis of BHK-21 and KC cells infected with AHSV-9.** (A) Agarose gel electrophoretic pattern of chromosomal DNA extracted from mock-infected (P) and AHSV-infected BHK-21 cells at different times post-infection (12 - 72 h). Apoptotic U937 cells served as a positive control (+). (B) Agarose gel electrophoretic pattern of chromosomal DNA extracted from mock-infected (P) and AHSV-infected KC cells over a time course of 7 days. The sizes of the molecular weight marker, GeneRuler™ 1 kb DNA ladder (Fermentas), are indicated to the left of the figure.

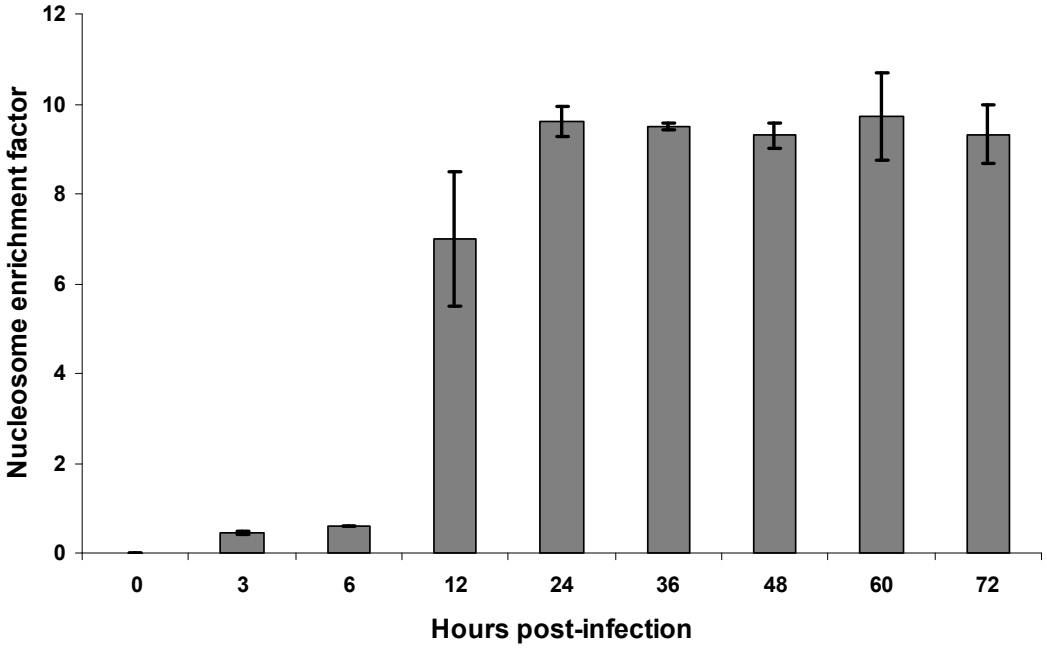

Fig. 4.4 **Enrichment of nucleosomes in the cytoplasm of BHK-21 cells infected with AHSV-9.** Cytoplasmic extracts were prepared from AHSV-infected BHK-21 cells at different times post-infection and pipetted into a streptavidin-coated microtitre plate. The samples were incubated with a mixture of anti-histone-biotin and anti-DNA-peroxidase antibodies. The biotinylated anti-histone antibody binds to the histone component of the nucleosomes and the streptavidin-coated microtitre plate, whereas the peroxidase-labelled DNA-specific antibody binds to the DNA component of the nucleosomes. After removal of the unbound antibodies, the nucleosomes were detected by measuring peroxidase activity with ABTS as substrate. The nucleosome enrichment factor was subsequently calculated, as described under Materials and Methods. The data are means ± SD of two independent experiments.

4.3.3 Caspase-3 activation in AHSV-infected BHK-21 cells

In the previous sections, it was shown that infection of BHK-21 cells with AHSV-9 resulted in morphological and biochemical hallmarks associated with the induction of apoptosis. To gain insight into the mechanism of AHSV-induced apoptosis, activation of caspase-3, a key agent of apoptosis, was examined. Caspase-3 plays a central role in apoptosis by acting as the effector caspase in both the extrinsic and intrinsic apoptotic pathways (Hengartner, 2000; Duprez *et al*., 2009). To investigate, BHK-21 cells were infected with AHSV-9 and the caspase-3 enzyme activity in cytoplasmic extracts, prepared over a time course of 72 h, was measured by proteolytic cleavage of the chromogenic substrate DEVD-*p*NA. This assay is based on the recognition by caspase-3 of the DEVD (Asp-Glu-Val-Asp) amino acid sequence linked to the chromophore *p*-nitroanilide (*p*NA). Upon cleavage of the labeled peptide by caspase-3, free *p*NA is released with a resulting increase in absorbance measurements. Comparison of the absorbance of released *p*NA from AHSV-infected cells with that of uninfected BHK-21 cells makes it possible to determine the increase in caspase-3 activity.

The results, presented in Fig. 4.5, indicated that the caspase-3 activity in AHSV-infected BHK-21 cells increased gradually from 0 until 12 h post-infection. Between 12 and 18 h post-infection, there was a steep increase in caspase-3 activity and after 24 h post-infection, the caspase-3 activity decreased gradually until 72 h post-infection. This decrease in caspase-3 activity may have been due to lysis of the infected BHK-21 and is in agreement with results reported by Medina *et al*. (1997). Based on these results, it was concluded that AHSV-9 infection of BHK-21 cells induces apoptosis with the activation of the executioner caspase, caspase-3.

4.3.4 Mitochondrial membrane depolarization in AHSV-infected BHK-21 cells

Although it was shown that caspase-3 was activated in AHSV-9 infected BHK-21 cells, the assay does not allow for determining whether caspase-3 was activated through the extrinsic or intrinsic apoptosis pathway. To elucidate the upstream events and to evaluate the role of mitochondria in this process, the mitochondrial membrane potential of AHSV-infected BHK-21 cells was subsequently examined. Depolarization of the mitochondrial outer membrane is an early, pivotal event in the intrinsic (or mitochondrial) apoptotic signaling pathway, resulting in the release of

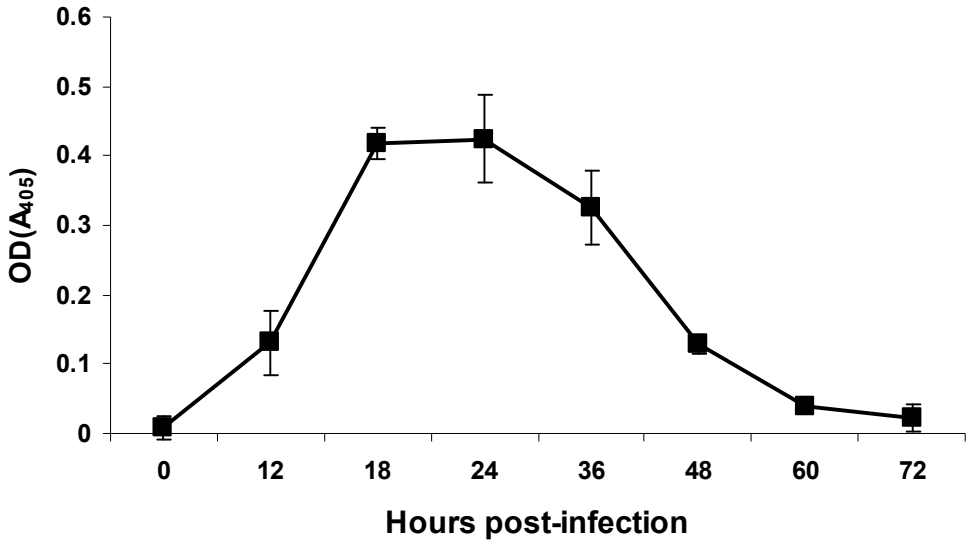

Fig. 4.5 **Activation of caspase-3 associated with AHSV-induced apoptosis in BHK-21 cells.** Cytoplasmic extracts, each containing 200 µg total protein, were prepared from uninfected and AHSV-infected BHK-21 cells at different times post-infection. Following incubation with the caspase-3 synthetic substrate DEVD-*p*NA, the liberated *p*NA was quantified at 405 nm in an ELISA plate reader. The data is presented as an increase in caspase-3 activity. Data are expressed as mean ± SD of three independent experiments.

several proapoptotic proteins from the mitochondrial intermembrane space to the cytosol (Chipuk and Green, 2008). This allows for the recruitment and activation of caspase-9, which, in turn, activates caspase-3. Caspase-3 is crucial for the execution of apoptotic cell death (Duprez *et al*., 2009). To investigate, BHK-21 cells were infected with AHSV-9 and the cells were stained with the lipophilic cation DePsipher™, which is used to indicate loss of the mitochondrial membrane potential. The virus-infected cells were analyzed by both flow cytometry and confocal microscopy. In healthy cells with polarized mitochondrial membranes, the DePsipher™ reagent easily enters cells and fluoresces brightly red in its multimeric form within healthy mitochondria. In apoptotic cells with a disturbed mitochondrial membrane potential, the dye cannot accumulate within the mitochondria and remains in the cytoplasm in its green fluorescent monomeric form. Thus, apoptotic cells showing primarily green fluorescence are readily differentiated from healthy cells that show red fluorescence. As a positive control, BHK-21 cells treated with the protonophore FCCP were included in the assays. FCCP is known for its ability to uncouple oxidative phosphorylation in mitochondria, thus resulting in depolarization of the mitochondrial membrane (Dispersyn *et al*., 1999).

Flow cytometric analysis of AHSV-infected BHK-21 cells, treated with the DePsipher™ reagent over a time course of 24 h, indicated a progressive loss of mitochondrial membrane potential from 0 to 24 h post-infection, as evidenced by an increase in the green-to-red (FL1/FL2) fluorescence form of the mitochondria-binding dye DePsipher™. Indeed, the FL1/FL2 ratio of virus-infected cells at 24 h post-infection was comparable to that obtained for BHK-21 cells incubated with FCCP for 24 h (Fig. 4.6). To furthermore confirm these results the control and AHSV-infected cells were examined by confocal microscopy at 24 h post-infection, following incubation of the cell monolayers with the DePsipher™ reagent. In uninfected BHK-21 cells, red fluorescent aggregates were observed in the mitochondria, indicating a lack of apoptosis (Fig. 4.7A, B and C). In contrast, in AHSV-infected BHK-21 cells, green fluorescence was observed that was localized to the cell cytoplasm, indicating that the mitochondrial membrane potential was disturbed (Fig. 4.7D, E and F). These results were in agreement with that observed in BHK-21 cells treated with FCCP (Fig. 4.7G and H). Overall, these results therefore suggest that infection of BHK-21 cells by AHSV-9 resulted in mitochondrial depolarization, and apoptosis induction involves the activation of the intrinsic apoptotic signaling pathway.

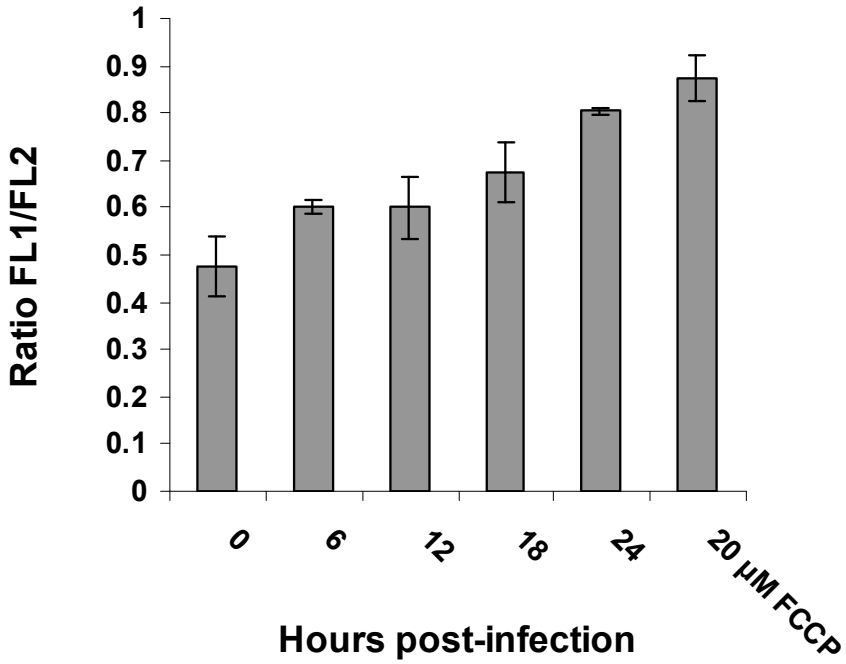

Fig. 4.6 **Mitochondrial membrane depolarization in BHK-21 cells infected with AHSV-9.** AHSV-infected BHK-21 cells were treated with DePsipher™ at the indicated times post-infection, and analyzed by flow cytometry. BHK-21 cells treated with FCCP were included as a positive control in the analysis. An increase in the ratio of green (FL1)/red (FL2) fluorescence is indicative of mitochondrial membrane depolarization. Results are mean values ± SD of two independent experiments.

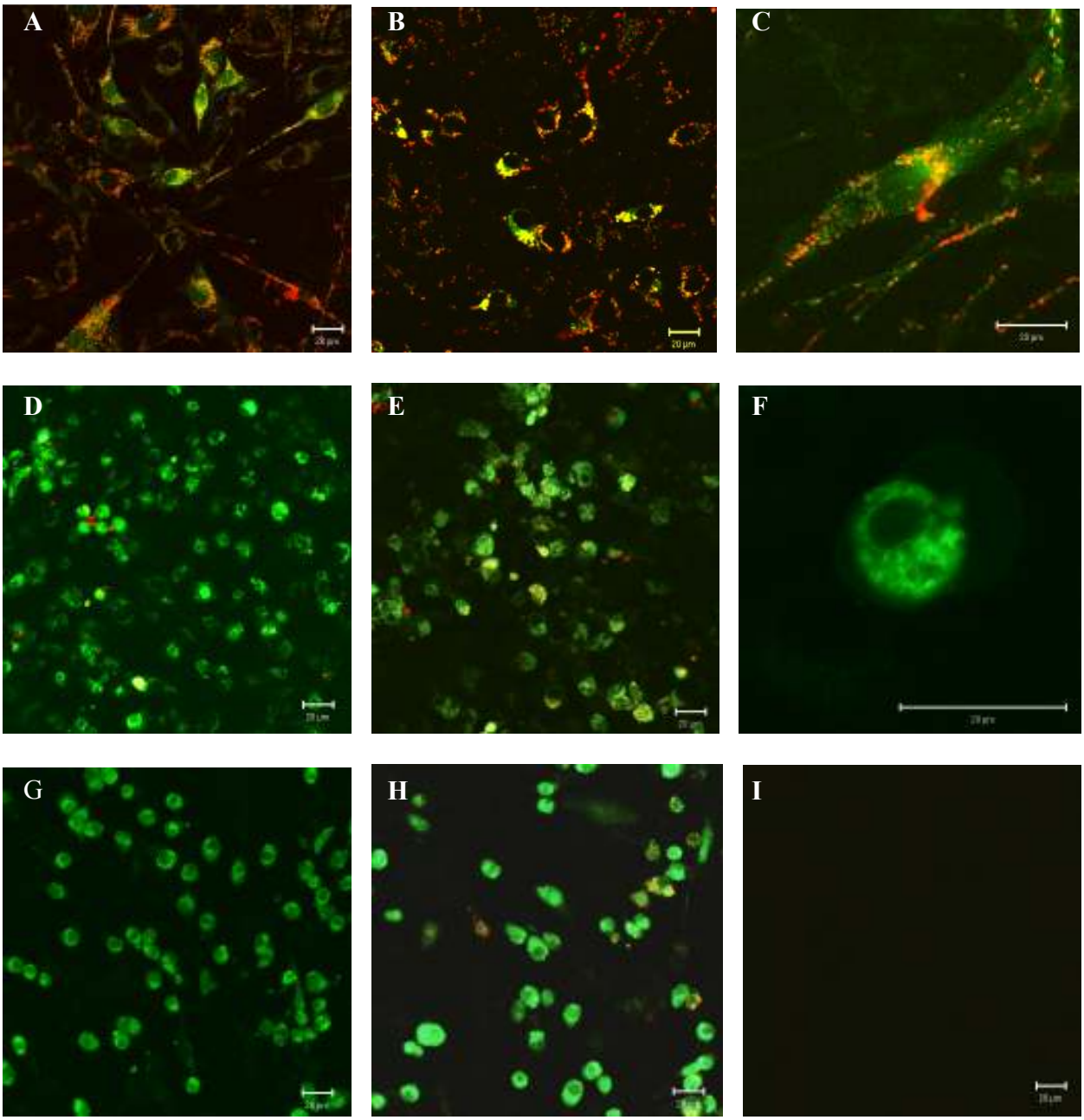

Fig. 4.7 **Confocal scanning laser microscopy of AHSV-infected BHK-21 cells stained with DePsipher™.** Uninfected BHK-21 cells (A, B and C), AHSV-infected BHK-21 cells (D, E and F) and BHK-21 cells treated with FCCP (G and H) were examined at 24 h post-infection with a Zeiss LSM S10 META confocal microscope fitted with bypass filters for fluorescein (505-550 nm) and rhodamine (560-615 nm). Representative fields are shown. No fluorescence was observed in uninfected BHK-21 cells without the DePsipher™ reagent (I). Micrographs C and F are enlarged to indicate the difference in fluorescence between a healthy (C) and an apoptotic (F) cell. Bar = 20 µm.

4.4 DISCUSSION

African horse sickness virus (AHSV) is vectored by haematophagous *Culicoides* spp. to equids and causes severe oedema and haemorrhages in horses, but is asymptomatic in the insect host (Mellor and Hamblin, 2004; Wilson *et al*., 2009). This is also reflected in tissue culture where AHSV causes rapid cell death in infected mammalian cells in culture, whereas infection of insect cells are unapparent and show no CPE (Osawa and Hazrati, 1965; Mirchamsy *et al.*, 1970). The basis for this differential host response is not known, but may be due to the induction of apoptosis in infected mammalian cells. Indeed, analyses of endothelial cells of animals infected with AHSV indicated ultrastructural changes that could be suggestive of apoptosis (Gómez-Villamandos *et al*., 1999). Various reports have indicated that infection of mammalian cells by viruses induces apoptosis, as well as a variety of signal transduction pathways (Brojatsch *et al*., 1996; Jan and Griffin, 1999; Connolly *et al*., 2000; Gadaleta *et al*., 2002). There are two common pathways for the induction of apoptosis, *i.e.* the extrinsic pathway, which is primarily initiated by virus attachment to receptors, and the intrinsic pathway, which is mediated by damage to the mitochondria (Jin and El-Deiry, 2005; Xu and Shi, 2007; Duprez *et al*., 2009). In this part of the investigation, a series of experiments were undertaken to examine the induction of apoptosis during AHSV-9 infection of mammalian and insect cells, and to identify effectors of AHSV-induced apoptosis.

Examination of AHSV-infected BHK-21 cells by light and transmission electron microscopy showed the presence of morphological hallmarks associated with the induction of apoptosis, which included cell shrinkage and detachment, nuclear chromatin condensation, blebbing of the plasma membrane and the formation of apoptotic bodies. These morphological alterations are a consequence of biochemical changes that occur during apoptosis (Wyllie, 1981; Kerr *et al*., 1984; Schwartzman and Cidlowski, 1993). Nuclear changes, *e.g.* chromatin condensation and apoptotic body formation, are the result of both DNA cleavage and proteolysis of key nuclear polypeptides (Earnshaw *et al*., 1999; Nicholson, 1999; Fischer *et al*., 2003). The loss of overall cell shape has been attributed to caspase cleavage of gelsolin and fodrin proteins, while detachment of cells from the surface has been attributed to caspase cleavage of the adherence junction proteins β-catenin and plakoglobin γ-catenin (Kothakota *et al*., 1997; Schmeiser *et al*., 1998; Hengartner, 2000). Moreover, caspase cleavage and subsequent activation of the proapoptotic kinase ROCK1

results in blebbing of the plasma membrane (Coleman *et al*., 2001), whereas caspase-dependent cleavage of nuclear proteins, such as lamin-A and lamin-B, are associated with nuclear shrinkage (Rao *et al*., 1996). It thus follows that cellular caspases play a key role in apoptosis (Alnemri *et al*., 1996; Li and Yuan, 2008).

During apoptosis, the excision of nucleosome chains by Topoisomerase II and DNAse I/DNAse II is routinely used as a biochemical marker of apoptosis (Wyllie, 1980; 1981; Earnshaw, 1995). Caspase-activated deoxyribonuclease (CAD)/DNA fragmentation factor 40 (DFF40), a 40-kDa nuclear enzyme, is activated by caspase-3 and promotes apoptotic DNA degradation (Enari *et al*., 1998; Cao *et al*., 2001). Consequently, BHK-21 cells infected with AHSV-9 were examined for nuclear DNA fragmentation and activation of caspase-3. Caspase-3 is a key executioner molecule of the caspase cascade that leads to apoptosis (Hengartner, 2000). In virus-infected BHK-21 cells the onset and timing of DNA fragmentation, as evidenced by the enrichment of endosomes in the cytoplasm of AHSV-infected cells, coincided with the activation of caspase-3. Both DNA fragmentation and caspase-3 activity were first observed at 12 h post-infection and reached a maximum at 24 h post-infection. No further increase in DNA fragmentation was observed, thus indicating that at 24 h post-infection the nuclear DNA had been fragmented in almost all of the cells. Indeed, the DNA laddering pattern became more random from 48 h post-infection onwards, most likely due to non-specific nucleolysis of already fragmented nuclear DNA (Koyama and Adachi, 1997). In contrast, the caspase-3 activity in AHSV-infected cells decreased gradually until 72 h post-infection, possibly due to increasing cell lysis. These results differ from those reported for BTV in which DNA fragmentation is observed at 36 h post-infection and caspase-3 is activated at 24 h post-infection in virus-infected mammalian cells (Mortola *et al*., 2004; Stewart and Roy, 2010). Interestingly, it has been observed previously that cells infected with AHSV display a much stronger cytopathic effect at early times after infection than cells infected with BTV (Wirblich *et al*., 2006), suggesting that these two orbiviruses may differ in virulence. It is tempting to speculate that the apparent difference in virulence may reflect on AHSV having to replicate as rapidly as possible (and by implication quicker than BTV) to avoid the cellular machinery being shut down by apoptosis. This may have the added advantage of rapid spreading of progeny virions to neighboring cells following apoptosis-induced

cell lysis. Alternatively, it may also be that the difference in virulence is due to differences in the cytotoxicity of different membrane permeabilizing viral proteins, *e.g.* NS3 and/or VP5.

In the intrinsic pathway apoptosis is triggered by internal signals, mainly mediated and controlled by Bcl-2 family members, which lead to disruption of the mitochondrial transmembrane potential (Green and Kroemer, 2004; Chipuk and Green, 2008). Once mitochondrial depolarization occurs, cell death is precipitated through the release of molecules such as cytochrome c and Smac/DIABLO. To determine whether AHSV-9 causes mitochondria damage, virus-infected BHK-21 cells were examined following incubation of the cell monolayers with DePsipher™, an indicator of mitochondrial membrane depolarization. AHSV-9 infection of BHK-21 cells resulted in mitochondrial depolarization as early as 6 h post-infection and increased gradually until 24 h post-infection. These results therefore indicate that the intrinsic mitochondrial signaling pathway is involved in AHSV-induced apoptosis. These results are in agreement with those presented for orthoreovirus (Kominsky *et al*., 2002a) and BTV (Nagaleekar *et al*., 2007), both of which activate the intrinsic apoptosis pathway following loss of mitochondrial membrane potential. The early stage at which mitochondrial depolarization occurs in AHSV-infected BHK-21 cells may indicate that apoptosis is triggered by a virus-induced event early in the infection cycle. In this regard, it is noteworthy that exogenous treatment of mammalian cells with purified recombinant BTV VP2 and VP5 proteins, but not with each protein used separately, was sufficient to trigger an apoptotic response (Mortola *et al.*, 2004). This would suggest that both outer capsid proteins play an important role in apoptosis induction and furthermore implies that receptor binding alone is likely insufficient to trigger apoptosis, but that virus uncoating in the endosome is also required. Interestingly, apoptosis induction in reovirus-infected mammalian cells is reported to require viral disassembly in cellular endosomes, but not viral transcription and replication (Connolly and Dermody, 2002; Danthi *et al*., 2006). It may therefore be that the process of apoptosis for orbiviruses, such as AHSV and BTV, is very similar to that of orthoreoviruses.

In contrast to AHSV-infected mammalian cells, there were no morphological or biochemical signs of apoptosis in a cell line derived from *C. sonorensis*, despite prolonged exposure of the KC insect cells to AHSV-9 (7 days) and expression of viral proteins. Although apoptosis in insect

cells has been documented (Clarke and Clem, 2003; Claveria and Torres, 2003; Kornbluth and White, 2005), this finding suggests that the signaling pathway for the induction of apoptosis is not triggered by AHSV infection of insect cells. The results are similar to those reported for other arboviruses, such as Sindbis virus (Karpf and Brown, 1998), La Crosse virus (Borucki *et al*., 2002), Dengue virus (Courageot *et al*., 2003), BTV (Mortola *et al*., 2004) and West Nile virus (Li and Stollar, 2004). All of these viruses replicate to high titres in both insect vector and vertebrate cells, but CPE is only observed in infected vertebrate cells and strongly correlates with the amount of apoptosis seen in the cells. It is plausible that the invasion, replication and dissemination strategy of AHSV, as well as the above viruses, may act differently in insect cells compared to mammalian cells. Indeed, one of the major morphological differences observed during infection of insect and mammalian cells in culture are that BTV appears to preferentially bud from the plasma membrane of insect cells, thus leaving the cells intact. In contrast, in mammalian cell culture, a high proportion of virus remains cell-associated, leading to eventual cell lysis (Hyatt *et al.*, 1989; Guirakhoo *et al.*, 1995). Moreover, in this study, immunoblot analyses of AHSV-infected BHK-21 and KC cell lysates detected the nonstructural protein NS2 at 12 h and 3 days post-infection, respectively, indicating that there may be a difference in the rate of virus replication in the respective cell cultures.

Collectively, the results obtained in this part of the investigation indicated that AHSV induced apoptosis in mammalian cells, but not in insect cells. Specifically, it was demonstrated that apoptosis is induced in virus-infected mammalian cells via the intrinsic apoptotic pathway, following mitochondrial membrane depolarization that results in subsequent activation of caspase-3. Despite these first steps, further studies are needed to gain insights into several aspects of AHSV-induced apoptosis. These include, amongst other, examining the role, if any, of the extrinsic apoptotic pathway in AHSV-induced apoptosis, the identification of viral proteins responsible for inducing apoptosis and the role of AHSV-induced apoptosis in AHSV pathogenesis. Such studies will not only extend knowledge regarding AHSV-host interactions, but may also pave the way to developing new strategies for the prevention and control of AHSV infections.

CHAPTER FIVE

CONCLUDING REMARKS

African horse sickness virus (AHSV) particles are composed of seven structural proteins organized into two concentric capsids that encapsidate the genome of ten double-stranded RNA (dsRNA) segments (Verwoerd *et al.*, 1972; Roy *et al.*, 1994b). The outer capsid is composed of two major structural proteins, VP2 and VP5, which, in turn, encapsidate the internal capsid, or core, and is composed of two major proteins (VP3 and VP7) and three minor proteins (VP1, VP4 and VP6). AHSV also encodes four nonstructural proteins (NS1, NS2 and NS3/NS3A) that are considered to play important roles in virus assembly and release. In contrast to the nonstructural proteins (Uitenweerde *et al.*, 1995; van Staden *et al.*, 1995; Maree and Huismans, 1997), not much is known regarding the biological function of the AHSV structural proteins. Interestingly, the outer capsid proteins of various members of the *Reoviridae* family, such as bluetongue virus (BTV) (Mortola *et al.*, 2004) and reovirus (Tyler *et al.*, 1995; Connolly and Dermody, 2002), have been implicated in the induction of apoptosis in infected mammalian cells. Consequently, the primary aims of this investigation were to functionally characterize the VP5 protein of AHSV and to determine whether AHSV can induce apoptosis in infected mammalian cells and by which mechanism. In this conclusion, the new information that has evolved during this investigation will be summarized and suggestions regarding future research will be made.

An RNA interference (RNAi)-based approach was initially used to investigate the biological relevance of AHSV VP5. RNAi is an evolutionary conserved cellular pathway that induces degradation of target mRNA in a sequence-specific manner, leading to post-transcriptional silencing of gene expression (Fire *et al.*, 1998). Consequently, it has become a widely used research tool whereby loss-of-function phenotypes can be generated and thereby allow virus gene function to be determined (López and Arias, 2004; Cuadras *et al.*, 2006; Ayala-Breton *et al.*, 2009; Kobayashi *et al.*, 2009). In mammalian cell cultures, RNAi is most commonly induced by exogenously delivered small interfering RNA (siRNA) (Elbashir *et al.*, 2001a; Caplen *et al.*, 2001) or endogenously expressed short hairpin RNA (shRNA) (Brummelkamp *et al.*, 2002b; Rubinson *et al.*, 2003; Shen *et al.*, 2003). During the course of this investigation, both approaches were explored as a means to silence expression of the AHSV VP5 gene. By making use of an *in vitro* model of infection, results were obtained indicating VP5-directed shRNAs were not capable of reducing the VP5 mRNA levels in virus-infected Vero cells. In contrast, different VP5-directed siRNAs resulted in a modest reduction (1.8- to 2.5-fold) of VP5 mRNA expression

in virus-infected BHK-21 cells (Chapter 2). Since there are presently no reliable methods to select for effective RNAi effector molecules without empirical testing, these results indicate that there may be room for improvement in searching for the ideal sequence or region in VP5 that may yield the optimum activity. It is, however, interesting to note that in comparative analyses between the use of siRNAs and shRNAs to silence gene expression of the AHSV NS2 protein, it was found that siRNAs were much more efficacious in silencing gene expression compared to their shRNA counterparts (M.A. Nieuwoudt and D.J. Patterson, unpublished data). Similar results have also been reported in the literature (Bridge *et al.*, 2003; Lambeth *et al.*, 2007). Despite the success and usefulness of RNAi-based gene silencing approaches, several shortcomings to this technology have been identified, including the transient nature of the gene silencing in the case of siRNAs (Elbashir *et al.*, 2002; Dykxhoorn *et al.*, 2003; Rao *et al.*, 2009), induction of apoptosis in the case of using vector-based RNAi approaches (Ghodgaonkar *et al.*, 2009; Kandan-Kulangara *et al.*, 2010) and the inability to study mutant versions of selected genes in the absence of complete gene silencing. Many of these hurdles can be overcome if a reverse genetic system was available for AHSV that would allow for genetic manipulation of the virus. Strategies to rescue infectious viruses from cloned cDNA or *in vitro* transcribed synthetic RNA transcripts has only recently been reported for some members of the *Reoviridae* family, including reovirus (Kobayashi *et al.*, 2007; 2010) and BTV (Boyce *et al.*, 2008). Notably, during the completion of this research project, a publication appeared describing the recovery of infectious AHSV from core-derived viral transcripts and showed that reassortment viruses could be derived by mixing the core-derived transcripts with an *in vitro*-derived T7 transcript (Matsuo *et al.*, 2010). Although this probably does not reflect a "true" reverse genetic system, it does nevertheless indicate that it may indeed be possible to develop reverse genetic system for AHSV. It can be envisaged that the successful development of a reverse genetic approach for AHSV would greatly advance research in this field and therefore should be explored in greater detail.

Despite the use of two different approaches and seven different RNAi effector molecules, silencing of AHSV VP5 gene expression in mammalian cells was inefficient. This therefore necessitated that an alternative approach be adopted whereby its possible biological role in virus infection could be investigated. For this purpose, VP5 was tagged with gluthathione *S*-transferase (GST) and expressed by a recombinant baculovirus in *Spodoptera frugiperda* (Sf-9)

insect cells. The VP5 protein was shown to permeabilize the Sf-9 cells, indicating cytotoxicity. By taking structural features of VP5 into account, a series of N- and C-terminal truncated VP5 proteins were generated and their biological activity was compared with the parental VP5 protein. Truncated VP5 proteins that included the N-terminal 43 amino acids (comprising of two amphipathic α-helices) exhibited membrane permeabilizing activity, and subsequent exogenous addition of synthetic VP5 peptides indicated that both these α-helices are required for membrane permeabilization (Chapter 3). The ability of VP5 to destabilize membranes may be indicative of a role during the early stages of virus infection, most likely following virus internalization but prior to cell penetration of the transcriptionally active cores. Recently it has been reported that the VP5 protein of BTV interacts with lipid rafts, as well as with plasma membrane-associated NS3, thus suggesting that these interactions may be important during virus assembly and egress (Bhattacharya and Roy, 2008). However, the VP5 protein of all nine AHSV serotypes lacks the conserved membrane-docking domain identified in VP5 sequences of BTV and the closely related epizootic hemorrhagic disease virus (EHDV). Considering that the assembly of the outer capsid proteins VP2 and VP5 onto the core is unlikely to occur in the virus inclusion body (VIB) structures (Modrof *et al.*, 2005; Kar *et al.*, 2007), this raises some interesting future questions regarding intracellular trafficking of the AHSV VP5 protein, as well as when and where in the cell VP5 is assembled into maturing virions. Since results obtained in this investigation indicated that intracellularly expressed AHSV VP5 by means of a baculovirus recombinant was capable of inducing membrane permeabilization, it follows that VP5 is likely to possess a unique signal for its membrane targeting. Thus, whether lipid rafts participate in the transport, morphogenesis and release of AHSV or whether the virus follows an as-yet-undescribed route from the cytosol to the plasma membrane warrants further investigation.

Although AHSV infects both mammalian and insect cells in culture, severe cytopathic effects (CPE) leading to rapid cell death are only observed in infected mammalian cells (Osawa and Hazrati, 1965; Mirchamsy *et al*., 1970). The ability of AHSV to replicate in these two distinct cell types and induce dramatically different phenotypes thus provided an ideal model system to determine whether apoptosis is induced by AHSV following infection of susceptible cells. Consequently, apoptosis was investigated in BHK-21 mammalian cells and *Culicoides sonorensis* (KC) insect cells infected with AHSV-9. The infected cell monolayers were

examined for several key indicators of apoptosis, namely cell morphology, chromosomal DNA fragmentation and caspase-3 activation. The results indicated that AHSV infection induced apoptosis in the BHK-21 cells, but not in the KC insect cells. Furthermore, flow cytometry analyses and confocal laser scanning microscopy of virus-infected BHK-21 cells stained with DePsipher™ revealed the loss of mitochondrial membrane potential. These results therefore indicate that AHSV-induced apoptosis involves the intrinsic apoptosis signaling pathway (Chapter 4). It has been reported that other members of the *Reoviridae* family, *e.g.* BTV (Nagaleekar *et al*., 2007; Stewart and Roy, 2010) and reovirus (Richardson-Burns *et al.*, 2002; Clarke *et al*., 2005), induce apoptosis through activation of both the intrinsic and extrinsic apoptosis signaling pathways. Future studies should therefore be aimed at investigating the involvement of the extrinsic signaling pathway in AHSV-induced apoptosis. These studies should also be extended to include investigations of NF-κβ and interferon regulatory factors, both of which have roles in initiating an antiviral environment as part of the cellular innate immune response (Connolly *et al.*, 2000; Iwamura *et al.*, 2001). It would also be of interest to determine whether the AHSV outer capsid proteins are sufficient to trigger apoptosis, as had been reported for BTV (Mortola *et al.*, 2004), and through which mechanism(s). Interestingly, Meiring *et al.* (2009) reported that Vero cells infected with a monoreassortant AHSV, which contained nine genome segments from AHSV-4 and the S10 genome segment from AHSV-2, had titres of up to ten-fold higher than the respective parent viruses. In addition, the CPE of the monoreassortant virus was less severe than that of both parental virus and a CellTiter-Blue® cell viability assay indicated that 85% of the infected cells were still viable at 48 h post-infection. Since several viroporins have been shown to induce apoptosis (Madan *et al*., 2008), it would thus be of interest to determine whether NS3 might also be involved in apoptosis induction. The induction of apoptosis by members of the *Reoviridae* family, notably rotavirus (Sato *et al*., 2006), reovirus (Richardson-Burns and Tyler, 2004) and BTV (Umeshappa *et al*., 2010), has been shown to play a major role in the pathogenesis of these virus infections. To determine whether this is true for AHSV, it will be essential to investigate caspase activation and the role of apoptosis in African horse sickness disease in susceptible animals. It can be envisaged that such studies could, in the long-term, aid in the identification of apoptosis inhibitors that may reduce disease severity and thus provide a novel strategy for treating or limiting virus-induced tissue damage following virus infection.

In summary, this study has shown that the VP5 protein of AHSV-9 is a membrane destabilizing protein and that this activity is associated with the N-terminal 43 amino acids of VP5. It was furthermore shown that, in contrast to insect cells, AHSV-9 induces apoptosis in infected mammalian cells and involves the intrinsic apoptosis signaling pathway. A greater understanding of the biological importance of VP5, as well as the initiators and nature of the pathways involved in AHSV-induced apoptosis may in future aid the design of alternative strategies whereby the virus can be controlled or lessen the impact of African horse sickness disease.

PUBLICATIONS AND CONGRESS CONTRIBUTIONS

Conference contributions

1. **Stassen**, **L**., Huismans, H. and Theron, J. (2008). African horse sickness virus induces apoptosis in cultured mammalian cells. Bio-08 joint Conference of the South African Society for Microbiology, South African Society for Biotechnology and South African Society of Biochemistry and Molecular Biology, 21-25 January 2008, Grahamstown, South Africa.

2. **Stassen**, **L**., Barnes, W.A., Nieuwoudt, M.A., Huismans, H., van Staden, V. and Theron, J. (2008) Suppression of African horse sickness virus gene expression by siRNA and shRNA in mammalian cells. 20th Biennial Congress of the South African Genetics Society, 27-29 March 2008, Pretoria, South Africa.

3. **Stassen**, **L**., Huismans, H. and Theron, J. (2009). African horse sickness virus-induced cell death in mammalian cell cultures. 10th International Symposium on Double-Stranded RNA viruses, 21-25 June 2009, Hamilton Island, Great Barrier Reef, Australia.

Publications

Stassen, **L**., Huismans, H. and Theron, J. (2011). Membrane permeabilization of the African horse sickness virus VP5 protein is mediated by two N-terminal amphipathic α-helices. Arch. Virol. 156, 711-715.

Stassen, **L**., Huismans, H. and Theron, J. (2011). African horse sickness virus induces apoptosis in mammalian cells. Submitted

REFERENCES

Aagaard, L., Amarzguioui, M., Sun, G., Santos, L.C., Ehsani, A., Prydz, H. and Rossi, J.J. (2007). A facile lentiviral vector system for expression of doxycycline-inducible shRNAs: Knockdown of the pre-miRNA processing enzyme Drosha. *Mol. Ther.* 15, 938-945.

Acehan, D., Jiang, X., Morgan, D.G., Heuser, J.E., Wang, X. and Akey, C.W. (2002). Three dimensional structure of the apoptosome: Implications for assembly, procaspase-9 binding, and activation. *Mol. Cell* 9, 423-432.

Agosto, M.A., Ivanovic, T. and Nibert, M.L. (2006). Mammalian reovirus, a nonfusogenic nonenveloped virus, forms size-selective pores in a model membrane. *Proc. Natl. Acad. Sci. USA* 103, 16496-16501.

Alembekov, I.R., Kretova, O.V., Gashnikova, N.M., Pokrovsky, A.G. and Tchurikov, N.A. (2009). Efficiency of the RNA interference induced by the genetic constructs expressing siRNAs depends on promoter strength. *Mol. Biol.* 43, 344-347.

Alexopoulou, L., Holt, A.C., Medzhirov, R. and Flavell, R.A. (2001). Recognition of double-stranded RNA and activation of NF-kappaβ by Toll-like receptor 3. *Nature* 413, 732-738.

Alnemri, E.S., Livingston, D.J., Nicholson, D.W., Salvesen, G., Thornberry, N.A., Wong, W.W. and Yuan, J. (1996). Human ICE/CED-3 protease nomenclature. *Cell* 87, 171.

Altschul, S.F., Madden, T.L., Schaffer, A.A., Zhang, J., Zhang, Z., Miller, W. and Lipman, D.J. (1997). Gapped BLAST and PSI-BLAST: A new generation of protein database search programs. *Nucleic Acids Res.* 25, 3389-3402.

Amarzguioui, M., Holen, T., Babaie, E. and Prydz, H. (2003). Tolerance for mutations and chemical modifications in a siRNA. *Nucleic Acids Res.* 31, 589-595.

Amarzguioui, M., Rossi, J.J. and Kim, D. (2005). Approaches for chemically synthesized siRNA and vector-mediated RNAi. *FEBS Lett.* 579, 5974-5981.

Ameres, S.L., Martinez, J. and Schroeder, R. (2007) Molecular basis for target RNA recognition and cleavage by human RISC. *Cell* 130, 101-112.

Anderson, E.M., Birmingham, A., Baskerville, S., Reynolds, A., Maksimova, E., Leake, D., Fedorov, Y., Karpilow, J. and Khvorova, A. (2008). Experimental validation of the importance of seed complement frequency to siRNA specificity. *RNA* 14, 853-861.

Ayala-Breton, C., Arias, M., Espinosa, R., Romero, P., Arias, C.F. and Lopez, S. (2009). Analysis of the kinetics of transcription and replication of the rotavirus genome by RNA interference. *J. Virol.* 83, 8819-8834.

Bagchi, P., Dutta, D., Chattopadhyay, S., Mukherjee, A., Halder, U.C., Sarkar, S., Kobayashi, N., Komoto, S., Taniguchi, K. and Chawla-Sarkar, M. (2010). Rotavirus non-structural protein-1 suppresses virus-induced cellular apoptosis to facilitate viral growth by activating the cell-survival pathways during early stages of infection. *J. Virol.* 84, 6834-6845.

Baker, K.A., Dutch, R.E., Lamb, R.A. and Jardetzky, T.S. (1999). Structural basis for paramyxovirus-mediated membrane fusion. *Mol. Cell* 3, 309-319.

Baker, M. and Prasad, B.V. (2010). Rotavirus cell entry. *Curr. Top. Microbiol. Immunol.* 343, 121-148.

Banan, M. and Puri, N. (2004). The ins and outs of RNAi in mammalian cells. *Curr. Pharm. Biotechnol.* 5, 441-450.

Banerjee, M. and Johnson, J.E. (2008). Activation, exposure and penetration of virally encoded membrane-active polypeptides during non-enveloped virus entry. *Curr. Prot. Pept. Sci.* 9, 16-27.

Bao, Q. and Shi, Y. (2007). Apoptosome: A platform for the activation of initiator caspases. *Cell Death Differ.* 14, 56-65.

Barnard, J.H. (1998). Epidemiology of African horse sickness and the role of the zebra in South Africa. *Arch. Virol.* (*Suppl.*) 14, 13-19.

Barton, E.S., Chappell, J.D., Connolly, J.L., Forrest, J.C. and Dermody, T.S. (2001). Reovirus receptors and apoptosis. *Virology* 290, 173-180.

Basak, A.K., Gouet, P., Grimes, J., Roy, P. and Stuart, D. (1996). Crystal structure of the top domain of African horse sickness virus VP7: Comparison with Bluetongue virus VP7. *J. Virol.* 70, 3797-3806.

Basak, A.K., Stuart, D.I. and Roy, P. (1992). Preliminary crystallographic study of bluetongue virus capsid protein, VP7. *J. Mol. Biol.* 228, 687-689.
Beaton, A.R., Rodriguez, J., Reddy, Y.K. and Roy, P. (2002). The membrane trafficking protein calpactin forms a complex with bluetongue virus protein NS3 and mediates virus release. *Proc. Natl. Acad. Sci. USA* 99, 13154-13159.
Benedict, C.A., Norris, P.S. and Ware, C.F. (2002). To kill or be killed: Viral evasion of apoptosis. *Nature Immunol.* 3, 1013-1018.
Benedict, C.A., Norris, P.S., Prigozy, T.I., Bodmer, J.L., Mahr, J.A., Garnett, C.T., Martinon, F., Tschopp, J., Gooding, L.R. and Ware, C.F. (2001). Three adenovirus E3 proteins cooperate to evade apoptosis by tumor necrosis factor-related apoptosis-inducing ligand receptor-1 and -2. *J. Biol. Chem.* 276, 3270-3278.
Bernstein, E., Caudy, A.A., Hammond, S.M. and Hannon, G.J. (2001). Role for a bidentate ribonuclease in the initiation step of RNA interference. *Nature* 409, 363-366.
Bertin, J., Armstrong, R.C., Ottilie, S., Martin, D.A., Wang, Y., Banks, S., Wang, G.H., Senkevich, T.G., Alnemri, E.S., Moss, B., Lenardo, M.J., Tomaselli, K.J. and Cohen, J.I. (1997). Death-effector domain-containing herpesvirus and poxvirus proteins inhibit both Fas-and TNFR1-induced apoptosis. *Proc. Natl. Acad. Sci. USA* 94, 1172-1176.
Bhattacharya, B. and Roy, P. (2008). Bluetongue virus outer capsid protein VP5 interacts with membrane lipid rafts via a SNARE domain. *J. Virol.* 82, 10600-10612.
Bhattacharya, B., Noad, R.J. and Roy, P. (2007). Interaction between Bluetongue virus outer capsid protein VP2 and vimentin is necessary for virus egress. *Virol. J.* 4, 7.
Birnbaum, M.J., Clem, R.J. and Miller, L.K. (1994). An apoptosis-inhibiting gene from a nuclear polyhedrosis virus encoding a polypeptide with Cys/His sequence motifs. *J. Virol.* 68, 2521-2528.
Birnboim, H.C. and Doly, J. (1979). A rapid alkaline extraction procedure for screening recombinant plasmid DNA. *Nucleic Acids Res.* 7, 1513-1523.
Blumenstiel, J.P. and Hartl, D.L. (2005). Evidence for maternally transmitted small interfering RNA in the repression of transposition in *Drosophila virilis*. *Proc. Natl. Acad. Sci. USA* 102, 15965-15970.
Boatright, K.M., Renatus, M., Scott, F.L., Sperandio, S., Shin, H., Pedersen, I.M., Ricci, J.E., Edris, W.A., Sutherlin, D.P., Green, D.R. and Salvesen, G.S. (2003). A unified model for apical caspase activation. *Mol. Cell.* 11, 529-541.
Boden, D., Pusch, O., Lee, F., Tucker, L., Shank, P.R. and Ramratnam, B. (2003). Promoter choice affects the potency of HIV-1 specific RNA interference. *Nucleic Acids Res.* 31, 5033-5038.
Boise, L.H., Gonzalez-Garcia, M., Postema, C.E., Ding, L., Lindsten, T., Turka, L.A., Mao, X., Nuñez, G. and Thompson, C.B. (1993). Bcl-x, a *bcl-2*-related gene that functions as a dominant regulator of apoptotic cell death. *Cell* 74, 597-608.
Borucki, M.K., Kempf, B.J., Blitvich, B.J., Blair, C.D. and Beaty, B.J. (2002). La Crosse virus: Replication in vertebrate and invertebrate hosts. *Microbes Infect.* 4, 341-350.
Boyce, M., Cristina, C.P.C. and Roy, P. (2008). Development of reverse genetics systems for bluetongue virus: Recovery of infectious virus from synthetic RNA transcripts. *J. Virol.* 82, 8339-8348.
Boyce, M., Wehrfritz, J., Noad, R. and Roy, P. (2004). Purified recombinant bluetongue virus VP1 exhibits RNA replicase activity. *J. Virol.* 78, 3994-4002.
Boyle, J.S. and Lew, A.M. (1995). An inexpensive alternative to glassmilk for DNA purification. *Trends Genet.* 11, 8.
Braasch, D.A., Jensen, S., Liu, Y., Kaur, K., Arar, K., White, M.A. and Corey, D.D. (2003). RNA interference in mammalian cells by chemically-modified RNA. *Biochemistry* 42, 7967-7975.
Bremer, C.W. (1976). A gel electrophoretic study of the protein and nucleic acid components of African horsesickness virus. *Onderstepoort J. Vet. Res.* 43, 193-199.
Bremer, C.W., Huismans, H. and van Dijk, A.A. (1990). Characterization and cloning of the African horsesickness virus genome. *J. Gen. Virol.* 71, 793-799.
Bridge, A.L., Pebernard, S., Ducraux, A., Nicoulaz, A.L. and Iggo, R. (2003). Induction of an interferon response by RNAi vectors in mammalian cells. *Nature Genet.* 34, 263-264.

Brojatsch, J., Naughton, J., Rolls, M.M., Zingler, K. and Young, J.A. (1996). CAR1, a TNFR-related protein, is a cellular receptor for cytopathic avian leukosis-sarcoma viruses and mediates apoptosis. *Cell* 87, 845-855.

Brookes, S.M., Hyatt, A.D. and Eaton, B.T. (1993). Characterization of virus inclusion bodies in bluetongue virus infected cells. *J. Gen. Virol.* 74, 525-530.

Broquet, A.H., Lenoir, C., Gardet, A., Sapin, C., Chwetzoff, S., Jouniaux, A.M., Lopez, S., Trugnan, G., Bachelet, M. and Thomas, G. (2007). Hsp70 negatively controls rotavirus protein biovailability in Caco-2 cells infected by the rotavirus RF strain. *J. Virol.* 81, 1297-1304.

Brown, C.C. and Dardiri, A.H. (1990). African horsesickness: A continuing menace. *J. Am. Vet. Med. Assoc.* 196, 2019-2021.

Brown, G.C. and Borutaite, V. (2008). Regulation of apoptosis by the redox state of cytochrome c. *Biochim. Biophys. Acta* 1777, 877-881.

Brown, K.M., Chu, C.Y. and Rana, T.M. (2005). Target accessibility dictates the potency of human RISC. *Nature Struct. Mol. Biol.* 12, 469-470.

Brown, M. and Faulkner, P. (1977). A plaque assay for nuclear polyhedrosis viruses using a solid overlay. *J. Gen. Virol.* 36, 361-364.

Brown, S.E., Morrison, H.G., Karabatsos, N. and Knudson, D.L. (1991). Genetic relatedness of two new Orbivirus serogroups: Orungo and Lebombo. *J. Gen. Virol.* 72, 1065-1072.

Brummelkamp, T.R., Bernards, R. and Agami, R. (2002a). A system for stable expression of short interfering RNAs in mammalian cells. *Science* 296, 550-553.

Brummelkamp, T.R., Bernards, R. and Agami, R. (2002b). Stable suppression of tumorgenicity by virus-mediated RNA-interference. *Cancer Cell* 2, 243-247.

Burger, L. (2006). Silencing African horsesickness virus VP7 protein expression *in vitro* by RNA interference. M.Sc Thesis, Department of Microbiology and Plant Pathology, Faculty of Biological and Agricultural Sciences, University of Pretoria, South Africa.

Burroughs, J.N., O'Hara, R.S., Smale, C.J., Hamblin, C., Walton, A., Armstrong, R. and Mertens, P.P.C. (1994). Purification and properties of virus particles, infectious subviral particles, cores and VP7 crystals of African horsesickness virus serotype 9. *J. Gen. Virol.* 75, 1849-1857.

Calisher, C.H. and Mertens, P.P.C. (1998). Taxonomy of African horse sickness viruses. *Arch. Virol.* (*Suppl.*) 14, 3-11.

Callus, B.A. and Vaux, D.L. (2007). Caspase inhibitors: Viral, cellular and chemical. *Cell Death Differ.* 14, 73-78.

Campagna, M., Eichwald, C., Vascotto, F. and Burrone, O.R. (2005). RNA interference of rotavirus segment 11 mRNA reveals the essential role of NSP5 in the virus replicative cycle. *J. Gen. Virol.* 86, 1481-1487.

Cao, G., Pei, W., Lan, J., Stetler, R.A., Luo, Y., Nagayama, T., Graham, S.H., Yin, X.M., Simon, R.P. and Chen, J. (2001). Activated DNase/DNA fragmentation factor 40 mediates apoptotic DNA fragmentation in transient cerebral ischemia and in neuronal cultures. *J. Neurosci.* 21, 4678-4690.

Caplen, N.J., Parrish, S., Imani, F., Fire, A. and Morgan, R.A. (2001). Specific inhibition of gene expression by small double-stranded RNAs in invertebrate and vertebrate systems. *Proc. Natl. Acad. Sci. USA* 98, 9742-9747.

Carmell, M.A., Xuan, Z., Zhang, M.Q. and Hannon, G.J. (2002). The Argonaute family: Tentacles that reach into RNAi, developmental control, stem-cell maintenance, and tumorgenesis. *Genes Dev.* 16, 2733-2742.

Carthew, R.W. and Sontheimer, E.J. (2009). Origins and mechanisms of miRNAs and siRNAs. *Cell* 136, 642-655.

Carvalho, J., Arnold, M.M. and Nibert, M.L. (2007). Silencing and complementation of reovirus core protein mμ2: Functional correlations with mμ2-microtubule association and differences between virus- and plasmid-derived mμ2. *Virol.* 364, 301-316.

Castanotto, D., Li, H. and Rossi, J.J. (2002). Functional siRNA expression from transfected PCR products. *RNA* 8, 1454-1460.

Celma, C.C.P. and Roy, P. (2009). A viral nonstructural protein regulates bluetongue virus trafficking and release. *J. Virol.* 83, 6806-6816.
Cerutti, H. and Casas-Mollano, J.A. (2006). On the origin and functions of RNA-mediated silencing: From protists to man. *Curr. Genet.* 50, 81-99.
Chan, F.D., Berger, J.M. and Kim, P.S. (1997). Core structure of gp41 from the HIV envelope glycoprotein. *Cell* 89, 263-273.
Chandran, K., Farsetta, D.L. and Nibert, M.L. (2002). Strategy for nonenveloped virus entry: A hydrophobic conformer of the reovirus membrane protein µ1 mediates membrane disruption. *J. Virol.* 76, 9920-9933.
Chang, D.W., Xing, Z., Capacio, V.L., Peter, M.E. and Yang, X. (2003). Interdimer processing mechanism of procaspase-8 activation. *EMBO J.* 22, 4132-4142.
Chang, T.J., Juan, C.C., Yin, P.H., Chin, C.W. and Tsay, H.J. (1998). Up-regulation of beta-actin, cyclophilin and GAPDH in N1S1 rat hepatoma. *Oncol. Rep.* 5, 469-471.
Chaïbi, C., Cotte-Laffitte, J., Sandré, C., Esclatine, A., Servin, A.L., Quéro, A.-M. and Géniteau-Legendre, A. (2005). Rotavirus induces apoptosis in fully differentiated human intestinal Caco-2 cells. *Virology* 332, 480-490.
Chen, M. and Wang, J. (2002). Initiator caspases in apoptosis signaling pathways. *Apoptosis* 7, 313-319.
Chen, M., Granger, A.J., VanBrocklin, M.W., Payne, W.S., Hunt, H., Zhang, H., Dodgson, J.B. and Holmen, S.L. (2007). Inhibition of avian leukosis virus replication by vector-based RNA interference. *Virology* 365, 464-472.
Chipuk, J.E. and Green, D.R. (2008). How do Bcl-2 proteins induce mitochondrial outer membrane permeabilization? *Trends Cell Biol.* 18, 157-164.
Chiu, Y.L. and Rana, T.M. (2002). RNAi in human cells: Basic structural and functional features of small interfering RNA. *Mol. Cell* 10, 549-561.
Chowdhury, I., Tharakan, B. and Bhat, G. (2006). Current concepts in apoptosis: The physiological suicide program revisited. *Cell. Mol. Biol. Lett.* 11, 506-525.
Chowdhury, I., Tharakan, B. and Bhat, G.K. (2008). Caspases - An update. *Comp. Biochem. Physiol.* 151, 10-27.
Chuma, T., Le Blois, H., Sanchez-Vizcaino, J.M., Diaz-Laviada, M. and Roy, P. (1992). Expression of the major core antigen VP7 of African horsesickness virus by a recombinant baculovirus and its use as a group-specific diagnostic reagent. *J. Gen. Virol.* 73, 925-931.
Clarke, P. and Tyler, K.L. (2009). Apoptosis in animal models of virus-induced disease. *Nature Rev. Microbiol.* 7, 144-155.
Clarke, P., Beckham, J.D., Leser, J.S., Hoyt, C.C. and Tyler, K.L. (2009). Fas-mediated apoptotic signaling in the mouse brain following reovirus infection. *J. Virol.* 83, 6161-6170.
Clarke, P., Meintzer, S.M., Spalding, A.C., Johnson, G.L. and Tyler, K.L. (2001). Caspase 8-dependent sensitization of cancer cells to TRAIL-induced apoptosis following reovirus-infection. *Oncogene* 20, 6910-6919.
Clarke, P., Meinzter, S.M., Wang, Y., Moffitt, L.A., Richardson-Burns, S.M., Johnson, G.L. and Tyler, K.L. (2004). JNK regulates the release of pro-apoptotic mitochondrial factors in reovirus-infected cells. *J. Virol.* 78, 13132-13138.
Clarke, P., Richardson-Burns, S.M., DeBiasi, R.L. and Tyler, K.L. (2005). Mechanisms of apoptosis during reovirus infection. *Curr. Top. Microbiol. Immunol.* 289, 1-24.
Clarke, T.E. and Clem, R.J. (2003). Insect defenses against virus infection: The role of apoptosis. *Int. Rev. Immunol.* 22, 401-424.
Claveria, C. and Torres, M. (2003). Mitochondrial apoptotic pathways induced by *Drosophila* programmed cell death regulators. *Biochem. Biophys. Res. Commun.* 304, 531-537.
Clem, R. J. (2007). Baculoviruses and apoptosis: A diversity of genes and responses. *Curr. Drug Targets* 8, 1069-1074.
Clem, R.J., Fechheimer, M. and Miller, L.K. (1991) Prevention of apoptosis by a baculovirus gene during infection of insect cells. *Science* 254, 1388-1390.

Coetzer, J.A.W. and Erasmus, B.J. (1994). African horsesickness. In: Infectious Diseases of Livestock. J.A.W. Coetzer, G.R. Thomson and R.C. Tustin (Eds.), pp. 460-475, Oxford University Press, Cape Town.

Cohen, S.N., Chang, A.C.Y. and Hsu, L. (1972). Nonchromosomal antibiotic resistance in bacteria: Genetic transformation of *Escherichia coli* by R-factor DNA. *Proc. Natl. Acad. Sci. USA* 69, 2110-2114.

Coleman, M.L., Sahai, E.A., Yeo, M., Bosch, M., Dewar, A. and Olson, M.F. (2001). Membrane blebbing during apoptosis results from caspase-mediated activation of Rock I. *Nature Cell Biol.* 3, 339-345.

Connolly, J.L. and Dermody, T.S. (2002). Virion disassembly is required for apoptosis induced by reovirus. *J. Virol.* 76, 1632-1641.

Connolly, J.L., Rodgers, S.E., Clarke, P., Ballard, D.W., Kerr, D.L., Tyler, K.L. and Dermody, T.S. (2000). Reovirus-induced apoptosis requires activation of transcription factor NF-κβ. *J. Virol.* 74, 2981-2989.

Courageot, M.P., Catteau, A. and Despres, P. (2003). Mechanisms of Dengue virus-induced cell death. *Adv. Virus Res.* 60, 157-186.

Cowley, J.A. and Gorman, B.M. (1987). Genetic reassortants for identification of the genome segment coding for the bluetongue virus hemagglutinin. *J. Virol.* 61, 2304-2306.

Cowley, J.A., Walker, P.J. and Gorman, B.M. (1992). Recognition sites in assembly of bluetongue viruses. In: Bluetongue, African horse sickness and related orbiviruses. Proceedings of the Second International Symposium. T.E. Walton and B.I. Osborn (Eds.), pp. 423-432. CRC Press, London.

Csorba, T., Pantaleo, V. and Burgyán, J. (2009). RNA silencing: An antiviral mechanism. *Adv. Virus Res.* 75, 35-71.

Cuadras, M.A., Bordier, B.B., Zambrano, J.L., Ludert, J.E. and Greenberg, H.B. (2006). Dissecting rotavirus particle-raft interaction with small interfering RNAs: Insights into rotavirus transit through the secretory pathway. *J. Virol.* 80, 3935-3946.

Czauderna, F., Fechtner, M., Dames, S., Aygün, H., Klippel, A., Pronk, G.J., Giese, K. and Kaufmann, J. (2003a). Structural variations and stabilising modifications of synthetic siRNAs in mammalian cells. *Nucleic Acids Res.* 31, 2705-2716.

Czauderna, F., Santel, A., Hinz, M., Fechtner, M., Durieux, B., Fisch, G., Leenders, F., Arnold, W., Giese, K., Klippel, A. and Kaufmann, J. (2003b). Inducible shRNA expression for application in a prostate cancer mouse model. *Nucleic Acids Res.* 31, e127.

Danial, N.N. and Korsmeyer, S.J. (2004). Cell death: Critical control points. *Cell* 116, 205-219.

Danthi, P., Guglielmi, K.M., Kirchner, E., Mainou, B., Stehle, T. and Dermody, T.S. (2010). From touchdown to transcription: The reovirus cell entry pathway. *Curr. Top. Microbiol. Immunol.* 343, 91-119.

Danthi, P., Hansberger, M.W., Campbell, J.A., Forrest, J.C. and Dermody, T.S. (2006). JAM-A-independent, antibody-mediated uptake of reovirus into cells leads to apoptosis. *J. Virol.* 80, 1261-1270.

Danthi, P., Kobayashi, T., Holm, G.H., Hansberger, M.W., Abel, T.W. and Dermody, T.S. (2008). Reovirus apoptosis and virulence are regulated by host cell membrane-penetration efficiency. *J. Virol.* 82, 161-172.

Davis, M.P., Bottley, G., Beales, L.P., Killington, R.A., Rowlands, D.J. and Tuthill, T.J. (2008). Recombinant VP4 of human rhinovirus induces permeability in model membranes. *J. Virol.* 82, 4169-4174.

de Waal, P.J. and Huismans, H. (2005). Characterization of the nucleic acid binding activity of inner core protein VP6 of African horse sickness virus. *Arch. Virol.*150, 2037-2050.

DeBiasi, R.L., Clarke, P., Meintzer, S., Jotte, R., Kleinschmidt-Demasters, B.K., Johnson, G.L. and Tyler, K.L. (2003). Reovirus-induced alteration in expression of apoptosis and DNA repair genes with potential roles in viral pathogenesis. *J. Virol.* 77, 8934-8947.

Decker, T. and Lohmann-Matthes, M.L. (1988). A quick and simple method for the quantitation of lactate dehydrogenase release in measurements of cellular cytotoxicity and tumor necrosis factor (TNF) activity. *J. Immunol. Methods* 115, 61-69.

Déctor, M.A., Romero, P., López, S. and Arias, C.F. (2002). Rotavirus gene silencing by small interfering RNAs. *EMBO Rep.* 3, 1175-1180.
Degterev, A., Boyce, M. and Yuan, J. (2003). A decade of caspases. *Oncogene* 22, 8543-8567.
DeMaula, C.D., Bonneau, K.R. and MacLachlan, J. (2000). Changes in the outer capsid proteins of bluetongue virus serotype ten that abrogate neutralization by monoclonal antibodies. *Virus Res.* 67, 59-66.
DeMaula, C.D., Jutila, M.A., Wilson, D.W. and MacLachlan, N.J. (2001). Infection kinetics, prostacyclin release and cytokine-mediated modulation of the mechanism of cell death during bluetongue virus infection of cultured ovine and bovine pulmonary artery and lung microvascular endothelial cells. *J. Gen. Virol.* 82, 787-794.
Denisova, E., Dowling, W., LaMonica, R., Shaw, R., Scarlata, S., Ruggeri, F. and Mackow, E.R. (1999). Rotavirus capsid protein VP5* permeabilizes membranes. *J. Virol.* 73, 3147-3153.
Desagher, S., Osen-Sand, A., Nichols, A., Eskes, R., Montessuit, S., Lauper, S., Maundrell, K., Antonsson, B. and Martinou, J.C. (1999). Bid-induced conformational change of Bax is responsible for mitochondrial cytochrome c release during apoptosis. *J. Cell Biol.* 144, 891-901.
Deveraux, Q.L. and Reed, J.C. (1999). IAP family proteins: Suppressors of apoptosis. *Genes Dev*. 13, 239-252.
Deveraux, Q.L., Roy, N., Stennicke, H.R., Van Arsdale, T., Zhou, Q., Srinivasula, S.M., Alnemri, E.S., Salvesen, G.S. and Reed, J.C. (1998). IAPs block apoptotic events induced by caspase-8 and cytochrome c by direct inhibition of distinct caspases. *EMBO J.* 17, 2215-2223.
Deveraux, Q.L., Takahashi, R., Salvesen, G.S. and Reed, J.C. (1997). X-linked IAP is a direct inhibitor of cell-death proteases. *Nature* 388, 300-304.
Ding, C. and Cantor, C.R. (2004). Quantitative analysis of nucleic acids – the last few years of progress. *J. Biochem. Mol. Biol.* 37, 1-10.
Dispersyn, G., Nuydens, R., Connors, R., Borgers, M. and Geerts, H. (1999). Bcl-2 protects against FCCP-induced apoptosis and mitochondrial membrane potential depolarization in PC12 cells. *Biochim. Biophys. Acta* 1428, 357-371.
Doench, J.G., Petersen, C.P. and Sharp, P.A. (2003). siRNAs can function as miRNAs. *Genes Dev.* 17, 438-442.
Donze, O. and Picard, D. (2002). RNA interference in mammalian cells with siRNA synthesized with T7 RNA polymerase. *Nucleic. Acids Res.* 30, e46.
Dowling, W., Denisova, E., LaMonica, R. and Mackow, E.R. (2000). Selective membrane permeabilization by the rotavirus VP5* protein is abrogated by mutations in an internal hydrophobic domain. *J. Virol.* 74, 6368-6376.
du Plessis, M. and Nel, L.H. (1997). Comparative sequence analysis and expression of the M6 gene, encoding the outer capsid protein VP5 of African horsesickness virus serotype nine. *Virus Res.* 47, 41-49.
Du, C., Fang, M., Li, Y., Li, L. and Wang, X. (2000). Smac, a mitochondrial protein that promotes cytochrome c-dependent caspase activation by eliminating IAP inhibition. *Cell* 102, 33-42.
Du, Q., Thonberg, H., Wang, J., Wahlestedt, C. and Liang, Z. (2005). A systematic analysis of the silencing effects of an active siRNA at all single-nucleotide mismatched target sites. *Nucleic Acids Res.* 33, 1671-1677.
Duckett, C.S., Nava, V.E., Gedrich, R.W., Clem, R.J., Van Dongen, J.L., Gilfillan, M.C., Shiels, H., Hardwick, J.M. and Thompson, C.B. (1996). A conserved family of cellular genes related to the baculovirus *iap* gene and encoding apoptosis inhibitors. *EMBO J.* 15, 2685-2694.
Dufour, B., Moutou, F., Hattenberger, A.M. and Rodhain, F. (2008). Global change: Impact, management risk approach and health measures – the case of Europe. *Rev. Sci. Tech.* 27, 529-550.
Duprez, L., Wirawan, E., Vanden Berghe, T. and Vandenabeele, P. (2009). Major cell death pathways at a glance. *Microbes Infect.* 11, 1050-1062.
Dutta, D., Bagchi, P., Chatterjee, A., Nayak, M.K., Mukherjee, A., Chattopadhyay, S., Nagashima, S., Kobayashi, N., Komoto, S., Taniguchi, K. and Chawla-Sarkar, M. (2009). The molecular chaperone heat shock protein-90 positively regulates rotavirus infection. *Virology* 391, 325-333.

Dykxhoorn, D.M., Novina, C.D. and Sharp, P.A. (2003). Killing the messenger: Short RNAs that silence gene expression. *Nature Rev. Mol. Cell Biol.* 4, 457-467.
Earnshaw, W.C. (1995). Nuclear changes in apoptosis. *Curr. Opin. Cell Biol.* 7, 337-343.
Earnshaw, W.C., Martins, L.M. and Kaufmann, S.H. (1999). Mammalian caspases: Structure, activation, substrates, and functions during apoptosis. *Annu. Rev. Biochem*. 68, 383-424.
Eaton, B.T. and Crameri, G.S. (1989). The site of bluetongue virus attachment to glycophorins from a number of animal erythrocytes. *J. Gen. Virol.* 70, 3347-3353.
Eaton, B.T., Hyatt, A.D. and Brookes, S.M. (1990). The replication of bluetongue virus. *Curr. Top. Microbiol. Immunol.* 162, 89-118.
Eaton, B.T., Hyatt, A.D. and White, J.R. (1988). Localization of the nonstructural protein NS1 in bluetongue virus-infected cells and its presence in virus particles. *Virol.* 163, 527-537.
Ekert, P.G., Silke, J., Hawkins, C.J., Verhagen, A.M. and Vaux, D.L. (2001). DIABLO promotes apoptosis by removing MIHA/XIAP from processed caspase 9. *J. Cell Biol.* 152, 483-490.
el Hasnaoui, H., el Harrak, M., Zientara, S., Laviada, M. and Hamblin, C. (1998). Serological and virological responses in mules and donkeys following inoculation with African horse sickness virus serotype 4. *Arch. Virol.* (*Suppl.*) 14, 29-36.
Elbashir, S.M., Harborth, J., Lendeckel, W., Yalcin, A., Weber, K. and Tuschl, T. (2001a). Duplexes of 21-nucleotide RNAs mediate RNA interference in cultured mammalian cells. *Nature* 411, 494-498.
Elbashir, S.M., Harborth, J., Weber, K. and Tuschl, T. (2002). Analysis of gene function in somatic mammalian cells using small interfering RNAs. *Methods* 26, 199-213.
Elbashir, S.M., Lendeckel, W. and Tuschl, T. (2001b). RNA interference is mediated by 21 and 22-nucleotide RNAs. *Genes Dev.* 15, 188-200.
Elbashir, S.M., Martinez, J., Patkaniowska, A., Lendeckel, W. and Tuschl, T. (2001c). Functional anatomy of siRNAs for mediating efficient RNAi in *Drosophila melanogaster* embryo lysate. *EMBO J.* 20, 6877-6888.
Elmore, S. (2007). Apoptosis: A review of programmed cell death. *Toxicol. Pathol.* 35, 495-516.
Enari, M., Sakahira, H., Yokoyama, H., Okawa, K., Iwamatsu, A. and Nagata, S. (1998). A caspase-activated DNase that degrades DNA during apoptosis, and its inhibitor ICAD. *Nature* 391, 43-50.
Epand, R.M., Shai, Y., Segrest, J.P. and Anantharamaiah, G.M. (1995). Mechanisms for the modulation of membrane bilayer properties by amphipathic helical peptides. *Biopolymers* 37, 319-338.
Erasmus, B.J. (1973). The pathogenesis of African horse sickness. In: Equine infectious disease III. Proceedings of the Third International Conference of Equine Infectious Disease. J.T. Bryans and H. Gerber (Eds.), pp. 1-11. Karger, Basel.
Erasmus, B.J. (1976). A new approach to polyvalent immunization against African horsesickness. Proceeding of the Fourth International Conference of Equine Infectious Diseases, Lyon, pp. 401-403. Princeton, N.J. Veterinary Publications, Inc.
Erasmus, B.J., Young, E., Pieterse, L.M. and Boshoff, S.T. (1978). The susceptibility of zebra and elephants to African horsesickness virus. *J. Equine Med. Surg.* (*Suppl.*) 1, 409-413.
Estes, M.K., Graham, D.Y. and Mason, B.B. (1981). Proteolytic enhancement of rotavirus infectivity: Molecular mechanisms. *J. Virol.* 39, 879-888.
Falanga, A., Cantisani, M., Pedone, C. and Galdiero, S. (2009). Membrane fusion and fission: Enveloped viruses. *Protein Pept Lett.* 16, 751-759.
Fassi-Fihri, O., el Harrak, M. and Fassi-Fehri, M.M. (1998). Clinical, virological and immune responses of normal and immunosuppressed donkeys (*Equus asinus africanus*) after inoculation with African horse sickness virus. *Arch. Virol.* (*Suppl.*) 14, 49-56.
Fesik, S.W. (2000). Insights into programmed cell death through structural biology. *Cell* 103, 273-282.
Finkel, E. (2001). The mitochondrion: Is it central to apoptosis? *Science* 292, 624-626.
Fire, A., Xu, S., Montgomery, M.K., Kostas, S.A., Driver, S.E. and Mello, C.C. (1998). Potent and specific genetic interference by double-stranded RNA in *Caenorhabditis elegans*. *Nature* 391, 806-811.
Fischer, R., Baumert, T. and Blum, H.E. (2007). Hepatitis C virus infection and apoptosis. *World J. Gastroenterol.* 13, 4865-4872.

Fischer, U., Jänicke, R.U. and Schulze-Osthoff, K. (2003). Many cuts to ruin: A comprehensive update of caspase substrates. *Cell Death Differ.* 10, 76-100.
Fish, R.J. and Kruithof, E.K. (2004). Short-term cytotoxic effects and long-term instability of RNAi delivered using lentiviral vectors. *BMC Mol. Biol.* 3, 5-9.
Forzan, M., Marsh, M. and Roy, P. (2007). Bluetongue virus entry into cells. *J. Virol.* 81, 4819-4827.
Forzan, M., Wirblich, C. and Roy, P. (2004). A capsid protein of nonenveloped bluetongue virus exhibits membrane fusion activity. *Proc. Natl. Acad. Sci. USA* 101, 2100-2105.
Foss, D.L., Baarsch, M.J. and Murtaugh, M.P. (1998). Regulation of hypoxanthine phosphoribosyltransferase, glyceraldehyde-3-phosphate dehydrogenase and β-actin mRNA expression in porcine immune cells and tissues. *Animal Biotechnol.* 9, 67-78.
Francki, R.I.B., Fauquet, C.M., Knudson, D.L. and Brown, F. (1991). Classification and nomenclature of viruses. Fifth Report of the International Committee on Taxonomy of Viruses. Springer, Wien New York. *Arch. Virol.* (*Suppl.*) *2*.
French, T.J., Inumaru, S. and Roy, P. (1989). Expression of two related nonstructural proteins of bluetongue virus (BTV) type 10 in insect cells by a recombinant baculovirus: Production of polyclonal ascitic fluid and characterization of the gene product in BTV-infected BHK cells. *J. Virol.* 63, 3270-3278.
Fuentes-Prior, P. and Salvesen, G.S. (2004). The protein structures that shape caspase activity, specificity, activation and inhibition. *Biochem. J.* 384, 201-232.
Gadaleta, P., Vacotto, M. and Coulombie, F. (2002). Vesicular stomatitis virus induces apoptosis at early stages in the viral cycle and does not depend on virus replication. *Virus Res.* 86, 87-92.
Gale, P., Brouwer, A., Ramnial, V., Kelly, L., Kosmider, R., Fooks, A.R. and Snary, E.L. (2009). Assessing the impact of climate change on vector-borne viruses in the EU through the elicitation of expert opinion. *Epidemiol. Infect.* 7, 1-12.
Galluzzi, L., Brenner, C., Morselli, E., Touat, Z. and Kroemer, G. (2008). Viral control of mitochondrial apoptosis. *PLoS Pathogens* 4, e1000018.
Gan, J., Tropea, J.E., Austin, B.P., Court, D.L., Waugh, D.S. and Ji, X. (2006). Structural insight into the mechanism of double-stranded RNA processing by ribonuclease III. *Cell* 124, 355-366.
Ge, Q., Ilves, H., Dallas, A., Kumar, P., Shorenstein, J., Kazakov, S.A. and Johnston, B.H. (2010). Minimal-length short hairpin RNAs: The relationship of structure and RNAi activity. *RNA* 16, 106-117.
Ghodgaonkar, M.M., Sha, R.G., Kandan-Kulangara, F., Affar, E.-B., Qi, H.H., Wiemer, E. and Shah, G.M. (2009). Abrogation of DNA vector-based RNAi during apoptosis in mammalian cells due to caspase-mediated cleavage and inactivation of Dicer-1. *Cell Death Differ.* 16, 858-868.
Gibson, L., Holmgreen, S.P., Huang, D.C., Bernard, O., Copeland, N.G., Jenkins, N.A., Sutherland, G.R., Baker, E., Adams, J.M. and Cory, S. (1996). Bcl-w, a novel member of the Bcl-2 family, promotes cell survival. *Oncogene* 13, 665-675.
Giering, J.C., Grimm, D., Storm, T.A. and Kay, M.A. (2008). Expression of shRNA from tissue-specific pol II promoter is an effective and safe RNAi therapeutic. *Mol. Ther.* 16, 1630-1636.
Golantsova, N.E., Gorbunova, E.E. and Mackow, E.R. (2004). Discrete domains within the rotavirus VP5* direct peripheral membrane association and membrane permeability. *J. Virol.* 78, 2037-2044.
Golks, A., Brenner, D., Fritsch, C., Krammer, P.H. and Lavrik, I.N. (2005). C-FLIPR: A new regulator of death receptor-induced apoptosis. *J. Biol. Chem*. 280, 14507-14513.
Gómez-Villamandos, J.C., Sánchez, C., Carrasco, L., Laviada, M.D., Bautista, M.J., Martínez-Torrecuadrada, J., Sánchez-Vizcaíno, J.M. and Sierra, M.A. (1999). Pathogenesis of African horse sickness: Ultrastructural study of the capillaries in experimental infection. *J. Comp. Path.* 121, 101-116.
Gorman, B.M. (1979). Variation in Orbiviruses. *J. Gen. Virol.* 44, 1-15.
Gorman, B.M. (1985). Speciation in orbiviruses. *Prog. Clin. Biol. Res.* 178, 275-278.
Gorman, B.M. (1992). An overview of orbiviruses. In: Bluetongue, African horse sickness and related orbiviruses. Proceedings of the Second International Symposium. T.E. Walton and B.I. Osburn (Eds.), pp. 335-348. CRC Press, London.
Gorman, B.M. and Taylor, J. (1985). Orbiviruses. In: Field's Virology. B.N. Fields and D.M. Knipe (Eds.), pp. 275-278. Raven Press, New York.

Gou, D., Jin, N. and Liu, L. (2003). Gene silencing in mammalian cells by PCR-based short hairpin RNA. *FEBS Lett.* 548, 113-118.
Gou, D., Weng, T., Wang, Y., Wang, Z., Zhang, H., Gao, L., Chen, Z., Wang, P. and Liu, L. (2007). A novel approach for the construction of multiple shRNA expression vectors. *J. Gene Med.* 9, 751-763.
Gould, A.R. and Hyatt, **A.D.** (1994). The orbivirus genus, diversity, structure, replication and phylogenetic relationships. *Comp. Immunol. Microbiol. Infect. Dis.* 17, 163-188.
Gould, A.R. and Pritchard, L.I. (1988). The complete nucleotide sequence of the outer coat protein, VP5, of the Australian bluetongue virus (BTV) serotype 1 reveals conserved and non-conserved sequences. *Virus Res.* 9, 285-292.
Gray, D.C., Hoeflich, K.P., Peng, L., Gu, Z., Gogineni, A., Murray, L.J., Eby, M., Kljavin, N., Seshagiri, S., Cole, M.J. and Davis, D.P. (2007). pHUSH: A single vector system for conditional gene expression. *BMC Biotechnol.* 7, 61.
Gredell, J.A., Berger, A.K. and Walton, S.P. (2008). Impact of target mRNA structure on siRNA silencing efficiency: A large-scale study. *Biotechnol. Bioeng.* 100, 744-755.
Green, D.R. and Kroemer, G. (2004). The pathophysiology of mitochondrial cell death. *Science* 305, 626-629.
Grimes, J.M., Burroughs, J.N., Gouet, P., Diprose, J.M., Malby, R., Zientara, S., Mertens, P.P. and Stuart, D.I. (1998). The atomic structure of the bluetongue virus core. *Nature* 395, 470-478.
Grishok, A., Pasquinelli, A., Conte, D., Li, N., Parrish, S., Ha, I., Baillie, D., Fire, A., Ruvkun, G. and Mello, C. (2001). Genes and mechanisms related to RNA interference regulate expression of the small temporal RNAs that control *C. elegans* developmental timing. *Cell* 106, 23-34.
Gross, A., McDonnell, J.M. and Korsmeyer, S.J. (1999). Bcl-2 family members and the mitochondria in apoptosis. *Genes Dev.* 13, 1899-1911.
Grubman, M. and Lewis, S. (1992). Identification and characterisation of the structural and non-structural proteins of African horse sickness virus and determination of the genome coding assignments. *Virology* 186, 444-451.
Guinea, R. and Carrasco, L. (1994). Influenza virus M2 protein modifies membrane permeability in *E. coli* cells. *FEBS Lett.* 343, 242-246.
Guirakhoo, F., Catalan, J.A. and Monath, T.P. (1995). Adaption of bluetongue virus in mosquito cells results in overexpression of NS3 proteins and release of virus particles. *Arch. Virol.* 140, 967-974.
Gupta, S., Schoer, R.A., Egan, J.E., Hannon, G.J. and Mittal, V. (2004). Inducible, reversible, and stable RNA interference in mammalian cells. *Proc. Natl. Acad. Sci. USA* 101, 1927-1932.
Guthrie, A.J. (2007). African horse sickness. In: Equine infectious diseases. D.C. Sellon and M. Long (Eds.), pp. 164-170, Suanders Elsevier, Missouri.
Hacein-Bey-Abina, S., Von Kalle, C., Schmidt, M., McCormack, M.P., Wulffraat, N., Leboulch, P., Lim, A., Osborne, C.S., Pawliuk, R., Morillon, E., Sorensen, R., Forster, A., Fraser, P., Cohen, J.I., de Saint Basile, G., Alexander, I., Wintergerst, U., Frebourg, T., Aurias, A., Stoppa-Lyonnet, D., Romana, S., Radford-Weiss, I., Gross, F., Valensi, F., Delabesse, E., Macintyre, E., Sigaux, F., Soulier, J., Leiva, L.E., Wissler, M., Prinz, C., Rabbitts, T.H., Le Deist, F., Fischer, A. and Cavazzana-Calvo, M. (2003). LMO2-associated clonal T cell proliferation in two patients after gene therapy for SCID-X1. *Science* 302, 415-419.
Haley, B. and Zamore, P.D. (2004). Kinetic analysis of the RNAi enzyme complex. *Nature Struct. Mol. Biol.* 11, 599-606.
Hall, T.A. (1999). BioEdit: A user-friendly biological sequence alignment editor and analysis program for Windows 95/98/NT. *Nucleic Acids Symp. Ser.* 41, 95-98.
Hammond, S.M., Bernstein, E., Beach, D. and Hannon, G.J. (2000). An RNA-directed nuclease mediates post-transcriptional gene silencing in *Drosophila* cells. *Nature* 404, 293-296.
Han, Z. and Harty, R.N. (2004). The NS3 protein of bluetongue virus exhibits viroporin-like properties. *J. Biol. Chem.* 279, 43092-43097.

Harborth, J., Elbashir, S.M., Vandenburgh, K., Manninga, H., Scaringe, S.A., Weber, K. and Tuschl, T. (2003). Sequence, chemical, and structural variation of small interfering RNAs and short hairpin RNAs and the effect on mammalian gene silencing. *Antisense Nucleic Acid Drug Dev.* 13, 83-105.
Hassan, S.H. and Roy, P. (1999). Expression and functional characterization of bluetongue virus VP2 protein: Role in cell entry. *J. Virol.* 73, 9832-9842.
Hassan, S.H., Wirblich, C., Forzan, M. and Roy, P. (2001). Expression and functional characterization of bluetongue virus VP5 protein: Role in cellular permeabilization. *J. Virol.* 75, 8356-8367.
Hassani, Z., Francois, J.C., Alfama, G., Dubois, G.M., Paris, M., Giovannangeli, C. and Demeneix, B.A. (2007). A hybrid CMV-H1 construct improves efficiency of PEI-delivered shRNA in the mouse brain. *Nucleic Acids Res*. 35, e65.
Hay, S. and Kannourakis, G. (2002). A time to kill: Viral manipulation of the cell death program. *J. Gen. Virol.* 83, 1547-1564.
Hayama, E. and Li, J.K. (1994). Mapping and characterization of antigenic epitopes and the nucleic acid-binding domains of VP6 protein of bluetongue viruses. *J. Virol.* 68, 3604-3611.
Heinonen, J.E., Mohamed, A.J., Nore, B.F. and Smith, C.I. (2005). Inducible H1 promoter-driven lentiviral siRNA expression by stuffer reporter deletion. *Oligonucleotides* 15, 139-144.
Hengartner, M.O. (2000). The biochemistry of apoptosis. *Nature* 407, 770-776.
Henry, S.D., van der Wegen, P., Metselaar, H.J., Tilanus, H.W., Scholte B.J. and van der Laan, L.J. (2006). Simultaneous targeting of HCV replication and viral binding with a single lentiviral vector containing multiple RNA interference expression cassettes. *Mol. Ther.* 14, 485-493.
Hewat, E.A., Booth, T.F. and Roy, P. (1992). Structure of bluetongue virus particles by cryoelectron microscopy. *J. Struct. Biol.* 109, 61-69.
Hewish, D.R. and Burgoyne, L.A. (1973). Chromatin sub-structure. The digestion of chromatin DNA at regularly spaced sites by a nuclear deoxyribonuclease. *Biochem. Biophys. Res. Commun.* 52, 504-510.
Hirsch, A.J. (2010). The use of RNAi-based screens to identify host proteins involved in viral replication. *Future Microbiol.* 5, 303-311.
Holen, T., Amarzguioui, M., Wiiger, M.T., Babaie, E. and Prydz, H. (2002). Positional effects of short interfering RNAs targeting the human coagulation trigger Tissue Factor. *Nucleic Acids Res.* 30, 1757-1766.
Howell, P.G. (1962). The isolation and identification of further antigenic types of African horse sickness virus. *Onderstepoort J. Vet. Res.* 29, 139-149.
Howie, H.L., Katzenellenbagen, R.A. and Galloway, D.A. (2009). Papilloma virus E6 proteins. *Virology* 384, 324-334.
Hsieh, A.C., Bo, R., Manola, J., Vazquez, F., Bare, O., Khvorova, A., Scaringe, S., Sellers, W.R. (2004). A library of siRNA duplexes targeting the phosphoinositide 3-kinase pathway: Determinants of gene silencing for use in cell-based screens. *Nucleic Acids Res.* 32, 893-901.
Hu, Y., Ding, L., Spencer, D.M. and Nunez, G. (1998). WD-40 repeat region regulates Apaf-1 self-association and procaspase-9 activation. *J. Biol. Chem.* 273, 33489-33494.
Huismans, H. (1979). Protein synthesis in bluetongue virus-infected cells. *Virol.* 92, 385-396.
Huismans, H. and Els, H.J. (1979). Characterization of tubules associated with the replication of three different orbiviruses. *Virol.* 92, 397-406.
Huismans, H. and Erasmus, B.J. (1981). Identification of the serotype-specific and group-specific antigens of bluetongue virus. *Onderstepoort J. Vet. Res.* 48, 51-58.
Huismans, H., van der Walt, N.T., Cloete, M. and Erasmus, B.J. (1987a). Isolation of a capsid protein of bluetongue virus that induces a protective immune response in sheep. *Virol.* 157, 172-179.
Huismans, H., van Dijk, A.A. and Bauskin, A.R. (1987b). *In vitro* phosphorylation and purification of a nonstructural protein of bluetongue virus with affinity for single-stranded RNA. *J. Virol.* 61, 3589-3595.
Hutvagner, G. and Simard, M.J. (2008). Argonaute proteins: Key players in RNA silencing. *Nature Rev. Mol. Cell Biol.* 9, 22-32.
Hyatt, A.D. and Eaton, B.T. (1988). Ultrastructural distribution of the major capsid proteins within bluetongue virus and infected cells. *J. Gen. Virol*. 69, 805-815.

Hyatt, A.D., Eaton, B.T. and Brookes, S.M. (1989). The release of bluetongue virus from infected cells and their superinfection by progeny virus. *Virology* 173, 21-34.
Hyatt, A.D., Eaton, B.T. and Lunt, R. (1987). The grid-cell-culture technique: The direct examination of virus-infected cells and progeny viruses. *J. Microscopy* 145, 97-106.
Hyatt, A.D., Gould, A.R., Coupar, B. and Eaton, B.T. (1991). Localisation of the non-structural protein NS3 in bluetongue infected cells. *J. Gen. Virol.* 72, 2263-2267.
Hyatt, A.D., Zhao, Y. and Roy, P. (1993). Release of bluetongue virus-like particles from insect cells is mediated by BTV nonstructural protein NS3/NS3A. *Virology* 193, 592-603.
Inumaru, S., Ghiasi, H. and Roy, P. (1987). Expression of bluetongue virus group-specific antigen VP3 in insect cells by a baculovirus vector: Its use for detection of bluetongue virus antibodies. *J. Gen. Virol.* 68, 1627-1635.
Isakovic, A., Jankovic, T., Harhaji, L., Kostic-Rajacic, S., Nikolic, Z., Vajs, V. and Trajkovic, V. (2008). Antiglioma action of xanthones from *Gentiana kockiana*: Mechanistic and structure-activity requirements. *Bioorg. Med. Chem.* 16, 5683-5694.
Itoh, N., Yonehara, S., Ishii, A., Yonehara, M., Mizushima, S., Sameshima, M., Hase, A., Seto, Y. and Nagata, S. (1991). The polypeptide encoded by the cDNA for human cell surface antigen Fas can mediate apoptosis. *Cell* 66, 233-243.
Iwamura, T., Yoneyama, M., Yamaguchi, K., Suhara, W., Mori, W., Shiota, K., Okabe, Y., Namiki, H. and Fujita, T. (2001). Induction of IRF-3/-7 kinase and NF-kappaβ in response to double-stranded RNA and virus infection: Common and unique pathways. *Genes Cells* 6, 375-388.
Iwata, H., Yamagawa, M. and Roy, P. (1992). Evolutionary relationships among the gnat-transmitted orbiviruses that cause African horse sicknes, bluetongue, and epizootic hemorrhagic disease is evidenced by their capsid protein sequences. *Virology* 191, 251-261.
Jackson, A.L., Bartz, S.R., Schelter, J., Kobayashi, S.V., Burchard, J., Mao, M., Li, B., Cavet, G. and Linsley, P.S. (2003). Expression profiling reveals off-target gene regulation by RNAi. *Nature Biotechnol.* 21, 635-637.
Jackson, A.L., Burchard, J., Leake, D., Reynolds, A., Schelter, J., Guo, J., Johnson, J.M., Lim, L., Karpilow, J., Nichols, K., Marshall, W., Khvorova, A. and Linsley, P.S. (2006). Position-specific chemical modification of siRNAs reduces "off-target" transcript silencing. *RNA* 12, 1197-1205.
Jan, J.T. and Griffin, D.E. (1999). Induction of apoptosis by Sindbis virus occurs at cell entry and does not require viral replication. *J. Virol.* 73, 10296-10302.
Jiang, J., Serinkan, B.F., Tyurina, Y.Y., Borisenko, G.G., Mi, Z., Robbins, P.D., Schroit, A.J. and Kagan, V.E. (2003). Peroxidation and externalization of phosphatidylserine associated with release of cytochrome c from mitochondria. *Free Radic. Biol. Med.* 35, 814-825.
Jin, Z. and El-Deiry, W.S. (2005). Overview of cell death signaling pathways. *Cancer Biol. Ther.* 4, 139-163.
Jinek, M. and Doudna, J.A. (2009). A three-dimensional view of the molecular machinery of RNA interference. *Nature* 457, 405-412.
Johnson, C.R. and Jarvis, W.D. (2004). Caspase-9 regulation: An update. *Apoptosis* 9, 423-427.
Kahlon, J., Sugiyama, K. and Roy, P. (1983). Molecular basis of bluetongue virus neutralization. *J. Virol.* 48, 627-632.
Kandran-Kulangara, F., Shah, R.G., Affar el, B. and Shah, G.M. (2010). Persistence of different forms of transient RNAi during apoptosis in mammalian cells. *PLoS One* 5: e12263.
Kanzaki, L.I., Ornelas, S.S. and Argañaraz, E.R. (2008). RNA interference and HIV-1 infection. *Rev. Med. Virol.* 18, 5-18.
Kar, A.K. and Roy, P. (2003). Defining the structure-function relationships of bluetongue virus helicase protein VP6. *J. Virol.* 77, 11347-11356.
Kar, A.K., Bhattacharya, B. and Roy, P. (2007). Bluetongue virus RNA binding protein NS2 is a modulator of viral replication and assembly. *BMC Mol. Biol.* 8, 4.
Kar, A.K., Ghosh, M. and Roy, P. (2004). Mapping the assembly pathway of Bluetongue virus scaffolding protein VP3. *Virol.* 324, 387-399.

Kariko, K., Bhuyan, P., Capodici, J. and Weissman, D. (2004b). Small interfering RNAs mediate sequence-independent gene suppression and induce immune activation by signaling through Toll-like receptor 3. *J. Immunol.* 172, 6545-6549.
Kariko, K., Bhuyan, P., Capodici, J., Ni, H., Lubinski, J., Friendman, H. and Weissman, D. (2004a). Exogenous siRNA mediates sequence-independent gene suppression by signaling through Toll-like receptor-3. *Cells Tiss. Org.* 177, 132-138.
Karpf, A.R. and Brown, D.T. (1998). Comparison of Sindbis virus-induced pathology in mosquito and vertebrate cell cultures. *Virology* 240, 193-201.
Karpf, A.R., Blake, J.M. and Brown, D.T. (1997). Characterization of the infection of *Aedes albopictus* cell clones by Sindbis virus. *Virus Res.* 50, 1-13.
Kawasaki, H., Suyama, E., Lyo, M. and Taira, K. (2003). siRNA generated by recombinant human Dicer induce specific and significant but target site-independent gene silencing in human cells. *Nucleic Acids Res.* 31, 981-987.
Ke, N., Godzik, A. and Reed, J.C. (2001). Bcl-B, a novel Bcl-2 family member that differentially binds and regulates Bax and Bak. *J. Biol. Chem.* 276, 12481-12484.
Kerr, J.F., Wyllie, A.H. and Currie, A.R. (1972). Apoptosis: A basic biological phenomenon with wide-ranging implications in tissue kinetics. *Br. J. Cancer* 26, 239-257.
Kerr, J.F.R., Bishop, C.J. and Searle, J. (1984). Apoptosis. In: Recent Advances in Histopathology. P.P. Anthony and R.N.M. Mac-Sween (Eds.), pp. 1-15, Churchill Livingstone, Edinburgh.
Ketzinel-Gilad, M., Shaul, Y. and Galun, E. (2006). RNA interference for antiviral therapy. *J. Gene Med.* 8, 933-950.
Khvorova, A., Reynolds, A. and Jayasena, S.D. (2003). Functional siRNAs and miRNAs exhibit strand bias. *Cell*, 115, 209-216.
Kiefer, M.C., Brauer, M.J., Powers, V.C., Wu, J.J., Umansky, S.R., Tomei, L.D. and Barr, P.J. (1995). Modulation of apoptosis by the widely distributed Bcl-2 homologue Bak. *Nature* 374, 736-739.
Kim, D.H., Behlke, M.A., Rose, S.D., Chang, M.S., Choi, S. and Rossi, J.J. (2005). Synthetic dsRNA Dicer substrates enhance RNAi potency and efficacy. *Nature Biotechnol.* 23, 222-226.
Kim, K., Lee, Y.S. and Carthew, R.W. (2007). Conversion of pre-RISC to holo-RISC by Ago2 during assembly of RNAi complexes. *RNA* 13, 22-29.
Kischkel, F.C., Lawrence, D.A., Tinel, A., LeBlanc, H., Virmani, A., Schow, P., Gazdar, A., Blenis, J., Arnott, D. and Ashkenazi, A. (2001). Death receptor recruitment of endogenous caspase-10 and apoptosis initiated in the absence of caspase-8. *J. Biol. Chem.* 276, 46639-46646.
Knudson, D.L. and Monath, T.P. (1990). Orbiviruses. In: Field's Virology. B.N. Fields and D.M. Knipe (Eds.), pp. 1405-1433. Raven Press, New York.
Kobayashi, T., Antar, A.A., Boehme, K.W., Danthi, P., Eby, E.A., Guglielme, K.M., Holm, G.H., Johnson, E.M., Maginnis, M.S., Naik, S., Skelton, W.B., Wetzel, J.D., Wilson, G.J., Chappell, J.D. and Dermody, T.S. (2007). A plasmid-based reverse genetics system for animal double-stranded RNA viruses. *Cell Host Microbe* 1, 147-157.
Kobayashi, T., Chapell, J.D., Danthi, P. and Dermody, T.S. (2006). Gene-specific inhibition of reovirus replication by RNA interference. *J. Virol.* 80, 9053-9063.
Kobayashi, T., Ooms, L.S., Chappell, J.D. and Dermody, T.S. (2009). Identification of functional domains in reovirus replication proteins μNS and μ2. *J. Virol*. 83, 2892-2906.
Kobayashi, T., Ooms, L.S., Ikizler, M., Chappell, J.D. and Dermody, T.S. (2010). An improved reverse genetics system for mammalian orthoreoviruses. *Virology* 398, 194-200.
Kominsky, D.J., Bickel, R.J. and Tyler, K.L. (2002a). Reovirus-induced apoptosis requires mitochondrial release of Smac/DIABLO and involves reduction of cellular inhibitor of apoptosis protein levels. *J. Virol.* 76, 11414-11424.
Kominsky, D.J., Bickel, R.J. and Tyler, K.L. (2002b). Reovirus-induced apoptosis requires both death-receptor- and mitochondrial-mediated caspase-dependent pathways of cell death. *Cell Death Differ.* 9, 926-933.

Kornberg, R.D. (1974). Chromatin structure: A repeating unit of histones and DNA. *Science* 184, 868-871.
Kornbluth, S. and White, K. (2005). Apoptosis in *Drosophila*: Neither fish nor fowl (nor man, nor worm). *J. Cell Sci.* 118, 1779-1787.
Korsmeyer, S.J., Wei, M.C., Saito, M., Weiler, S., Oh, K.J. and Schlesinger, P.H. (2000). Proapoptotic cascade activates Bid, which oligomerizes Bak or Bax into pores that result in the release of cytochrome c. *Cell Death Differ*. 7, 1166-1173.
Korzeniewski, C. and Callewaert, D.M. (1983). An enzyme-release assay for natural cytotoxicity. *J. Immunol. Methods* 64, 313-320.
Kothakota, S., Azuma, T., Reinhard, C., Klippel, A., Tang, J., Chu, K., McGarry, T.J., Kirschner, M.W., Koths, K., Kwaiatkowski, D.J. and Williams, L.T. (1997). Caspase-3-generated fragment of gelsolin: Effector of morphological change in apoptosis. *Science* 278, 294-298.
Koyama, A.H. and Adachi, A. (1997). Induction of apoptosis by herpex simplex virus type 1. *J. Gen. Virol.* 78, 2909-2912.
Kozopas, K.M., Yang, T., Buchan, H.L., Zhou, P. and Craig, R.W. (1993). Mcl1, a gene expressed in programmed myeloid cell differentiation, has sequence similarity to Bcl2. *Proc. Natl. Acad. Sci. USA* 90, 3516-3520.
Krammer, P.H. (1998). The CD95(APO-1/Fas)/CD95L system. *Toxicol. Lett.* 102/103, 131-137.
Kretschmer-Kazemi Far, R. and Sczakiel, G. (2003). The activity of siRNA in mammalian cells is related to structural target accessibility: A comparison with antisense oligonucleotides. *Nucleic Acids Res.* 31, 4417-4424.
Kumar, S. (2007). Caspase function in programmed cell death. *Cell Death Differ*. 14, 32-43.
Kuwana, T.L., Bouchier-Hayes, L., Chipuk, J.E., Bonzon, C., Sullivan, B.A., Green, D.R. and Newmeyer, D.D. (2005). BH3 domains of BH3-only proteins differentially regulate Bax-mediated mitochondrial membrane permeabilization both directly and indirectly. *Mol. Cell* 17, 525-535.
Kyte, J. and Doolittle, R.F. (1982). A simple method for displaying the hydrophobic character of a protein. *J. Mol. Biol.* 157, 105-142.
Laegreid, W.W. (1996). African horsesickness. In: Virus infections of vertebrates, Vol. 6. Virus Infections of Equines. M.J. Studdert (Ed.), pp. 101-123. Elsevier Press, Amsterdam.
Laemmli, U.K. (1970). Cleavage of structural proteins during the assembly of the head of bacteriophage T4. *Nature* 227, 680-685.
Lagunoff, M. and Caroll, P.A. (2003). Inhibition of apoptosis by the gamma-herpesviruses. *Int. Rev. Immunol.* 22, 373-399.
Lambeth, L.S., Moore, R.J., Muralitharan, M.S. and Doran, T.J. (2007). Suppression of bovine viral diarrhea virus replication by small interfering RNA and short hairpin RNA-mediated RNA interference. *Vet. Microbiol.* 119, 132-143.
Lamkanfi, M., Festjens, N., Declercq, W., Vanden Berghe, T. and Vandenabeele, P. (2007). Caspases in cell survival, proliferation and differentiation. *Cell Death Differ*. 14, 44-55.
Laviada, M.D., Roy, P., Sanchez-Vizcaino, J.M. and Casal, J.I. (1995). The use of African horse sickness virus NS3 protein, expressed in bacteria, as a marker to differentiate infected from vaccinated horses. *Virus Res.* 38, 205-218.
Le Blois, H., French, T., Mertens, P.P., Burroughs, J.N. and Roy, P. (1992). The expressed VP4 protein of bluetongue virus binds GTP and is the candidate guanylyl transferase of the virus. *Virology* 189, 757-761.
Lecatsas, G. (1968). Electron microscopic study of the formation of bluetongue virus. *Onderstepoort J. Vet. Res.* 35, 139-149.
Lecellier, C.H., Dunoyer, P., Arar, K., Lehmann-Che, J., Eyquem, S., Himber, C., Saib, A. and Voinnet, O. (2005). A cellular microRNA mediates antiviral defense in human cells. *Science* 308, 557-560.

Lee, N.S., Dohjima, T., Bauer, G., Li, H., Li, M.J., Ehsani, A., Salvaterra, P. and Rossi, J. (2002). Expression of small interfering RNAs targeted against HIV-1 rev transcripts in human cells. *Nature Biotechnol.* 20, 500-505.
Letai, A., Bassik, M.C., Walensky, L.D., Sorcinelli, M.D., Weiler, S. and Korsmeyer, S.J. (2002). Distinct BH3 domains either sensitize or activate mitochondrial apoptosis, serving as prototype cancer therapeutics. *Cancer Cell* 2, 183-192.
Levy, H., Fraenkel-Conrat, H. and Owens, R.A. (1994). Virology. Third edition, pp. 1-7. Prentice Hall, New Jersey.
Li, H., Zhu, H., Xu, C.J. and Yuan, J. (1998). Cleavage of Bid by caspase 8 mediates the mitochondrial damage in the Fas pathway of apoptosis. *Cell* 94, 491-501.
Li, J. and Yuan, J. (2008). Caspases in apoptosis and beyond. *Oncogene* 27, 6194-6205.
Li, L., Lin, X., Khvorova, A., Fesik, S. and Shen, Y. (2007a). Defining the optimal parameters for hairpin-based knockdown constructs. *RNA* 13, 1765-1774.
Li, M.L. and Stollar, V. (2004). Alphaviruses and apoptosis. *Int. Rev. Immunol.* 23, 7-24.
Li, Q., Li, H., Blitvich, B.J. and Zhang, J. (2007b). The *Aedes albopictus* inhibitor of apoptosis 1 gene protects vertebrate cells from bluetongue virus-induced apoptosis. *Insect Mol. Biol.* 16, 93-105.
Li, S., Zhao, Y., He, X., Kim, T.H., Kuharsky, D.K., Rabinowich, H., Chen, J., Du, C. and Yin, X.M. (2002). Relief of extrinsic pathway inhibition by the Bid-dependent mitochondrial release of Smac in Fas-mediated hepatocyte apoptosis. *J. Biol. Chem.* 277, 26912-26920.
Lin, X., Ruan, **X., Anderson, M.G., McDowell, J.A., Kroeger, P.E., Fesik, S.W. and Shen, Y.** (2005). siRNA-mediated off-target gene silencing triggered by a 7 nt complementation. *Nucleic Acids Res.* 33, 4527-4535.
Lingel, A., Simon, B., Izaurralde, E. and Sattler, M. (2004). Nucleic acid 39-end recognition by the Argonaute2 PAZ domain. *Nature Struct. Mol. Biol.* 11, 576-577.
Liu, C.M., Liu, D.P., Dong, W.J. and Liang, C.C. (2004). Retrovirus vector-mediated stable gene silencing in human cells. *Biochem. Biophys. Res. Commun.* 313, 716-720.
López, S. and Arias, C.F. (2004). Virus gene silencing by RNA interference. *Virus Res.* 102, 1-2.
López, T., Camacho, M., Zayas, M., Nájera, R., Sánchez, R., Arias, C.F. and López, S. (2005a). Silencing the morphogenesis of rotavirus. *J. Virol.* 79, 184-192.
López, T., Rojas, M., Ayala-Bretón, C., López, S. and Arias, C.F. (2005b). Reduced expression of the rotavirus NSP5 gene has a pleiotropic effect on virus replication. *J. Gen. Virol.* 86, 1609-1617.
Lord, C.C., Woolhouse, M.E. and Barnard, B.J. (1997). Transmission and distribution of virus serotypes: African horse sickness in zebra. *Epidemiol. Infect.* 118, 43-50.
Loudon, P.T. and Roy, P. (1992). Interaction of nucleic acids with core-like and subcore-like particles of bluetongue virus. *Virology* 191, 231-236.
Lowy, R.J. (2003). Influenza virus induction of apoptosis by intrinsic and extrinsic mechanisms. *Int. Rev. Immunol.* 22, 425-449.
Lu, Z.J. and Mathews, D.H. (2007). Efficient siRNA selection using hybridization thermodynamics. *Nucleic Acids Res.* 36, 640-647.
Luo, K.Q. and Chang, D.C. (2004). The gene-silencing efficiency of siRNA is strongly dependent on the local structure of mRNA at the targeted region. *Biochem. Biophys. Res. Commun.* 318, 303-310.
Luo, X., Budihardjo, I., Zou, H., Slaughter, C. and Wang, X. (1998). Bid, a Bcl2 interacting protein, mediates cytochrome c release from mitochondria in response to activation of cell surface death receptors. *Cell* 94, 481-490.
Lymperopoulos, K., Wirblich, C., Brierley, I. and Roy, P. (2003). Sequence specificity in the interaction of bluetongue virus non-structural protein 2 (NS2) with viral RNA. *J. Biol. Chem.* 278, 31722-31730.
Ma, J.B., Ye, K. and Patel, D.J. (2004). Structural basis for overhang-specific small interfering RNA recognition by the PAZ domain. *Nature* 429, 318-322.
Mackay, I.M., Arden, K.E. and Nitsche, A. (2002). Real-time PCR in virology. *Nucleic Acids Res.* 30, 1292-1305.

MacLachlan, N.J. and Guthrie, A.J. (2010). Re-emergence of bluetongue, African horse sickness, and other orbivirus diseases. *Vet. Res.* 41, 35.

MacLachlan, N.J., Balasuriya, U.B., Davis, N.L., Collier, M., Johnston, R.E., Ferraro, G.L. and Guthrie, A.J. (2007). Experiences with new generation vaccines against equine viral arteritis, West Nile disease and African horse sickness. *Vaccine* 25, 5577-5582.

Macrae, I.J., Zhou, K., Li, F., Repic, A., Brooks, A.N., Cande, W.Z., Adams, P.D. and Doudna, J.A. (2006). Structural basis for double-stranded RNA processing by Dicer. *Science* 311, 195-198.

Manche, L., Green, S.R., Schmedt, C. and Mathews, M.B. (1992). Interactions between double-stranded RNA regulators and the protein kinase DAI. *Mol. Cell. Biol.* 12, 5238-5248.

Manjunath, N., Wu, H.W., Subramanya, S. and Shankar, P. (2009). Lentiviral delivery of short hairpin RNAs. *Adv. Drug Deliv. Rev.* 61, 732-745.

Maree, F.F. and Huismans, H. (1997). Characterization of tubular structures composed of nonstructural protein NS1 of African horsesickness virus expressed in insect cells. *J. Gen. Virol.* 78, 1077-1082.

Maree, S., Durbach, S. and Huismans, H. (1998). Intracellular production of African horsesickness virus core-like particles by expression of the two major core proteins, VP3 and VP7, in insect cells. *J. Gen. Virol.* 79, 333-337.

Markovic, Z., Todorovic-Markovic, B., Kleut, D., Nikolic, N., Vranjes-Djuric, S., Misirkic, M., Vucicevic, L., Janjetovic, K., Isakovic, A., Harhaji, L., Babic-Stojic, B., Dramicanin, M. and Trajkovic, V. (2007). The mechanism of cell-damaging reactive oxygen generation by colloidal fullerenes. *Biomaterials* 28, 5437-5448.

Marshall, J.J. and Roy, P. (1990). High level expression of the two outer capsid proteins of bluetongue virus serotype 10: Their relationship with the neutralization of virus infection. *Virus Res.* 15, 189-195.

Marshall, O.J. (2004). PerlPrimer: Cross-platform, graphical primer design for standard, bisulphite and real-time PCR. *Bioinformatics* 20, 2471-2472.

Martelli, A.M., Zweyer, M., Ochs, R.L., Tazzari, P.L., Tabellini, G., Narducci, P. and Bortul, R. (2001). Nuclear apoptotic changes: An overview. *J. Cell. Biochem.* 82, 634-646.

Martin, S.J. and Green, D.R. (1995). Protease activation during apoptosis: Death by a thousand cuts? *Cell* 82, 349-352.

Martin, S.J., Reutelingsperger, C.P., McGahon, A.J., Rader, J.A., van Schie, R.C., LaFace, D.M. and Green, D.R. (1995). Early redistribution of plasma membrane phosphatidylserine is a general feature of apoptosis regardless of the initiating stimulus: Inhibition by overexpression of Bcl-2 and Abl. *J. Exp. Med.* 182, 1545-1556.

Martinez, J. and Tuschl, T. (2004). RISC is a 5' phosphomonoester-producing RNA endonuclease. *Genes Dev.* 18, 975-980.

Martinez, J., Patkaniowska, A., Urlaub, H., Luhrmann, R. and Tuschl, T. (2002). Single-stranded antisense siRNAs guide target RNA cleavage in RNAi. *Cell* 110, 563-574.

Martinez-Torrecuadrada, J.L., Diaz-Laviada, M., Roy, P., Sanchez, C., Vela, C., Sanchez-Vizcaino, J.M. and Casal, J.I. (1996). Full protection against African horsesickness (AHS) in horses induced by baculovirus-derived AHS virus serotype 4 VP2, VP5 and VP7. *J. Gen. Virol.* 77, 1211-1221.

Martinez-Torrecuadrada, J.L., Iwata, H., Venteo, A., Casal, I. and Roy, P. (1994). Expression and characterization of two outer capsid proteins of African horsesickness virus: The role of VP2 in virus neutralization. *Virology* 202, 348-359.

Martinez-Torrecuadrada, J.L., Langeveld, J.P.M., Meloen, R.H. and Casal, J.I. (2001). Definition of neutralizing sites on African horse sickness virus serotype 4 VP2 at the level of peptides. *J. Gen. Virol.* 82, 2415-2424.

Martinez-Torrecuadrada, J.L., Langeveld, J.P.M., Venteo, A., Sanz, A., Dalsgaard, K., Hamilton, W.D.O., Meloen, R.H. and Casal, J.I. (1999). Antigenic profile of African horse sickness virus serotype 4 VP5 and identification of a neutralizing epitope shared with bluetongue virus and epizootic hemorrhagic disease virus. *Virology* 257, 449-459.

Martin-Latil, S., Mousson, L., Autret, A., Colbère-Garapin, F. and Blondel, B. (2007). Bax is activated during rotavirus-induced apoptosis through the mitochondrial pathway. *J. Virol.* 81, 4457-4464.

Martinon, F., Hofmann, K. and Tschopp, J. (2001). The pyrin domain: A possible member of the death domain-fold family implicated in apoptosis and inflammation. *Curr. Biol.* 11, R118-R120.
Maruri-Avidal, L., López, S. and Arias, C.F. (2008). Endoplasmic reticulum chaperones are involved in the morphogenesis of rotavirus infectious prticles. *J. Virol.* 82, 5368-5380.
Matranga, C., Tomari, Y., Shin, C., Bartel, D.P. and Zamore, P.D. (2005). Passenger-strand cleavage facilitates assembly of siRNA into Ago2-containing RNAi enzyme complexes. *Cell* 123, 607-620.
Matsuo, E., Celma, C.C.P. and Roy, P. (2010). A reverse genetics system of African horse sickness virus reveals existence of primary replication. *FEBS Lett.* 584, 3386-3391.
McAnuff, M.A., Rettig, G.R. and Rice, K.G. (2007). Potency of siRNA versus shRNA mediated knockdown *in vivo*. *J. Pharm. Sci.* 96, 2922-2930.
McIntosh, B.M. (1958). Immunological types of horse sickness virus and their significance in immunization. *Onderstepoort J. Vet. Res.* 27, 465-538.
Medina, V., Edmonds, B., Young, G.P., James, R., Appleton, S. and Zalewski, P.D. (1997). Induction of caspase-3 protease activity and apoptosis by butyrate and trichostatin A (inhibitors of histone deacetylase): Dependence on protein synthesis and synergy with a mitochondrial/cytochrome c-dependent pathway. *Cancer Res*. 57, 3697-3707.
Meiring, T.L., Huismans, H. and van Staden, V. (2009). Genome segment reassortment identified non-structural protein NS3 as a key protein in African horsesickness virus release and alteration of membrane permeability. *Arch. Virol.* 154, 263-271.
Meister, G. and Tuschl, T. (2004). Mechanisms of gene silencing by double-stranded RNA. *Nature* 431, 343-349.
Mellor, P.S. (1993). African horsesickness: Transmission and epidemiology. *Vet. Res.* 24, 199-212.
Mellor, P.S. (1994). Epizootiology and vectors of African horse sickness virus. *Comp. Immunol. Microbiol. Infect. Dis.* 17, 287-296.
Mellor, P.S. and Hamblin, C. (2004). African horse sickness. *Vet. Res.* 35, 445-466.
Mellor, P.S., Boorman, J. and Jennings, M. (1975). The multiplication of African horse sickness virus in two species of *Culicoides*. *Arch. Virol.* 47, 351-356.
Mertens, P. (2004). The dsRNA viruses. *Virus Res.* 101, 3-13.
Mertens, P.P. and Diprose, J. (2004). The bluetongue virus core: A nano-scale transcription machine. *Virus Res.* 101, 29-43.
Mertens, P.P.C., Burroughs, J.N., Walton, A., Welby, M.P., Fu, H., O'Hara, R.S., Brookes, S.M. and Mellor, P.S. (1996). Enhanced infectivity of modified bluetongue virus particles for two insect cell lines and for two *Culicoides* vector species. *Virology* 217, 582-593.
Mi, J., Li, Z.Y., Ni, S., Steinwaerder, D. and Lieber, A. (2001). Induced apoptosis supports spread of adenovirus vectors in tumors. *Hum. Gene Ther.* 12, 1343-1352.
Miller, V.M., Xia, H., Marrs, G.L., Gouvion, C.M., Lee, G., Davidson, B.L. and Paulson, H.L. (2003). Allele-specific silencing of dominant disease genes. *Proc. Natl. Acad. Sci. USA* 100, 7195-7200.
Mirchamsy, H., Hazrati, A., Bahrami, S. and Shafyi, A. (1970). Growth and persistent infection of African horse sickness virus in a mosquito cell line. *Am. J. Vet. Res.* 31, 1755-1761.
Mittal, V. (2004). Improving the efficiency of RNA interference in mammals. *Nature Rev. Genet.* 5, 355-365.
Miyagishi, M. and Taira, K. (2002). U6 promoter-driven siRNAs with four uridine 3' overhangs efficiently suppress targeted gene expression in mammalian cells. *Nature Biotechnol.* 20, 497-500.
Mizukoshi, N., Sakamoto, K., Iwata, A., Tsuchiya, T., Ueda, S., Apiwatnakorn, B., Kamada, M. and Fukusho, A. (1993). The complete nucleotide sequence of African horsesickness virus serotype 4 (vaccine strain) segment 4, which encodes the minor core protein VP4. *Virus Res.* 28, 299-306.
Modrof, J., Lymperopoulos, K. and Roy, P. (2005). Phosphorylation of Bluetongue virus nonstructural protein 2 is essential for formation of viral inclusion bodies. *J. Virol.* 79, 10023-10031.
Mohr, S., Bakal, C. and Perrimon, N. (2010). Genomic screening with RNAi: Results and challenges. *Annu. Rev. Biochem.* 79, 37-64.

Montero, H., Arias, C.F. and López, S. (2006). Rotavirus protein NSP3 is not required for viral protein synthesis. *J. Virol.* 80, 9031-9038.
Montgomery, M.K., Xu, S. and Fire, A. (1998). RNA as a target of double-stranded RNA-mediated genetic interference in *Caenorhabditis elegans*. *Proc. Natl. Acad. Sci. USA* 95, 15502-15507.
Moore, C.B., Guthrie, E.H., Huang, M.T.-H. and Taxman, D.J. (2010). Short hairpin RNA(shRNA): Design, delivery and assessment of gene knockdown. *Methods Mol. Biol.* 629, 141-158.
Mortola, E. and Larsen, A. (2009). Infección por el virus de la Lengua azul: Activación de señales celulares que inducen apoptosis. *Rev. Argent. Microbiol.* 41, 134-140.
Mortola, E., Noad, R. and Roy, P. (2004). Bluetongue virus outer capsid proteins are sufficient to trigger apoptosis in mammalian cells. *J. Virol.* 78, 2875-2883.
Murphy, K.M., Streips, U.N. and Lock, R.B. (2000). Bcl-2 inhibits a Fas-induced conformational change in the Bax N terminus and Bax mitochondrial translocation. *J. Biol. Chem.* 275, 17225-17228.
Myers, J.W., Jones, J.T., Meyer, T. and Ferrel, J.E. (2003). Recombinant Dicer efficiently converts large dsRNA into siRNAs suitable for gene silencing. *Nature Biotechnol.* 21, 324-328.
Nagaleekar, V.K., Tiwari, A.K., Kataria, R.S., Bais, M.V., Ravindra, P.V. and Kumar, S. (2007). Bluetongue virus induces apoptosis in cultured mammalian cells by both caspase-dependent extrinsic and intrinsic apoptotic pahways. *Arch. Virol*. 152, 1751-1756.
Naito, Y., Yoshimura, J., Morishita, S. and Ui-Tei, K. (2009). siDirect 2.0: Updated software for designing functional siRNA with reduced seed-dependent off-target effect. *BMC Bioinformatics* 10, 392.
Nayak, A., Berry, B., Tassetto, M., Kunitomi, M., Acevedo, A., Deng, C., Krutchinsky, A., Gross, J., Antoniewski, C. and Andino, R. (2010). Cricket paralysis virus antagonizes Argonaute 2 to modulate antiviral defense in *Drosophila*. *Nature Struct. Mol. Biol.* 17, 547-554.
Newton, K., Meyer, J.C., Bellamy, A.R. and Taylor, J.A. (1997). Rotavirus nonstructural glycoprotein NSP4 alters plasma membrane permeability in mammalian cells. *J. Virol.* 71, 9458-9465.
Nibert, M.L., Schiff, L.A. and Fields, B.N. (1991). Mammalian reovirus contains a myristoylated structural protein. *J. Virol.* 65, 1960-1967.
Nicholson, D.W. (1999). Caspase structure, proteolytic substrates, and function during apoptotic cell death. *Cell Death Differ*. 6, 1028-1042.
Nykänen, A., Haley, B. and Zamore, P.D. (2001). ATP requirements and small interfering RNA structure in the RNA interference pathway. *Cell* 107, 309-321.
O'Brien, V. (1998). Viruses and apoptosis. *J. Gen. Virol.* 79, 1833-1845.
O'Donnell, S.M., Hansberger, M.W., Connolly, J.L., Chappell, M.J., Watson, M.J., Pierce, J.M., Wetzel, J.D., Han, W., Barton, E.S., Forrest, J.C., Valyi-Nagy, T., Yull, F.E., Blackwell, T.S., Rottman, J.N., Sherry, B. and Dermody, T.S. (2005). Organ specific roles for transcription factor NF-κβ in reovirus-induced apoptosis and disease. *J. Clin. Investig.* 115, 2341-2350.
O'Donnell, S.M., Holm, G.H., Pierce, J.M., Tian, B., Watson, M.J., Chari, R.S., Ballard, D.W., Brasier, A.R. and Dermody, T.S. (2006). Identification of an NF-κβ-dependent gene network in cells infected by mammalian reovirus. *J. Virol.* 80, 1077-1086.
Odegard, A.L., Chandran, K., Zhang, X., Parker, J.S., Baker, T.S. and Nibert, M.L. (2004). Putative autocleavage of outer capsid protein μ1, allowing release of myristoylated peptide μ1N during particle uncoating, is critical for cell entry by reovirus. *J. Virol*. 78, 8732-8745.
Oellerman, R.A., Els, H.J. and Erasmus, B.J. (1970). Characterization of African horse sickness virus. *Arch. Gesammte Virusforsch.* 29, 163-174.
Ohrt, T., Mutze, J., Staroske, W., Weinmann, L., Hock, J., Crell, K., Meister, G. and Schwille, P. (2008). Fluorescence correlation spectroscopy and fluorescence cross-correlation spectroscopy reveal the cytoplasmic origination of loaded nuclear RISC *in vivo* in human cells. *Nucleic Acids Res.* 36, 6439-6449.
Oldfield, S., Hirasawa, T. and Roy, P. (1991). Sequence conservation of the outer capsid protein, VP5, of bluetongue virus, a contrasting feature to the outer capsid protein VP2. *J. Gen. Virol.* 72, 449-451.
Olejniczak, M., Galka, P. and Krzyzosiak, W.J. (2009). Sequence-non-specific effects of RNA interference triggers and microRNA regulators. *Nucleic Acids Res.* 38, 1-16.

Oltvai, Z.N., Milliman, C.L. and Korsmeyer, S.J. (1993). Bcl-2 heterodimerizes *in vivo* with a conserved homolog, Bax, that accelerates programmed cell death. *Cell* 74, 609-619.
Osaki, M., Oshimura, M. and Ito, H. (2004). PI3K-Akt pathway: Its functions and alterations in human cancer. *Apoptosis* 9, 667-676.
Osawa, Y. and Hazrati, A. (1965). Growth of African horse sickness virus in monkey kidney cell cultures. *Am. J. Vet. Res.* 25, 505-511.
Overhoff, L., Alken, M., Far, R.K., Lemaitre, M., Llebleu, B., Sczakiel, G. and Robbins, I. (2005). Local RNA target structure influences siRNA efficacy: A systematic global analysis. *J. Mol. Biol.* 348, 871-881.
Owens, R., Limn, C. and Roy, P. (2004). Role of an arbovirus nonstructural protein in cellular pathogenesis and virus release. *J. Virol.* 78, 6649-6656.
Paddison, P.J., Caudy, A.A. and Hannon, G.J. (2002a). Stable suppression of gene expression by RNAi in mammalian cells. *Proc. Natl. Acad. Sci. USA* 99, 1443-1448.
Paddison, P.J., Caudy, A.A., Bernstein, E., Hannon, G.J. and Conklin, D.S. (2002b). Short hairpin RNAs (shRNAs) induce sequence-specific silencing in mammalian cells. *Genes Dev.* 16, 948-958.
Papadakis, E.S., Finegan, K.G., Wang, X., Robinson, A.C., Guo, C., Kayahara, M. and Tournier, C. (2006). The regulation of Bax by c-Jun N-terminal protein kinase (JNK) is a prerequisite to the mitochondrial-induced apoptotic pathway. *FEBS Lett.* 580, 1320-1326.
Parker, J.S., Roe, S.M. and Barford, D. (2005). Structural insights into mRNA recognition from a PIWI domain-siRNA guide complex. *Nature* 434, 663-666.
Parker, R. and Song, H. (2004). The enzymes and control of eukaryotic mRNA turnover. *Nature Struct. Mol. Biol.* 11, 121-127.
Patel, R., T'wallant, N.C., Herbert, M.H., White, D., Murison, J.G. and Reid, G. (2009). The potency of siRNA-mediated growth inhibition following silencing of essential genes is dependent on siRNA design and varies with target sequence. *Oligonucleotides* 19, 317-328.
Paul, C.P., Good, P.D., Winer, I. and Engelke, D.R. (2002). Effective expression of small interfering RNA in human cells. *Nature Biotechnol.* 20, 505-508.
Paule, M.R. and White, R.J. (2000). Survey and summary: Transcription by RNA polymerases I and III. *Nucleic Acids Res.* 28, 1283-1298.
Peek, A.S. and Behlke, M.A. (2007). Design of active small interfering RNAs. *Curr. Opin. Mol. Ther.* 9, 110-118.
Penaloza, C., Lin, L., Lockshin, R.A. and Zakeri, Z. (2006). Cell death in development: Shaping the embryo. *Histochem. Cell Biol.* 126, 149-158.
Peng, J., Zhao, Y., Mai, J., Pang, W.K., Wei, X., Zhang, P. and Xu, Y. (2005). Inhibition of hepatitis B virus replication by various RNAi constructs and their pharmacodynamic properties. *J. Gen. Virol.* 86, 3227-3234.
Pfaffl, M.W., Horgan, G.W. and Dempfle, L. (2002). Relative expression software tool (REST) for group-wise comparison and statistical analysis of relative expression results in real-time PCR. *Nucleic Acids Res.* 30, e36.
Pfaffl, M.W., Tichopad, A., Prgomet, C. and Neuvians, T.P. (2004). Determination of stable housekeeping genes, differentially regulated target genes and sample integrity: BestKeeper – Excel-based tool using pair-wise correlations. *Biotechnol. Lett.* 26, 509-515.
Pham, J.W., Pellino, J.L., Lee, Y.S., Carthew, R.W. and Sontheimer, E.J. (2004). A Dicer-2-dependent 80S complex cleaves targeted mRNAs during RNAi in *Drosophila. Cell* 117, 83-94.
Pitti, R.M., Marsters, S.A., Ruppert, S., Donahue, C.J., Moore, A. and Ashkenazi, A. (1996). Induction of apoptosis by Apo-2 ligand, a new member of the tumor necrosis factor cytokine family. *J. Biol. Chem.* 271, 12687-12690.
Potgieter, A.C., Cloete, M., Pretorius, P.J. and van Dijk, A.A. (2003). A first full outer capsid protein sequence data-set in the *Orbivirus* genus (family *Reoviridae*): Cloning, sequencing, expression and analysis of a complete set of full-length outer capsid VP2 genes of the nine African horsesickness virus serotypes. *J. Gen. Virol.* 84, 1317-1326.

Prasad, B.V.V., Yamaguchi, S. and Roy, P. (1992). Three-dimensional structure of single-shelled BTV. *J. Virol.* 66, 2135-2142.
Pronk, G.J., Ramer, K., Amiri, P. and Williams, L.T. (1996). Requirement of an ICE-like protease for induction of apoptosis and ceramide generation by REAPER. *Science* 271, 808-810.
Provost, P., Dishart, D., Doucet, J., Frendewey, D., Sameulsson, B. and Radmark, O. (2002). Ribonuclease activity and RNA binding of recombinant human Dicer. *EMBO J.* 21, 5864-5874.
Qin, X.-F., An, D.S., Chen, I.S.Y. and Baltimore, D. (2003). Inhibiting HIV-1 infection in human T cells by lentiviral-mediated delivery of small interfering RNA against CCR5. *Proc. Natl. Acad. Sci. USA* 100, 183-188.
Radonić, A., Thulke, S., Bae, H.-G., Műller, M.A., Siegert, W. and Nitsche, A. (2005). Reference gene selection for quantitative real-time PCR analysis in virus infected cells: SARS coronavirus, Yellow fever virus, Human Herpesvirus-6, Camelpox virus and Cytomegalovirus infections. *Virol. J.* 2, 7.
Radonić, A., Thulke, S., Mackay, I.M., Landt, O., Siegert, W. and Nitsche, A. (2004). Guideline to reference gene selection for quantitative real-time PCR. *Biochem. Biophys. Res. Commun*. 313, 856-862.
Ramadevi, N. and Roy, P. (1998). Bluetongue virus core protein VP4 has nucleoside triphosphate phosphohydrolase activity. *J. Gen. Virol.* 79, 2475-2480.
Ramadevi, N., Burroughs, J.N., Mertens, P.P.C., Jones, I.M. and Roy, P. (1998). Capping and methylation of mRNA by purified recombinant VP4 protein of bluetongue virus. *Proc. Natl. Acad. Sci. USA* 95, 13537-13542.
Randall, G., Grakoui, A. and Rice, C.M. (2003). Clearance of replicating hepatitis C virus replicon RNAs in cell culture by small interfering RNAs. *Proc. Natl. Acad. Sci. USA* 100, 235-240.
Rao, C.D., Kiuchi, A. and Roy, P. (1983). Homologous terminal sequences of the genome double-stranded RNAs of bluetongue virus. *J. Virol.* 46, 378-383.
Rao, D.D., Vorhies, J.S., Senzer, N. and Nemunaitis, J. (2009). siRNA vs shRNA: Similarities and differences. *Adv. Drug Deliv. Rev.* 61, 746-759.
Rao, L., Perez, D. and White, E. (1996). Lamin proteolysis facilitates nuclear events during apoptosis. *J. Cell Biol.* 135, 1441-1455.
Rasmussen, R. (2001). Quantification on the LightCycler. In: Rapid cycle real-time PCR, methods and applications. S. Meuer, C. Wittwer and K. Nakagawara (Eds.), pp. 21-34. Springer Press, Heidelberg.
Reading, P.C., Khanna, A. and Smith, G.L. (2002). Vaccinia virus CrmE encodes a soluble and cell surface tumor necrosis factor receptor that contributes to virus virulence. *Virology* 292, 285-298.
Renatus, M., Zhou, Q., Stennicke, H.R., Snipas, S.J., Turk, D., Bankston, L.A., Liddington, R.C. and Salvesen, G.S. (2000). Crystal structure of the apoptotic suppressor CrmA in its cleaved form. *Structure* 8, 789-797.
Reynolds, A., Anderson, E.M., Vermeulen, A., Fedorov, Y., Robinson, K., Leake, D., Karpilow, J., Marshall, W.S. and Khvorova, A. (2006). Induction of the interferon response by siRNA is cell type- and duplex-length-dependent. *RNA* 12, 988-993.
Reynolds, A., Leake, D., Boese, Q., Scaringe, S., Marshall, W.S. and Khvorova, A. (2004). Rational siRNA design for RNA interference. *Nature Biotechnol.* 22, 326-330.
Richardson-Burns, S.M. and Tyler, K.L. (2004). Regional differences in viral growth and central nervous system injury correlate with apoptosis. *J. Virol.* 78, 5466-5475.
Richardson-Burns, S.M., Kominsky, D.J. and Tyler, K.L. (2002). Reovirus-induced neuronal apoptosis is mediated by caspase-3 and is associated with the activation of death receptors. *J. Neurovirol.* 8, 365-380.
Riedl, S.J. and Salvesen, G.S. (2007). The apoptosome: Signaling platform of cell death. *Nature Rev. Mol. Cell Biol.* 8, 405-413.
Root, D.E., Hacohen, N., Hahn, W.C., Lander, E.S. and Sabatini, D.M. (2006). Genome scale loss-of-function screening with a lentiviral RNAi library. *Nature Methods* 3, 715-719.
Rossi, J.J. (2008). Expression strategies for short hairpin RNA interference triggers. *Hum. Gene Ther.* 19, 313-317.

Rothe, M., Pan, M.G., Henzel, W.J., Ayres, T.M. and Goeddel, D.V. (1995). The TNFR2-TRAF signaling complex contains two novel proteins related to baculoviral inhibitor of apoptosis proteins. *Cell* 83, 1243-1252.
Roulston, A., Marcellus, R.C. and Branton, P.E. (1999). Viruses and apoptosis. *Annu. Rev. Microbiol.* 53, 577-628.
Roy, N., Deveraux, Q.L., Takahashi, R., Salvesen, G.S. and Reed, J.C. (1997). The c-IAP-1 and c-IAP-2 proteins are direct inhibitors of specific caspases. *EMBO J.* 16, 6914-6925.
Roy, P. (2001). Orbiviruses. In: Field's Virology, fourth edition. D.M. Knipe, P.M. Howley, D.E. Griffin, R.A. Lamb and M.A. Martin (Eds.), pp 1835-1869, Lippincott Williams and Wilkins, Philadelphia.
Roy, P. (2008). Functional mapping of Bluetongue virus proteins and their interactions with host proteins during virus replication. *Cell Biochem. Biophys.* 50, 143-157.
Roy, P. and Noad, R. (2006). Bluetongue virus assembly and morphogenesis. *Curr. Top. Microbiol. Immunol.* 309, 87-116.
Roy, P., Adachi, A., Urakawa, T., Booth, T.F. and Thomas, C.P. (1990). Identification of bluetongue virus VP6 protein as a nucleic acid-binding protein and the localization of VP6 in virus-infected vertebrate cells. *J. Virol.* 64, 1-8.
Roy, P., Bishop, D.H.L., LeBlois, H. and Erasmus, B.J. (1994a). Long-lasting protection of sheep against bluetongue challenge after vaccination with virus-like particles: Evidence for homologous and partial heterologous protection. *Vaccine* 12, 805-811.
Roy, P., French, T. and Erasmus, B.J. (1992). Protective efficacy of virus-like particles for bluetongue disease. *Vaccine* 10, 28-32.
Roy, P., Fukusho, A., Ritter, D.G. and Lyons, D. (1988). Evidence for genetic relationship between RNA and DNA viruses from the sequence homology of a putative polymerase gene of bluetongue virus with that of vaccinia virus: Conservation of RNA polymerase genes from diverse species. *Nucleic Acids Res.* 16, 11759-11767.
Roy, P., Mertens, P.P. and Casal, I. (1994b). African horse sickness virus structure. *Comp. Immunol. Microbiol. Infect. Dis.* 17, 243-273.
Rozen, S. and Skaletsky, H. (2000). Primer3 on the www for general users and for biologist programmers. *Methods Mol. Biol.* 132, 365-386.
Rubinson, D.A., Dillon, C.P., Kwiatkowski, A.V., Sievers, C., Yang, L., Kopinja, J., Zhang, M., McManus, M.T., Gertler, F.B., Scott, M.L. and Van Parijs, L. (2003). A lentivirus-based system to functionally silence genes in primary mammalian cells, stem cells and transgenic mice by RNA interference. *Nature Genet.* 33, 401-406.
Sambrook, J. and Russel, D.W. (2001). Molecular cloning: A laboratory manual. Cold Spring Harbor Laboratory Press, Cold Spring Harbor, New York.
Samuel, M.A., Morrey, J.D. and Diamond, M.S. (2007). Caspase-3-dependent cell death of neurons contributes to the pathogenesis of West Nile virus encephalitis. *J. Virol.* 81, 2614-2623.
Sato, A., Iizuka, M., Nakagomi, O., Suzuki, M., Horie, Y., Konno, S., Hirasawa, F., Sasaki, K., Shindo, K. and Watanabe, S. (2006). Rotavirus double-stranded RNA induces apoptosis and diminishes wound repair in rat intestinal epithelial cells. *J. Gastroenterol. Hepatol.* 21, 521-530.
Sattar, R., Ali, S.A. and Abbasi, A. (2003). Molecular mechanism of apoptosis: Prediction of three-dimensional structure of caspase-6 and its interactions by homology modeling. *Biochem. Biophys. Res. Commun.* 308, 497-504.
Scaffidi, C., Medema, J.P., Krammer, P.H. and Peter, M.E. (1997). FLICE is predominantly expressed as two functionally active isoforms, caspase-8/a and caspase-8/b. *J. Biol.Chem.* 272, 26953-26958.
Schaack, J. (2005). Induction and inhibition of innate inflammatory responses by adenovirus early region proteins. *Viral Immunol.* 18, 79-88.
Scherer, L.J., Yildiz, Y., Kim, J., Cagnon, L., Heale, B. and Rossi, J.J. (2004). Rapid assessment of anti-HIV siRNA efficacy using PCR-derived Pol III shRNA cassettes. *Mol. Ther.* 10, 597-603.
Schmeiser, K., Hammond, E.M., Roberts, S. and Grand, R.J. (1998). Specific cleavage of gamma catenin by caspases during apoptosis. *FEBS Lett.* 433, 51-57.

Schmittgen, T.D. and Zakrajsek, B.A. (2000). Effect of experimental treatment on housekeeping gene expression: Validation by real-time, quantitative RT-PCR. *J. Biochem. Biophys. Methods* 46, 69-81.
Schuck, S., Manninen, A., Honsho, M., Fullekrug, J. and Simons, K. (2004). Generation of single and double-knockdowns in polarized epithelial cells by retrovirus-mediated RNA interference. *Proc. Natl. Acad. Sci. USA* 101, 4912-4917.
Schwartzman, R.A. and Cidlowski, J.A. (1993). Apoptosis: The biochemistry and molecular biology of programmed cell death. *Endocrinol. Rev.* 14, 133-151.
Schwarz, D.S., Hutvágner, G., Du, T., Xu, Z., Aronin, N. and Zamore, P.D. (2003). Asymmetry in the assembly of the RNAi enzyme complex. *Cell* 115, 199-208.
Schweizer, A., Briand, C. and Grutter, M.G. (2003). Crystal structure of caspase-2, apical initiator of the intrinsic apoptotic pathway. *J. Biol. Chem*. 278, 42441-42447.
Selvey, S., Thompson, E.W., Matthaei, K., Lea, R.A., Irving, M.G. and Griffiths, L.R. (2001). Beta-actin – an unsuitable internal control for RT-PCR. *Mol. Cell. Probes* 15, 307-311.
Shah, K., Garner, H.R., White, M.A., Shames, D.S. and Minna, J.D. (2007). sIR: siRNA Information Resource, a web-based tool for siRNA sequence design and analysis and an open access siRNA database. *BMC Bioinformatics* 8, 178.
Shao, Y., Chan, C.Y., Maliyekkel, A., Lawrence, C.E., Roninson, I.B. and Ding, Y. (2007). Effect of target secondary structure on RNAi efficiency. *RNA* 13, 1631-1640.
Shen, C., Buck, A.K., Liu, X., Winkler, M. and Reske, S.N. (2003). Gene silencing by adenovirus-delivered siRNA. *FEBS Lett.* 539, 111-114.
Shi, Y. (2002). Mechanisms of caspase activation and inhibition during apoptosis. *Mol. Cell* 9, 459-470.
Shisler, J., Yang, C., Walter, B., Ware, C. and Gooding, L. (1997). The adenovirus E3-10.4K/14.5K complex mediates loss of cell surface Fas (CD95) and resistance to Fas-induced apoptosis. *J. Virol.* 71, 8299-8306.
Shrey, K., Suchit, A., Nishant, M. and Vibha, R. (2009). RNA interference: Emerging diagnostics and therapeutics tool. *Biochem. Biophys. Res. Commun.* 386, 273-277.
Sidahmed, A.M. and Wilkie, B. (2010). Endogenous antiviral mechanisms of RNA interference: A comparative biology perspective. *Methods Mol. Biol.* 623, 3-19.
Siolas, D., Lerner, C., Burchard, J., Ge, W., Linsley, P.S., Paddison, P.J., Hannon, G.J. and Cleary, M.A. (2005). Synthetic shRNAs as potent RNAi triggers. *Nature Biotechnol.* 23, 227-231.
Sledz, C.A., Holko, M., de Veer, M.J., Silverman, R.H. and Williams, B.R. (2003). Activation of the interferon system by short-interfering RNAs. *Nature Cell Biol.* 5, 834-839.
Sohail, M., Doran, G., Riedemann, J., Macaulay, V. and Southern, E.M. (2003). A simple and cost-effective method for producing small interfering RNAs with high efficacy. *Nucleic Acids Res.* e38.
Sprick, M.R., Rieser, E., Stahl, H., Grosse-Wilde, A., Weigand, M.A. and Walczak, H. (2002). Caspase-10 is recruited to and activated at the native TRAIL and CD95 death inducing signaling complexes in a FADD-dependent manner but can not functionally substitute caspase-8. *EMBO J.* 21, 4520-4530.
Stark, G.R., Kerr, I.M., Williams, B.R., Silverman, R.H. and Schreiber, R.D. (1998). How cells respond to interferons. *Annu. Rev. Biochem.* 67, 227-264.
Stassen, L., Huismans, H. and Theron, J. (2007). Silencing of African horse sickness virus VP7 protein expression in cultured cells by RNA interference. *Virus Genes* 35, 777-783.
Stauber, N., Martinez-Costas, J., Sutton, G., Monastyrskaya, K. and Roy, P. (1997). Bluetongue virus VP6 protein binds ATP and exhibits an RNA-dependent ATPase function and a helicase activity that catalyze the unwinding of double-stranded RNA substartes. *J. Virol.* 71, 7220-7226.
Stennicke, H.R., Ryan, C.A. and Salvesen, G.S. (2002). Reprieval from execution: The molecular basis of caspase inhibition. *Trends Biochem. Sci.* 27, 94-101.
Stewart, M.E. and Roy, P. (2010). Role of cellular caspases, nuclear factor-kappaβ and interferon regulatory factors in Bluetongue virus infection and cell fate. *Virol. J.* 7, 362.
Stoltz, M.A., van der Merwe, C.F., Coetzee, J. and Huismans, H. (1996). Subcellular localization of the nonstructural protein NS3 of African horsesickness virus. *Onderstepoort J. Vet. Res.* 63, 57-61.

Stram, Y. and Kuzntzova, L. (2006). Inhibition of viruses by RNA interference. *Virus Genes* 32, 299-306.
Stuart, D.I. and Grimes, J.M. (2006). Structural studies on orbivirus proteins and particles. *Curr. Top. Microbiol. Immunol.* 309, 221-244.
Stuart, D.I., Gouet, P., Grimes, J., Malby, R., Diprose, J., Zientara, S., Burroughs, J.N. and Mertens, P.P.C. (1998). Structural studies of orbivirus particles. *Arch. Virol.* 14, 235-250.
Subramanya, S., Kim, S.S., Manjunath, N. and Shankar, P. (2010). RNA interference-based therapeutics for human immunodeficiency virus HIV-1 treatment: Synthetic siRNA or vector-based shRNA? *Expert Opin. Biol. Ther.* 10, 201-213.
Suda, T., Takahashi, T., Golstein, P. and Nagata, S. (1993). Molecular cloning and expression of the Fas ligand, a novel member of the tumor necrosis factor family. *Cell* 75, 1169-1178.
Sui, G., Soohoo, C., Affar el, B., Gay, F., Shi, Y. and Forrester, W.C. (2002). A DNA vector-based RNAi technology to suppress gene expression in mammalian cells. *Proc. Natl. Acad. Sci. USA* 99, 5515-5520.
Summers, M.D. and Smith, G.E. (1987). A manual of methods for Baculovirus vectors and insect cell culture procedures. *Texan Agric. Exp. Station Bull.* 1555.
Sun, W., Pertzev, A. and Nicholson, A.W. (2005). Catalytic mechanism of *Escherichia coli* ribonuclease III: Kinetic and inhibitor evidence for the involvement of two magnesium ions in RNA phosphodiester hydrolysis. *Nucleic Acids Res.* 33, 807-815.
Sundararajan, R. and White, E. (2001). E1B 19K blocks Bax oligomerization and tumor necrosis factor α-mediated apoptosis. *J. Virol.* 75, 7506-7516.
Suzuki, T., Higgins, P.J. and Crawford, D.R. (2000). Control selection for RNA quantitation. *BioTechniques* 29, 332-337.
Suzuki, Y., Nakabayashi, Y. and Takahashi, R. (2001). Ubiquitin-protein ligase activity of x-linked inhibitor of apoptosis protein promotes proteasomal degradation of caspase-3 and enhances its anti-apoptotic effect in FAS-induced cell death. *Proc. Natl. Acad. Sci. USA* 98, 8662-8667.
Swanepoel, R., Erasmus, B.J., Williams, R. and Taylor, M.B. (1992). Encephalitis and chorioretinitis associated with neurotropic African horsesickness virus infection in laboratory workers. Part III. Virological and serological investigations. *S. Afr. Med. J.* 81, 458-461.
Tafer, H., Ameres, S.L., Obernosterer, G., Gebeshuber, C.A., Schroeder, R., Martinez, J. and Hofacker, I.L. (2008). The impact of target site accessibility on the design of effective siRNAs. *Nature Biotechnol.* 26, 578-583.
Takahashi, K., Kawai, T., Kumar, H., Sato, S., Yonehara, S. and Akira, S. (2006). Roles of caspase-8 and caspase-10 in innate immune responses to double-stranded RNA. *J. Immunol.* 176, 4520-4524.
Takahashi, Y., Yamaoka, K., Nishikawa, M. and Takakura, Y. (2009). Quantitative and temporal analysis of gene silencing in tumor cells induced by small interfering RNA or short hairpin RNA expressed from plasmid vectors. *J. Pharm. Sci.* 98, 74-80.
Tan, B.-H., Nason, E., Staeuber, N., Jiang, W., Monastryrskaya, K. and Roy, P. (2001). RGD tripeptide of bluetongue virus VP7 protein is responsible for core attachment to *Culicoides* cells. *J. Virol.* 75, 3937-3947.
Tartaglia, L.A., Ayres, T.M., Wong, G.H. and Goeddel, D.V. (1993). A novel domain within the 55 kDa TNF receptor signals cell death. *Cell* 74, 845-853.
Taxman, D.J., Livingstone, L.R., Zhang, J., Conti, B.J., Iocca, H.A., Williams, K.L., Lich, J.D., Ting, J.P-Y. and Reed, W. (2006). Criteria for effective design, construction, and gene knockdown by shRNA vectors. *BMC Biotechnology* 6, 7.
Taylor, M.B., van der Meyden, C.H., Erasmus, B.J., Reid, R., Labuschagne, J.H., Dreyer, L. and Prozesky, O.W. (1992). Encephalitis and chorioretinitis associated with neurotropic African horse sicknessvirus infection in laboratory workers. IV. Experimental infection of the vervet monkey *Cercopithecus pygerythrus*. *S. Afr. J. Med. Sci.* 81, 462-467.
ter Brake, O., Konstantinova, P., Ceylan, M. and Berkhout, B. (2006). Silencing of HIV-1 with RNA interference: A multiple shRNA approach. *Mol. Ther.* 14, 883-892.

Thellin, O., Zorzi, W., Lakaye, B., De Borman, B., Coumans, B., Hennen, G., Grisar, T., Igout, A. and Heinen, E. (1999). Housekeeping genes as internal standards: Use and limits. *J. Biotechnol.* 75, 291-295.

Theron, J. and Nel, L.H. (1997). Stable protein-RNA interaction involves the terminal domains of bluetongue virus mRNA, but not the terminally conserved sequences. *Virology* 229, 134-142.

Theron, J., Uitenweerde, J.M., Huismans, H. and Nel, L.H. (1994). Comparison of the expression and phosphorylation of the non-structural protein NS2 of three different orbiviruses: Evidence that the phosphorylation modulates ssRNA-binding and involves an ubiquitous cellular kinase. *J. Gen. Virol.* 75, 3401-3411.

Thomas, C.P., Booth, T.F. and Roy, P. (1990). Synthesis of bluetongue viral-coded phosphoprotein and formation of inclusion bodies by recombinant baculovirus in insect cells: It binds the single-stranded RNA species. *J. Gen. Virol.* 71, 2073-2083.

Thorley, J.A., McKeating, J.A. and Rappoport, J.Z. (2010). Mechanisms of viral entry: Sneaking in the front door. *Protoplasma* 244, 15-24.

Timmer, J.C. and Salvesen, G.S. (2007). Caspase substrates. *Cell Death Differ.* 14, 66-72.

Tomari, Y. and Zamore, P.D. (2005). Perspective: Machines for RNAi. *Genes Dev.* 19, 517-529.

Tomari, Y., Du, T., Haley, B., Schwarz, D.S., Bennett, R., Cook, H.A., Koppetsch, B.S., Theurkauf, W.E. and Zamore, P.D. (2004). RISC assembly defects in the *Drosophila* RNAi mutant Armitage. *Cell* 116, 831-841.

Tsai, B. (2007). Penetration of nonenveloped viruses into the cytoplasm. *Annu. Rev. Cell Dev. Biol.* 23, 23-43.

Tuschl, T., Zamore, P.D., Lehmann, R., Bartel, D.P. and Sharp, P.A. (1999). Targeted mRNA degradation by double-stranded RNA *in vitro*. *Genes Dev.* 13, 3191-3197.

Tyler, K.L., Squier, M.K., Rodgers, S.E., Schneider, B.E., Oberhaus, S.M., Grdina, T.A., Cohen, J.J. and Dermody, T.S. (1995). Differences in the capacity of reovirus strains to induce apoptosis are determined by the viral attachment protein σ1. *J. Virol.* 69, 6972-6979.

Ui-Tei, K., Naito, Y., Takahashi, F., Haraguchi, T., Ohki-Hamazaki, H., Juni, A., Ueda, R. and Saigo, K. (2004). Guidelines for the selection of highly effective siRNA sequences for mammalian and chick RNA interference. *Nucleic Acids Res.* 32, 936-948.

Uitenweerde, J.M., Theron, J., Stoltz, M.A. and Huismans, H. (1995). The multimeric nonstructural NS2 proteins of Bluetongue virus, African horsesickness virus, and Epizootic hemorrhagic disease virus differ in their single-stranded RNA-binding ability. *Virology* 209, 624-632.

Umeshappa, C.S., Singh, K.P., Nanjundappa, R.H. and Pandey, A.B. (2010). Apoptosis and immuno-suppression in sheep infected with bluetongue virus serotype-23. *Vet. Microbiol.* 144, 310-318.

Unwalla, H.J., Li, M.J., Kim, J.D., Li, H.T., Ehsani, A., Alluin, J. and Rossi, J.J. (2004). Negative feedback inhibition of HIV-1 by TAT-inducible expression of siRNA. *Nature Biotechnol.* 22, 1573-1578.

Urakawa, T., Ritter, G.D. and Roy, P. (1989). Expression of largest RNA segment and synthesis of VP1 protein of bluetongue virus in insect cells by recombinant baculovirus: Association of VP1 protein with RNA polymerase activity. *Nucleic Acids Res.* 17, 7395-7401.

Uren, A.G., Coulson, E.J. and Vaux, D.L. (1998). Conservation of baculovirus inhibitor of apoptosis repeat proteins (BIRPs) in viruses, nematodes, vertebrates and yeasts. *Trends Biochem. Sci.* 23, 159-162.

Uren, A.G., Pakusch, M., Hawkins, C.J., Puls, K.L. and Vaux, D.L. (1996). Cloning and expression of apoptosis inhibitory protein homologs that function to inhibit apoptosis and/or bind tumor necrosis factor receptor-associated factors. *Proc Natl Acad Sci USA* 93, 4974-4978.

van de Wetering, M., Oving, I., Muncan, V., Pon Fong, M.T., Brantjes, H., van Leenen, D., Holstege, F.C., Brummelkamp, T.R., Agami, R. and Clevers, H. (2003). Specific inhibition of gene expression using a stably integrated, inducible small-interfering-RNA vector. *EMBO Rep.* 4, 609-615.

van Dijk, A.A. and Huismans, H. (1988). *In vitro* transcription and translation of bluetongue virus mRNA. *J. Gen. Virol.* 69, 573-581.

van Niekerk, M., Smit, C.C., Fick, W.C., van Staden, V. and Huismans, H. (2001). Membrane association of African horsesickness virus nonstructural protein NS3 determines its cytotoxicity. *Virol.* 279, 499-508.
Van Rensburg, L.B.J., De Clerk, J., Groenewald, H.B. and Botha, W.S. (1981). An outbreak of African horsesickness in dogs. *J. S. Afr. Vet. Assoc.* 52, 323-325.
van Rij, R.P. and Berezikov, E. (2009). Small RNAs and the control of transposons and viruses in *Drosophila*. *Trends Microbiol.* 17, 163-171.
van Staden, V. and Huismans, H. (1991). A comparison of the genes which encode nonstructural protein NS3 of different orbiviruses. *J. Gen. Virol.* 72, 1073-1090.
van Staden, V., Stoltz, M.A. and Huismans, H. (1995). Expression of nonstructural protein NS3 of African horsesickness virus (AHSV): Evidence for a cytotoxic effect of NS3 in insect cells, and characterization of the gene products in AHSV-infected Vero cells. *Arch. Virol.* 140, 289-306.
Vaux, D.L., Cory, S. and Adams, J.M. (1988). Bcl-2 gene promotes haemopoietic cell survival and cooperates with c-myc to immortalize pre-B cells. *Nature* 335, 440-442.
Venter, G.J., Graham, S.D. and Hamblin, C. (2000). African horse sickness epidemiology: Vector competence of South African *Culicoides* species for virus serotypes 3, 5 and 8. *Med. Vet. Entomol.* 14, 245-250.
Verhagen, A.H., Ekert, P.G., Pakusch, M., Silke, J., Connolly, L.M., Reid, G.E., Moritz, R.L., Simpson, R.J. and Vaux, D.L. (2000). Identification of DIABLO, a mammalian protein that promotes apoptosis by binding to and antagonizing IAP proteins. *Cell* 102, 43-53.
Vermeulen, A., Behlen, L., Reynolds, A., Wolfson, A., Marshall, W.S., Karpilow, J. and Khvorova, A. (2005). The contributions of dsRNA structure to Dicer specificity and efficiency. *RNA* 11, 674-682.
Verwoerd, D.W. and Huismans, H. (1969). On the relationship between bluetongue, African horsesickness and reoviruses: Hybridization studies. *Onderstepoort J. Vet. Res.* 36, 175-179.
Verwoerd, D.W., Els, H.J., De Villiers, E.M. and Huismans, H. (1972). Structure of bluetongue virus capsid. *J. Virol.* 10, 783-794.
Vickers, T.A., Koo, S., Bennett, C.T., Crooke, S.T., Dean, N.M. and Baker, B.F. (2003). Efficient reduction of target RNAs by small interfering RNA and RNase H-dependent antisense agents. A comparative analysis. *J. Biol. Chem.* 278, 7108-7118.
Vlassov, A.V., Korba, B., Farrar, K., Mukerjee, S., Seyhan, A.A., Ilves, H., Kaspar, R., Kazakov, S.A. and Johnston, B.H. (2007). shRNAs targeting hepatitis C: Effects of sequence and structural feature, and comparison with siRNA. *Oligonucleotides* 17, 223-236.
Wade-Evans, A.M., Pan, Z.Q. and Mertens, P.P. (1988). Sequence analysis and *in vitro* expression of a cDNA clone of genome segment 5 from bluetongue virus, serotype 1 from South Africa. *Virus Res.* 11, 227-240.
Wadhwa, R., Kaul, S.C., Miyagishi, M. and Taira, K. (2004). Vectors for RNA interference. *Curr. Opin. Mol. Ther.* 6, 367-372.
Wang, H.-W., Noland, C., Siridechadilok, B., Taylor, D.W., Ma, E., Felderer, K., Doudna, J. and Nogales, E. (2009). Structural insights into RNA processing by the human RISC-loading complex. *Nature Struct. Mol. Biol.* 16, 1148-1153.
Wang, K., Yin, X.M., Chao, D.T., Milliman, C.L. and Korsmeyer, S.J. (1996). Bid: A novel BH3 domain-only death agonist. *Genes Dev.* 10, 2859-2869.
Wang, Q., Contag, C.N., Ilves, H., Johnston, B.H. and Kaspar, R.L. (2005). Small hairpin RNAs efficiently inhibit hepatitis C IRES-mediated gene expression in human tissue culture cells and a mouse model. *Mol. Ther.* 12, 562-568.
Wang, X.W., Gibson, M.K., Vermeulen, W., Yeh, H., Forrester, K., Stürzbecher, H.W., Hoeijmakers, J.H. and Harris C.C. (1995). Abrogation of p53-induced apoptosis by the hepatitis B virus X gene. *Cancer Res.* 55, 6012-6016.
Weber, C.H. and Vincenz, C. (2001). The death domain superfamily: A tale of two interfaces? *Trends Biochem. Sci.* 26, 475-481.

Weil, D., Garcon, L., Harper, M., Dumenil, D., Dautry, F. and Kress, M. (2002). Targeting the kinesin Eg5 to monitor siRNA transfection in mammalian cells. *BioTechniques* 33, 1244-1248.
Weisinger, G., Gavish, M., Mazurika, C. and Zinder, O. (1999). Transcription of actin, cyclophilin and glyceraldehyde phosphate dehydrogenase genes: Tissue- and treatment specificity. *Biochim. Biophys. Acta* 1446, 225-232.
Weissenhorn, W., Hinz, A. and Gaudin, Y. (2007). Virus-membrane fusion. *FEBS Lett.* 581, 2150-2155.
Wertz, I.E. and Dixit, V.M. (2010). Signaling to NF-kβ: Regulation by ubiquitination. *Cold Spring Harb. Perspect. Biol.* 2, a003350.
Westerhout, E.M. and Berkhout, B. (2007). A systemic analysis of the effect of target RNA structure on RNA interference. *Nucleic Acids Res.* 35, 4322-4330.
Wetzel, H., Nevill, E.M. and Erasmus, B.J. (1970). Studies on the transmission of African horsesickness. *Onderstepoort J. Vet. Res.* 37, 165-168.
White, E. (1998). Regulation of apoptosis by adenovirus E1A and E1B oncogenes. *Semin. Virol.* 8, 505-513.
White, J.M. (1990). Viral and cellular membrane fusion proteins. *Annu. Rev. Physiol*. 52, 675-697.
White, J.M., Delos, S.E., Brecher, M. and Schornberg, K. (2008). Structures and mechanisms of viral membrane fusion proteins: Multiple variations on a common theme. *Crit. Rev. Biochem. Mol. Biol.* 43, 189-219.
Wiley, D.C. and Skehel, J.J. (1987). The structure and function of the hemagglutinin membrane glycoprotein of influenza virus. *Annu. Rev. Biochem*. 56, 365-394.
Wiley, S.R., Schooley, K., Smolak, P.J., Din, W.S., Huang, C.P., Nicholl, J.K., Sutherland, G.R., Smith, T.D., Rauch, C., Smith, C.A. and Goodwin, R.G. (1995). Identification and characterization of a new member of the TNF family that induces apoptosis. *Immunity* 3, 673-682.
Williams, C.F., Inoue, T., Lucus, A.-M., Zanotto, P.M.A. and Roy, P. (1998). The complete sequence of four major structural proteins of African horse sickness virus serotype 6: Evolutionary relationships within and between the orbiviruses. *Virus Res.* 53, 53-73.
Wilson, A., Mellor, P.S., Szmaragd, C. and Mertens, P.P.C. (2009). Adaptive strategies of African horse sickness virus to facilitate vector transmission. *Vet. Res.* 40, 16.
Wirblich, C., Bhattacharya, B. and Roy, P. (2006). Nonstructural protein 3 of bluetongue virus assists virus release by recruiting ESCRT-I protein Tsg101. *J. Virol.* 80, 460-473.
Wiznerowicz, M., Szulc, J. and Trono, D. (2006). Tuning silence: Conditional systems for RNA interference. *Nature Methods* 3, 682-688.
Wolter, K.G., Hsu, Y.T., Smith, C.L., Nechushtan, A., Xi, X.G. and Youle, R.J. (1997). Movement of Bax from the cytosol to mitochondria during apoptosis. *J. Cell Biol.* 139, 1281-1292.
Wooddell, C.I., Van Hout, C.V., Reppen, T., Lewis, D.L. and Herweijer, H. (2005). Long-term RNA interference from optimized siRNA expression constructs in adult mice. *Biochem. Biophys. Res. Commun.* 334, 117-127.
Wu, X., Chen, S.Y., Iwata, H., Compans, R.W. and Roy, P. (1992). Multiple glycoproteins synthesized by the smallest RNA segment (S10) of bluetongue virus. *J. Virol.* 66, 7104-7112.
Wu, Y., Tibrewal, N. and Brige, R.B. (2006). Phospohatidylserine recognition by phagocytes: A view to kill. *Trends Cell Biol.* 16, 189-197.
Wyllie, A.H. (1980). Glucocorticoid-induced thymocyte apoptosis is associated with endogenous endonuclease activation. *Nature* 284, 555-556.
Wyllie, A.H. (1981). Cell death: A new classification separating apoptosis from necrosis. In: Cell death in biology and pathology. I.D. Bowen and R.A. Lockshin (Eds.), pp. 9-34, Chapman and Hall, London.
Wyllie, A.H., Beattie, G.J. and Hargreaves, A.D. (1981). Chromatin changes in apoptosis. *Histochem. J.* 13, 681-692.
Wyllie, A.H., Kerr, J.F.R. and Currie, A.R. (1980). Cell death: The significance of apoptosis. *Int. Rev. Cytol.* 68, 251-306.

Xia, H., Mao, Q., Paulson, H.L. and Davidson, B.L. (2002). siRNA-mediated gene silencing *in vitro* and *in vivo*. *Nature Biotechnol.* 20, 1006-1010.
Xu, G. and Shi, Y. (2007). Apoptosis signaling pathways and lymphocyte homeostasis. *Cell Res.* 17, 759-771.
Xu, G., Cirilli, M., Huang, Y., Rich, R.L., Myszka, D.G. and Wu, H. (2001). Covalent inhibition revealed by the crystal structure of the caspase-8/p35 complex. *Nature* 410, 494-497.
Yang, D., Buchholz, F., Huang, Z., Goga, A., Chen, C.-Y., Brodsky, F.M. and Bishop, J.M. (2002). Short RNA duplexes produced by hydrolysis with *Escherichia coli* RNase III mediate effective RNA interference in mammalian cells. *Proc. Natl. Acad. Sci. USA* 99, 9942-9947.
Yang, E., Zha, J., Jockel, J., Boise, L.H., Thompson, C.B. and Korsmeyer, S.J. (1995). Bad, a heterodimeric partner for Bcl-XL and Bcl-2, displaces Bax and promotes cell death. *Cell* 80, 285-291.
Yeh, W.C., Itie, A., Elia, A.J., Ng, M., Shu, H.B., Wakeham, A., Mirtsos, C., Suzuki, N., Bonnard, M., Goeddel, D.V. and Mak, T.W. (2000). Requirement for Casper (c-FLIP) in regulation of death receptor-induced apoptosis and embryonic development. *Immunity* 12, 633-642.
Yu, J.Y., DeRuiter, S.L. and Turner, D.L. (2002). RNA interference by expression of short-interfering RNAs and hairpin RNAs in mammalian cells. *Proc. Natl. Acad. Sci. USA* 99, 6047-6052.
Yu, J.Y., Taylor, J., DeRuiter, S.L., Vojtek, A.B. and Turner, D.L. (2003). Simultaneous inhibition of GSK3α and GSK3β using hairpin siRNA expression vectors. *Mol. Ther.* 7, 228-236.
Yuan, J., Shaham, S., Ledoux, S., Ellis, H.M. and Horvitz, H.R. (1993). The *C. elegans* cell death genes *ced3* encodes a protein similar to mammalian interleukin-1β-converting enzyme. *Cell* 75, 641-652.
Zamore, P.D., Tuschl, T., Sharp, P.A. and Bartel, P. (2000). RNAi: Double-stranded RNA directs the ATP-dependent cleavage of mRNA at 21 to 23 nucleotide intervals. *Cell* 101, 25-33.
Zhang, H., Fabrice, A.K., Jaskiewicz, L., Westhof, E. and Filipowicz, W. (2004). Single processing centre models for human Dicer and bacterial RNase III. *Cell* 118, 57-68.
Zhang, L., Chandran, K., Nibert, M.L. and Harrison, S.C. (2006). Reovirus μ1 structural rearrangements that mediate membrane penetration. *J. Virol.* 80, 12367-12376.
Zhang, X., Boyce, M., Bhattacharya, B., Zhang, X., Schein, S., Roy, P. and Zhou, Z.H. (2010). Bluetongue virus coat protein VP2 contains sialic acid-binding domains, and VP5 resembles enveloped virus fusion proteins. *Proc. Natl. Acad. Sci. USA* 107, 6292-6297.
Zhao, L.J., Jian, H. and Zhu, H. (2003). Specific gene inhibition by adenovirus-mediated expression of small interfering RNA. *Gene* 316, 137-141.
Zhou, H. and Zeng, X. (2009). Energy profile and secondary structure impact shRNA efficacy. (2009). *BMC Genomics* 10 (Suppl 1), S9.
Zhou, L., Jiang, G., Chan, G., Santos, C.P., Severson, D.W. and Xiao, L. (2005). Michelob_x is the missing inhibitor of apoptosis protein antagonist in mosquito genomes. *EMBO Rep.* 6, 769-774.
Zinke, M., Kendl, S., Singethan, K., Fehrholz, M., Reuter, D., Rennick, L., Herold, M.J. and Schneider-Schaulies, J. (2009). Clearance of measles virus from persistently infected cells by short hairpin RNA. *J. Virol.* 83, 9423-9431.